Nádia Sofia Pereira Gonçalves

PERIPHERAL NEUROINFLAMMATION AND NOVEL POTENTIAL THERAPEUTIC TARGETS IN FAMILIAL AMYLOIDOTIC POLYNEUROPATHY

Tese de Candidatura ao grau de Doutor em Ciências Veterinárias submetida ao Instituto de Ciências Biomédicas Abel Salazar da Universidade do Porto.

Orientador – Professora Doutora Maria João Saraiva

Categoria – Professor catedrático

Afiliação – Instituto de Ciências Biomédicas Abel Salazar da Universidade do Porto.

Este trabalho foi financiado pela Fundação para a Ciência e a Tecnologia SFRH/BD/ 74304/2010, FCOMP-01-0124-FEDER-022718 (PEST-c/SAU/LA0002/2011 and PTDC/SAU-ORG/111313/2009) FCOMP-01-0124-FEDER-028406 (PTDC/BIM-MEC/0282/2012) e co-financiado pelo POPH/FSE.

A beleza das coisas existe no espírito de quem as contempla.

David Hume

Acknowledgements

Muitas foram as pessoas que contribuíram para o meu crescimento pessoal e profissional ao longo destes anos. A todos os que contribuíram direta ou indiretamente com paciência e amizade o meu obrigada!

À Professora Maria João Saraiva por me ter dado a oportunidade de integrar a sua equipa, por toda a disponibilidade e entusiasmo que sempre demonstrou pelo meu trabalho e pela abertura que sempre teve às minhas sugestões científicas. A paixão que sente pela ciência e o seu brio profissional são contagiantes e muito me ajudaram a crescer enquanto investigador. E porque a motivação não se fica apenas pelo laboratório, não podia deixar de agradecer pelos bons momentos partilhados em congressos nacionais e internacionais.

À Professora Fátima Gartner, directora do meu programa doutoral, muito agradeço a disponibilidade, simpatia e gentileza que sempre demonstrou perante as minhas dúvidas e questões.

Ao Doutor Paulo Vieira pelo seu pragmatismo e incentivo que sempre deu a este projeto. Agradeço-lhe pela energia e dinamismo com que sempre discutimos ciência e por ter sido uma peça fundamental na minha formação e na progressão dos trabalhos que deram origem a esta tese.

À Doutora Ana Paula Pêgo agradeço o seu apoio incansável e o entusiasmo demonstrado na nossa colaboração científica.

À Doutora Mónica Sousa agradeço todas as sugestões, críticas e comentários que contribuíram para a qualidade deste trabalho.

Ao Rui Fernandes e à Doutora Paula Sampaio por toda a ajuda prestada com os estudos de microscopia eletrónica e de fluorescência.

À Paula Magalhães pela simpatia e ajuda na genotipagem e no PCR em tempo real.

Ao grupo de Neurobiologia Molecular, particularmente à Maria Teixeira Coelho, Alda Henriques, Diana Martins e João Moreira por todos os almoços, sushizadas, gargalhadas e momentos de amizade que partilhamos. À Paula Gonçalves por todos os processamentos de parafina e de microscopia eletrónica.

A special thanks to Yohei Misumi for the extraordinary scientific discussions and friendship.

À equipa das festarolas João Valente, Ricardo Celestino, Rita Mota, Raquel Monteiro, Ana Duarte, Ângela Brito, Ritisse de Barros, Carlos Resende, João Vinagre e Bárbara Gonçalves. Obrigada pelo companheirismo, por me aturarem sempre com um sorriso na cara, por tornarem míticas as noites de Halloween e por estarem sempre presentes.

Um agradecimento especial à Luciana Moreira pelos momentos partilhados na escrita da tese e por toda a ajuda com a formatação deste trabalho. Obrigada pela paciência!

Não posso deixar de agradecer às minhas eternas amigas Isabel Domingues, Viviana Barros e Maria Molinos que me acompanham há já muitos anos e que me dão a sua preciosa amizade.

À Dona Lurdes e à Nela que com a sua calma sempre me mostraram o lado positivo de todas as coisas. À Bi e à Diana, que já são minhas sobrinhas adotadas, por todo o carinho e amizade.

Aos meus pais um agradecimento muito especial, pois sem eles nada disto teria sido possível. Obrigada por acreditarem em mim, pelo amor, dedicação, valores incutidos e por serem os meus melhores amigos.

Ao meu maninho Tiago por tudo o que percorremos juntos, pelas conversas e pela amizade sincera.

Ao Nelson que é um pilar na minha vida. Obrigada por me fazeres ver a vida de uma forma mais alegre e pela felicidade com que juntos vivemos.

Agradeço ao Instituto de Ciências Biomédicas Abel Salazar (ICBAS) da Universidade do Porto onde me formei, por me ter voltado a acolher, desta vez como aluna de doutoramento.

Agradeço ao Instituto de Biologia Molecular e Celular (IBMC) por ter proporcionado as condições essenciais ao desenvolvimento desta tese.

Finalmente, um agradecimento à Fundação para a Ciência e Tecnologia por me conceder uma bolsa de doutoramento (SFRH/BD/74304/2010).

De acordo com o disposto no n.º 1 do artigo 34.º do Decreto-Lei n.º 74/2006, republicado pelo Decreto-Lei n.º 115/2013, 1.ª série, n.º 151 de 7 de Agosto de 2013, constam nesta dissertação os artigos já publicados, que a seguir se discriminam:

Gonçalves NP, Teixeira-Coelho M, Saraiva MJ (2015) Protective role of Anakinra against transthyretin mediated axonal loss and cell death in a mouse model of Familial Amyloidotic Polyneuropathy. *J Neuropathol Exp Neurol*, 74(3): 203-217.

Gonçalves NP, Costelha S, Saraiva MJ (2014) Glial cells in Familial Amyloidotic Polyneuropathy. *Acta Neuropathol Commun,* 2:177.

Gonçalves NP, Vieira P, Saraiva MJ (2014) Interleukin-1 signaling pathway as a therapeutic target in transthyretin amyloidosis. *Amyloid*, 21(3): 175-184.

Gonçalves NP, Teixeira-Coelho M, Saraiva MJ (2014) The inflammatory response to sciatic nerve injury in a Familial Amyloidotic Polyneuropathy mouse model. *Exp Neurol*, 257: 76-87.

Gonçalves NP, Oliveira H, Pêgo AP, Saraiva MJ (2012) A novel nanoparticle delivery system for in vivo targeting of sciatic nerve: impact on regeneration. *Nanomedicine (Lond)*, 7(8): 1167-1180.

Table of contents

Abbreviation list

8-OHdG	8-hydroxy-2' -deoxyguanosine
18S	18S ribosomal RNA
Aβ	Amyloid beta
AAV	Adeno-associated Virus
ANS	Autonomic nervous system
AP-1	Activator protein 1
Apaf-1	Apoptotic protease activating factor 1
Arg-1	Arginase-1
ASO	Anti-sense oligonucleotides
ATF	Activating transcription factor
Bcl-2	B-cell lymphoma 2
BDNF	Brain-derived neurotrophic factor
Bid	BH3 interacting domain death agonist
BiP	Binding immunoglobulin protein
Bp	Base pairs
CCL2	Chemokine (C-C motif) ligand 2
CD45	Lymphocyte common antigen
CD11b	Cluster of differentiation molecule 11b
cDNA	Complemmentary DNA
C/EBP	CCAAT/enhancer binding protein
CH	Chitosan
CHROX	Chitosan labeled with rhodamine
CNS	Central nervous system
CREB	cAMP response element-binding protein
CSF	Cerebrospinal fluid
Cxcl-3	Chemokine (C-X-C motif) ligand 3
Cxcl-2	Chemokine (C-X-C motif) ligand 2
Cxcl-12	Chemokine (C-X-C motif) ligand 12
DA	Degree acetylation
DAMPs	Damage-associated molecular pattern molecules
DAPI	4’.6-diamino-2-phenylindole
DLK	Dual leucine zipper kinase
DLS	Dynamic light scattering
DRG	Dorsal root ganglia
ECM	Extracellular matrix

EEA1	Early Endosome Antigen 1
EGCG	Epigallocatechin gallate
eIF2α	Eukaryotic Initiation Factor 2 alpha
ELISA	Enzyme-linked immunosorbent assay
ER	Endoplasmic reticulum stress
ERAD	Endoplasmic-reticulum-associated protein degradation
ERK	Extracellular-signal-regulated kinase
FAC	Familial Amyloidotic Cardiomyopathy
FAP	Familial Amyloidotic Polyneuropathy
FasL	Fas Ligand
GAG	Glycosaminoglycan
GAP-43	Growth associated protein 43
GAPDH	Glyceraldehyde 3-phosphate dehydrogenase
GM-CSF	Macrophage colony stimulating factor
HDAC5	Histone deacetylase 5
HDL	High density lipoprotein
HIV-1	Human immunodeficiency virus type 1
HNE	Hydroxynonenal
Hnf-4	Hepatocyte nuclear factor-4
Hnf-3β	Hepatocyte nuclear factor 3 beta
Hsf-1	Heat shock factor 1
Hsp	Heat shock protein
IBA-1	Ionized calcium-binding adapter molecule 1
IgG	Immunoglobulin G
IHC	Immunohistochemistry
IKBα	Nuclear factor of kappa light polypeptide gene enhancer in B-cells inhibitor alpha
IL-1RI	Interleukin-1 receptor type I
IL-1Ra	Interleukin-1 receptor antagonist
IL-1β	Interleukin-1 beta
IL-1α	Interleukin-1 alpha
IL-6	Interleukin 6
IL-10	Interleukin 10
iNOS	Inducible nitric oxide
IRAK1	Interleukin-1 receptor-associated kinase 1
IRE1	Inositol-requiring protein 1
JNK	Signal transduction by the c-Jun N-terminal kinase

KO	Knockout
Lamp-1	Lysosome-associated membrane glycoprotein 1
LDL	Low-density lipoprotein
LIF	Leukemia inhibitory factor
Ly6G	Lymphocyte antigen 6G
MHC	Major histocompatibility complex
MMP-9	Matrix metalloproteinase-9
mRNA	Messenger RNA
Myd88	Myeloid differentiation primary response gene 88
NF-κB	Nuclear factor kB
NGAL	Neutrophil gelatinase-associated lipocalin
NGF	Nerve growth factor
NPY	Neuropeptide Y
Oct-6	Octamer transcription factor 6
PBS	Phosphate buffer saline
PDI	Polydispersity index
PERK	Pancreatic ER kinase (PKR)-like ER kinase
PGP 9.5	Protein gene product 9.5
PKA	Protein kinase A
PLA_2	Phospholipase A2
PNS	Peripheral nervous system
qPCR	Real-time polymerase chain reaction
RAGE	Receptor for advanced glycation end products
RAGs	Regeneration associated genes
RAP	Receptor-associated protein
RBP	Retinol binding protein
RNAi	Interference RNA
SAP	Serum amyloid P component
SEM	Standard error of the mean
SFI	Sciatic functional index
siRNA	Small interfering RNA
SQ-IHC	Semi-quantitative immunohistochemistry
SSA	Senil systemic amyloidosis
STAT3	Signal transducer and activator of transcription 3
T_4	Thyroxine
tBid	truncated Bid
TEM	Transmission electron microscopy

TIMP-1	Metallopeptidase inhibitor 1
TLR	Toll-like receptor
TNF-α	Tumor necrosis factor alpha
TTR	Transthyretin
TUDCA	Tauroursodeoxycholic acid
UPR	Unfolded protein response
WT	Wild-type

Abstract

Familial Amyloidotic Polyneuropathy (FAP) is a neurodegenerative disorder, characterized by the extracellular deposition of transthyretin (TTR) aggregates and amyloid fibrils, particularly at the peripheral and autonomic nervous systems (PNS and ANS, respectively). TTR is a homotetrameric protein synthesized mainly by the liver, choroid plexuses of the brain and retinal epithelium, acting as a physiological carrier of thyroxine and retinol. Over 100 single point mutations have been identified in the *TTR* gene being the most common associated with FAP the substitution of a methionine for a valine at position 30 of the polypeptide chain (V30M). The molecular mechanisms related to neurodegeneration in FAP are still poorly understood; however, evidence suggests that non-fibrillar aggregates are the major neurotoxic culprits in the pathological process. Thus, signs of endoplasmic reticulum (ER) stress, extracellular matrix (ECM) remodeling, heat shock response, inflammation and oxidative stress are present since the earlier stages of disease. Synthesis of interleukin-1β (IL-1β) by axons of the peripheral nerve from FAP patients has been associated with nerve fiber degeneration, which consequently creates a feed-forward mechanism aggravating the disease phenotype. Thus, a balanced cytokine environment is fundamental, as uncontrolled pro-inflammatory responses culminate in tissue damage and cell death.

In this work, we studied the role of ECM remodeling and inflammation in the progress of FAP to open new avenues for novel therapeutic approaches. We demonstrated *in vivo* that upregulation of heparan sulfate proteoglycans promote TTR polymerization. Given the relationship between inflammation and ECM remodeling, we next investigated whether a pro-inflammatory stimulus might influence TTR deposition. Using a nerve injury model we found for the first time that neuroinflammation triggers TTR expression and non-fibrillar deposition in the peripheral nerve and that FAP mice are impaired in their ability to recruit innate immune cells and regenerate after damage. These findings prompt us to test *in vivo* the effect of the anti-inflammatory drug Anakinra on pathology progression. Our results revealed that Anakinra efficiently impairs TTR non-fibrillar deposition in the sciatic nerve, inhibits production of intermediate molecules of the IL-1 signaling pathway and lowers the levels of apoptotic, oxidative and ER stress associated biomarkers. Moreover, by treating FAP transgenic mice with Anakinra, 48 hours before sciatic nerve ligation, we were able to prevent nerve TTR non-fibrillar deposition and expression, rescuing the observed phenotype. In addition, activation of apoptotic cascades was diminished and accompanied by an improved regenerative response.

The multi-target properties of Anakinra together with its low toxicity in humans, prompt us to propose anti-inflammatory therapy in the treatment of TTR-related amyloidosis. Future

therapies for FAP will probably encompass for a combinatorial approach targeting multiple pathways of the disease.

Previous studies demonstrate soluble non-mutated TTR internalization by a variety of cell types, for instance through the megalin receptor. Here we evaluate internalization of TTR by glial cells of the PNS and ANS. We found that TTR was internalized *in vivo* by Schwann cells and satellite cells of both nervous systems, through an endocytic process. Partially colocalization between TTR and early endosome antigen 1 (EEA1) or lysosome-associated membrane glycoprotein 1 (Lamp-1) suggests TTR translocation along the endosomal compartment to lysosomes for degradation. Additional studies will be imperative to uncover the underlying molecular mechanisms.

Taken together, this work contributed to disclose new disease platforms important for modulation of TTR amyloidosis, which might be key targets for future therapy.

Resumo

A Polineuropatia Amiloidótica Familiar (PAF) é uma doença neurodegenerativa caracterizada pela deposição extracelular de agregados de transtirretina (TTR) e fibras de amilóide, especialmente nos sistemas nervoso periférico e autonómico (SNP e SNA, respetivamente). A TTR é uma proteína homotetramérica produzida sobretudo pelo fígado, pelo plexo coróide no cérebro e pelo epitélio da retina, cuja principal função é o transporte de tiroxina e retinol. Mais de 100 mutações no gene da *TTR* foram já identificadas sendo a mutação principal associada à PAF a substituição de uma metionina por uma valina na posição 30 da cadeia polipeptídica (V30M). Os mecanismos moleculares relacionados com a neurodegenerescência na PAF são pouco conhecidos, no entanto há evidência de que os agregados não-fibrilares de TTR serão as espécies mais tóxicas para o desenrolar desta patologia. Deste modo, stress do retículo endoplasmático (RE), remodelação da matriz extracelular (ME), resposta associada a choque térmico, inflamação e stress oxidativo estão presentes desde o estadio inicial da doença. A síntese de interleucina-1β (IL-1β) pelos axónios dos nervos periféricos de doentes PAF tem sido associada com a degenerescência das fibras nervosas, consequentemente criando um mecanismo de feedback positivo, agravando o fenótipo da doença. Assim sendo, um perfil de produção de citocinas equilibrado é fundamental, uma vez que respostas pro-inflamatórias descontroladas culminam em dano tecidular e morte celular.

Neste trabalho, propusemo-nos a estudar o papel da remodelação da ME e da inflamação na progressão e desenvolvimento da PAF de forma a abrir novos caminhos na procura de estratégias terapêuticas. Demonstramos *in vivo* que um aumento de proteoglicanos de heparano sulfato contribuí para a polimerização da TTR. Dada a relação entre remodelação da ME e inflamação, de seguida fomos investigar de que forma é que um estímulo inflamatório pode influenciar a deposição de TTR. Através de um modelo de lesão de nervo periférico observamos *in vivo* que a inflamação pode de facto levar à deposição não-fibrilar de TTR e aumentar a sua síntese local no nervo. Mais ainda, os murganhos transgénicos para a PAF recrutam menos células do sistema imune inato e têm uma regeneração nervosa também comprometida. Estes dados levaram-nos a testar o efeito *in vivo* de uma terapia anti-inflamatória com Anacinra na patologia da PAF. Os nossos resultados revelaram que o tratamento com Anacinra inibiu com eficiência a deposição não-fibrilar de TTR no nervo ciático, reduziu a síntese de moléculas da via de sinalização da IL-1 e diminuiu os níveis de biomarcadores relacionados com a apoptose e stress oxidativo ou do RE. Mais ainda, o tratamento de animais transgénicos para a PAF com Anacinra, 48 horas antes de realizar a ligação do

nervo ciático, preveniu a deposição não-fibrilar e a expressão local de TTR, permitindo reverter o fenótipo observado em resposta a um estímulo inflamatório. Além disso, com este tratamento foi prevenida a ativação de cascatas apoptóticas, acompanhada por uma melhoria na resposta regenerativa do nervo.

As propriedades multifatoriais do Anacinra juntamente com a baixa toxicidade em humanos levam-nos a propôr esta terapia anti-inflamatória para o tratamento de amiloidoses de TTR. Terapias futuras para a PAF vão sem dúvida passar por uma abordagem combinatória, tendo como alvo múltiplas vias da doença.

Estudos anteriores demonstram que a TTR nativa é internalizada por diversos tipos de células, por exemplo através do recetor da megalina. Com este trabalho nós avaliamos a internalização de TTR pelas células da glia dos SNP e SNA. Vimos que a TTR é internalizada pelas células de Schwann e pelas células satélite de ambos os sistemas nervosos, por um processo endocítico. A colocalização parcial entre a TTR e um marcador de endossomas precoces (EEA1) ou com uma glicoproteína da membrana dos lisossomas (Lamp-1) sugere translocação de alguma TTR ao longo do compartimento endosomal para degradação nos lisossomas. Estudos adicionais serão essenciais de forma a esclarecer os mecanismos que operam por detrás destas observações. Em conclusão, este trabalho contribuiu para a descoberta de novos fatores importantes para a modulação das amiloidoses de TTR, que podem ser alvos principais para futuras terapias.

General Introduction

General Introduction

Transthyretin

In 1942 a protein travelling faster than albumin on an electrical field was named prealbumin. It circulates as a tetramer composed of identical 127 amino acid monomers in cerebrospinal fluid (CSF) (Kabat et al., 1942) and plasma (Seibert and Nelson, 1942). Knowledge regarding physiological roles of this protein in the transport of thyroxine (T_4) and retinol (Raz and Goodman, 1969), lead to a change of its name to transthyretin (TTR) in 1981 by the International Union of Biochemists.

In a phylogenetic context, TTR is a highly conserved protein found in several vertebrate species. More recently, TTR-like proteins have been found in prokaryotes, nematodes and plants, eventually without the ability to bind T_4 or similar ligands (Hennebry et al., 2006).

Mutations in the human *TTR* gene are associated with amyloidoses, a group of disorders characterized by the extracellular accumulation of amyloid deposits (Westermark, 1998), clinically termed Familial Amyloidotic Polyneuropathy (FAP) or Cardiomiopathy (FAC) when point mutations result in protein deposition in the peripheral and autonomic nervous systems (PNS and ANS) or heart, respectively.

Transthyretin gene structure and dynamics

The single gene encoding *TTR* is found on chromosome 18, more precisely in the 18q11.2-q12.1 region (Whitehead et al., 1984), spans about 7 kilobases and has four exons and three introns (Sasaki et al., 1985; Tsuzuki et al., 1985). The first exon, with 95 base pairs (bp) long, encodes a leader peptide of 20 amino acids and the first three amino acid residues of the mature protein, while exons 2 (131 bp), 3 (136 bp) and 4 (253 bp) hold the coding sequences for residues 4-47, 48-92 and 93-127 of the mature protein, respectively. Introns 1 and 3 have two independent open reading frames (Tsuzuki et al., 1985) with unclear functions since these are not transcribed to be expressed as independent polypeptides *in vivo* neither as part of functional transcripts (Soares et al., 2003). In the 5'-flanking region, a TATA box, a CAAT box and two overlapping sequences homologous to glucocorticoid responsive elements were identified. Additionally, in the 3'-untranslated region, downstream from the coding sequence, a polyadenylation signal (AATAAA) is present (Sasaki et al., 1985).

The *TTR* gene is highly conserved through evolution; mouse and rat *Ttr* genes share 82% and 90% homology, respectively, with the human *TTR* sequence (Costa et al., 1986). A

proximal promoter and a distal enhancer are the two major regulatory domains present in the 5' flanking region of the *TTR* gene. The *TTR* promoter is bound by nuclear transcription enhancing factors, namely hepatocyte nuclear factors 1, 3, 4 and 6, CCAAT/enhancer binding proteins (c/EBP) and the the activator protein 1 (AP-1) (Costa et al., 1990).

TTR is mainly synthesized by liver hepatocytes and the choroid plexuses of the brain, secreting the protein into plasma and CSF, respectively (Soprano et al., 1985; Dickson et al., 1986). Moreover, *in vivo* studies noticed that synthesis and secretion of TTR are regulated independently in the liver and choroid plexus (Dickson et al., 1986) suggesting the presence of different regulation factors between tissues. The choroid plexus consists of modified ependymal cells that secrete 10 times more *TTR* mRNA than the liver, when expressed as tissue/weight, representing TTR 20% of the total ventricular proteins in the CSF (concentration levels range from 5 to 20 µg/mL) (Vatassery et al., 1991). More than 90% of plasma circulating TTR arises from liver production. Plasma TTR levels are age dependent since they increase gradually after birth until reach the adult concentration of 200-400 µg/mL (Goldsmith and Munson, 1987), beginning to decline at age 50. Importantly, TTR plasma levels have been useful for the control of nutritional and inflammatory status in several conditions (Dickson et al., 1982; Potter and Luxton, 1999).

Low amounts of the *TTR* gene have been also detected in stomach, namely in gastric ghrelin cells (Walker et al., 2013), heart, skeletal muscle, spleen (Soprano et al., 1985), human placenta (McKinnon et al., 2005), pancreas, retinal pigment epithelium in the eye (Westermark and Westermark, 2008) and Schwann cells of the peripheral nerve (Murakami et al., 2010). Recently, *TTR* expression in hippocampal and cortical neuron cultures has also been suggested (Li et al., 2011). This system highlights a prominent example for the differential regulation of *TTR* in different cell types, since the heat shock factor 1 (*Hsf-1*) was found as a regulator for *TTR* transcription in primary hippocampal neurons but not in hepatocytes (Wang et al., 2014).

TTR is expressed during embryonic development and throughout life; nevertheless it does not seem to be essential since TTR knockout (KO) mice shows normal fetal development, fertility and life span (Episkopou et al., 1993).

TTR has a fast turnover rate with a biological half-life of approximately 2 days in humans (Socolow et al., 1965) and 29 h in Buffalo rats (Dickson et al., 1982). The mechanism for TTR cellular uptake is not fully understood, however liver and kidney are thought to be the two major active organs for TTR degradation, with 15% of TTR being excreted in urine (Makover et al., 1988). Additionally, some studies revealed that TTR internalization by the liver and kidney is receptor-mediated. One endocytic receptor has been described based on cell culture studies, which is megalin, a multi-ligand binding receptor found in the

plasma membrane of many epithelial cells, mediating TTR internalization by the kidney and dorsal root ganglia (DRG) (Sousa et al., 2000a; Fleming et al., 2009). A yet unidentified receptor member of low-density lipoprotein (LDL) family sensitive to receptor-associated protein (RAP) seems to be involved in TTR uptake by the liver (Sousa and Saraiva, 2001). Additionally, TTR interacts with the receptor for advanced glycation end products (RAGE) with a Kd of 120 nM (Sousa et al., 2000b; Monteiro et al., 2006a).

Transthyretin structure

The *TTR* cDNA codes for a mature polypeptide chain of 127 amino acids being the protein secreted in the form of a tetramer, with 55 KDa, of identical subunits (Blake et al., 1974). Each monomer is composed of 8 β-sheet strands (denoted A-H), organized into 4-stranded β-sheets (DAGH and CBEF), and a short α-helix, located between E and F. Strands F and H of each monomer can join edge-to-edge to form a dimer through hydrogen bonding (Blake et al., 1978) (Figure 1).

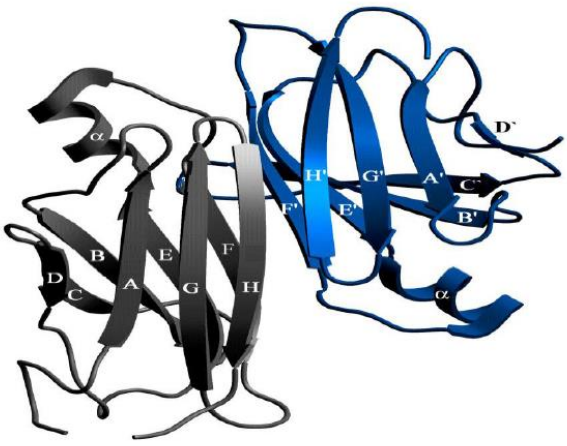

Figure 1 – Ribbon diagram of the wild-type TTR dimer. A TTR dimer is originated when two TTR monomers join side-by-side. Adapted from Protein Data Bank 1ETB.

The association of two dimers, through hydrophobic contacts, form the native TTR tetrameric structure (Figure 2). The dimer-dimer contact is mediated by only eight backbone hydrogen bonds and these associations are substantially weaker than those between the two monomers in a dimer. Non-covalent assembly of the tetramer creates a 50 Å long central hydrophobic channel comprising two symmetrical binding sites for thyroxine with distinct binding constants. As these binding sites exhibit negative cooperativity, due to an allosteric communication between them, only one molecule of T_4

bounds to TTR tetramer (Irace and Edelhoch, 1978). The position of T_4 in the spacious channel is defined by charged amino acids Lys15 and Glu54. Another TTR ligand – retinol binding protein (RBP) has four binding sites located at the surface of the TTR molecule (Monaco et al., 1995).

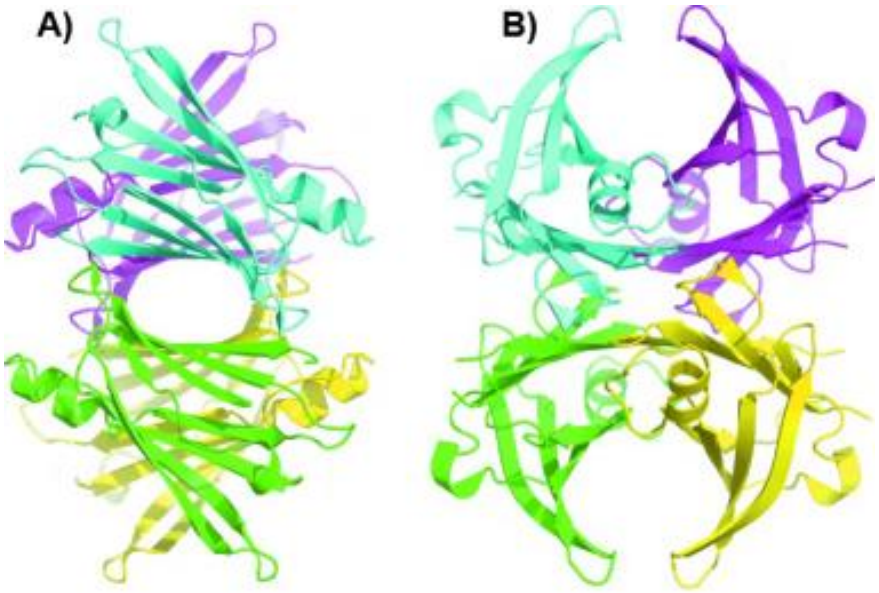

Figure 2 – Diagram denoting TTR quaternary structure. Front view along the bivalent T_4 binding channel (**A**) and side view perpendicular to the binding channel (**B**). The four identical monomers are represented in different colors. The concave shaped β-sheet saddle constitutes the dimer-dimer interface, leaving a central channel (adapted from Haupt et al., 2014).

From a structural point of view, TTR is a very stable protein; however the existence of genetic point mutations may alter the structural stability of the molecule. For instance, the substitution of a methionine for a valine at position 30 of the polypeptide chain (V30M) results in distortion of the T_4 binding cavity leading to a lower binding affinity and TTR destabilization (Hamilton et al., 1993).

Transthyretin physiological functions

TTR homotetramer acts as a transport protein for about 15% of circulating plasma thyroxine and almost all retinol (vitamin A, 95%), through the formation of a complex with RBP (Kanai et al., 1968). However, during the last years, several other functions have been associated with this molecule.

Transthyretin as a transporter protein

Thyroid hormones are primarily responsible for regulation of metabolism and for normal mammalian development. The major form of thyroid hormone in the blood is thyroxine (T_4), which has a longer half-life than triiodothyronine (T_3), the active hormone derived from T_4 deiodination (Palha, 2002). Thyroxine is a tyrosine-based hormone synthesized by the follicular cells of the thyroid gland and its production is regulated by the thyroid stimulating hormone released from the pituitary gland. In humans, most of the T_4 circulating in the bloodstream is transported by thyroxine binding globulin, 20% is transported by albumin and 15% bounds TTR (Bartalena, 1990). In contrast, TTR is the major T_4 carrier in plasma rodents and in the CSF of both rodents and humans (Bartalena and Robbins, 1993). Thus, the stoichiometry of T_4 binding to TTR is higher in the CSF as compared to that in serum (Palha, 2002). However, the role of TTR in the physiology of thyroid hormones is not yet fully understood. Studies with TTR KO mice suggested that TTR is not required for normal T_4 metabolism since regardless of a two-fold decrease in total circulating T_4 levels, these animals were still euthyroid without major phenotypic abnormalities or altered thyroid gland morphology (Episkopou et al., 1993; Palha et al., 1994). In addition, Palha and colleagues (Palha et al., 1997) showed that T_4 levels in CSF of TTR null mice were 30% decreased, but with no differences in brain T_4 content. Moreover, it was previously described that T_4 distribution from the CSF into the brain was TTR-dependent and mediated by receptor endocytosis (Kassem et al., 2006). In addition, an important role for TTR on T_4 transport across the placenta was recently described (Landers et al., 2009). All together these results point towards a preferential relevance for the TTR-T_4 interaction in the brain; however, further studies need to be performed to elucidate TTR role in thyroid hormone homeostasis.

TTR is also involved in the transport of retinol (vitamin A), an essential molecule for several biological functions, namely embryonic development, growth, cellular differentiation, reproduction and vision (Gudas, 2012). RBP is formed in the endoplasmic reticulum (ER) of hepatocytes and associates with TTR, before being secreted to the bloodstream (Kanai et al., 1968). The formation of the complex TTR-RBP-retinol, usually

in a 1:1:1 stoichiometry, prevents loss of RBP through the renal glomeruli (Kanai et al., 1968; Monaco et al., 1995). Retinol-RBP complex binds on the exterior of TTR tetramer utilizing four symmetric-related RBP binding sites; however steric hindrance prevents the binding of more than two RBP molecules. Nevertheless, due to the limiting RBP concentration in plasma, only one RBP molecule is transported by TTR under physiological conditions (Monaco et al., 1995). Consequently, RBP binding to TTR leads to a 70% decrease in its internalization, suggesting that the TTR tetramer is taken up without RBP (Sousa and Saraiva, 2001).

Despite presenting significant lower plasma levels of retinol and RBP, due to increased renal filtration, TTR null mice show normal retinol concentration in tissues and no signs of vitamin A deficiency (van Bennekum et al., 2001). These findings suggest that TTR probably acts as a retinol reservoir, preventing its loss via kidneys. Kawaguchi and coworkers reported a specific receptor for cellular uptake of RBP-retinol, the transmembrane protein “stimulated by retinoic acid 6” (STRA6) that is mostly expressed in brain, eye, kidney, spleen and reproductive tract (Kawaguchi et al., 2007). Circulating retinol may be recycled by liver multiple times before degradation. Recently, a novel RBP transporter regulating retinol homeostasis in liver, intestine and adipose tissue was identified, the RBP receptor-2 (Alapatt et al., 2013).

It has been shown that other molecules can interact with TTR such as noradrenaline oxidation products, retinoic acid, pterin, perlecan, lysosomal-associated membrane protein 1 (Lamp-1) and metallothionein 2 (Liz et al., 2010). However, little is known about the functions assigned by these interactions. Additionally, several compounds sharing molecular structural similarities with T_4 can bind TTR in the T_4 channel; among them are non-steroid anti-inflammatory drugs like flufenamic acid or diflunisal, natural isoflavones (genistein) and polyphenols (resveratrol and curcumin) (Almeida et al., 2004; Sekijima et al., 2008). Recently, *in vitro* studies highlight the binding of epigallocatechin gallate (EGCG) to the surface of the TTR tetramer, which were further corroborated with the complex crystal structure (Ferreira et al., 2009; Miyata et al., 2010). Discovery and characterization of the interaction between these small molecules and TTR is of major importance due to their effect on TTR stabilization with possible therapeutic actions for TTR amyloidosis.

Transthyretin as a novel protease

A small fraction of plasma TTR is associated with high density lipoproteins (HDL) through binding to apolipoprotein A-I (apoA-I) (Sousa et al., 2000c). Further investigation revealed the proteolytic activity of TTR. Thus, *in vitro* studies showed that TTR is a non-canonical serine protease able to cleave apoA-I in its C-terminus (Liz et al., 2004). This phenomena lead to a reduced ability of apoA-I in cholesterol efflux, which can increase development of atherosclerosis (Liz et al., 2007). Yet, the *in vivo* role of TTR in HDL biology requires further evaluation. Although the catalytic machinery of TTR remains unclear it was recently described that a small fraction of TTR is active as a metallopeptidase since metal chelators abolished its activity (Liz et al., 2012).

It was reported that neuropeptide Y (NPY), acting as a neurotransmitter in the brain and in the ANS, can be also cleaved *in vitro* by TTR thus promoting neurite outgrowth (Liz et al., 2009).

Evidence suggests a protective role of TTR in Alzheimer's disease. Costa and colleagues showed that TTR cleaves amyloid β (Aβ) originating smaller and less amyloidogenic peptides than the full length counterpart. Furthermore, TTR species suppress Aβ aggregation *in vitro* suggesting Aβ proteolysis by TTR (Costa et al., 2008a; Costa et al., 2008b; Li et al., 2013).

Transthyretin in the nervous system

Recent studies have been implicating TTR as an important molecule in the nervous system physiology. To clearly understand the role of this protein in neurobiology, characterization of TTR null mice is being fundamental.

Concerning the central nervous system (CNS), it was shown that TTR KO animals presented lower signs of depressive-like behavior and increased exploratory activity, suggesting a link between TTR and behavior (Sousa et al., 2004). Later, these observations were ascribed to the increased levels of norepinephrine in the limbic forebrain and NPY, which among others holds anti-depressant properties (Nunes et al., 2006). Further supporting a role for TTR in cognition, it was shown that TTR null mice presented memory impairment (Buxbaum et al., 2008). Moreover, recent data, using RBP KO animals, revealed that the phenotype of TTR KO mice is not related to TTR function as an RBP carrier since both strains display memory and motor deficits, cortical and hippocampal neuronal loss, some degree of gliosis and reduction in proliferating neuroblasts in the subventricular zone (Buxbaum et al., 2014).

Evidence supports a role for TTR in neuroprotection after cerebral ischemia. Using a model of permanent middle cerebral artery occlusion in TTR KO mice, deficient for the

heat shock response, Santos and colleagues found increased infarct area, cerebral edema and increased microglial response in these animals as compared with the wild-type (WT) situation (Santos et al., 2010a). Still, the mechanisms behind these observations require further investigation.

TTR has been suggested to play a key role in the modulation of Aβ aggregation, a major feature of Alzheimer's disease. It was shown that TTR binds to Aβ preventing amyloid fibril formation and cellular toxicity (Schwarzman et al., 1994). Moreover, several studies reported decreased levels of TTR in CSF (Serot et al., 1997) and plasma (Han et al., 2011; Ribeiro et al., 2012) in patients with Alzheimer's disease, turning TTR to a potential biomarker in the neurochemical differential diagnosis of this disorder. In addition, a neuroprotective role for TTR in Alzheimer's disease has been suggested by inhibition of Aβ fibril formation and consequent protection of neurons from oligomer-induced toxicity and amelioration of cognitive functions (Ribeiro et al., 2012; Cascella et al., 2013; Li et al., 2013; Ribeiro et al., 2014). However, this phenomenon needs further investigation.

Differential TTR levels have also being found in diverse neurological conditions. For instance TTR has been proposed as an early biomarker for frontotemporal dementia, Guillain-Barré syndrome and Parkinson's disease since its levels are upregulated in plasma or CSF from patients (Vieira and Saraiva, 2014).

Very recently, a role for TTR in 14-3-3ζ metabolism was suggested as the hippocampus of TTR KO mice presented lower levels of this protein due to increased lysosomal degradation (Vieira et al., 2013). In addition, *in vitro* and *in vivo* studies suggest that TTR regulates insulin-like growth factor receptor I at the transcriptional and translational levels, triggering receptor nuclear translocation (Vieira et al., 2014). Taken together, these results unravel a new function for naïve TTR in neuroprotection.

Regarding TTR roles in the PNS, Fleming and coworkers, showed that mouse TTR WT plays an important role in nerve regeneration, since TTR KO animals presented slower nerve conduction velocity, impaired sensorimotor recovery and lower fiber density after nerve crush (Fleming et al., 2007). A few years later, the underlying mechanism behind TTR neuritogenic activity was proven to be its internalization by a megalin mediated clathrin-dependent pathway in sensory neurons (Fleming et al., 2009). Very recently, studies with *Caenorhabditis elegans* show that a TTR-like protein (TTR-52) is critical for successful axonal regenerative fusion (Neumann et al., 2015), further reinforcing the importance of this protein for proper axonal growth.

Other functions of transthyretin

TTR tetramer has been considered a functional protein in pancreatic β-cells, promoting insulin release and protecting against β-cell apoptosis (Refai et al., 2005). In addition, it was demonstrated that TTR may bind glucose-regulated proteins at the plasma membrane being thus internalized into the β-cell via a clathrin-dependent pathway (Dekki et al., 2012). Furthermore, TTR KO mice evidenced impaired recovery of blood glucose and lower levels of glucagon in the islets of Langerhans, suggesting that TTR expressed in pancreatic α-cells might play an important role in glucose homeostasis (Su et al., 2012).

Transthyretin molecular variants

More than 100 TTR mutations have been identified, resulting from point substitutions in the polypeptide chain. The only exception is the mutation V122 consequent to one amino acid deletion at position 122. From all TTR mutations (an updated list can be found at http://amyloidosismutations.com/mut-attr.php), 98 are associated with amyloidoses (Benson and Kincaid, 2007). Amyloidoses are rare diseases caused by extracellular deposition of insoluble misfolded proteins, disrupting normal tissue function (Westermark, 1998). TTR-related amyloidosis are phenotypic heterogeneous and although the major clinical feature is sensorimotor polyneuropathy, cardiomyopathy, carpal tunnel syndrome, vitreopathy or leptomeningeal involvement occur as well. Most affected individuals are heterozygous for the pathological mutation, expressing both WT and mutant TTR (Benson and Kincaid, 2007). The most common TTR mutation associated with peripheral neuropathy is V30M (Saraiva et al., 1984). This TTR variant is present worldwide with major endemic areas in northern Portugal, northern Sweden and Japan (Andrade, 1952; Saraiva et al., 1984; Benson and Kincaid, 2007). The penetrance rate of V30M induced disease varies and sometimes cases of early-onset (≤ 35 years) and late-onset (≥ 50 years) coexists in the same family. Indeed, younger generations are usually associated with more severe phenotypes and disease anticipation (Lemos et al., 2014), correlating with differences in clinical findings (Koike et al., 2004). The most amyloidogenic variant often leading to an early-onset with both cardiac and neurologic involvement is the replacement of a leucine by a proline at position 55 (L55P) (Jacobson et al., 1992). Several heterozygous individuals, carriers of two different TTR mutations, usually in different alleles, have been reported. For instance, patients with T119M or the R104H non-pathogenic variants, in addition to the V30M mutation, present milder phenotypes and

slower disease progression, due to increased stabilization of the protein tetrameric structure (Longo Alves et al., 1997).
The most prevalent mutation in the United States is V122I affecting 3-4% of African Americans and leading to a late-onset restrictive cardiomyopathy (Jacobson et al., 1996).
TTR WT protein has a tendency to aggregate with ageing, depositing primarily in the heart, but also in the gut and carpal tunnel, condition denominated senile systemic amyloidosis (SSA). It is thus not associated with any TTR variant but affects 10-25% of the elderly population over 80 years of age (Pitkänen et al., 1984; Westermark, 2005). Furthermore, 9% of TTR mutations give rise to leptomeningeal amyloidosis, including those derived from the TTR mutation L12P, considered as one of the most aggressive variants (Brett et al., 1999).
The study of TTR variants is of major importance for deeply characterization of TTR-related amyloidosis and to provide novel insights regarding therapeutic strategies.

Familial Amyloidotic Polyneuropathy

Familial Amyloidotic Polyneuropathy (FAP) was first described by Corino de Andrade in northern Portugal in 1952 (Andrade, 1952). Over the next two decades, Japan and Sweden were found as other large foci (Araki et al., 1968; Andersson, 1976). This type of hereditary amyloidosis was characterized histologically by generalized atypical amyloid, affecting particularly the peripheral nerves. Amyloid is a heterogeneous material with distinctive β-sheet fibrils identified by green birefringence under polarized light, after staining with alkaline alcoholic Congo red (Puchtler and Sweat, 1965). TTR was identified as the precursor of amyloid in this setting (Costa et al., 1978) and later the most common mutation, V30M, was recognized (Saraiva et al., 1984), becoming a biochemical marker for FAP (Saraiva et al., 1985). Deep ultrastructural characterization of amyloid deposits show that fibrils are typically straight nonbranching filaments, with several lenghs and with approximately 10 nm diameter (Coimbra and Andrade, 1971a; Inoue et al., 1998).
Until 20 years ago, FAP was believed to be a disease restricted to endemic areas; however, with progress in technology, nowadays it is known that this disorder, despite being rare, is distributed worldwide with cases diagnosed in Spain, France, Italy, Greece, United States of America and Brasil (Ando et al., 2005). In Portugal the prevalence of FAP is estimated to be 1 in 538 individuals while in Europe the

incidence of this genetic disorder is estimated to be less than 1 in 100,000 individuals (Ando et al., 2013).

Pathological features of Familial Amyloidotic Polyneuropathy

FAP is an autosomal dominant neurodegenerative disorder characterized by the deposition of TTR aggregates and amyloid fibrils in the connective tissue of several organs, with exception of the CNS and liver parenchyma, affecting particularly the PNS (Coimbra and Andrade, 1971 a, b). The onset of clinical symptoms generally occurs between the third and fourth decade of life but with great variations across different populations (Ando et al., 2013). Patients with early-onset presentation deteriorate quickly while in carriers with the late-onset, the polyneuropathy progresses slowly with different pathological presentations (Koike et al., 2004; Planté-Bordeneuve and Said, 2011). This peculiar form of nerve length-dependent polyneuropathy is fatal in about 10 years on average, varying accordingly to endemic region, genotype and clinical symptoms (Ando et al., 2013). Symptoms start with sensory involvement in the lower limbs, particularly impaired thermal sensibility and neuropathic pain. The sensory deficit gradually progresses relentlessly to the upper limbs and motor deficit appears in the distal lower limbs with walking becoming increasingly difficult also caused by loss of balance, weight loss and muscle wasting. Due to the random distribution of TTR amyloid in the peripheral nerves, carpal tunnel syndrome might be an early non-specific manifestation of FAP. Life-threatening autonomic dysfunction is generally present in FAP patients with early-onset since the first stage of disease including orthostatic hypotension, erectile dysfunction, postprandial diarrhea, constipation or both alternately, nausea, vomiting, dysuria and urinary retention. Cardiac involvement occurs in about 50-80% of FAP patients leading to amyloid restrictive cardiomyopathy with episodes of arrhythmias, syncope or even sudden death. Additional symptoms often found include vitreous opacity, dry eye, glaucoma, nephritic syndrome, renal failure and anemia due to low levels of erythropoietin (Sousa and Saraiva, 2003; Ando et al., 2005; Planté-Bordeneuve and Said, 2011; Ando et al., 2013; Ando et al., 2014). Despite being a multi-symptom disease, CNS manifestations in FAP are rare, regardless of leptomeningeal amyloid deposition (Said and Planté-Bordeneuve, 2009).

At post-mortem examination, amyloid deposits are found in almost every tissue. In peripheral nerve specimens, TTR deposits as amyloid are characteristically found in the endoneurium in close contact with Schwann cells and collagen fibrils (Figure 3). With disease progress, axonal fiber degeneration begins in the unmyelinated and small

diameter myelinated fibers together with invasion and destruction of endoneurial blood vessels. In advanced cases, electroneurophysiological studies demonstrate loss of larger myelinated fibers with demyelination in points of contact with endoneurial clumps of amyloid. Very recently, novel neurophysiological markers of early TTR induced neuropathy were established and proposed as novel tests for FAP diagnosis (Conceição et al., 2014).

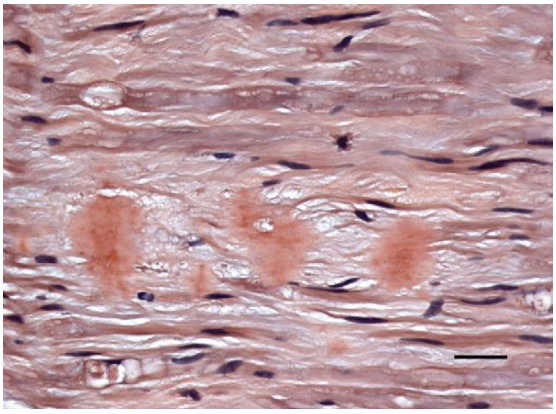

Figure 3 – TTR amyloid deposits in the endoneurium highlighted by Congo red staining. Longitudinal section of a paraffin-embedded nerve biopsy specimen from a 30-year-old man carrying the V30M mutation. Scale bar 10 µm (from Planté-Bordeneuve and Said, 2011).

Amyloid fibrils might occasionally invade the cytoplasm of degenerating Schwann cells due to disruption of the basal lamina (Coimbra and Andrade, 1971b; Thomas and King, 1974), thus impairing nutritional support to several unmyelinated fibers and accounting for early unmyelinated axonal loss. Consequently, abundant groups of flat sheets of Schwann cells processes without axons (bands of Büngner) and Wallerian degeneration are often found in FAP nerve biopsies. In ganglia, amyloid deposition occurs in the stroma in close contact with satellite cells leading to neuron chromatolysis and progressive cell death (Sobue et al., 1990); therefore, these neuronal lesions might produce a distally symmetrical polyneuropathy characterized by the loss of small caliber fibers (Thomas and King, 1974). The deleterious effect of endoneurial amyloid deposits might also be due to a mechanical and toxic effect to the tissue. Moreover, in severely affected cases, vessel walls may be destructed or occluded by amyloid, leading to vascular permeability, interstitial edema and ischemia, thus contributing to the progressive polyneuropathy. Recently, Congo red positive material was detected in circulation, suggesting the presence of TTR aggregates in blood (Liu et al., 2014).

Mechanisms for transthyretin amyloidogenesis

Although remarkable progress has been made regarding TTR amyloidogenesis, the precise molecular mechanisms underlying amyloid fibril formation are not completely understood. It is now accepted that several factors might be involved in the pathogenesis of TTR amyloidosis. First among them is the structure of the native precursor protein, as amino acid substitutions usually destabilize the primary protein, dictating the inheritance of the disease (Benson and Kincaid, 2007). Biophysical studies demonstrate that under acid conditions or increased temperature, WT and mutant TTR tetramers can dissociate into non-native monomers with low conformational stability, originating high molecular mass soluble aggregates that self-assemble leading to the formation of unsoluble fibrils in an infinitely propagating fashion (Figure 4) (Colon and Kelly, 1992; Lai et al., 1996; Quintas et al., 2001). Indeed, X-ray diffraction studies have suggested that TTR monomers or dimers are the intermediate moiety and the building blocks for the pathway of amyloid fibril formation (Blake and Serpell, 1996). In addition, stability of the TTR tetramer has been pointed out as the most important factor for amyloid fibril initiation. In fact, there is a correlation between the thermodynamic stability of TTR variants and their potential to form modified monomers and soluble aggregates. For instance, crystallographic studies have shown that the mutation V30M forces the two β-sheets of each monomer to become more apart, resulting in a distortion of the T_4-binding pocket, associated with reduced affinity for T_4 and lower protein stability (Hamilton et al., 1993).

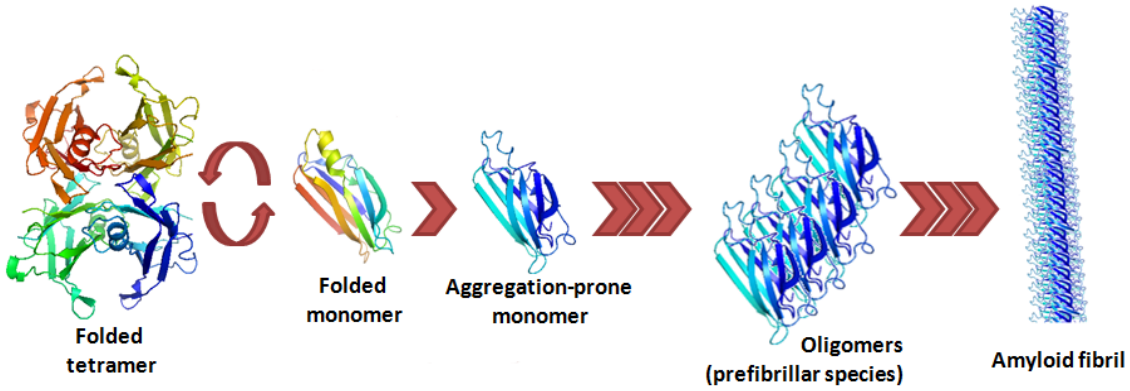

Figure 4 – Hypothetical model for TTR amyloid cascade. Tetramer dissociation into non-native monomers is the first and rate-limiting step for amyloid fibril formation. This unfolded monomer is prone to aggregation, leading to the formation of intermediate species such as oligomers/aggregates finally ending in insoluble amyloid fibrils (adapted from Azevedo et al., 2013).

The rate of amyloid formation and growth is dependent on TTR concentration, thus the quality control system of the cell, such as ER retention or protein degradation by the proteasome (ERAD), might be an important factor determining amyloidogenesis (Sekijima et al., 2005). The presence of an N-glycosylated circulating TTR secreted from FAP liver that is able to escape from ERAD, was recently described (Teixeira and Saraiva, 2013). However, its implication for the etiopathogenesis of the disease needs further clarification.
Although the conformational hypothesis having oligomeric TTR as the nucleus of the polymerization is currently the most accepted theory, proteolytic cleavage may well be a determinant factor in FAP pathogenesis. This theory is supported by findings of the presence of C-terminal TTR fragments in amyloid deposits extracted from FAP patients, raising the hypothesis that proteolytic processing might prompt amyloid fibril formation (Bergström et al., 2005). Moreover, fibril type has been associated with the clinical and pathological phenotypes since patients with truncated TTR in the amyloid deposits present a late-onset form of disease and packed/short fibrils as compared with patients with early-onset disease, who did not exhibit TTR fragments in amyloid deposits (Ihse et al., 2008). Gaining more insight into this issue, recent data demonstrate that the main component of the *ex vivo* fibrils derived from the TTR variant S52P was the fragment corresponding to residues 49-127, thus supporting the important role of proteolytic cleavage for TTR amyloid fibrillogenesis (Mangione et al., 2014). However, the referred proteolytic fragments are not always detected in TTR fibrils (Tawara et al. 1983), therefore despite the release of small peptides might contribute to the initiation or progression of FAP pathology, the role of proteolysis in TTR amyloidogenesis seems to be not an essential mechanism behind amyloid formation, further needing deeply investigation.

Composition of transthyretin amyloid deposits

Amyloids from different disorders might share a common rich cross-β structure and similar pathways for fibril formation; however, they have different compositions. In TTR amyloidosis, all deposits contain a set of accessory molecules, regardless of the fibril precursor. Indeed, affinity between TTR and glycosaminoglycans (GAGs) was previously demonstrated, with evidence that GAGs may be involved in TTR deposition (Inoue et al., 1998; Noborn et al., 2011; Bourgault et al., 2011). GAGs are a heterogeneous group of highly sulfated polysaccharides regulating several physiological processes, such as development or cell adhesion. The common sulfated GAGs are dermatan sulfate, chondroitin sulfate and heparan sulfate, which differ in the structure of the carbohydrate backbone and in sulfate groups. GAGs are usually found in the ECM attached to a core

protein, as proteoglycans (Häcker et al., 2005). Heparan sulfate proteoglycans might be present extracellularly or at cell surface and have been frequently associated with TTR amyloid deposits (Noborn et al., 2011). In fact, Noborn and colleagues showed that heparan sulfate or heparin are able to prompt TTR aggregation and fibrillogenesis both *in vitro* and in a transgenic *Drosophila melanogaster* model of amyloidosis. The mechanism behind this interaction was dependent on the size of heparin, extent of sulfation, pH, TTR concentration and conformation (Noborn et al., 2011). Additional *in vitro* studies demonstrate that larger GAGs are able to interact with multiple TTR aggregates at the same time and that they preferentially bind to pre-formed aggregate species, enhancing its self-assembly, changing TTR quaternary structure, thus increasing the formation of amyloid fibrils (Bourgault et al., 2011). These studies represent an important piece of the puzzle to better understand how GAGs accelerate the amyloidogenic process. For instance, endoneurium is rich in proteoglycans, which might contribute for the tissue selectivity of TTR deposition. Also, the sulfation degree of heparan sulfate increases with age, which may explain the deposition of naïve TTR in the elderly population, giving rise to SSA.

Besides proteoglycans, amyloid fibrils also contain other ubiquitous components, like serum amyloid P component (SAP) and several basement membrane constituents, such as fibronectin, laminin or collagen type IV (Pepys, 2001; Misumi et al., 2009). SAP is a plasma glycoprotein and an important molecule favoring fibrillogenesis since it is estimated that 14% of the dry mass of amyloid deposits is formed by SAP. It is postulated that SAP is non-covalently linked to amyloid deposits, preventing proteolytic breakdown, thus retarding their clearance (Pepys, 2001). Hence, this molecule has been very useful for the clinical diagnosis of amyloidosis through scintigraphy analysis, where radio-labelled protein locate areas of amyloid deposition (Hawkins and Pepys, 1995). Recently, SAP protection against the cytotoxicity of amyloidogenic aggregates was also suggested (Andersson et al., 2013).

Ultrastructural analysis of cardiomyocytes and vascular smooth muscle cells from FAP patients provide evidence that TTR amyloid fibrils formed first at the basement membrane with simultaneous increase in the biosynthesis of membrane components, like laminin, collagen type IV and fibronectin. These micro-environmental changes function as a scaffold for the amyloid fibril growth and this chain reaction could affect *in vivo* fibril turnover and dynamics, contributing for FAP pathogenesis (Misumi et al., 2009).

Animal models of human amyloidoses

TTR amyloidoses are the prototypic protein folding disorders, with protein deposition occurring extracellularly, frequently taking place distant from the site of synthesis. The development of recombinant molecular techniques made possible to analyse folding and misfolding mechanisms, for instance by adding small molecules or peptides able to accelerate or inhibit fibril formation. Despite the first insights into protein aggregation provided by the *in vitro* studies or autopsy analyses, more precise notions of pathogenesis and protein roles are awaited. Thus, several animal models have been generated to allow disease modeling, deeply knowledge regarding pathophysiological mechanisms or development of new therapeutic strategies.

Experimental models based on transgenic expression of normal or mutant forms of TTR in *Drosophila melanogaster* have been generated. TTR V30M flies presented reduced lifespan and neurological impairment, while flies with human TTR WT showed a mild phenotype, similar to that of SSA patients (Berg et al., 2009). In addition, a double mutant form overexpressing either the clinically relevant mutant TTR L55P, or the highly destabilized engineered mutant TTR-A was constructed (Pokrzywa et al., 2007), denoting intracellular aggregates and amyloid filaments in fat body cells (Pokrzywa et al., 2010). The introduction of amyloid precursors in flies compresses the time necessary to obtain a disease phenotype; however, the comparison of a highly mitotic model to mammals might be problematic as cellular and molecular phenotypes could have major differences. Thus, a mammalian model rather than flies would seem to be favored. Several mouse models for TTR amyloidosis have been created but until this moment none of the murine transgenic models exhibit perfect characteristics. Regarding FAP, the first mouse model utilized cDNA's encoding the amyloidogenic allele *TTR* V30M driven by the metallothionein promoter (Sasaki et al., 1986; Sasaki et al., 1989). Zinc induced the expression of *TTR* but circulating levels were too small and no amyloid deposition was detected, suggesting that such a construct would not generate a useful disease model. Subsequently, transgenic mice with the intact human *TTR* V30M gene, with a 6.0 kb of sequence upstream to the initiation site, were generated. These animals showed similar TTR levels in plasma as found in humans and presented appropriate tissue specific TTR expression and deposition (gut, heart, skin, kidney) beginning at about 9 months of age. Nevertheless, the PNS and ANS were spared (Nagata et al., 1995; Takaoka et al., 1997).

Gene depletion (KO) technology allows for gene silencing, generating animals with a totally different phenotype. In 1993, Episkopou and colleagues developed a *Ttr* KO mouse to investigate the TTR roles, namely in embryonic development (Episkopou et al., 1993). Since then, this strain has been widely used to address several aspects of TTR biology. In

a collaborative work, *Ttr* KO mice were crossed with the 6.0-TTR V30M transgenic mice, creating animals with the human *TTR* V30M variant but lacking the endogenous mouse *Ttr* gene. These mice contained 30-60 copies of the human gene and at 24 months of age, TTR deposition resembled that of human FAP patients, but still without deposition in PNS or ANS, not displaying peripheral or autonomic neuropathy (Kohno et al., 1997). Although they were considered moderately successful, these animals still provide means to define new disease biomarkers, to find novel factors modeling disease progression or to evaluate potential therapeutic agents.

Transgenic animals carrying the highly amyloidogenic *TTR* variant L55P were first developed by Teng and coworkers (Teng et al., 1995); however, this strain showed no deposition phenotype even at 2 years of age. Later on, mice with *TTR* L55P construct were crossed onto the murine *Ttr* null background. Non-fibrillar TTR deposition was found earlier in both gastrointestinal tract and skin, while amyloid deposits started to accumulate in these organs approximately at 8 months of age (Sousa et al., 2002). These findings suggested that murine *Ttr* inhibited aggregation and deposition of the highly unstable human TTR L55P variant. However, since TTR deposits were not found involving the nervous system, a new attempt to generate a more accurate model was tried. In 2010, a new mouse model emerged by crossing animals with the V30M mutation, in a *Ttr* null background, with mice KO or heterozygous for the *Hsf-1*. The impaired chaperone response led to relatively early TTR gastrointestinal deposits and, for the first time, protein deposition in the PNS and ANS (Santos et al., 2010b). Moreover, this novel model displayed signs of inflammatory and oxidative stress replicating nerve pathology of asymptomatic carriers of FAP. Overall, this study pointed out the involvement of genes related to the unfolded protein response (UPR) in the neuroprotection against tissue damage elicited by TTR aggregates.

Very recently, through liver specific adeno-associated virus (AAV) gene transfer, a new somatic transgenic mouse line was settled. Viral shocks with TTR L12P (a very aggressive mutant) were administered to TTR KO mice which, after 3 months treatment, presented TTR L12P aggregates inside hepatocytes, found to be degraded by the lysosomal proteolytic system (Batista et al., 2013). This novel model replicates the pathological features displayed by patients with the TTR L12P mutation, namely the severe protein deposition in liver, opening new windows of action for the establishment of innovative models based on gene therapy.

The effect of genetic factors, with manipulation of genome, can be easily assessed in transgenic mouse models; however, their small size makes difficult certain types of manipulation. A Japanese group chose to develop a transgenic rat model expressing the human TTR V30M, under the action of mouse albumin promoter, favoring studies on liver

transplantation. Nevertheless, this model only showed non-fibrillar TTR deposits in colon at very late ages (Ueda et al., 2007).

In addition to the mouse models above described for FAP, an additional mouse model for SSA, overexpressing human TTR WT is also available. Non-fibrillar TTR deposits are present earlier and over age 18 months and amyloid deposits are frequently found in heart and kidney, similar to lesions characterizing age-related fibrillogenesis in humans (Teng et al., 2001).

In summary, it is unquestionable that murine transgenic models for TTR amyloidoses have provided interesting insights into the pathogenesis of these disorders. Although they might raise mechanistic questions that probably are ultimately answered only in more reductionist experimental systems, moving a drug to the clinical practice will certainly require extensive animal testing. Despite all the recent efforts, the perfect animal model for FAP was still not established since none of the referred above models develop peripheral neuropathy.

Mechanisms for cytotoxicity in Familial Amyloidotic Polyneuropathy

While most attention has been focused on amyloid fibrils, different studies evidence that low molecular mass aggregated species are the most cytotoxic culprits. The observation of aggregated non-fibrillar forms of TTR, negative for Congo red staining, in nerve biopsies from asymptomatic FAP carriers dates back to 2001 (Sousa et al., 2001a). Using microscopic and cell viability assays, Sousa and colleagues also demonstrated that these are the most toxic species, in contrast to the fibril counterpart, and that in advanced stages of disease, non-fibrillar TTR aggregates coexist with fibrillar forms in nerve tissue (Figure 5). Based on these results and on the density of nerve fibers, a scoring system was developed for the classification of patient material and stage of disease. Patients classified as FAP 0 have no reduction in the number of fibers, presenting only non-fibrillar TTR aggregates deposition; FAP 1 patients present a discrete decrease in fiber density and fibrillar TTR deposition starts to appear; FAP 2 and 3 have evident or severe fiber reduction, respectively, with extensive amyloid deposition.

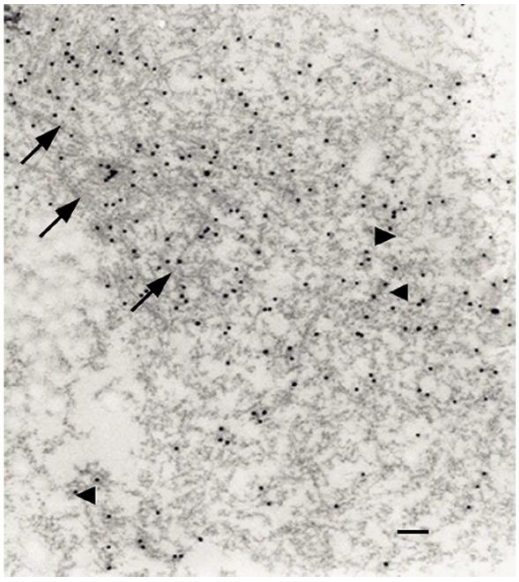

Figure 5 – Photomicrograph of TTR electron immunocytochemistry in an FAP nerve. Arrows pointed out fibrillar TTR deposition while arrowheads denote TTR non-fibrillar aggregates. Scale bar: 100 nm (from Sousa and Saraiva, 2003).

Later on, it was shown *in vitro* that monomeric or relatively small, rapidly formed TTR aggregates, of a maximum size of six subunits, were the major cytotoxic intermediates (Reixach et al., 2004). Further studies characterized these aggregated forms of TTR using dynamic light scattering (DLS) and the presence of smaller intermediate species was found to be correlated with calcium influx (Hou et al., 2007). Altogether, these data

indicates that cellular toxicity starts at early stages of FAP disease, predominantly consequent to the presence of non-fibrillar TTR aggregates. Although the precise molecular mechanisms mediating cytotoxicity in FAP are not yet fully understood, several pathways, including ER stress, apoptosis, ECM remodeling, oxidative stress and inflammation have been implicated.

Endoplasmic reticulum stress and the unfolded protein response

It seems increasingly probable that dysregulation of intracellular calcium homeostasis may represent the common primary mechanism of pathogenesis of amyloid related neurodegenerative disorders. Calcium is critical to normal cell physiology and the function of excitable cells. The calcium ion gradient across cells is maintained by plasma membrane calcium-ATPase pump and the sodium/calcium exchanger that are able to actively release it into the extracellular space. In addition, calcium might also be sequestered into intracellular organelle stores by the ER ATPase pump (Surmeier and Schumacker, 2013). Recently, it has become apparent that calcium regulation also affects ER function and the unfolded protein response (UPR) (Mattson, 2012). ER dysfunction and stress leads to inappropriate protein folding with consequent accumulation of misfolded molecules and UPR activation. This adaptive response is dependent on three basic transmembrane signaling sensors like inositol-requiring enzyme 1 (IRE1), activating transcription factor 6 (ATF-6) and pancreatic ER kinase (PKR)-like ER kinase (PERK). All the main transducers are activated in a process dependent on the ER-resident chaperone binding immunoglobulin protein (BiP/Grp78). In non-stressed conditions, BiP binds to the ER luminal domain of these transmembrane protein receptors, repressing the UPR. When overwhelming load of misfolded proteins or overexpression of proteins occurs, higher levels of BiP are required to bind them, leading to its dissociation from IRE1, ATF-6 and PERK, which in turn become active. Thus, upon BiP release, IRE1 and PERK oligomerize, inducing autophosphorylation and allowing for the activation of transcription factors involved in the UPR, such as X-box-binding protein (XBP1) and phosphorylated eukaryotic translation initiation factor 2α (eIF2α), able to reduce protein burden in the ER by decreasing initial protein translation. On the other hand, ATF-6 translocates to the Golgi apparatus, where it is cleaved for migration to the nucleus, initiating transcription of genes related to the UPR (Xu et al., 2005; Szegezdi et al., 2006). In summary, most of the adaptive measures involve activation of transcription factors and upregulation of ER chaperones to enhance the folding capacity of ER, promote ER-associated degradation (ERAD) and inhibit general translation, aiming at restoring the normal ER function (Xu et al., 2005; Szegezdi et al., 2006; Colgan et al., 2011).

A connection between ER stress and FAP was previously demonstrated. Indeed, increased levels of the ER-resident chaperone BiP were found both in tissues from FAP patients and from an FAP mouse model, in close relation with TTR deposition; effect that seems to be dependent on calcium mobilization from the ER to the cytosol (Teixeira et al., 2006). Additional results demonstrate proteolysis of ATF-6 and phosphorylation of eIF2α. These mechanisms that initially might be protective, switches from pro-survival to pro-apoptotic if protein aggregation persists and the stress cannot be resolved. During prolonged ER stress, all the upstream mentioned signals ultimately result in caspase activation, with ordered and sequential dismantling of the cell. Caspase-12 has been proposed as a key mediator in ER stress-related apoptosis (Nakagawa et al., 2000). The mechanism involved in its activation is not yet fully clear but evidence suggests cleavage of caspase-12 through calpain activation, secondary to calcium release during the ER stress response (Nakagawa and Yuan, 2000). Involvement of caspase-12 mediated ER-specific apoptosis was demonstrated for FAP. *In vitro* studies disclose activation and cleavage of the pro-caspase-12 into an activated fragment when neuroblastoma cells were incubated with TTR aggregates, hence reinforcing the role of these intermediary species for cytotoxicity in FAP (Macedo et al., 2010).

Traditional BiP-mediated ERAD, retrogradely transport the misfolded proteins from the ER to cytosol towards further degradation by the ubiquitin proteasome system. Protein ubiquitination is the major pathway of non-lysosomal proteolysis of intracellular proteins, which are then recognized by the 26S proteasome. Aberration of this system leads to the dysregulation of cellular homeostasis with accumulation of damaged, oxidized or misfolded proteins (Wang and Maldonado, 2006). It is the case of FAP disease, where ubiquitin expression is increased in tissues from human patients and transgenic mouse lines presenting TTR deposition, but accompanied by a significant decrease in proteasome activity, indicating proteasome impairment triggered by TTR aggregates (Santos et al., 2007).

It has been proposed that membrane permeabilization triggered by TTR aggregates may be a key event in the pathophysiology of amyloidosis. Supporting this idea, Cecchi and coworkers proposed that membrane fluidity and disruption, raised by TTR aggregates, correlate with disturbances in calcium homeostasis, representing an important mechanism for TTR amyloid pathogenesis (Cecchi et al., 2005). In addition, calcium release from ER stores can modulate cell death and toxicity. In this regard, *in vitro* studies denote that increased levels of the chaperone BiP, following cell stimulation with TTR aggregates, involves calcium mobilization from the ER through ryanodine receptors, as it can be suppressed by dantrolene (Teixeira et al., 2006). Later, studies with human neuroblastoma cells demonstrated that TTR aggregates rapidly induced an increase in the

concentration of intracellular calcium due to an influx of extracellular pools, mainly via voltage-gated calcium channels (Hou et al., 2007). Although calcium mobilization seems to have an important role for cytotoxicity in FAP, the mechanisms underlying this process need further investigation.

Apoptosis and mitochondrial dysfunction

Neuronal death underlies the symptoms of a broad array of neurodegenerative diseases, including multiple sclerosis, FAP, Alzheimer's, Parkinson's and Huntington's diseases. The mainly shared pathway for neuronal death is apoptosis, a process characterized by chromatin condensation, nuclear fragmentation, decreased cellular volume but maintenance of organelle integrity (Ghavami et al., 2014). Caspases are evolutionarily conserved cysteine proteases and the main propagators of the apoptotic program at the cellular level. These enzymes are present in the cytoplasm as inactive forms and need to be cleaved by proteolysis for activation. Ligation of external cell death inducing molecules (for example tumor necrosis factor α – TNF-α or Fas ligand – FasL) to death receptors, such as Fas or p75 neurotrophin receptor, result in caspase-8 activation, which in turn activate downstream effector caspases, like caspase-3 (Raoul et al., 2000). Extrinsic apoptosis might also be triggered when the extracellular concentrations of trophic factors (for example brain-derived neurotrophic factor (BDNF) or nerve growth factor (NGF)) fall below a certain threshold, leading to the transduction of lethal signals (Galluzzi et al., 2012). In contrast, the intrinsic apoptotic pathway is triggered by internal stress (starvation, oxidative stress, free radical damage, cytosolic calcium overload or cellular dysfunction), with activation of caspase-9 and decrease in mitochondrial transmembrane potential, culminating with cytochrome *c* release into the cytosol. Both death signaling pathways lead to activation of the executioner caspase-3 but intercommunication between both pathological settings might occur through cleavage of B-cell lymphoma 2 (Bcl-2) interacting domain (Bid), forming truncated Bid (t-Bid), which later promotes mitochondrial cytochrome *c* release and caspase-9 activation (Figure 6) (Ghavami et al., 2014).

Programmed cell death is crucial for normal neural development and physiologic aging, playing a key role in the construction of an efficient neuronal network. However, under pathologic conditions, it is also co-responsible for the loss of neurons associated with neurodegenerative disorders (Tendi et al., 2010). The main molecular components of the apoptotic program in neurons include caspases and members of the Bcl-2 family proteins. Thus, after an insult, release of apoptotic regulators Bax and Bak from complexes with anti-apoptotic Bcl-2 molecules, lead to their insertion into outer mitochondrial membrane contributing to cytochrome *c* release (Figure 6) (Ghavami et al., 2014).

Activation of apoptotic signaling platforms in FAP have been demonstrated by evidence of DNA fragmentation, increased levels of caspase-3 (Sousa et al., 2001b), Bax, caspase-8 and overactivation of Fas death receptor (Macedo et al., 2007) in tissues from FAP patients.

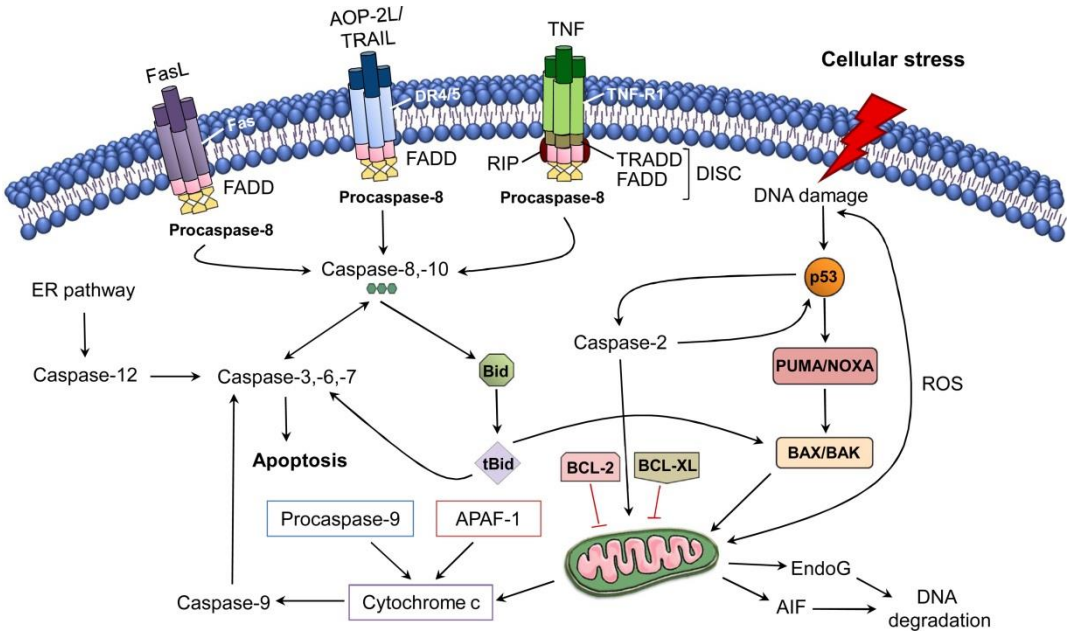

Figure 6 – Schematic representation of apoptotic platforms. Apoptosis might be triggered by binding of external stress ligands (FasL, TNF-related apoptosis-inducing ligand (APO-2L/TRAIL), TNF-α) to cell surface death receptors (Fas, DR4, DR5, TNF-R1). The intrinsic apoptotic pathway can be activated by p53 upon DNA damage, following exposure to cellular stress. A cross-talk between the intrinsic and extrinsic pathways can occur by cleavage of Bid to form tBid, by caspase-8, which is a strong activator of the mitochondrial apoptotic pathway (from Ghavami et al., 2014).

Together with the ER, mitochondria constitute the major storage compartment for intracellular calcium ions (Galluzzi et al., 2012). Calcium might lead to cell death by inducing mitochondrial dysfunction and release of cytochrome *c*. Once this molecule has been released into cytosol, it is able to interact with the apoptotic protease activating factor 1 (Apaf-1) for the subsequent recruitment of pro-caspase-9 into the apoptosome. Thus, formation of apoptosome leads to an amplificatory loop for caspase-9 activation and induction of apoptosis (Ghavami et al., 2014). Until some years ago, there was no evidence for an important role of mitochondria in FAP, since levels of both Bcl-2 and Apaf-1 were not altered in tissues with TTR deposition (Macedo et al., 2007). However, recently, mitochondrial proteins involved in cell energetics were found differentially represented in abdominal white adipose tissue from patients with TTR amyloidosis. By

proteomic analysis, ATP synthase subunits α and β were found downregulated in patients, which lead authors to hypothesize that impairment in mitochondrial function and energy production might play a key role in TTR-triggered cardiomyopathy (Brambilla et al., 2013). Mitochondria constitute the most prominent source of ATP and play an additional critical role in autophagy. Defects in the autophagic machinery or mitochondrial dynamics might play a pathological role in cancer or in neurodegenerative disorders, as neurons are among the most energy-consuming cell types (Galluzzi et al., 2012); however, the role of autophagy in FAP is yet to be clarified.

Heat shock response

Molecular chaperones are proteins that assist the folding and the assembly of other macromolecular structures, preventing incorrect alterations and aggregation. Many chaperones are heat shock proteins (Hsps), that is, proteins expressed in response to elevated temperatures, ischemic injury, oxidative or other cellular stresses, constitutively and inducibly expressed in the nervous system (Richter et al., 2010). The heat shock response is primarily regulated by the transcription factor Hsf-1. In resting cells, Hsf-1 is associated with Hsp-90 and Hsp-70 in the cytoplasm. Upon stress, these Hsps dissociate from the Hsf-1, allowing for its phosphorylation and nucleus translocation, where it binds to the promoter of several Hsp genes, mediating their transcription (Benarroch, 2011). There is increasing evidence that Hsps could be crucial modulators of neurotoxicity in Alzheimer's, Parkinson's and Huntington's diseases. Likewise, colocalization between molecular chaperones Hsp-70 or Hsp-27 with amyloid fibrils has been detected in all these neurodegenerative disorders, indicating an inadequate refold and degradation of the amyloid species or representing chaperone loss of function (Benarroch, 2011). Substantial data indicate heat shock response activation also in FAP. Therefore, increased levels of Hsp-70, Hsp-27 and Hsf-1 were noticed in salivary glands and nerve biopsies from FAP patients (Santos et al., 2008). Consistent with this view, Santos and coworkers demonstrated that the lack of Hsf-1 induced an extensive and earlier mouse phenotype when compared with other models of FAP (Santos et al., 2010b). In addition, non-fibrillar TTR deposition in the PNS and ANS was achieved, for the first time in an animal model, further reinforcing the role of the heat shock response in the modulation of TTR burden. Subsequent studies raised the importance of the heat shock response in the pathological mechanisms taking place in FAP, namely by the demonstration of increased expression of αB-crystallin and clusterin in tissues from FAP patients and mouse models, most likely triggered by the deposition of TTR aggregates (Magalhães et al., 2010; Magalhães and Saraiva, 2011).

Extracellular matrix remodeling

The extracellular matrix (ECM) is one of the most important regulators of cellular and tissue homeostasis. Dynamic remodeling of the ECM is essential for development, wound healing, cell proliferation, adhesion, migration and cell differentiation (Lu et al., 2011). Despite multiple regulatory mechanisms, sustained dysregulation of the ECM dynamics can result in life-threatening pathological conditions, such as Alzheimer's disease or cancer (Lu et al., 2011; Mizoguchi et al., 2011). Excessive ECM dynamics is also a feature of FAP. Through microarray analysis of salivary glands from FAP patients, increased expression of ECM related genes was noticed, namely biglycan, neutrophil gelatinase-associated lipocalin (NGAL) and matrix metalloproteinase-9 (MMP-9) (Sousa et al., 2005). Interestingly, although MMP-9 has the ability to degrade TTR aggregates and fibrils *in vitro*, authors observed that in the presence of SAP, TTR fibrils become resistant to MMP-9 proteolysis. Later on, these results were corroborated in an FAP mouse model being biglycan overexpression already present in the preliminary stages of disease while NGAL, MMP-9, tissue inhibitor of metalloproteinase 1 (TIMP-1) and also chondroitin sulfate, increased only in amyloid laden tissues (Cardoso et al., 2008). Histological examination also revealed increased expression of laminin, fibronectin, collagen type IV and heparan sulfate in close association with amyloid fibrils deposition in cardiomyocytes (Misumi et al., 2009; Noborn et al., 2011). Thus, the excessive or uncontrolled remodeling of the ECM observed in FAP disease, might probably contribute to neurodegeneration.

Inflammation and oxidative stress

Neuroinflammation is a protective immune response involving host cells, blood vessels, proteins and other mediators, intending elimination of the initial cause of injury, for cell repair. When neuroinflammation is a long-standing and self-perpetuating response, persisting long after the initial insult, results in a sustained release of pro-inflammatory mediators, increased oxidative and nitrosative stress. The sustained release of cytokines and chemokines works to perpetuate the inflammatory cycle, leading to a positive feedback loop. Thus, rather than serving as a protective response, chronic neuroinflammation is most often detrimental and damaging to the nervous system (Frank-Cannon et al., 2009). Neurodegenerative disorders, including multiple sclerosis, Alzheimer's, Parkinson's and Huntington's diseases have been associated with chronic neuroinflammation and elevated levels of pro-inflammatory cytokines. Neuropathological studies indicate that neuroinflammation is not a simple response to an already existing pathology but may begin prior to significant loss of neuronal populations, modifying

disease progression (Rogers, 1995). In this way, activation of the inflammatory response was also observed in preliminary stages of FAP with upregulation of TNF-α, interleukin-1β (IL-1β) and macrophage-colony stimulating factor, in sural nerve biopsies from asymptomatic carriers (Sousa et al., 2001a; Sousa et al., 2001b). Cytokine-driven neuroinflammation, occurring in earlier stages of disease indicate that TTR aggregates exert a neuronal pro-inflammatory response; however, if an inflammatory stimulus is also able to trigger TTR deposition, remains unanswered. With disease progress, levels of neuroinflammation increased, with *IL-1β* mRNA transcripts found mainly in endoneurial axons (Sousa et al., 2001b). The proposed mechanism underlying these observations was the binding of TTR species to RAGE with activation of extracellular signal-regulated kinases (ERK) 1/2, nuclear factor κB (NF-κB) translocation and consequent transcription of pro-inflammatory proteins (Sousa et al., 2000b; Sousa et al., 2001b; Monteiro et al., 2006). NF-κB is a transcription factor essential for amplification, maintenance and tuning down of inflammatory responses (Ben-Neriah and Karin, 2011). Under resting conditions, NF-κB dimers are bound to inhibitory IκBα (nuclear factor of kappa light polypeptide gene enhancer in B-cells inhibitor, alpha) proteins in the cytoplasm. Several extracellular signals might activate the IκB kinase which phosphorylates IκBα, targeting this protein for ubiquitination and proteasome degradation. Consequently, NF-κB is released and translocates into the nucleus contributing for the transcription of several genes, self-perpetuating the overactivated inflammatory response (Oeckinghaus et al., 2011). In support of this idea, p50, one of the NF-κB subunits was found upregulated, with a predominant nucleus distribution, in tissues from FAP patients (Sousa et al., 2000b).

To explore the eventual balance between pro and anti-inflammatory events in FAP, histological analysis for the interleukin-10 (IL-10) was performed in human sural nerve biopsies. Surprisingly, expression of IL-10 was noticed only in advanced cases of disease, suggesting that activation of anti-inflammatory mechanisms might occur to late, being not sufficient to control inflammation (Sousa et al., 2005). A striking feature of FAP is the absence of an immune/inflammatory infiltrate, despite the production of pro-inflammatory cytokines by axons, indicating that other mechanisms might be operating to prevent recruitment of effector cells (Misu et al., 1999; Sousa et al., 2001b). In line with this observation, a non-optimal activation of Schwann cells was noted, since upon the injury stimulus provided by TTR aggregates, these cells had no ability to express chemokines and neurotrophic factors, important for tissue regeneration (Sousa et al., 2001b). Thus, this lack of Schwann cells responsiveness may contribute for neuronal dysfunction present in FAP.

Very recently, a novel diagnostic technique was developed, allowing *in vivo* detection of nerve injury. Hence, by magnetic resonance neurography, lower limb nerve injury could

be detected and quantified *in vivo* on microstructural level in symptomatic FAP patients, and also in yet asymptomatic gene carriers, in whom imaging detection precedes clinical and electrophysiological manifestation (Kollmer et al., 2014). Despite the need for deeply interpretation of imaging signals, this new imaging data would be valuable for the evaluation of the effectiveness of novel therapeutic agents on halting disease progression and may have future implications also for the diagnostic of other distally-symmetric polyneuropathies.

Another link between inflammation and TTR amyloidosis comes from studies in a mouse model resembling human senile systemic amyloidosis (SSA). Through a microarray screening, it was found that, even before TTR starts to accumulate in the heart, cardiac gene transcription differs from that of WT littermates, primarily in the expression of a large number of genes associated with inflammation and immune response, raising the hypothesis that TTR burden might be triggered in response to multiple subclinical inflammatory traumas and that a robust immune inflammatory transcriptional profile might precede TTR deposition in tissues (Buxbaum et al., 2012).

The neuronal cell oxidative stress response has an intense role regarding neurodegeneration. Though, oxygen is imperative for life, imbalanced metabolism and excess reactive oxygen and nitrogen species generation is believed to be involved in the pathogenesis of several neurodegenerative disorders. In this way, free radical attack on neural cells contributes for protein or DNA injury, inflammation, tissue damage and subsequent cellular apoptosis (Uttara et al., 2009). The involvement of oxidative stress also in FAP has been reported. First, markers of lipid peroxidation, such as hydroxynonenal (HNE) and thiobarbituric acid reactive substances (TBARS) were found increased in human colon biopsy samples of FAP patients (Ando et al., 1997). A subsequent study demonstrates the increased expression of inducible form of nitric oxide synthase (iNOS) and 3-nitrotyrosine, in nerves from patients and asymptomatic carriers (Sousa et al., 2001b). It is known that reactive nitrogen species such as nitric oxide can react with superoxide to produce peroxynitrite, a powerful oxidant that in turn nitrates thyrosine originating 3-nitrotyrosine (Melo et al., 2011). Therefore, 3-nitrotyrosine is a potent biomarker for nitrosative stress. Other markers of oxidative stress, like 8-hydroxydeoxyguanosine and glutaredoxin 1 were observed increasingly expressed in tissues from FAP patients and mouse models of disease (Macedo et al., 2007) further reinforcing the role of oxidative stress in the pathomechanisms of this disease.

Overall, a spectrum of environmental cues, mitochondrial dysfunction, ER stress, calcium dysregulation, inflammation, cell death and oxidative stress are known to evolve and form as a result of accumulation of aberrant misfolded proteins (Figure 7). Understanding the

relationships between disease mechanisms is critical for the development of therapeutic modalities to combat the progress of neurodegenerative disorders.

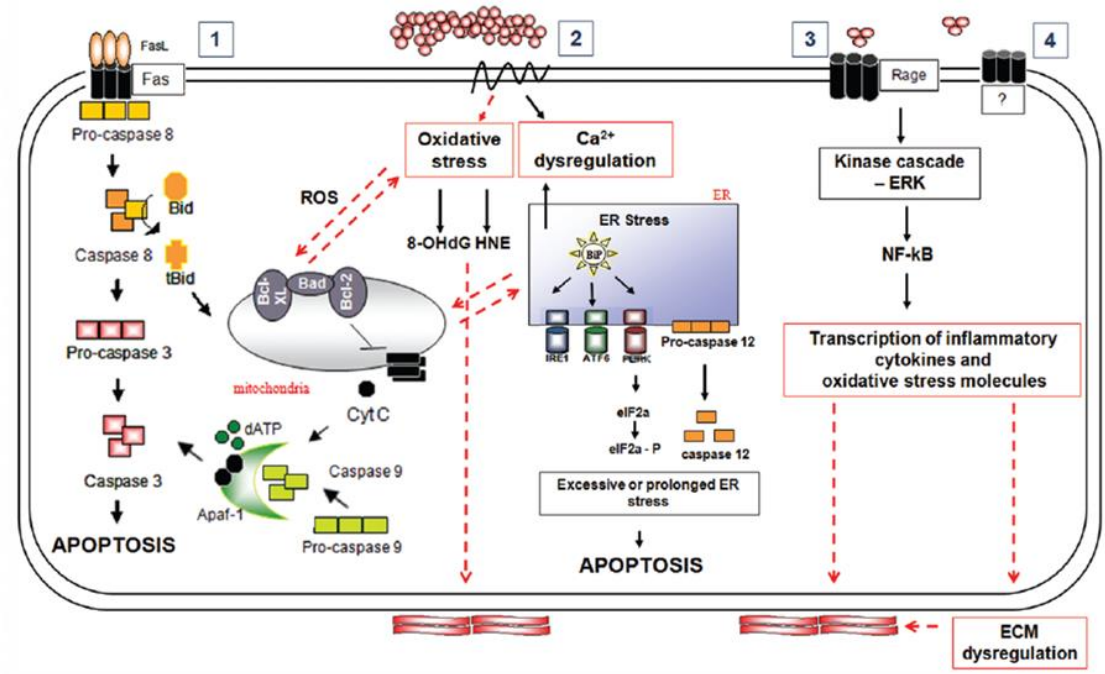

Figure 7 – Schematic representation of neurotoxicity induced by TTR aggregates. Extracellular non-fibrillar TTR aggregates interact with the cell membrane and with membrane receptors such as Fas or RAGE, ultimately leading to neurodegeneration. Calcium dysregulation, ER stress, apoptosis, activation of kinase cascades and NF-κB, with concomitant transcription of pro-inflammatory cytokines and oxidative stress molecules, are central networks in the molecular mechanisms underlying FAP disease. Moreover, newly formed oxidized species and inflammatory mediators might contribute to extracellular matrix components dysregulation and fibril formation. Additionally, other possible receptors may also be involved, particularly membrane receptors, subject that needs further clarification (from Saraiva et al., 2012).

Therapies for Familial Amyloidotic Polyneuropathy

FAP is a life-threatening disorder and few treatment options are available yet. Recent progress has modified prognosis and management of TTR amyloidosis by targeting different disease aspects, such as protein synthesis, stabilization, inhibition of TTR aggregation and fibril disruption by selective molecules (Figure 8). We next describe the main strategies adopted over the years to prevent or delay FAP pathology.

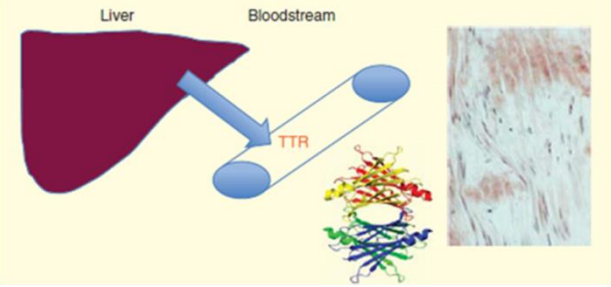

Target	Hepatocytes	Circulating TTR tetramer	Tissular amyloid deposits	Damaged tissue
Therapy	Liver transplantation	Tafamidis	Doxycycline-TUDCA	TUDCA
	ASOS	Diflunisal	Anti-SAP antibodies	Carvedilol
	siRNA	EGCG	Immunization	
	Gene therapy with AAV vectors	Curcumin	EGCG	
		Cyclodextrin	Curcumin	
		Molecular tweezers		

Figure 8 – Therapeutical approaches put forward so far for FAP (adapted from Adams et al., 2014).

Liver transplantation

Liver transplantation is so far the best therapeutic strategy for FAP. Liver transplant removes the main source of mutated TTR, slowing disease progression. However, it does not prevent development of arrhythmia and, in some cases, neuropathy might progress even after surgery. This suggests continued secretion of variant TTR from the choroid plexus, which may reach the endoneurium through the subarachnoid space (Ando et al., 2004; Planté-Bordeneuve and Said, 2011). In addition, preformed amyloid deposits might

act as a nidus enhancing further polymerization (Ueda and Ando, 2014). Nevertheless, improvement of the autonomic function with general well-being has been reported.
Very recent findings indicate that CNS clinical involvement occurs in TTR V30M patients, regardless of liver transplantation. In this way, focal neurological episodes arise due to progression of TTR deposition from the meninges and its vessels towards meningocortical vessels and the superficial brain parenchyma; suggesting that novel disease modifying therapies should consider brain TTR as a target (Maia et al., 2015).
Explanted FAP livers can be grafted into selected patients in domino liver transplantation. However, symptomatic neuropathy seems to occur after about 5 years (Stangou et al., 2005).
The best outcomes achieved with liver transplant occur when the procedure is done early in the course of FAP (de Carvalho et al., 2002). Thus, patients with severe polyneuropathy, poor nutritional status or autonomic dysfunction are not eligible for the procedure (Planté-Bordeneuve and Said, 2011). An additional number of limitations such as shortage of donors, surgery requirement, cost of the procedure, lifelong administration with immunosuppressants and lack of responsiveness regarding ocular or CNS complications put forward the development of novel alternative less-invasive therapeutic strategies for this disease (Ando, 2005).

Gene therapy

Gene therapy has arisen as a promising therapeutic strategy for FAP by preventing the transfer of genetic information from DNA to protein. It is a new non-invasive method preventing production of both mutant and wild-type *TTR*, thus reducing plasma TTR levels in a sustained fashion. The theory is that blocking *TTR* production by the liver at the translational level will lead to less non-fibrillar TTR species and amyloid deposition, halting disease progression (Hanna, 2014).
Antisense oligonucleotides (ASOs) are short synthetic single-stranded nucleotides, selectively binding to the target mRNA, thereby preventing production of the disease associated protein (Malik and Roy, 2011). Isis Pharmaceuticals has developed an ASO targeting *TTR* mRNA, designated ISIS-TTR_{RX}, preclinically characterized in transgenic mice expressing the human TTR I84S variant. One month treatment resulted in a significant decrease in both TTR liver expression and circulating plasma levels (Benson et al., 2006). Since ISIS-TTR_{RX} was found to be well tolerated, initiation of clinical trials was supported. Preliminary results demonstrate that after a month treatment, up to a 90% reduction in TTR levels was achieved in a study with healthy volunteers (Ackermann et al., 2012). Clinical trials with FAP patients are currently ongoing (Adams et al., 2014).

Another approach using interference RNA (RNAi) has been extensively studied for FAP, which take advantage of small interfering RNAs (siRNA) that mediate cleavage of target mRNA, thus silencing gene expression. A lipid nanoparticle formulation was developed by Alnylam Pharmaceuticals (ALN-TTR02) targeting a conserved sequence in mutant and non-mutant *TTR* mRNA, expressed specifically by the liver. In this way, the nanoparticle efficiently delivers the siRNA to hepatocytes where they are taken up by LDL receptors and released into the cytoplasm (Hanna, 2014). Animal models, healthy volunteers and FAP patients were already treated with ALN-TTR02 that was generally safe and well tolerated. In addition, sustained suppression of TTR plasma levels was observed, establishing proof of concept for an RNAi therapeutic tool, with Phase III clinical trials currently ongoing (Alvarez et al., 2010; Coelho et al., 2013; Adams et al., 2014). For intravenous injections of ALN-TTR02, premedication with steroids and anti-histaminic is necessary; therefore a formulation to be given subcutaneously has been tested, showing similar significant decrease in TTR plasma levels (Adams et al., 2014; Hannan et al., 2014).

These promising future therapeutic approaches can be extended to all forms of TTR amyloidosis since they are designed to prevent the expression of all *TTR* variants.

Based on previous results showing that incorporation of one subunit of TTR T119M into a predominantly V30M tetramer strongly stabilized the mixed tetramer against dissociation (Hammarström et al., 2001), a novel gene therapy approach using AAV vectors to deliver the TTR T119M variant into the liver of transgenic mice carrying the TTR V30M mutation, was very recently tested. Collectively, the authors described that somatic gene delivery of TTR T119M significantly reduced non-fibrillar TTR V30M deposition, BiP and MMP-9 levels in the gastrointestinal tract of treated animals, suggesting the possible use of this gene therapy approach in a prophylactic way to prevent FAP pathology (Batista et al., 2014).

Stabilization of transthyretin tetramers

It is widely accepted that dissociation of the TTR tetramer into compact non-native monomers, with low conformational stability, is the rate-limiting step for the process of amyloid fibril formation. Miroy and coworkers have shown that binding of T_4 to TTR tetramer stabilizes the native state over dissociation, thus inhibiting amyloidogenesis *in vitro* (Miroy et al., 1996). Because more than 99% of the T_4 binding sites are unoccupied, the strategy of administering small molecules that binds in the central hydrophobic channel to stabilize the native tetrameric structure, has been developed (Sekejima et al.,

2008). Several small molecules stabilizing TTR are now available but thus far only two drugs have come to the forefront to clinical development, namely diflunisal and tafamidis.
Diflunisal is a non-steroidal anti-inflammatory drug, which binds to T_4 binding sites, stabilizing serum TTR in amyloidotic patients (Tojo et al., 2006). It is being relatively well tolerated and in an open label study, some patients show amelioration of autonomic symptoms (Takahashi et al., 2014).
Tafamidis is another pharmacological chaperone, selectively binding to T_4 pocket for TTR stabilization. Safety was overall good with the most side effects being urinary tract infections and diarrhea. This potent stabilizer was approved in Europe and Japan for the treatment of FAP patients in the early stage of disease (Ueda and Ando, 2014). Results from clinical trials demonstrate that patients treated with tafamidis showed less neurological deterioration and slower disease progression (Bulawa et al., 2012; Coelho et al., 2012).
A number of structurally different small molecules that bind to TTR, increasing its stability have also been tested, such as epigallocatechin-3-gallate (EGCG) or curcumin. Similarly to diflunisal and tafamidis, curcumin interacts with TTR in the T_4 binding pocket, while EGCG binds at the protein surface. It was found that curcumin strongly suppressed TTR amyloid fibril formation by generating small "off-pathway" aggregates, while EGCG maintained most of the protein in a non-aggregated soluble form (Ferreira et al., 2009; Ferreira et al., 2011). Animal testing provide strong evidence for the benefic role of these selected polyphenols (Ferreira et al., 2012; Ferreira et al., 2013); however, clinical trials with FAP patients are still awaited.
Cyclodextrins are cyclic oligosaccharides composed of glucose units and one of its derivatives showed potent stabilization of TTR conformation by interacting with protein hydrophobic amino acids, especially tryptophan, in turn, suppressing TTR amyloid fibril formation (Jono et al., 2011). Additionally, a lys-specific molecular tweezer CLR01 has been shown to inhibit TTR aggregation and toxicity by interfering with hydrophobic and electrostatic interactions, redirecting TTR aggregation into the formation of innocuous assemblies (Sinha et al., 2011). When tested in a mouse model of FAP, CLR01 showed positive therapeutic effects thus being a promising disease-modifying agent for TTR amyloidosis (Ferreira et al., 2014).

Fibrils disrupters and amyloid clearance

Once TTR amyloid fibrils have deposited in the extracellular space, they are resistant to degradation and although they are currently not seen as the primary cause of FAP, it is known that amyloid deposits can induce organ dysfunction (Pepys, 2001). Consequently,

other therapeutic strategies for FAP involve molecules acting as fibril disruptors for the modulation of cellular stress and toxicity.

4'-iodo-4'-deoxydoxorubicin (IDOX) was described as an agent that could efficiently bind to TTR amyloid fibrils, disaggregating them into non-toxic species (Merlini et al., 1995; Cardoso et al., 2003). Nevertheless, since the use of this drug is associated with cardiotoxicity, less toxic compounds, such as doxycycline, have been evaluated (Cardoso et al., 2003). *In vitro* and *in vivo* studies showed that doxycycline was able to disaggregate TTR amyloid fibrils and to decrease biomarkers associated with the pathology (Cardoso et al., 2003; Cardoso and Saraiva, 2006), thus being a potential useful drug for FAP. Very recently, novel nanoconjugates based on doxycycline exhibited greater potential towards TTR fibril disaggregation being a promising therapeutics for advanced stages of disease (Conejos-Sánchez et al., 2015).

In addition, the above mentioned natural compounds EGCG and curcumin have also showed potential for TTR fibril disruption by converting existing fibrils into non-fibril conformers (Ferreira et al., 2009; Ferreira et al., 2011).

Since no inflammatory infiltrate is usually found near to amyloid deposits (Sousa et al., 2001b), immune therapies for the treatment of FAP may arise. By immunizing FAP transgenic mice with the TTR variant Y78F, Terazaki and coworkers observed reduction of both fibrillar and non-fibrillar TTR deposition within mice intestine, together with infiltration of lymphocytes and macrophages at sites of TTR deposition (Terazaki et al., 2006). These results indicate that immune therapies might be major candidates for the treatment of TTR amyloidosis.

Serum amyloid P component (SAP) is a universal element of amyloid fibrils, retarding their breakdown and clearance (Pepys, 2001). In this way, SAP has been proposed as a possible target for amyloidosis therapeutics (Pepys et al., 2002). Data from animal models receiving anti-human-SAP antibodies indicate that antibody mediate removal of this component, facilitating endogenous clearance of amyloid fibrils, without apparent adverse side effects (Bodin et al., 2010). This treatment seems to be clinically reasonable, therefore clinical trials with patients carrying systemic amyloidosis will be carried out soon (Hanna, 2014).

Anti-oxidant and anti-apoptotic treatments

Oxidative stress and apoptosis have been implicated in the pathological mechanisms underlying FAP disease (Saraiva et al., 2012). Therefore, anti-oxidant and anti-apoptotic therapy was attempted for the treatment of FAP by administrating tauroursodeoxhycholic

acid (TUDCA), a natural compound derived from biliary acids, to a mouse model of disease. Macedo and colleagues demonstrate that TUDCA decreases toxic TTR non-fibrillar aggregates deposition, as well as several disease associated biomarkers, but without a significant effect on mature fibrils (Macedo et al., 2008). A subsequent study combined the action of doxycycline with TUDCA for preclinical analysis (Cardoso et al., 2010). The authors showed a synergistic effect on lowering TTR deposits and associated biomarkers than either of the compounds alone. Based on this animal data, a Phase II open label study was conducted over a 12-month period. Preliminary results indicate that the combination of doxycycline with TUDCA stabilizes disease progression for at least 1 year (Obici et al., 2012).

In a different study, Macedo and coworkers postulated a possible therapeutical application of another anti-oxidative compound, carvedilol, a lipophilic non-selective β-adrenoreceptor antagonist with strong anti-oxidative effect, commonly used in different cardiovascular settings. Similarly as TUDCA, carvedilol was shown to decrease non-fibrillar TTR deposition and disease associated biomarkers namely, HNE, 8-OHdG and markers of ER stress as BiP and peIF2α (Macedo et al., 2010).

Hence, non-amyloid targets modulating the molecular pathways involved in aggregate-induced oxidative stress, cell death or inflammatory response, might be promising prophylactic strategies for FAP. Given the extensive number of proposed drugs, most likely the future therapy for FAP will encompass by a combinatorial approach.

Peripheral nerve regeneration

Nerve injury is a complex multi-cellular response that might be triggered by traumatic, inflammatory or autoimmune stimulus. In 1850, Augustus Waller described the disintegration of the frog nerves after axotomy, phenomena that have been collectively termed Wallerian degeneration (Waller, 1850). Decades later, Ramon y Cajal confirmed Waller observations and provided new histological insights, namely regarding axonal degeneration, leukocyte infiltration, Schwann cell responses and their importance for the regenerative process (Ramon y Cajal and May, 1928).

In practical terms, nerve TTR aggregates and amyloid fibrils deposition may behave similarly as an injury stimulus by compressing nerve fibers, ultimately leading to neurodegeneration. The major issues concerning Wallerian degeneration will be next described.

Wallerian degeneration

Wallerian degeneration comprises the rapid disintegration of the distal axons and the subsequent influx of immune cells, allowing the clearance of resulting debris and the formation of a favorable environment for regeneration to occur (Figure 9). Upon injury, axonal membrane of the distal stump undergoes beading and swelling (Gaudet et al., 2011). Within minutes after damage to the axonal membrane, calcium influx from extracellular and intracellular stores activates calpain, promoting local protein synthesis, increased cAMP levels and cytoskeleton rearrangements (George et al., 1995; Tedeschi and Bradke, 2013). Calcium entry into axoplasm and activation of the ubiquitin-proteasome system are required steps for granular disintegration of the cytoskeleton, characterized by the disassembly of microtubules and filaments that ultimately lead to axonal fragmentation and degradation. These processes are closely regulated by p38 mitogen-activated protein kinase and caspase-3, the former involved in axon degeneration by trophic factors withdrawal (Simon et al., 2012; Tedeschi and Bradke, 2013). Simultaneously, the blood-nerve barrier is compromised along the distal nerve portion, increasing perineurial permeability with consequent entry of blood-borne factors and inflammatory cells, crucial for tissue repair (Mizisin and Weerasuriya, 2011). Nerve degeneration and regenerative ability of the PNS are thus active processes, dependent on extrinsic and intrinsic factors. Besides the immune response, the role played by Schwann cells comprises the extrinsic category, while intrinsic factors include the transcriptional profile of the neuron cell body (Scheib and Höke, 2013).

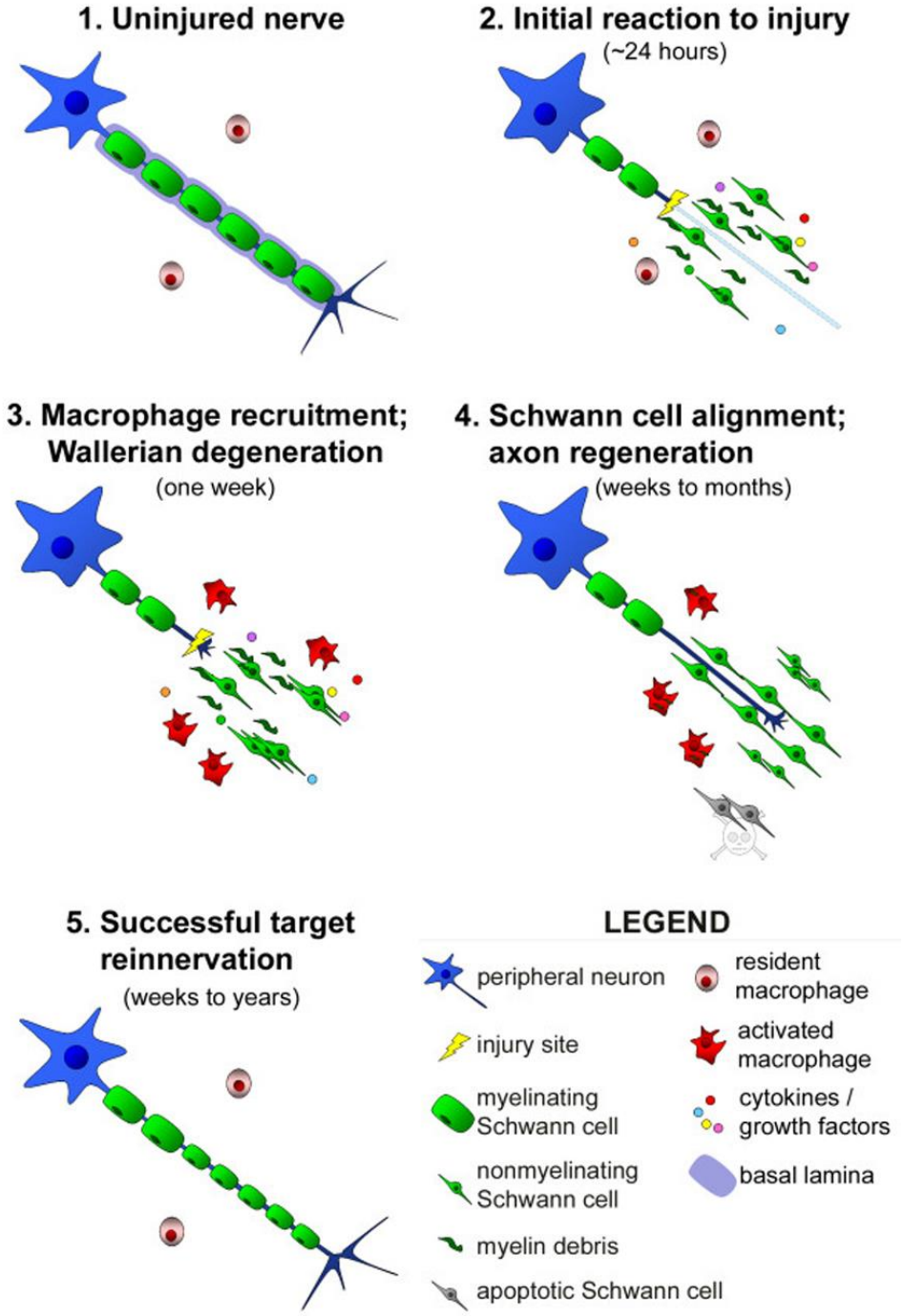

Figure 9 – Wallerian degeneration after peripheral nerve injury. A schematic representation of a single axon is shown. **1.** Normal nerve fiber maintaining synaptic contact with target cells. **2.** Injury results in distal fragmentation of axon and myelin. Schwann cells dedifferentiate with cytokine and growth factors production. **3.** Following, hematogenous macrophages are recruited contributing for clearance of myelin debris. **4.** Injured axons formed the growth cone and begin to regenerate along the bands of Büngner, originated from the Schwann cell alignment. **5.** Finally, successful regeneration and axon connection with peripheral targets takes place (from Gaudet et al., 2011).

The role of Schwann cells in Wallerian degeneration

Schwann cells arise from the neural crest during development and are the glial cells of the PNS (Figure 10). They constitute 90% of nucleated cells within the peripheral nerve and play crucial roles regarding nerve physiology, more precisely, trophic support to neurons and myelin insulation (Jessen and Mirsky, 2005; Gaudet et al., 2011). These cells can be divided in myelinating or ensheating Schwann cells. Myelinating Schwann cells associate to a single large caliber axon and form compact multi-layer myelin lamellae, providing insulation, pivotal for fast nerve conduction (Figure 10). In contrast, ensheating Schwann cells have multiple unmyelinated axonal segments embedded within grooves of its cytoplasmatic processes and plasma membrane, a structure termed Remak bundle (Figure 10).

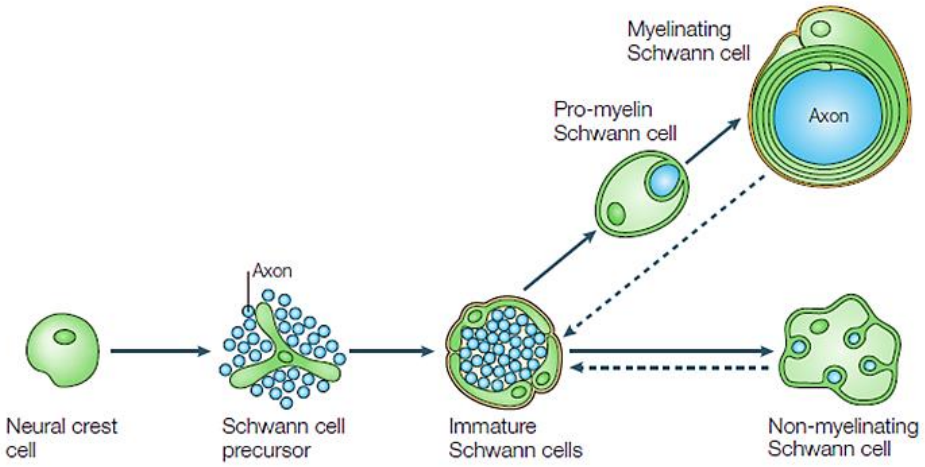

Figure 10 – Schematic illustration of the developmental transitions and Schwann cell organization in peripheral nerves. The embryonic phase of Schwann cell development involves three transient cell populations, namely migrating neural crest cells, Schwann cell precursors and immature Schwann cells. Myelination occurs only in Schwann cells that envelop large diameter axons; Schwann cells that wrap several small diameter axons, forming a Remak bundle, progress to become mature non-myelinating cells (from Jessen and Mirsky, 2005).

Soon after nerve damage, Schwann cells of the distal stump have the ability to revert back to a nondifferentiated, proliferative phenotype. This dedifferentiation stage involves transcriptional changes with downregulation of genes related to myelination, such as myelin-associated glycoprotein, with concomitant increased expression of trophic factors and regeneration-associated genes (like BDNF, NGF or growth associated protein 43 (GAP-43)) (Jessen and Mirsky, 2008; Gaudet et al., 2011). In addition, danger-associated molecular patterns (DAMPs), released from early axonal degeneration, induce toll-like receptor (TLR) signaling, mediated by myeloid differentiation primary response gene 88

(Myd88), leading to the breakdown of myelin and recruitment of immune cells (Boivin et al., 2007). Schwann cells express a variety of TLRs, including TLR2, TLR4, TLR7, TLR9 and TLR1 (Figure 11), the former upregulated after injury, making them the PNS sentinel cells (Goethals et al., 2010). When intracellular cascades are activated with nuclear translocation of NF-κB, Schwann cells are induced to express a variety of cytokines important for effective Wallerian degeneration, such as TNF-α, IL-6, IL-1α and β. TNF-α and IL-1 peaked at day 1 post-injury, before entry of inflammatory cells, and elicit production of chemokine C-C motif ligand 2 (CCL2), stressing the idea of their involvement in immune cell recruitment (Figure 11). Expression and activation of phospholipase A_2 (PLA_2) is also triggered by these pro-inflammatory cytokines and is a required step for the initiation of myelin breakdown. Furthermore, TNF-α and IL-1β prompt the production of MMP-9, necessary for the collapse of the blood-nerve barrier, stimulation of initial myelin disruption and monocyte migration (Defrancesco-Lisowitz et al., 2014; Brosius Lutz and Barres, 2014). Cytokines produced by Schwann cells might stimulate fibroblasts which in turn release IL-6 and granulocyte macrophage colony stimulating factor (GM-CSF), important for galectin-3 production by macrophages and Schwann cells (Saada et al., 1996) (Figure 12). Collectively, the fine-tune inflammatory response will be amplified with the ultimate goal of immune cell chemotaxis.

Upon myelin breakdown, Schwann cells begin to proliferate and align along their basal lamina to form bands of Büngner, which provide support and guide regenerating sprouts for axon growth (Scheib and Höke, 2013). The aligned Schwann cells induce nerve regeneration by secreting growth factors, their receptors and cell adhesion molecules, as laminin, one of the most prevalent ECM components in the PNS, essential for axon growth (Gaudet et al., 2011).

The best characterized axonal signals prompting phenotypic changes in Schwann cells, upon injury, are neuregulin-1 and c-Jun (Figure 12). In healthy nerves, neuregulin-1 induces proliferation and myelin production via the ErbB family of receptors. Ablation of this molecule during Wallerian degeneration results in severe defects regarding remyelination. Therefore, neuregulin-1 has shown a key role in reparative processes after nerve injury and might be partially involved in Schwann cell phenotypic changes (Fricker et al., 2011). c-Jun is a transcription factor required for efficient axonal regeneration. Recently, Arthur-Farraj and coworkers demonstrate that c-Jun reprograms the Schwann cell transcriptional profile to generate a repair cell, looking forward correct reinnervation and functional recovery after nerve insult (Arthur-Farraj et al., 2012). Denervated Schwann cells are the major phagocytic cells during the first days following injury. Several findings report that Schwann cells are immune competent cells able to express both major histocompatibility complex (MHC) classes I and II, upon stimulation, and behave as

primary antigen-presenting cells (Ydens et al., 2013). Some studies have proven that these cells are effective presenters of self-antigen, as they can phagocyte and degrade myelin or extracellular debris (Lilje, 2002). In summary, dedifferentiated Schwann cells promote nerve repair by proliferating, phagocyting myelin debris and mounting an immune response, with secretion of trophic factors, cytokines and chemokines, crucial for the activation and chemotaxis of innate immune cells.

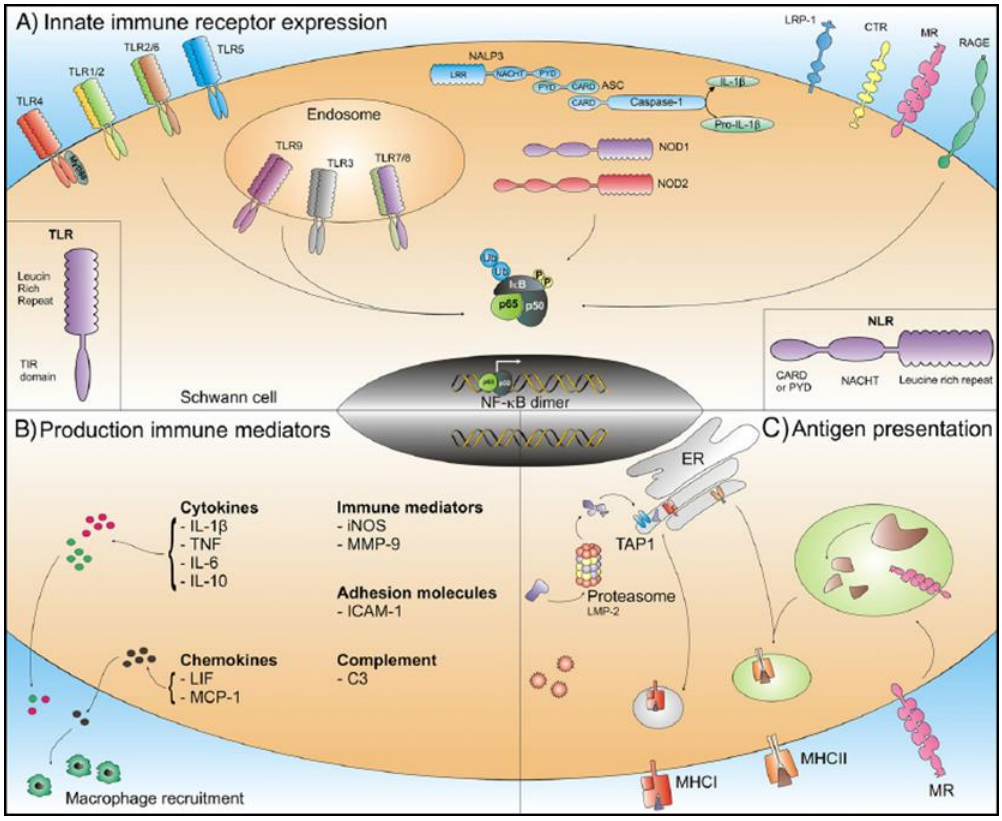

Figure 11 – Schematic representation of possible mechanisms elicited on Schwann cells after nerve insult. A) Despite expressing RAGE, low-density lipoprotein receptor-related protein-1 (LRP-1), C-type lectin and mannose receptors (CTR and MR, respectively), Schwann cells also express a broad range of TLR and NOD-like receptors, resulting in NF-κB activation upon injury. **B)** Dedifferentiated cells produce several cytokines, chemokines and other immune mediators, which further attract inflammatory cells. **C)** Schwann cells are immune competent cells since they have the ability to present antigen via the MHC type I and type II. Abbreviations not yet mentioned; CARD: caspase recruitment domain, ICAM: intercellular adhesion molecule, LIF: leukemia inhibitory factor, LMP-2: low molecular mass peptide-2, LRR: leucine rich repeat, MCP-1: monocyte chemoattractant protein-1 (also known as CCL2), NOD: nucleotide binding and oligomerization domain, PYD: pyrin domain, TAP1: antigen peptide transporter 1, TIR: Toll/interleukin receptor (from Ydens et al., 2013).

The immune cell response to peripheral nerve injury

Peripheral nerve injury is a complex response and involves multiple cell types. Whereas Schwann cells mediate myelin clearance in early stages of Wallerian degeneration, they are not the only important cell type in the distal nerve environment. Removal of myelin debris, growth factors production and remodeling of the ECM is also achieved by resident and recruited macrophages (Scheib and Höke, 2013). Resident endoneurial macrophages account for 2-9% of all cells in the uninjured nerve and express MHC molecules or complement receptor 3, essential for their functions regarding antigen presentation and surveillance (Mueller et al., 2003; Barrette et al., 2008). Evidence suggests that resident macrophages respond in the injured nerve before the accumulation of blood-derived monocytes, having an active phagocytic activity. In addition, together with Schwann cells, they produce cytokines and chemokines important for the recruitment of innate immune cells (Tofaris et al., 2002). Breakdown of the blood-nerve barrier allows the influx of serum components, like antibodies and complement, which then facilitate leucocyte recruitment and opsonize debris, enabling phagocytosis (Brück and Friede, 1990; Vargas et al., 2010). Neutrophils are the first innate immune cells to invade the injured tissue (Figure 12). They phagocyte debris and activate monocytes, having an important role regarding neuropathic pain (Austin and Moalem-Taylor, 2010; Gaudet et al., 2010).

By four days post-injury, large numbers of hematogenous monocytes begin to accumulate within the injured nerve, peaking between 7-14 days. Once in the tissue, monocytes differentiate into macrophages, which start to express cytokines and trophic factors, contributing for removal of inhibitory debris, ultimately aiding axon regeneration (Gaudet et al., 2010; Defrancesco-Lisowitz et al., 2014). Days or months after nerve damage, macrophages migrate through the basal lamina to nearby blood vessels or die by apoptosis (Kuhlmann et al., 2001).

Recently, studies on macrophage heterogeneity delineated this population into M1 (pro-inflammatory and cytotoxic) and M2 (anti-inflammatory and alternatively stimulated) stages of activation (Bastien and Lacroix, 2014). M1 macrophages are quickly recruited to injured nerves and are mostly involved in inflammation (releasing among others TNF-α, IL-1β and IL-6), proteolysis and phagocytosis. M2 macrophages are implicated in immune surveillance, tissue repair and wound healing, producing IL-10, arginase-1 (Arg-1) and several growth factors (Figure 12) (Ydens et al., 2012). M1 macrophages are present early after nerve insult but chemokine production by Schwann cells and resident macrophages, such as CCL2, drives macrophages towards an M2 phenotype, important for the control of inflammation (Sierra-Filardi et al., 2014). As a consequence, the levels of IL-10 start to increase, peaking at day 7 and remaining elevated through day 14 (Be'eri et

al., 1998). IL-10 activation gradually inhibits production of pro-inflammatory cytokines and downregulates expression of MMP-9 by macrophages, lowering leucocyte infiltration and myelin breakdown (Moore et al., 2001; Defrancesco-Lisowitz et al., 2014).

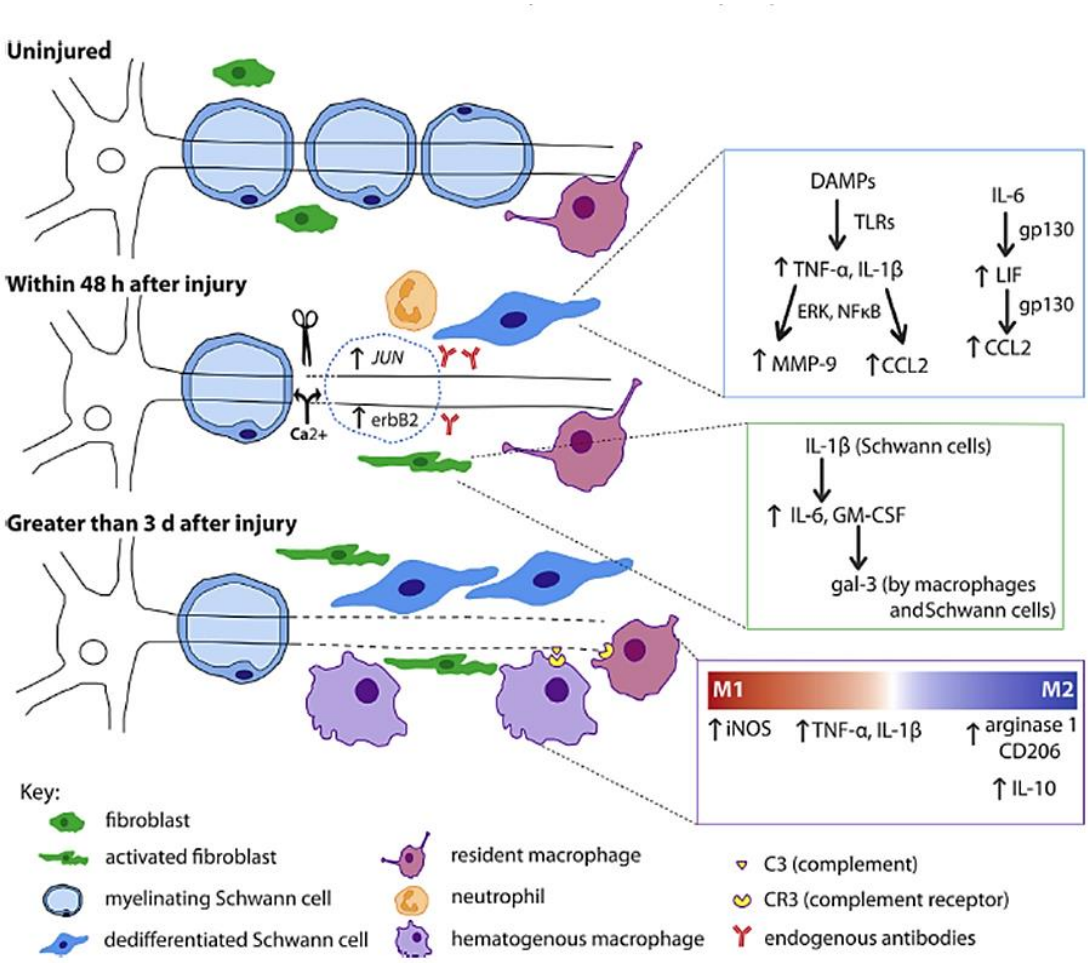

Figure 12 – Cellular types and intermediaries involved in Wallerian degeneration after nerve damage. Representative illustration denoting Schwann cell dedifferentiation consequent to calcium entry, axonal breakdown and upregulation of c-Jun and ErbB. Through TLR signaling, these cells produce pro-inflammatory cytokines and chemokines essential for the recruitment of innate immune cells. Fibroblasts also respond earlier with secretion of IL-6 and GM-CSF leading to galectin-3 expression by macrophages and Schwann cells, important for myelin phagocytosis. Neutrophils are the first innate cells to invade the peripheral nerve after injury. Hematogenous macrophages are recruited and enter the damaged tissue through the blood-nerve barrier disruption. Together with the resident macrophages, they can differentiate into M1 or M2 subtypes, with different cytokine profiles, and contribute for the clearance of myelin debris and nerve repair (from Defrancesco-Lisowitz et al., 2014).

The last phase of the immune response triggered after nerve injury is shaped by T lymphocytes which produce several pro or anti-inflammatory cytokines, modulating neuropathic pain behavior (Moalem et al., 2004).
Overall, these data suggests that the inflammatory response after nerve injury encompass a spectrum of activation stages that must be sensibly controlled, allowing for subsequent regeneration and repair.

Injury signaling to the cell body

Intrinsic and extrinsic cues are highly interconnected in the axon growth equation; for instance extrinsic signals are able to produce a multitude of changes in the neuronal cell body gene expression, following injury. This *de novo* synthesis of mRNAs and proteins mark a phenotypic switch characterized by a reduction in the machinery supporting synaptic transmission on behalf of axonal regeneration and survival (Defrancesco-Lisowitz et al., 2014). Upon injury, axons are depolarized due to an inversion in the calcium/sodium flux and this signal travels toward the cell body, stimulating local activation of protein synthesis (Bradke et al., 2012). When this calcium wave invades the ganglion soma, it triggers nuclear export of histone deacetylase 5 (HDAC5), leading to an increase in histone acetylation and further activation of the regenerative transcriptional program (Cho et al., 2013) (Figure 13). Then, newly synthesized molecules and structural components need to be shipped to the distant axon tip through anterograde transport (Figure 13). Besides axonal maintenance, anterograde transport is particularly relevant for axon supply with synaptic proteins, vesicles and organelles, especially mitochondria (Mar et al., 2014). Furthermore, the alteration of neuronal activity is dependent on axonal signaling that must be retrogradely transported to the cell soma. This aspect is achieved by the activation of adaptor proteins, such as dynactin, vimentin or importin, which facilitate the association of molecules with motor dynein for transport along cytoskeletal microtubules (Mar et al., 2014). Several injury signals locally activated are transported in a retrograde manner back to the cell body, like dual leucine kinase (DLK), ERK, signal transduction by the c-Jun N-terminal kinase (JNK) and signal transducer and activator of transcription 3 (STAT3) (Figure 13).
Recent observations highlight a dual role for DLK since this kinase might promote apoptosis or axon growth, depending on the neuron transcriptional program (Tedeschi and Bradke, 2013). Evidence with DLK null mice show that this molecule is likely involved in axon formation and neuronal migration and that it might regulate regeneration through influence on other injury driven molecules, such as STAT3 and JNK (Hirai et al., 2006; Shin et al., 2012). STAT3 is a positive injury signal contributing to axonal regeneration, the

expression of regeneration-associated genes (RAGs) and neuronal survival (Ben-Yaakov et al., 2012). Nerve injury also induces local activation of JNK that upon phosphorylation is translocated to the cell body within vesicular structures. Once in the neuron, JNK is required for the activation of the transcription factor c-Jun, thus increasing the expression of RAGs (Barnat et al., 2010). Another positive injury stimulus activated by phosphorylation is ERK. In the initial phase of Wallerian degeneration, ERK contribute for the dedifferentiation of Schwann cells and is then coupled to the retrograde transport machinery, in a process dependent on vimentin (Glenn et al., 2013). All together, these studies indicate that, in addition to neuronal cell bodies, axonally synthesized proteins are crucial for nerve regeneration.

The importance of axonal transport relies on the fact that its disruption leads to the onset of several neurodegenerative disorders, including amyotrophic lateral sclerosis, Charcot-Marie-Tooth, Alzheimer's and Huntington's diseases (Roy et al., 2005). However, wheter transport defects are cause or consequence of neurodegeneration is still under debate. The study of axonal transport in FAP is not yet disclosed and should be a topic of interest for future studies.

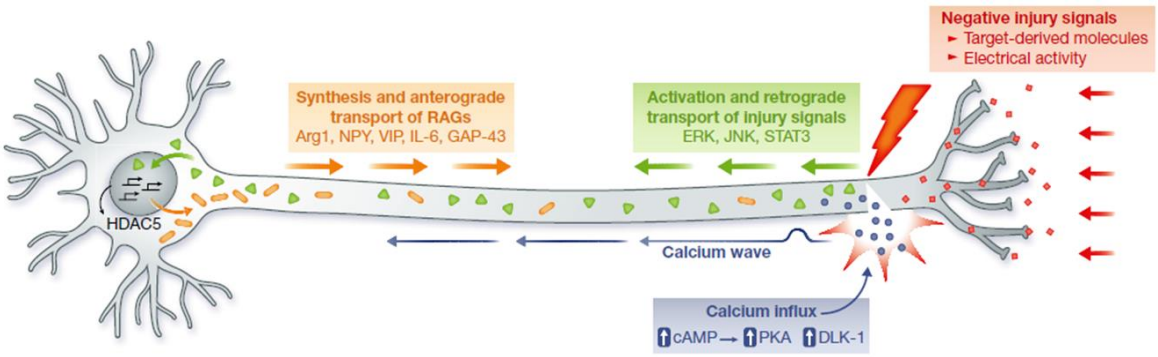

Figure 13 – Axonal transport following nerve injury. Most of the axonal transport is made along the microtubules dependent on cAMP, which in turn activates protein kinase A (PKA), signaling to DLK and promoting local protein synthesis and axonal elongation. Loss of electrical activity and removal of negative cues triggers axonal regeneration. When the calcium wave arrives to the cell body promote HDAC5 nuclear export and activation of the regenerative transcriptional program. Retrograde transport of positive injury signals including ERK, JNK and STAT3 is a potent driving force behind the intrinsic neuronal growth capacity. On the other hand, RAGs and other proteins expressed in the cell body reach the axon tip through anterograde transport. Abbreviation not yet mentioned; VIP: vasoactive intestinal peptide (from Mar et al., 2014).

Axonal elongation

After peripheral nerve injury, the distal stump undergoes Wallerian degeneration while the proximal stump begins regeneration. In this way, nerve fibers regrow from the distal tip of the proximal growing axon, the growth cone, to the distal end. Growth cones are highly specialized structures that control the rate and direction of axon elongation during development or after peripheral nerve damage. They are dynamic, actin-supported structures, shaped by assembly and reorganization of cytoskeletal elements (Bradke et al., 2012). To achieve a successful reinnervation, several key processes and extracellular cues need to be precisely regulated for correct directional guidance towards appropriate synaptic targets. These signals include neurotrophins, ECM proteins, neuronal adhesion molecules, expression of growth-associated proteins and RAGs. Neurotrophic factors, together with laminin, promote axon elongation by modulating cytoskeleton-binding proteins through activation of protein kinase B (AKT), which in turn inhibits glycogen synthase kinase-3β (GSK-3β), with consequent increase in microtubule speed in the growth cone, thus enhancing axon regeneration (Chen et al., 2007; Liz et al., 2014).

The first RAG to be identified was GAP-43 (Skene and Willard, 1981). It is a nervous tissue-specific cytoplasmic protein, expressed at high levels in neuronal growth cones and crucial for actin assembly and axon elongation. Overexpression of GAP-43 following injury is achieved by the retrogradely transported phosphorylated STAT-3 that in turn is a downstream molecule from the signal transduction of IL-6 and LIF, reinforcing the importance of cytokines in regeneration (Chen et al., 2007).

Arg-1 is a critical enzyme in polyamine synthesis and has been tied to axonal elongation due to its ability to overcome neurite growth inhibition by myelin associated glycoproteins (Cai et al., 2002).

The PKA-dependent pathway involved in cAMP mediated axon growth requires the downstream activation of several key transcription factors, including cyclic AMP-dependent transcription factor (ATF-3). This molecule is a reliable neuronal marker of injury and has demonstrated pro-regenerative qualities when neurons are cultured on permissive substrates, such as laminin (Seijffers et al., 2007). In addition, ATF-3 has been shown to influence neurite outgrowth and elongation (Defrancesco-Lisowitz et al., 2014).

Since the axonal skeleton is composed mainly by microtubules and microfilaments, successful axonal elongation depends also on tubulin and actin synthesis (Mar et al., 2014).

Upon appropriate length of axonal regrowth, Schwann cells redifferentiate in a proximal-to-distal direction and express myelin specific genes for timely remyelination. Once remyelination is complete, the expression of neurotrophins and their receptors return to

basal levels, target organs are finally reached and action potentials propagate normally. Overall, effective peripheral nerve regeneration has to be preceded by successful assembly of a new growth cone, increase in *de novo* protein synthesis, appropriate retrograde and anterograde transports, heightened responsiveness to trophic support and downregulation of inhibitory extracellular cues (Brosius Lutz and Barres, 2014). It is a robust but sometimes incomplete process with some drawbacks. Hence, in several cases regrowth does not lead to a complete functional recovery due to misrouting of regenerative sprouts, lack of efficient guidance mechanisms or increased branching of regenerating axons. These erroneous processes lead to incorrect reinnervation, motor deficits and disturbed sensory function (Hamilton et al., 2011).

Final remarks

In summary, successful regeneration depends on tightly controlled cellular and molecular programs and is only achieved in the presence of a permissive environment. So far, the regenerating properties of FAP peripheral nerves or their behavior to an injury stimulus remains unanswered. As such, further knowledge is needed to improve axonal regeneration or prevent neurodegeneration caused by the deposition of TTR aggregates and associated toxic signaling cascades. The present study addressed some of these issues to provide new insights on molecular signaling mechanisms associated with FAP pathology, in order to establish new potential therapeutic targets.

Research Project

Research Goals

In the present research project we proposed to clarify the FAP peripheral nerve response to an injury stimulus and the impact of inflammation and ECM remodeling in non-fibrillar TTR deposition. Alternative strategies for TTR amyloidosis are still awaited and this knowledge will allow for the development of novel therapeutic interventions. Additionally, we investigated the hypothesis of TTR internalization by cellular components of the PNS. Specifically, the following aims were covered:

Chapter I: Evaluate *in vivo* the influence of heparan sulfate proteoglycans in nerve TTR deposition;

Chapter II: Characterize the nerve response to injury, using an FAP mouse model, and investigate the effect of neuroinflammation over TTR deposition, contributing for a better understanding of the pathogenesis of TTR related amyloidosis;

Chapters III and IV: Propose a new therapeutic strategy for FAP, by *in vivo* preclinical studies with the anti-inflammatory drug Anakinra, and assess the effect of this protective approach regarding neuroregeneration after peripheral nerve insult.

Chapter V: Investigate the ability of glial cells for TTR internalization and degradation in tissues from an FAP mouse model and in sural nerve biopsies from FAP patients or healthy control subjects.

Chapter I

A novel nanoparticle delivery system for *in vivo* targeting of the sciatic nerve: evaluation of heparan sulfate influence on transthyretin deposition

A novel nanoparticle delivery system for *in vivo* targeting of the sciatic nerve: evaluation of heparan sulfate influence on transthyretin deposition

Nádia Pereira Gonçalves[1,2,3], Hugo Oliveira[4,5], Ana Paula Pêgo[1,4], Maria João Saraiva[1,2,3]

1) Instituto de Inovação e Investigação em Saúde (I3S), Universidade do Porto, Portugal
2) Unidade de Neurobiologia Molecular, IBMC – Instituto de Biologia Molecular e Celular, Universidade do Porto, 4150-180 Porto, Portugal
3) Instituto de Ciências Biomédicas de Abel Salazar, (ICBAS), Universidade do Porto, 4099-003 Porto, Portugal
4) INEB – Instituto de Engenharia Biomédica, Universidade do Porto, Rua do Campo Alegre, 823, 4150-180 Porto, Portugal;
5) Universidade do Porto, Faculdade de Engenharia, Rua Roberto Frias, s/n, 4200-465 Porto, Portugal

Running title: Heparan sulfate and TTR deposition

Abstract

Familial Amyloidotic Polyneuropathy (FAP) is an autosomal dominant neurodegenerative disorder characterized by extracellular deposition of mutant transthyretin (TTR) aggregates and amyloid fibrils, particularly in the peripheral nervous system (PNS). Recent studies indicate the potential involvement of heparan sulfate proteoglycans with amyloidogenic proteins and in modulation of TTR deposition. In the present work, nerve biopsies from human asymptomatic carriers and FAP patients were analyzed for heparan sulfate content and although mainly associated with amyloid fibrils, this molecule is also upregulated in earlier stages of disease, in association with non-fibrillogenic aggregates. Therefore, to study *in vivo* the role of glycosaminoglycans (GAGs) in TTR deposition, we developed a novel local delivery system into mice sciatic nerve using heparin/chitosan (CH) nanoparticles. To address drug release and diffusion throughout nerve tissue, fluorescently labeled CH and heparin were used and applied to sciatic nerves of wild-type (WT) mice. Our results show maximal absorption throughout the nerve extracellular matrix (ECM) at day 15 and no major inflammatory response activation, indicating this as a safe and biocompatible system for nerve delivery. Using this optimized system, heparin/CH nanoparticles were locally injected into sciatic nerve of transgenic mice carrying the most prevalent TTR mutation – V30M, in a *Ttr* null background and heterozygous for the heat shock factor 1 (*Hsf-1*), having in average 14 months of age. Contralateral nerve receiving uncoupled CH particles was used as control. Fifteen days after nanoparticles application, both heparan sulfate levels and non-fibrillar TTR deposition significantly increased in treated nerves, although no amyloid was detected, by Congo red staining. Our work demonstrates that changes in proteoglycan type and distribution could possibly account for alteration of the physical properties of tissues, increasing TTR deposition *in vivo*. Moreover, this new and versatile nanoparticle delivery system opens novel avenues in the field of neuropathology and probably in the design of therapeutic strategies targeting directly nerve tissue.

Introduction

Peripheral neuropathy is associated with damage to the peripheral nervous system (PNS), outside the brain and the spinal cord. PNS problems are common and encompass a large spectrum of traumatic injuries, diseases, tumors or iatrogenic lesions (Rodriguez et al., 2004). In peripheral neuropathies, such as diabetic neuropathy, polyradiculopathy, Charcot-Marie Tooth disease, Familial Amyloidotic Polyneuropathy (FAP), traumatic nerve lesions or secondary neuropathies due to alcoholism or HIV-1 infection are major causes to morbidity, being the conventional treatments primarily palliative rather than curative (Apfel, 1999). Symptoms depend on the type, number and localization of the affected nerves in the body, with pain or loss of sensation often produced.

FAP is an autosomal dominant neurodegenerative disorder characterized by extracellular deposition of mutant TTR aggregates and amyloid fibrils, particularly in the PNS (Coimbra and Andrade, 1971b). It is well known that extracellular matrix (ECM) remodeling contribute to the progress of this disease; some ECM-related genes are upregulated in nerve biopsies from FAP patients (Sousa et al., 2005) carrying the most prevalent TTR mutation, the V30M (Saraiva et al., 1984), and in tissues from FAP transgenic mouse models (Cardoso et al., 2008). One of those genes is biglycan that was found overexpressed at early stages of disease, before amyloid deposition (Sousa et al., 2005; Cardoso et al., 2008). Neutrophil gelatinase-associated lipocalin (NGAL), chondroitin sulfate and matrix metalloproteinase-9 (MMP-9) are upregulated only when TTR fibrils are already present, all colocalizing in later stages with amyloid deposits (Sousa et al., 2005; Cardoso et al., 2008). Heparan sulfate proteoglycans are glycoproteins of the ECM, covalently attached to chains of the glycosaminoglycan (GAG) heparan sulfate (Häcker et al., 2005). They have been identified as a codeposited component of amyloid in amyloid-related disorders (Ancsin, 2003), indicating that ECM remodeling occurs continuously until the later stages of disease. Moreover, recent *in vitro* studies and *in vivo* approaches in a *Drosophila* model indicate the potential involvement of heparin and heparan sulfate proteoglycans as enhancers of the amyloidogenic cascade, prompting TTR fibrillogenesis (Bourgault et al., 2011; Noborn et al., 2011; Di Domisio et al., 2012). In the present work our aim was to evaluate, in a mouse model of FAP, how changes in GAGs type and distribution could alter the nerve metabolism promoting TTR fibrillogenesis and deposition. In order to deliver drugs directly into the nerve tissue, while improving the half-life and efficacy of agents, a novel cationic nanoparticle-based delivery system composed of chitosan (CH) and heparin was established, having as long-term objective the development of novel therapeutic tools. We selected CH as a starting material in the design of vectors for heparin delivery to the nerve due to its well-established properties:

high biocompatibility, biodegradability, non-toxicity and non-antigenicity (Luo and Wang, 2014). Furthermore, CH presents a mucoadhesive character, which increases residual time at the target of absorption (Liu et al., 2007). In addition, it was previously reported that this biomaterial did not cause any damage to the nerve tissue when applied in nerve guides (Li et al., 2010).

Heparin is a polyanionic mucopolysaccharide and a well-known anticoagulant, associated to gastric ulcer healing (Lin et al., 2009). It has been used to optimize and extend the delivery kinetics of growth factors, prevent its degradation and enhance binding to cell surface receptors (Chu et al., 2010). Heparin has a similar structure with heparan sulfate; however, has a short biologic half-life (approximately one hour) and if directly injected in the sciatic nerve it will be rapidly cleared by phagocytic cells. Indeed the development of a delivery system that allows the release of heparin in a local and controlled fashion to the nerve tissue is paramount.

Main technical challenges are posed in order to achieve a safe and efficient delivery system to the peripheral nerve: (i) the drug must be efficiently absorbed; (ii) the administration has to be minimally invasive as not to induce severe secondary inflammatory reactions; (iii) sustained drug delivery must be attained and (iv) the delivered molecules need protection from biodegradative agents. Heparin, due to its highly negative charge can interact electrostatically with CH forming stable nanoparticles that will protect it from degradation while allowing it to be slowly released to the tissue (Liu et al., 2007; Boddohi et al., 2009). Thus, in the present work we prepared heparin/CH nanoparticles, studied heparin delivery as a function of time, evaluated the inflammatory response resulting from the nanoparticle delivery system and applied it to an FAP mouse model to address TTR nerve deposition.

Materials and Methods

Materials

Fluorescein labeled heparin (heparin-fluor) was purchased from Molecular Probes. The heparin used in the FAP mouse model (14 kDa, a kind gift from Dr. Jin Ping-Li, Upsala University, Sweden), was prepared from pig intestinal mucosa and had no anticoagulant activity. Technical grade CH (Chimarin™, degree acetylation (DA) 13%, apparent viscosity 8 mPas) was supplied by Medicarb. The average molecular weight of the starting material was found to be 7.8 ± 0.5x10^4 (GPC in 0.5 M CH_3COOH - 0.2 M CH_3COONa, 25ºC) (Moreira et al., 2009). Endotoxin levels of the purified CH extracts were assessed using the Limulus Amebocyte Lysate Assay (QCL-1000®), following the manufacturer's instructions. Endotoxin levels were found to be below 0.1 EU/mL, respecting the US Department of Health and Human Services guidelines for implantable devices. Matrigel™, with a protein concentration of 9.5 mg/mL and 2.0 EU/mL endotoxin units, was obtained from BD Biosciences. Unless mentioned otherwise, all reagents were obtained from Sigma-Aldrich and were of analytical grade.

Preparation of heparin/CH nanoparticles

A rhodamine activated derivative [5(6)-Carboxy-X-rhodamine N-succinimidyl ester, ROX; Fluka®] was used to label CH. In brief, 10 mg of CH was dissolved overnight in 10 mL of 1% acetic acid solution and added to an equal volume of ROX solution (0.13 mg/mL^{-1} in dehydrated methanol, Molecular Sieves, Merck). The reaction was let to occur for 3 h, under constant stirring, protected from light. The fluorescently-labeled CH (CHROX) was recovered by precipitation with 5 mL of 0.5 M NaOH. The precipitated polymer was washed with deionized water until no fluorescence was detected in the supernatant and, subsequently, freeze-dried. CH and CHROX solutions were prepared as follows: 10 mg of polymer was dissolved overnight in 4 mL of 1% acetic acid. Afterwards, 4 mL of 5 mM acetate buffer pH 5.5 was added and the pH of the solution adjusted to 5.5 with 1 M NaOH. The volume was completed to 10 mL with 5 mM acetate buffer pH 5.5 and the resulting solutions were stored at -20ºC until further use. Heparin-fluor was suspended in filtered ultrapure water to a final concentration of 1 mg/mL. Three kinds of CH particles were prepared, CH/heparin-fluor, CHROX/heparin-fluor and CH/heparin. All nanoparticle types were obtained by the addition of 10 µL of heparin solution into 25 µL of CH solution under vortex (100 rpm) for 30 s, at room temperature, according to Liu et al., (2007). Subsequently, the nanoparticles were let to stabilize for 15 min at room temperature

before further use. For comparison, 10 µL of heparin solution was mixed with 25 µL of a matrigel solution.

Characterization of heparin/CH nanoparticles

Particle size, polydispersity index (PDI) and zeta potential measurements were carried out on a dynamic light scattering (DLS) instrument (Zetasizer® Nano ZS). The Smoluchowski model was applied for zeta potential determination and cumulative analysis was used for mean particle size determination. All measurements were performed in triplicate, at 25°C. The morphology of prepared nanoparticles was examined by transmission electron microscopy (JEM-1400™). A total of 10 µL of nanoparticle suspension was placed onto a 300 mesh carbon-coated nickel grids for 2 min and after air-drying the samples were observed.

Human samples

Human tissue biopsy was performed after informed consent and approval from the Ethics Committee of the Hospital Geral de Santo António (Porto, Portugal), following the declaration of Helsinki. Archival sural nerve biopsy samples obtained from FAP V30M patients (*n*=3), asymptomatic carriers (*n*=3) and normal control subjects (*n*=3) were previously characterized for TTR deposition.

Animals and surgical procedures

Wild-type (WT) mice (in the 129/sv background with an average age of 12 months) and an FAP mouse model carrying the human V30M mutation, in an *Hsf-1* heterozygous background (Santos et al., 2010b), with 14 months-old, were used in the experiments (total *n*=48 for WT and *n*=5 for transgenic mice, as described throughout the text). The required total number of animals was approved by the Institute Ethical Committee (Porto, Portugal) as well as by the National General Veterinarian Board (Lisbon, Portugal). All animal experiments were carried out in accordance with the European Community Council Directive. The animals were anesthetized by intraperitoneal injection with a premixed solution containing ketamine (75 mg/kg) plus medetomidine (1 mg/kg). After skin incision and muscle dissection, the sciatic nerve was exposed in the mid-thigh and dissected free from the surrounding tissue. In the left side, heparin/CH nanoparticles were applied under the nerve; the right side served as control nerve for uncoupled CH nanoparticles. Animals were kept in the animal facility in a controlled-temperature room, maintained under a 12 h light/dark period and with water and food *ad libitum.* Mice were sacrificed and their sciatic

nerves exposed and excised either for direct observation by confocal microscopy or for processing in frozen and paraffin sections.

Fluorescence Microscopy

Sciatic nerves from mice that received CHROX/heparin-fluorescein labeled nanoparticles were taken to direct observation by confocal microscopy (Leica SP2 AOBS SE) for colocalization of heparin-fluor with CHROX in the tissue.

In most experiments that followed, the sciatic nerves were collected to a solution containing sodium m-periodate, L-lisine and 4% paraformaldehyde (MERCK) and left overnight at 4ºC followed by washing in 0.1 M Sorrenson´s phosphate buffer solution and cryoprotection (20% anhydrous glycerol and 0.4 M Sorrenson´s phosphate buffer). Eight µm frozen sections were cut using a freezing cryostat; immunofluorescence was performed and the slides were directly mounted with Vectashield with 4'.6-diamino-2-phenylindole (DAPI) (Vector). Antibodies used were: rabbit anti-collagen IV (1:600, Abcam), rabbit anti-protein gene product 9.5 (PGP 9.5, 1:800, Serotec) and rabbit anti-S-100 (1:100, DAKO). The secondary antibody was goat anti-rabbit Alexa Fluor 568 (Molecular Probes), diluted 1:1,000 in 4% fetal bovine serum and 1% bovine serum albumin in PBS blocking buffer. The slides were visualized in a Zeiss Axio Imager microscope.

Quantification of intensity of green fluorescence was performed using frozen sections of sciatic nerves. Each sample was evaluated in 4 or 5 different areas, using an inverted fluorescent microscope (Axiovert 200M, Zeiss). Fluorescence intensity was determined by image analysis using Axiovision software (4.8, Zeiss).

Immunohistochemistry and Double Immunofluorescence

In other experiments, sciatic nerves were collected to 10% formalin and embedded in paraffin blocks. Three µm-thick sections were deparaffinated in histoclear (National Diagnostics) and hydrated in a descent alcohol series. Endogenous peroxidase activity was inhibited with 3% hydrogen peroxide solution in methanol and sections were blocked with 4% fetal bovine serum and 1% bovine serum albumin in PBS. Primary antibodies used were: goat polyclonal anti-TNF-α (1:50, Santa Cruz Biotechnology), goat polyclonal anti-IL-1β (1:50, Santa Cruz Biotechnology), goat polyclonal anti-ionized calcium-binding adapter molecule 1 (IBA1), for macrophage detection, (1:200, Abcam), rabbit polyclonal anti-TTR (1:500, DAKO) and mouse monoclonal anti-heparan sulfate (1:100, Amsbio). Antigen visualization was performed with the 3.3´-diaminobenzidine (Sigma-Aldrich).

Semi-quantitative analysis of the immunostained area was performed with the Image Pro-plus software (Media Cybernetics). Results shown represent the area occupied by pixels corresponding to the immunohistochemical substrate's color that is normalized relatively to the total area, with the corresponding standard error of the mean (SEM). Each animal tissue was evaluated in five different areas with 20 X magnification.

For confocal microscopy, paraffin sections of human sural nerve biopsies and sciatic nerves from the FAP mouse model were deparaffinated, hydrated and double stained with rabbit anti-TTR (1:100, DAKO) and mouse anti-heparan sulfate (1:100, Amsbio). Donkey anti-rabbit Alexa Fluor 568 and goat anti-mouse Alexa Fluor 488 were used as secondary antibodies.

Congo red staining

The presence of amyloid deposits in treated sciatic nerves was investigated by Congo red staining and observation performed under polarized light. Briefly, deparaffinized tissue sections were incubated for 20 min with 0.01% sodium hydroxide in 80% ethanol saturated with sodium chloride followed by staining with 0.5% Congo red in the previous solution (Puchtler and Sweat, 1965). Next, preparations were washed with distilled water, stained with hematoxilin and analyzed under polarized light. In the positive controls, amyloid was identified by characteristic green birefringence.

Statistical Analysis

Statistical analysis was performed using GraphPad Prism 5.0 for Windows. Results are reported as mean ± SEM. Student's *t*-test or two-way analysis of variance (ANOVA) followed by Bonferroni post-test, were used and considered statistically significant when $*p<0.05$.

Results

Evaluation of heparan sulfate levels in human nerve biopsies

It was previously found *in vitro*, in a *Drosophila* model and in heart human specimens that TTR fibril extracts contain heparan sulfate proteoglycans (Bourgault et al., 2011; Noborn et al., 2011). Thus, we started by comparing heparan sulfate levels on sural nerve biopsies from FAP patients, asymptomatic carriers and healthy control subjects (*n*=3 per group). Histological examination revealed that this GAG is already upregulated in the earlier asymptomatic stage of disease, when only non-fibrillar TTR deposits are present in the peripheral nerve (Figure 1A). With disease progress, heparan sulfate immunoreactivity increases, in a pattern similar to TTR deposition (Figure 1A). In addition, using confocal microscopy, colocalization between TTR and heparan sulfate was noticed, corroborating the notion that this GAG is incorporated in FAP amyloid deposits (Figure 1B).

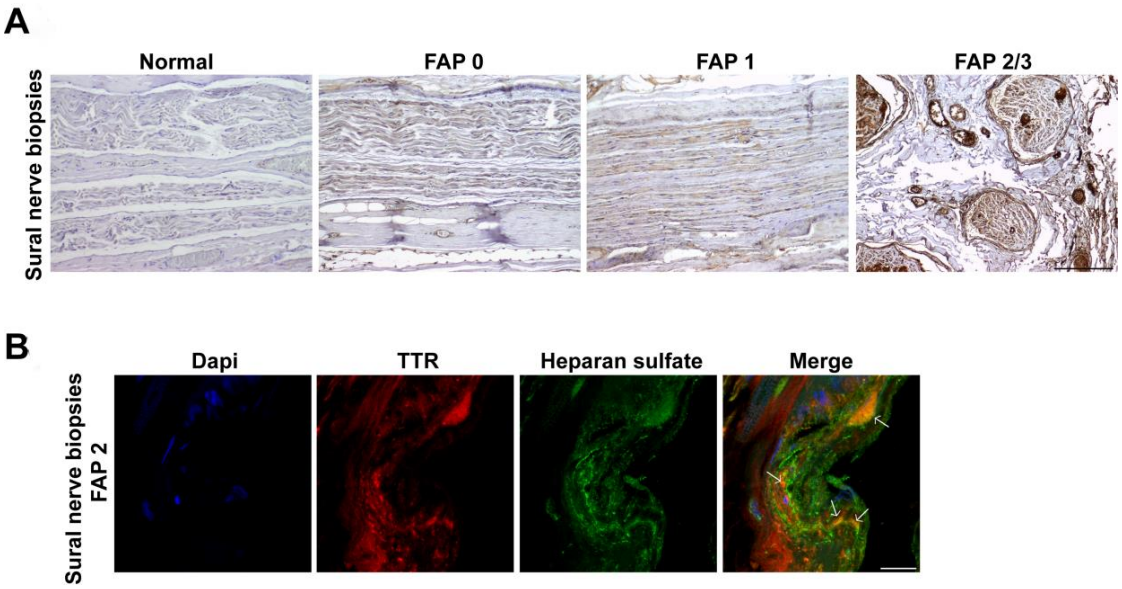

Figure 1 – Heparan sulfate immunoreactivity in human sural nerve biopsies. A) Histological examination of heparan sulfate levels in sural nerve biopsies from healthy control individuals (Normal), FAP asymptomatic carriers (FAP 0) and FAP patients with different patterns of amyloid deposition (FAP 1, 2 or 3). Scale bar 100 µm. **B)** Representative photomicrographs obtained with confocal microscopy showing colocalization (yellow and orange in merged panel, arrows) between TTR (red) and heparan sulfate (green) in sural nerve biopsies from FAP patients. Scale bar 15 µm.

Vehicle for the delivery system: Heparin/CH nanoparticles versus Matrigel

Based on the previous results, we aimed at developing a delivery system for the release of heparin into sciatic nerves of FAP mice, with the ultimate goal of understanding the heparan sulfate influence on TTR polymerization *in vivo*.

CH and matrigel were first assessed as vehicles for heparin nerve release. Distribution of fluorescent heparin in nerve frozen sections was compared 5, 10 and 15 days after application (*n*=3 WT animals for each time and each vehicle). Five days post-surgery, the spreading of heparin fluorescence was similar for both vehicles (Figure 2); at day 10 or 15, fluorescence was found at the surface of the nerve, most likely in the perineurium, in the group treated with heparin/matrigel while animals receiving heparin/CH nanoparticles showed heparin diffused into the nerve tissue, as documented in Figure 2 (day 15 not shown).

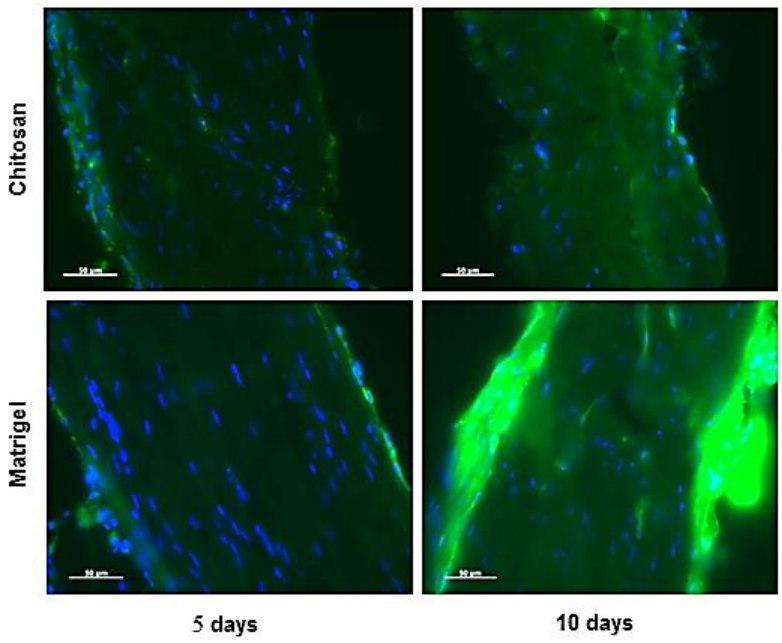

Figure 2 – Heparin-fluorescein diffusion pattern in nerve tissue, when conjugated with CH or matrigel. Representative fluorescence intensity of heparin, 5 and 10 days after CH nanoparticle or matrigel conjugate application. Sciatic nerve frozen sections were analyzed with an Axiovert microscope. Scale bar 50 µm.

These results, plus the biological advantages of CH, lead us to choose the CH-based system to continue the heparin delivery studies.

Characterization of Heparin/CH nanoparticles

The heparin/CH nanoparticle size (diameter, nm), PDI and zeta potential (mV) values are reported in Figure 3. As observed in Figure 3A a monomodal population was obtained in terms of size, with a positive net charge. The nanoparticles were spherical in shape as determined by electron microscopy analysis (Figure 3C) that corroborated the results of DLS in terms of the nanoparticle size.

A

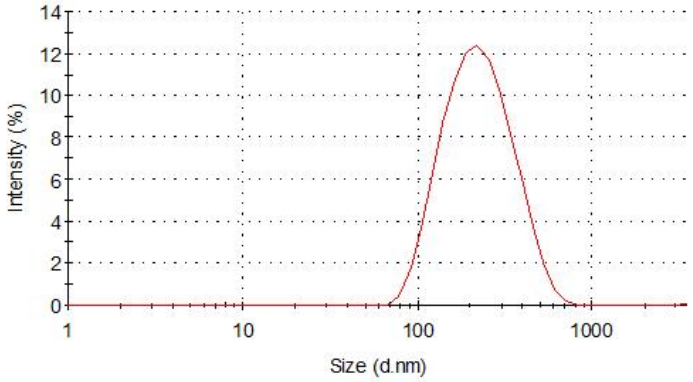

B

size (nm)	PDI	Zeta potential (mV)
198 ± 24.2	0.229 ±0.028	28.7 ± 4.1

C

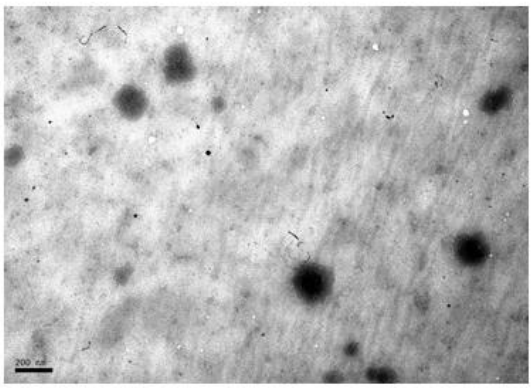

Figure 3 – Characterization of heparin/CH nanoparticles. A) & B) Size, PDI and zeta potential measurements, using DLS. **C)** Assessment of nanoparticle morphology and size by microscopy.

Heparin release in the sciatic nerve as a function of time

In order to monitor heparin release by CH and its diffusion throughout sciatic nerve, we conjugated CH with rhodamine (CHROX) before mixing with heparin-fluor; after 5, 10, 15, 30 and 45 days of application of CHROX/heparin-fluor nanoparticles in the sciatic nerves (*n*=3 animals for each time point), fresh, unprocessed nerves were analyzed by confocal

microscopy (Figure 4A). On day 5, both fluorochromes were detected at the surface of the nerve and merging suggested colocalization of CHROX with heparin-fluor. This surface colocalization was partially observed at day 10; however, at this time point, heparin-fluor was also found in the interior of the nerve, without CHROX colocalization as indicated by an arrow in Figure 4A. A control nerve with CHROX alone shows CH distribution only at the surface of the nerve. All together, these results indicated that heparin was being released by the CH nanoparticle, located at the surface and then diffused into the tissue. At day 15, CH particles were also diffusing into the nerve and heparin was released since regions with no colocalization were found, suggesting continuous delivery of the drug from the nanoparticle (arrows in Figure 4A). At day 10 the intensity of the green fluorescence signal was greater than on day 5 and this had increased by day 15 (Figure 4B). On day 30 a very weak green staining was visible, without CHROX signal, while at day 45 no signal was detected (data not shown). We therefore considered 15 days after application to be the best time for subsequent analyses of heparin tissue distribution.

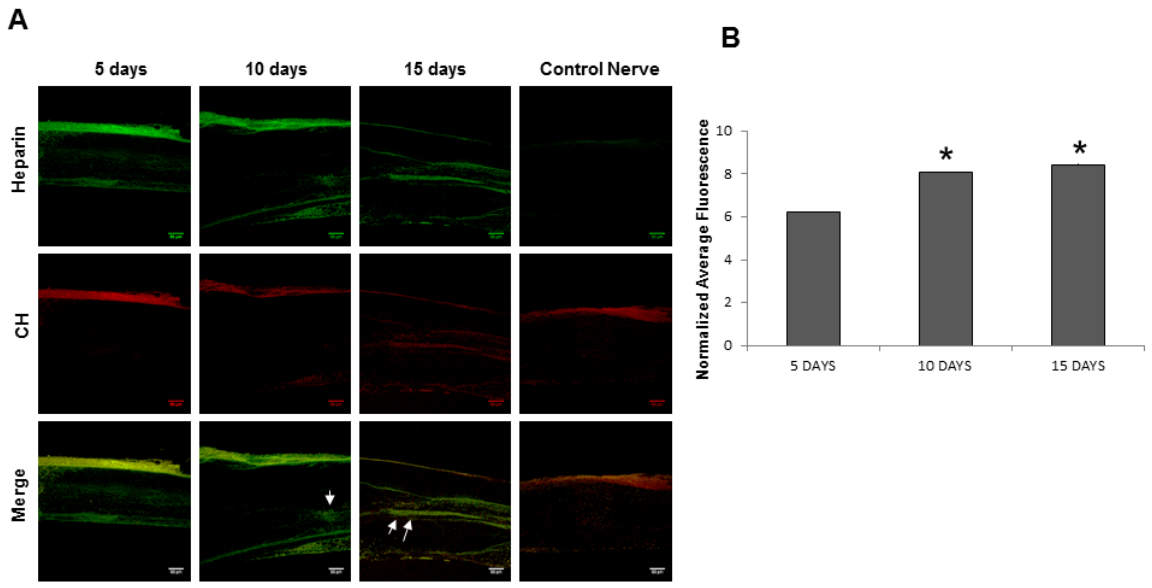

Figure 4 – Heparin release as a function of time studied in fresh unfixed nerve. A) Confocal photomicrographs denoting heparin-fluor in green and rhodamine-labeled CH in red. Superposition of the labels is shown (Merge). No colocalization of the two labels is indicated by arrows. Control nerve is rhodamine-CH (CHROX). Scale bar 50 µm. **B)** Semi-quantitative analysis of fluorescent heparin in the interior of the sciatic nerve. Bars represent normalized fluorescence intensity of analyzed image area reported as the mean ± SEM. SEM values are too small and would be virtually invisible on chart. *p<0.05, compared with 5 days.

Heparin localization within nerve structures

We next investigated the localization of released heparin in sciatic nerves, 15 days post-application (*n*=4). Frozen sections were analyzed by immunofluorescence with molecular markers of different nerve structures to colocalize with heparin-fluor (Figure 5). PGP 9.5 was used as a neuronal marker and S-100 as a marker of Schwann cells; with these markers few or none colocalization with fluorescent heparin was observed. Colocalization between heparin and collagen IV was clear; since collagen IV is the major constituent of the ECM, the results are indicative that heparin localized in the ECM and possibly at basement membranes of Schwann cells.

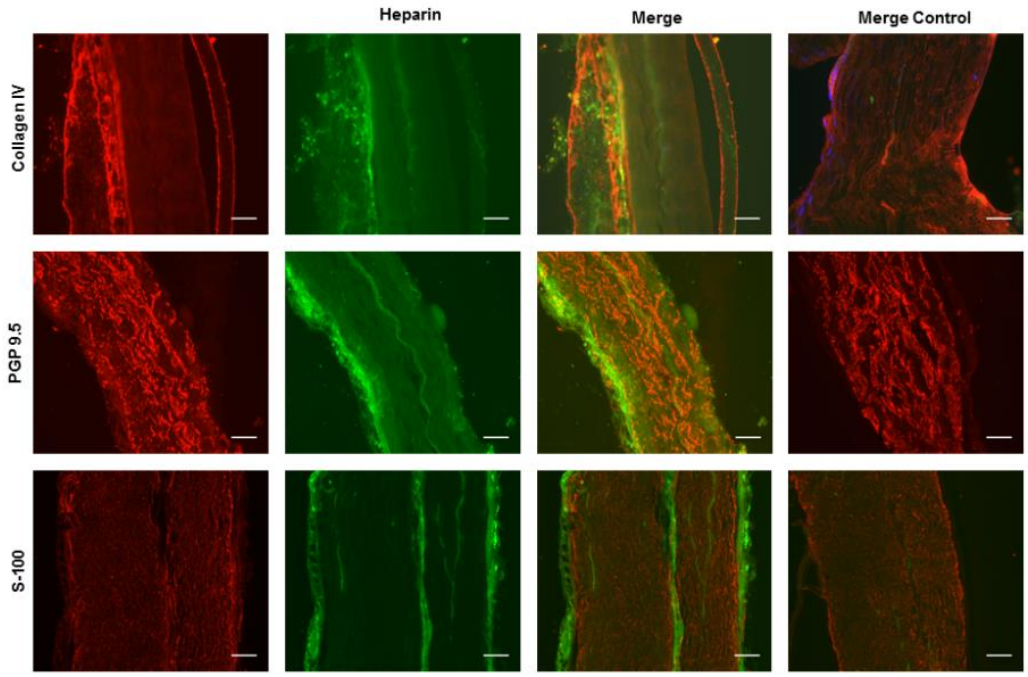

Figure 5 – Localization of heparin-fluorescein within nerve structures at day 15 after application of heparin/CH nanoparticles. Frozen sections through mice sciatic nerve were labeled with antibodies to collagen IV (red), PGP 9.5 (red) and S-100 (red). The green panel represents heparin-fluor. Superposition of the labels is shown (Merge). Colocalization was detected with collagen IV, in a higher extent than with axons (PGP 9.5) or Schwann cells (S-100), suggesting heparin delivery into the ECM. The control nerve derives from application of uncoupled CH in the contralateral nerve. Scale bar 100 µm.

Inflammatory Reactions

Macrophages and the pro-inflammatory cytokines TNF-α and IL-1β were evaluated by semi-quantitative immunohistochemistry (SQ-IHC) in paraffin sections at days 15, 30 and 45 (*n*=3 animals for each group) post-application of CH/heparin-fluor nanoparticles; as

control we used the contralateral nerves where uncoupled CH particles were deposited; *n*=2 mice treated with the same volume of water and sacrificed at day 15 served as sham. We could perceive some degree of macrophage activation on the time point of maximal heparin release to the interior of the nerve tissue when compared to the sham nerve; the slight activation was found to decrease with time, being virtually abolished at 45 days after nanoparticle application (Figure 6). The level of activation was similar to the control side (uncoupled CH), suggesting that the mild immunological reaction was attributable to the vehicle. TNF-α levels were increased in both nerves (CH/heparin and control uncoupled CH nanoparticles) at day 15 and also decreased with time (Figure 6). Forty-five days after, stabilization of the reactivity was observed. Comparing this response with sham nerve, we also concluded that the mild inflammatory reaction is due to CH and that a low percentage is due to surgery. The same situation was evident concerning IL-1β staining (data not shown).

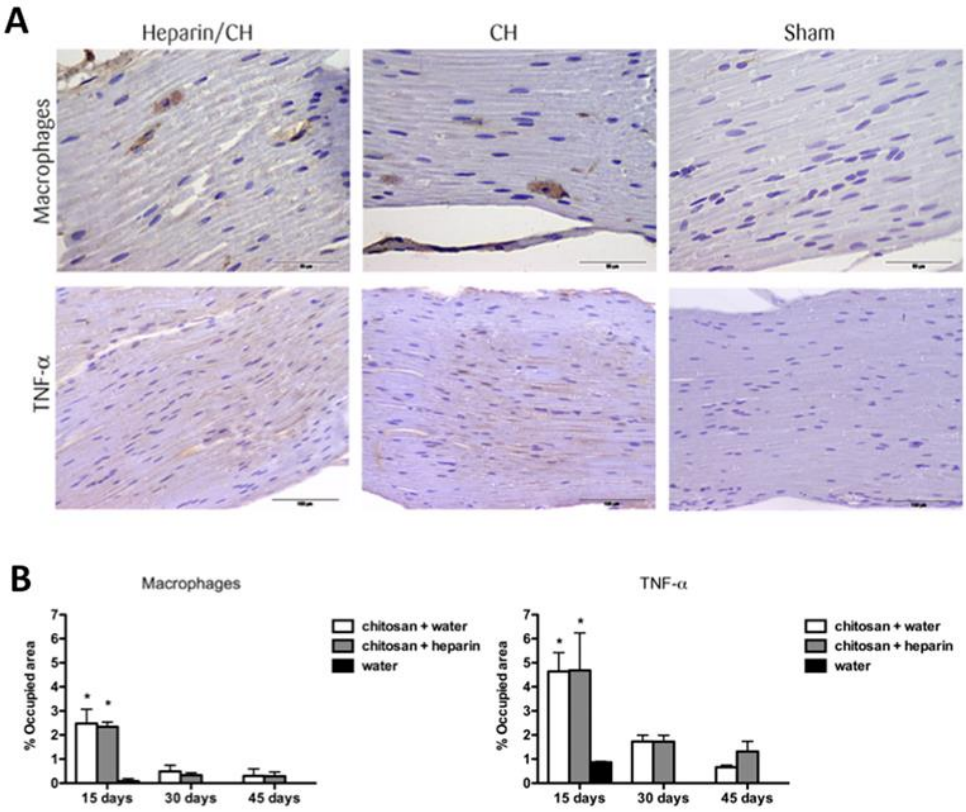

Figure 6 – Evaluation of the inflammatory response. A) Macrophage (scale bar 50 µm) and TNF-α (scale bar 100 µm) labeling in sciatic nerves treated with heparin coupled or uncoupled CH nanoparticles. Sham represents application of water. **B)** Histological examination demonstrated an increase in the levels of TNF-α and activated macrophages in treated nerves as compared with sham. In addition, a significant decrease of the inflammatory response with time was noticed (*p<0.05).

Effect of heparin delivery over TTR deposition in an FAP mouse model

After optimization and characterization of the delivery system, heparin/CH nanoparticles were applied into the sciatic nerve of TTR transgenic mice, to evaluate the effect of heparin on TTR deposition, *in vivo* (*n*=5). After 15 days, nerves were analyzed by immunohistochemistry and the levels of heparan sulfate and non-fibrillar TTR were both significantly increased in heparin treated nerves as compared with sham (Figure 7A). Congo red staining was negative, possibly because deposits were too small to be Congophilic. Moreover, areas of colocalization between TTR and heparan sulfate were perceived, suggesting that increase in heparan sulfate might contribute for TTR polymerization and deposition (Figure 7B).

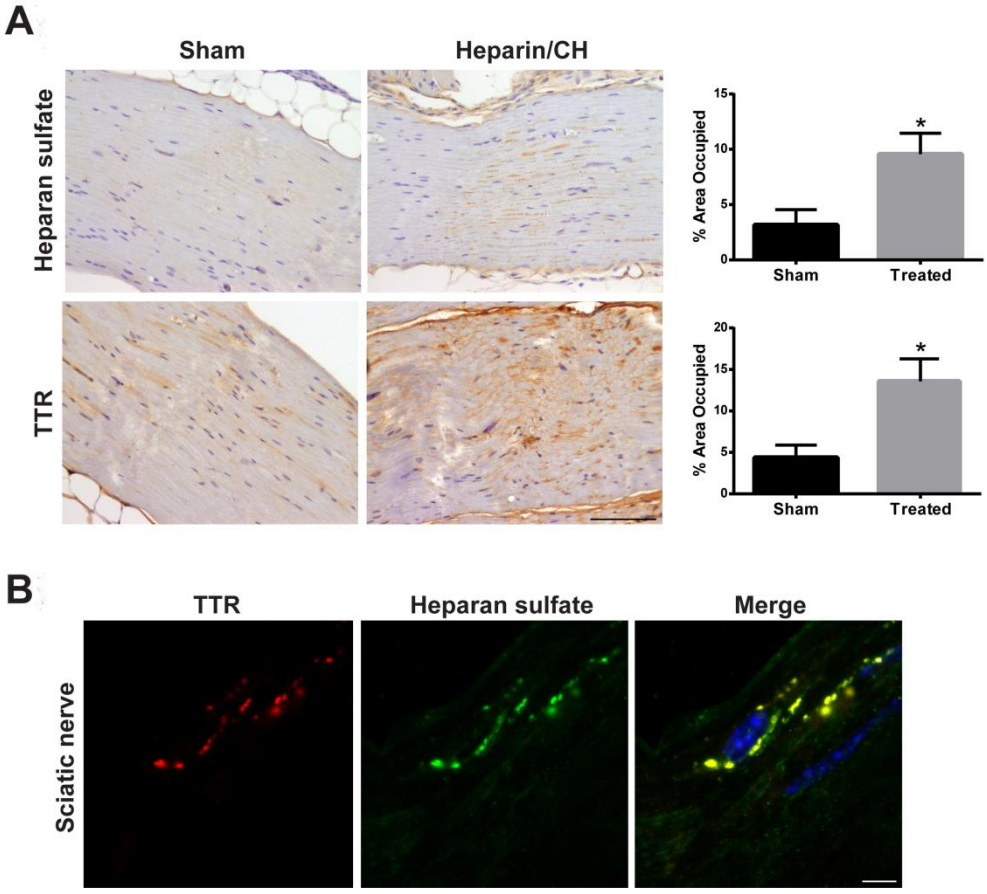

Figure 7 – Heparin release to the sciatic nerve upregulate local non-fibrillar TTR deposition in a mouse model of FAP. A) Representative SQ-IHC for TTR in sciatic nerve of Hsf/V30M mice treated with heparin/CH or uncoupled nanoparticles (sham). Scale bar 100 µm. Histograms represent quantification of immunohistochemical images and data is presented as percentage of area occupied ± SEM (*p<0.05). **B)** Double immunofluorescence between TTR and heparan sulfate in Hsf/V30M heparin/CH treated sciatic nerve, demonstrating colocalization between the 2 proteins (merged panel, scale bar 5 µm). Nuclei stained blue with DAPI.

Discussion

In this study, our primary goal was to evaluate if heparan sulfate was associated with TTR deposition in peripheral nerve biopsies from FAP patients. Immunohistological examination of sural nerves from patients, asymptomatic carriers and control individuals revealed substantial heparan sulfate accumulation within TTR amyloid deposits and also colocalization with non-fibrillar species. This finding prompts us to explore the potential of this GAG in TTR behavior and aggregation pathway in a mouse model of FAP disease. However, to address this point, a local delivery system into the sciatic nerve, based on heparin, need to be optimized.

Growing interest has been focused on nanomedicine as it can bring novel approaches towards the prevention, diagnosis and treatment of various diseases (Gharagozloo et al., 2015). CH is a natural polymer, with a cationic character that due to its biocompatibility and low cytotoxicity is emerging as a drug vehicle in tissue engineering and as a non-viral vector for gene therapy (Moreira et al., 2009).

Previous studies have been done to deeply characterize heparin/CH nanoparticles (Liu et al., 2007; Boddohi et al., 2009). Therefore some delivery systems were optimized in order to improve the absorption of heparin by the blood flow, locally by the gastric epithelium or by the lungs (Lin et al., 2009; Chen et al., 2009; Trapani et al., 2013). In these studies, nanoparticles were produced by combining positively charged chitosan with negatively charged heparin, in a ratio that produce minimum particle size with a positive zeta potential, strategy also followed in the present work. Initially CH and matrigel, in the form of nanoparticles and physical gel, respectively, were compared as vehicles for heparin release in the nerve. As CH-based nanoparticles were the only able to efficiently deliver heparin inside the nerves, this last was the chosen system to apply in the subsequent steps of the study. Nanosized heparin/CH particles were efficiently produced and found to be in the size range of what has been previously described in the literature (Mao et al., 2001; Oliveira et al., 2010), presenting several advantages regarding intra-nerve delivery. The condensation in the form of nanoparticles allows the penetration into the tissues and at the same time enables the escape from a number of cellular barriers, enzymatic degradation and cellular uptake, therefore enhancing drug delivery in the target tissues (Huang et al., 2002). Moreover, if a successful drug delivery system is aimed, a localized, effective and sustained release is paramount for its success. In view of these requirements, this novel delivery system has several advantages over other local systems, like miniosmotic pumps since these have a large size and could not be placed on mouse sciatic nerve for continuous delivery in time.

The degradation rate of the delivery system is a paramount factor when considering a sustained release throughout time. Indeed, CHROX based nanoparticles were detected up to 15 days post-administration, reinforcing its potential for a long-term drug release. As previously described, when CH (degree of de-acetylation 90%) was used as a vehicle for drug delivery, and after subcutaneous implantation in mice, its biodegradation occurred within 3 up to 14-28 days after the injection (Kofuji et al., 2002). In our case, we observed that on day 30 post-administration no signal was detected for CHROX based nanoparticles, suggesting that the polymer might be degraded in 15 to 30 days post-surgery. CH biodegradation by lysozyme leads to release of amino sugars of variable length, which have rapid clearance by the liver and kidney or can be incorporated into GAG metabolic pathways, ending up in skeletal muscle, articular cartilage or connective tissue (Baldrick et al., 2010).

CH nanoparticles promoted a mild inflammatory response, with activation of macrophages and increased cytokine production that decreased with time, being virtually abolished at 45 days after nanoparticle application. This observation complies with the expected intrinsic defense response of the body upon a mild exogenous stimulus. As no significant inflammatory reaction was triggered, CH seems to be an interesting material for use in the PNS, as previously shown with its use in the preparation of nerve guides (Li et al., 2010).

Finally, CHROX nanoparticles distribution throughout the nerve shows that this biomaterial, in the shape of nanoparticles, has the ability to enter into the nerve matrix. However, the majority of the nanoparticles are mainly detected in the periphery of the tissue, possibly due to the high surface densities of lipid moieties at the nerve surface that inhibit elevated penetration of the biomaterial (Pavinatto et al., 2007). Colocalization of CH and heparin occurred to some extent, indicating heparin continuous release from the nanoparticles and diffusion through the nerve matrix, as pointed out by colocalization with collagen IV.

ECM acts mechanically supporting the cells and regulates their behavior through specific interactions mediated by integrin receptors and proteoglycans, having high influence in axons or Schwann cells homeostasis (Sorokin et al., 2010). Thus, changes in the structure and composition of the ECM may alter tissue metabolism in several ways, such as triggering TTR nerve deposition. With optimization of the delivery system, we employed heparin/CH or uncoupled nanoparticles into sciatic nerves of FAP transgenic mice. In agreement with an earlier report using transgenic flies (Noborn et al., 2011), we confirmed that heparin was able to induce TTR aggregation *in vivo* also in transgenic mice carrying the V30M mutation; however, no positive Congo red material was detected, possibly related to the size of the aggregated species. It would be valuable to perform further

experiments using heparin with different lengths or sulfation degree or even using proteoglycans with different chain composition.

Understanding the pathological mechanisms and molecules underlying TTR deposition is of major value for prevention and treatment of TTR amyloidosis. Our data illustrate the important role of heparan sulfate/heparin in TTR aggregation and may assist in the design of potential therapeutic agents. For instance, the use of heparanase, an enzyme able to degrade this GAG, might be a promising future strategy for the exposure or breakdown of amyloid deposits (Jendresen et al., 2014). Furthermore, due to the extreme simplicity and versatility of this delivery system, it might open new avenues for the establishment of more suitable animal models and bring new viewpoints for study the influence of modulating proteins involved in neurodegeneration/regeneration.

Acknowledgments

This work was funded by FEDER funds through the Operational Competitiveness Program – COMPETE and by National Funds through FCT – Fundação para a Ciência e a Tecnologia under the project PTDC/SAU-ORG/111313/2009 and fellowships to NPG and HO, SFRH/BD/74304/2010 and SFRH/BD/22090/2005, respectively. The present work was also sponsored by POPH/FSE QREN program.

Authors would like to thank Dr. Paula Sampaio, Paula Gonçalves and Rui Fernandes from IBMC for the help with confocal microscopy, paraffin tissue processing and electron microscopy, respectively.

Chapter II

The inflammatory response to sciatic nerve injury in a Familial Amyloidotic Polyneuropathy mouse model

The inflammatory response to sciatic nerve injury in a Familial Amyloidotic Polyneuropathy mouse model

Nádia Pereira Gonçalves[1,2,3], Maria Teixeira-Coelho[1,2], Maria João Saraiva[1,2,3]

1) Instituto de Inovação e Investigação em Saúde (I3S), Universidade do Porto, Portugal
2) IBMC – Molecular Neurobiology, Instituto de Biologia Molecular e Celular, Porto, 4150-180 Portugal
3) Instituto de Ciências Biomédicas de Abel Salazar (ICBAS), Universidade do Porto, Porto, 4050-313 Portugal

Running title: Neuroinflammation in FAP

Abstract

Inflammation is a hallmark of several neurodegenerative disorders including Familial Amyloidotic Polyneuropathy (FAP). FAP is associated with extracellular deposition of mutant transthyretin (TTR), leading to degeneration of cells and tissues, particularly in the peripheral nervous system (PNS). With this work, our goal was to characterize the expression/deposition of TTR and the associated inflammatory immune response, induced by nerve injury, in wild-type (WT) mice and in a mouse model carrying the most common TTR mutation in FAP (V30M). Our results indicate that upon nerve injury TTR is significantly produced by Schwann cells and is dynamically regulated over time in V30M mice, accompanying a peak of inflammation. Strikingly, TTR V30M deposition in nerve tissue occurred, suggesting that inflammation contributes to TTR polymerization. In response to nerve injury, V30M mice display a downregulated innate immune response when compared to WT mice. More specifically, we saw decreased expression of cytokines and chemokines important for the recruitment of immune cells like macrophages and neutrophils, known to be important for the tissue regenerative process, which was found impaired in V30M mice. In conclusion, with this work we were able to characterize the biology of TTR both in WT and V30M animals, upon nerve injury, and found that TTR V30M impairs the inflammatory response necessary for nerve regeneration. Taken together, our findings suggest that inflammation is an important target to be considered in therapeutic strategies for FAP.

Introduction

Amyloidoses constitute a large group of acquired and hereditary disorders characterized by the extracellular accumulation of misfolded proteins, sharing a crossed β-sheet structure (Westermark, 2005). Among them, transthyretin (TTR) amyloidosis is the most common form of hereditary dominant systemic amyloidosis, in which TTR point mutations result in deposition of amyloidogenic species in different tissues (Benson and Kincaid, 2007). The TTR mutation most commonly associated with Familial Amyloidotic Polyneuropathy (FAP) is V30M (Saraiva et al., 1984) that leads to extracellular TTR deposition particularly at the peripheral and autonomic nervous systems (PNS and ANS, respectively), with neuropathy as a cardinal feature. TTR reaches the PNS through the cerebrospinal fluid, the blood-nerve barrier and over contact with peripheral nerve roots (Sousa and Saraiva, 2003) accumulating in the endoneurium, near Schwann cells, blood vessels and collagen fibrils, ultimately leading to neurodegeneration and cell death (Coimbra and Andrade, 1971b).

TTR functions as a carrier for thyroxine and retinol (Kanai et al., 1968) and is synthesized mainly by the liver and the choroid plexuses of the brain (Soprano et al., 1985). Recently, minute levels of *TTR* expression were also found in Schwann cells of the sciatic nerve (Murakami et al., 2010). The mechanism leading to TTR deposition in tissues include a decrease in its conformational stability with dissociation of the mutant homotetrameric form into unfolded monomers that self-assemble forming aggregates, oligomers and amyloid fibrils (Quintas el al., 2001).

The inflammatory response has been shown to be important for the development of peripheral neuropathies either by leading to deterioration or to amelioration of the disease process (Ydens et al., 2013). In the case of FAP, previous work with nerve biopsies from FAP patients shows the close association between production of inflammatory mediators and TTR non-fibrillar aggregates or amyloid fibrils deposition, suggesting a prominent role for inflammatory pathways in the progress of the disease (Sousa et al., 2001b). Additionally, infiltration of inflammatory cells in response to TTR aggregates or amyloid fibrils deposition in tissues from FAP patients would be expected. However, despite cytokine production by axons, no influx of such cells is found in FAP nerve biopsies (Misu et al., 1999; Sousa et al., 2001b), suggesting that mechanisms must operate to prevent or inhibit the correct innate immune response. TTR aggregates or amyloid material were never found in the PNS of the classical FAP animal models carrying the V30M mutation (Sasaki et al., 1986; Nagata el al., 1995; Kohno et al., 1997) which led us to hypothesize whether neuroinflammation might be a contributor for TTR production and deposition in the PNS. To address this possibility we induced nerve injury, in both wild-type (WT) and in

a well-described transgenic mouse for human TTR V30M, in a *Ttr* null background (V30M), and tested *in vivo* the local effect on TTR synthesis, deposition and the elicited inflammatory response.

Materials and Methods

Animals

Six months-old male and female WT and V30M mice, in the 129/Sv background, were used for the experiments. This was the chosen age since by this period, V30M mice have TTR non-fibrillar deposition in both the gastrointestinal tract and skin but not in the PNS (Kohno et al., 1997). Animals were housed in a controlled-temperature room, maintained under a 12 h light/dark period, with water and food *ad libitum*. One or 7 days after injury, mice were sacrificed with a lethal injection of a premixed solution containing ketamine and medetomidine.

All animal experiments were carried out in accordance with the European Community Council Directive (2010/63/EU) and the number of total animals for this research was approved by ethical committee and by National General Veterinarian Board.

Surgical procedures: Sciatic nerve injury

Anesthesia was induced with a premixed solution containing ketamine (75 mg/kg) plus medetomidine (1 mg/kg) and animals received a subcutaneous injection of butorfanol (1 mg/kg) prior to surgery. The thigh and legs were shaved, disinfected, the eyes coated to protect from drying and animals were then placed in abdominal position on a 37ºC heating pad. A skin incision of approximately 1 cm was made over the gluteal region exposing the left sciatic nerve from the sciatic notch to the point of trifurcation. The ischiocrural musculature was prepared with minimal tissue damage to ensure optimal conditions for functional recovery. Sciatic nerve ligation, adapted from the method described by Brumovsky et al., (2004) was performed using one ligature placed around the sciatic nerve at the mid-thigh level, with 5.0 silk. A sham operation was performed similarly at the contralateral side, except that the sciatic nerve was not constricted. The skin incision was closed with 5.0 silk suture and physiological saline solution was injected subcutaneously. Mice were kept in a recovery room with infrared heating lamp for 1-2 h. Post-surgical pain treatment consisted of supplying mice subcutaneously with butorfanol every 12 h for the first 48 h. The degree of constriction for each nerve after sacrifice and fixation was estimated under the dissection microscope and by microscopical observation of immunostained sections of the nerve. In all animals a decrease in the diameter of the nerve (without marked translucence) and swelling, proximal to the site of constriction, were observed. Animals did not show guarding behavior or autotomy, indicating slight constriction and not transection (Brumovsky et al., 2004).

Nociception evaluation

To compare the nociceptive response between WT and V30M mice after injury, hot-plate and Von Frey tests were performed.

The thermal response was assessed using the hot-plate test, with a standard temperature-controlled plate, prior to (day 0), 2 and 6 days after injury (*n*=9 WT and *n*=10 V30M mice). Mice were placed within a transparent Plexiglas box on a metal surface (hot-plate analgesia meter, IITC Life Science) at 52°C. Thirty seconds cut-off time was used for nonresponsive mice, to avoid possible tissue damage. The latency to respond with a hindpaw lick or shake/jump was measured and used as an index of nociception.

Von Frey filaments were used for the study of mechanical allodynia, before surgery and 5 days after injury (*n*=9 WT and *n*=10 V30M mice). Animals were placed in an opaque cage, to avoid visual stimulation, and let 20 min to adapt. Each Von Frey hair was applied to the skin of the mid-plantar surface of the hindpaw. This procedure was repeated 10 times with each filament, with an average of 20 s between consecutive applications. The force used started below the threshold of detection (0.026 g hair) and was increased until 5 or more positive scores had been obtained. The withdrawal threshold was expressed in grams.

Walking tract analysis

Walking tract analysis was performed in WT (*n*=9) and V30M mice (*n*=10) to compare functional recovery after injury. The hind feet of the mice were coated bilaterally with black nontoxic paint and the animals were then allowed to walk along a dark corridor, with ordinary white paper on the floor.

To calculate sciatic functional index (SFI) three classical parameters were determined both on the experimental and sham sides, namely: the distance from the heel to the third toe (print length), the distance from first to fifth toe (spreading of toes) and the distance from the second to the fourth toe (intermediary toe spreading). Footprints made at the beginning or the end of the trial were excluded and 3 values were measured from each run, for individual step parameter calculation. Tracks were analyzed according to the empirical equation developed by de Medinaceli et al., (1982) and adapted by Bain et al., (1989) and Hare et al., (1992): SFI = (-38.3 × print length factor) + (109.5 × toe spread factor) + (13.3 × intermediary toe spread factor) -8.8.

Immunohistochemistry (IHC) and double immunofluorescence

Sciatic nerve and L4-L6 dorsal root ganglia (DRG) from WT (*n*=5) and V30M mice (*n*=5), were excised, post-fixed in 10% formalin, embedded in paraffin blocks and cut longitudinally at 3 µm. Histoclear (National Diagnostics) was used to deparaffinate the sections that were thereafter hydrated in a descent alcohol series. Endogenous peroxidase activity was inhibited by 3% hydrogen peroxide in methanol and sections blocked with 4% fetal bovine serum and 1% bovine serum albumin in PBS. Primary antibodies used were: rabbit polyclonal anti-human TTR (1:1,000, DAKO), rabbit polyclonal anti-mouse TTR (1:1,500; Q-Biogen), goat polyclonal anti-TNF-α and IL-1β (1:25, Santa Cruz Biotechnology), rat monoclonal anti-F4/80 (1:50, Serotec), rabbit polyclonal anti-GAP-43 (1:1,000, Abcam), rabbit polyclonal anti-peripherin (1:1,500, Millipore) and rabbit polyclonal anti-ATF-3 (1:100, Santa Cruz Biotechnology). Secondary antibodies were biotinylated anti-rabbit, anti-rat (1:200, Vector) or anti-goat IgG (1:200, Abcam). ABC kit (Vector) with extravidin-peroxidase was used and labeling was performed with 3.3´-diaminobenzidine for antigen visualization. For densitometry analysis of the immunostained sections, 5 pictures at 20 X magnification were taken from different areas and quantified using the Image pro-plus 5.1 software. Results shown represent the area occupied by pixels corresponding to the substrate reaction color that is normalized relatively to the total image area, with the corresponding standard error of the mean (SEM).

For double immunofluorescence analyses in the PNS (*n*=4 mice per group), primary antibodies against human TTR (1:1,000), mouse TTR (1:1,500), mouse monoclonal anti-albumin (1:2,000, DAKO), mouse monoclonal anti-TAU (1:50, Calbiochem) and goat polyclonal anti-Oct-6 (1:25, Santa Cruz Biotechnology), were diluted using a blocking solution containing 10% fetal bovine serum, 1% bovine serum albumin and 0.5% Triton X-100. Secondary antibodies included donkey anti-rabbit Alexa Fluor 488, donkey anti-goat Alexa Fluor 568 and donkey anti-mouse Alexa Fluor 568 (1:1,000, Molecular Probes). Slides were mounted with Vectashield containing 4'.6-diamino-2-phenylindole (DAPI) (Vector) and visualized in a Zeiss Axio Imager or confocal microscope.

Congo red

The presence of amyloid deposits in PNS sections (*n*=5 WT and *n*=5 V30M mice) was investigated by Congo red staining according to the method of Puchtler and Sweat (1965). Briefly, deparaffinized tissues sections were incubated for 20 min with 0.01% NaOH in 80% ethanol saturated with NaCl followed by staining with 0.5% Congo red in the previous solution. The slides were then washed with tap water, stained with hematoxilin and

analyzed under polarized light. Amyloid was identified by the characteristic green birefringence, present in positive controls (stomach of old V30M mice).

ELISA IL-1β

The levels of IL-1β in injured and sham sciatic nerves from both WT (*n*=3) and V30M (*n*=3) mice were quantitatively determined by enzyme-linked immunosorbent assay (ELISA). Briefly, samples were homogenized in cell lysis buffer (Bio-Rad) containing a protease inhibitor cocktail (Bio-Rad) and 500 mM phenylmethylsulfonyl fluoride. After 3 times sonication with 10% power and 40% cycle, 4 s each, samples were centrifuged at 13,000 rpm for 15 min at 4ºC, supernatants collected and total protein concentration determined by the Bradford protein assay (Bio-Rad) for normalization. Sciatic nerves were diluted in 0.5% bovine serum albumin in PBS, as needed to a final concentration of 1.5 mg/mL.

Samples were run in duplicate and cytokine levels were analyzed according to the manufacturer's instructions (Bio-Rad Laboratories).

ELISA TTR

Determination of human TTR levels in plasma from V30M uninjured (*n*=6) and injured animals (*n*=6) was performed by ELISA, normalized to the total protein levels. A 96 well-plate was coated with rabbit anti-human TTR (Abcam) in 50 mM carbonate/bicarbonate buffer 9.6 pH, followed by application of TTR standards (2-37.5 ng/mL) and samples. After extensive washes, incubation with primary (sheep anti-hTTR, Abcam) and secondary antibodies (donkey anti-sheep, Sigma-Aldrich) was performed. SIGMAFAST^{TM} p-nitrophenyl phosphate tablets (Sigma-Aldrich) were used for color development and values obtained by measuring absorbance at 405 nm in a multiskan ascent microplate spectrophotometer (Thermo). Data were analyzed in 2nd-order polynomial quadratic equation, accordingly with guidelines from Alnylam Pharmaceuticals.

Real-time polymerase chain reaction (qPCR)

For messenger RNA (mRNA) extraction, injured and sham sciatic nerves from each strain (*n*=6 per group) were dissected free from surrounded tissues and frozen in RNA later (Ambion). Total mRNA was purified using RNeasy Mini columns (Qiagen), according to the manufacturer's instructions, and the quality of extracted mRNA was measured using Experion RNA StdSens Analysis Kit (Bio-Rad). Liver mRNA (*n*=5 per group) was purified using phenol extraction (Invitrogen). First-strand cDNA was synthesized using the SuperScript double-stranded cDNA Kit (Invitrogen) and subjected to qPCR, in duplicate,

using iQ Syber Green Super Mix (Bio-Rad). Reactions were analyzed on Bio-Rad iQ5 software. Primer sequences were designed using the Beacon software for the following genes: mouse *Ttr*, human *TTR*, *Il-1β*, *Il-6*, *Tnf-α*, *Il-10*, *Cxcl-3*, *Cxcl-2*, *Cxcl-12* and *Gapdh* (Annex). Calibration curves for target and housekeeping genes were constructed using 10-fold serial cDNA dilutions in duplicates and efficiency accepted between 95 and 117%. Differential expression was determined by the $2^{-\Delta\Delta CT}$ method using *Gapdh* as the housekeeping gene.

Flow cytometry

After mice anesthesia, injured sciatic nerves of both mouse models (*n*=9 per group) were dissected free from surrounding tissue and digested in fresh culture medium containing RPMI 1640 (Lonza), 10 mM HEPES, 5mg/mL bovine serum albumin, 1.6 mg/mL collagenase type IV, 200 µg/mL DNase I and 5 mM $CaCl_2$ (all from Sigma-Aldrich), 1 h at 37ºC. Single cell suspensions were filtered on a 70 µm cell strainer, pre-incubated with FcBlock reagent (BD Bioscience) and stained for their surface expression of CD11b and Ly6G (Biolegend). Characterization of neutrophil population was $CD11b^+$ and $Ly6G^+$. Samples were run on a FACS CALIBUR flow cytometer and analysis performed using FlowJo software.

Interference RNA experiment

For *in vivo* TTR-silencing studies, TTR or control siRNA (vehicle) were formulated into a lipid nanoparticle delivery system (Semple et al., 2010). WT (*n*=10) and V30M mice (*n*=10) were injected in the tail vein with mouse or human TTR siRNA, respectively, at a concentration of 1 mg/kg. A control group receiving vehicle was used, in both mouse models (*n*=9 WT and *n*=10 V30M). Two days after injection, sciatic nerve injury was performed as described above. Two days after injury, a re-injection was made and mice were sacrificed 7 days after the surgery. Sciatic nerve was processed as described above for IHC against mouse and human TTR and liver extracts used for TTR qPCR.

Immunogold labeling

Ultrathin sections of distal sciatic nerve stumps from V30M mice (*n*=4) were fixed on 0.2% glutaraldehyde and 2% paraformaldehyde, in phosphate buffer solution, for 2 h and subsequently embedded in LR white resin. Nerves were mounted onto nickel grids and after 10 min of sodium borohydrate treatment, grids were incubated in 2% gelatin for 20 min. Blocking in 2% bovine serum albumin in TBS for 1 h followed 5 min incubation in 20 mM glycine. Anti-human TTR (DAKO) diluted 1:100 in blocking buffer, was used as

primary antibody, overnight at 4ºC. In parallel, control sections without primary antibody were used. As secondary antibody, anti-rabbit immunoglobulins (British Biocell International, 1:20) coupled to 10 nm gold particles were used for 1 h at room temperature. Grids were subsequently washed 6 times for 10 min each in pure water and stained with uranyl acetate for 3 min and lead citrate for 30 s. Observation was performed in a Jeol JEM-1400 electron microscope.

Morphometric analysis

Morphometric studies were performed on the distal stump of injured sciatic nerves from WT (*n*=4) and V30M mice (*n*=4), 7 days after injury. A few mm length tissue was removed and fixed overnight in a 0.1 M phosphate buffer solution containing 1% glutaraldehyde and 4% paraformaldehyde. Tissues were washed for 30 min in 0.1 M phosphate buffer and post-fixed with 1% osmium tetroxide in 0.2 M phosphate buffer for 2 h. After a new wash of 30 min, the tissue was dehydrated using a series of graded alcohols and propylene oxide and finally embedded in epon. Half µm thick transverse sections were cut (using SuperNova Reichest Leica ultramicrotome) and stained with 1% toluidine blue, for 15 s, in an 80°C heating plate, before being examined on a light microscope.

Using semithin sections, total counts of myelinated fibers were carried out per animal, by counting 40 X magnified photographs covering the whole nerve area. To determine the density of unmyelinated fibers, ultrathin transverse sections were cut and stained with lead uranyl acetate. Sections were then mounted on mesh grids and visualized on a Zeiss 10C TEM. For each animal density analysis, 20 non-overlapping photographs (7,000 amplification), corresponding to 7052 μm^2 of each ultrathin section, were taken and fibers counted.

Statistical analysis

Quantitative data are expressed as mean ± standard error of the mean (SEM) and were analyzed by Student t-test, one-way or two-way ANOVA, followed by Bonferroni post-test. Statistical significance was established for $*p<0.05$, $**p<0.01$, $***p<0.001$.

Results

Sciatic nerve injury results in increased local *TTR* mRNA expression in the V30M mouse model

The expression of low levels of *TTR* mRNA in the sciatic nerve, in basal conditions, both in TTR V30M transgenic and WT mice was recently described (Murakami et al., 2010). In our study we first assessed expression of *TTR* mRNA in the sciatic nerve upon injury by ligation and found that one day post-injury, *TTR* mRNA expression in the nerve was downregulated both in WT and V30M mice when compared to the respective shams (Figure 1A). However, at 7 days post-lesion, expression of *TTR* mRNA in V30M mice was significantly upregulated as compared to the respective sham nerves, in contrast with WT mice where differences were not found (Figure 1A). Next, we investigated whether the increased *TTR* mRNA levels in the V30M mice resulted in TTR deposition in the nerve tissue. By SQ-IHC of injured and sham nerves of both mice strains, 7 days following damage, we found that nerve injury led to TTR immunoreactivity in both nerve segments being more prominent in the distal stump (Figure 1B). However, TTR relative concentration change was higher in the V30M mice as they presented a TTR fold change of 74 in the distal portion *versus* 26 fold in the WT animals, when compared to the respective sham nerves (Figure 1B). Importantly, WT mice have similar levels of TTR in plasma (Oliveira et al., 2011), when compared to V30M mice, and therefore this fold differences are not due to different copies of the human gene being expressed.

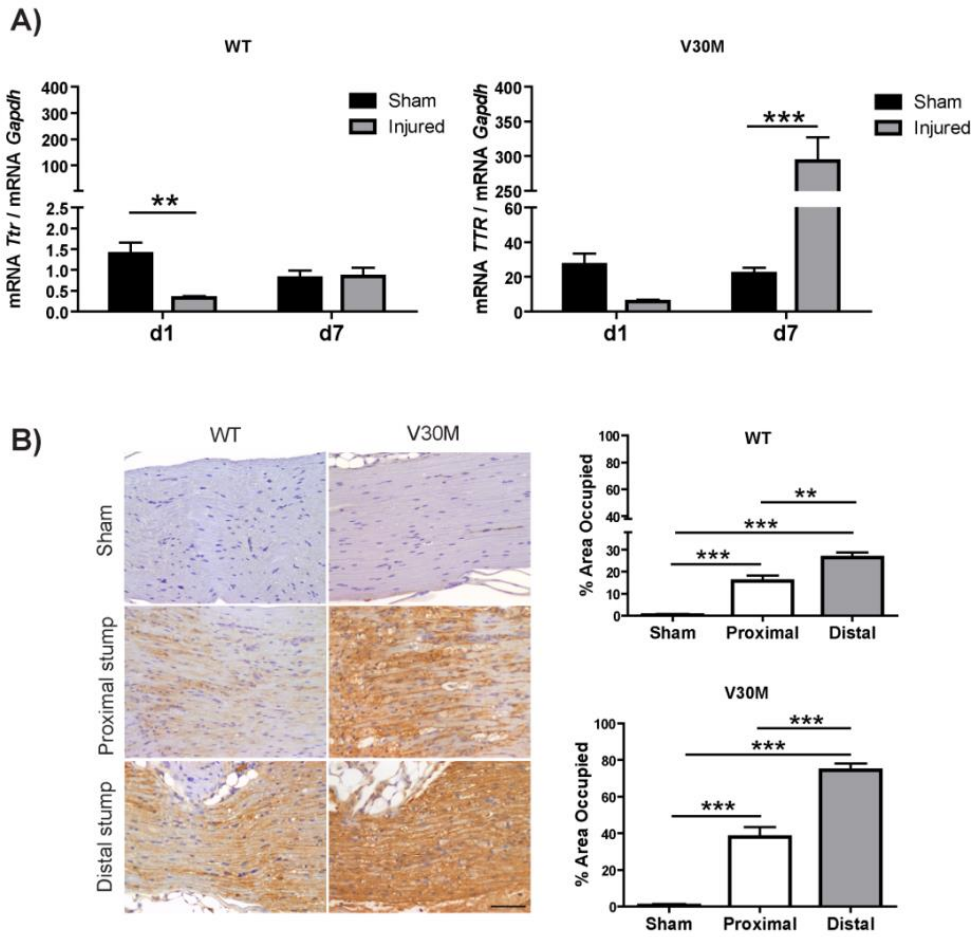

Figure 1 – Sciatic nerve injury leads to local upregulation of TTR V30M expression. A) Histograms represent *TTR* mRNA levels in the sciatic nerve of WT (left chart) and V30M mice (right chart), 1 and 7 days after lesion (*n*=6), as compared with sham nerves (*n*=6). **B)** Representative SQ-IHC against mouse (left panels) and human TTR (right panels) in the proximal and distal stumps, 7 days after sciatic nerve injury, as compared with respective sham nerves. Charts represent quantification of immunohistochemical images (*n*=5 V30M and *n*=5 WT mice; scale bar 100 µm; ***p*<0.01 and ****p*<0.001).

TTR V30M deposition in the PNS is tissue specific and locates at the extracellular matrix

Next, we wondered if the striking TTR deposition after injury in V30M mice was related to local synthesis and tissue reactivity or could derive from blood contamination. We started by determining if systemic TTR production was recapitulating the striking increase in *TTR* mRNA found in nerves of V30M mice. We found TTR plasma levels of injured and naïve V30M mice to be similar (Figure 2A), indicating that liver does not react to this injury model. Using double immunofluorescence and an antibody for albumin, an abundant

plasma protein, we observed that in WT mice the vast majority of TTR being present in the tissue derives from blood contamination (Figure 2B, Merge). However, the partial colocalization between albumin and TTR V30M, indicated that only some TTR V30M protein reached the nerve via the blood stream (Figure 2B, Merge). To confirm that, we further used immunogold for injured nerves of V30M mice and found TTR aggregates in the extracellular space, in close association with collagen fibrils (Figure 2C), indicating TTR deposition in V30M nerve to be tissue specific. However, the tissue was negative for amyloid deposits (data not shown), probably because these aggregated TTR forms are not sufficiently mature to appear as Congophilic deposits.

It was previously shown that siRNA targeting *TTR* expression by the liver is able to remove TTR deposits from tissues (Alvarez et al., 2010). Thus, by using this tool, and silencing *TTR* expression specifically in the liver (99% reduction of *TTR* synthesis, Figure 2D) we were able to prevent TTR deposition after injury (Figure 2E). Moreover, several cells in the sciatic nerves of V30M mice, but not of WT, still present intracellular TTR staining (Figure 2E, right panel). These cells showed colocalization of TTR with Oct-6 (Figure 2F), a standard marker for differentiated Schwann cells.

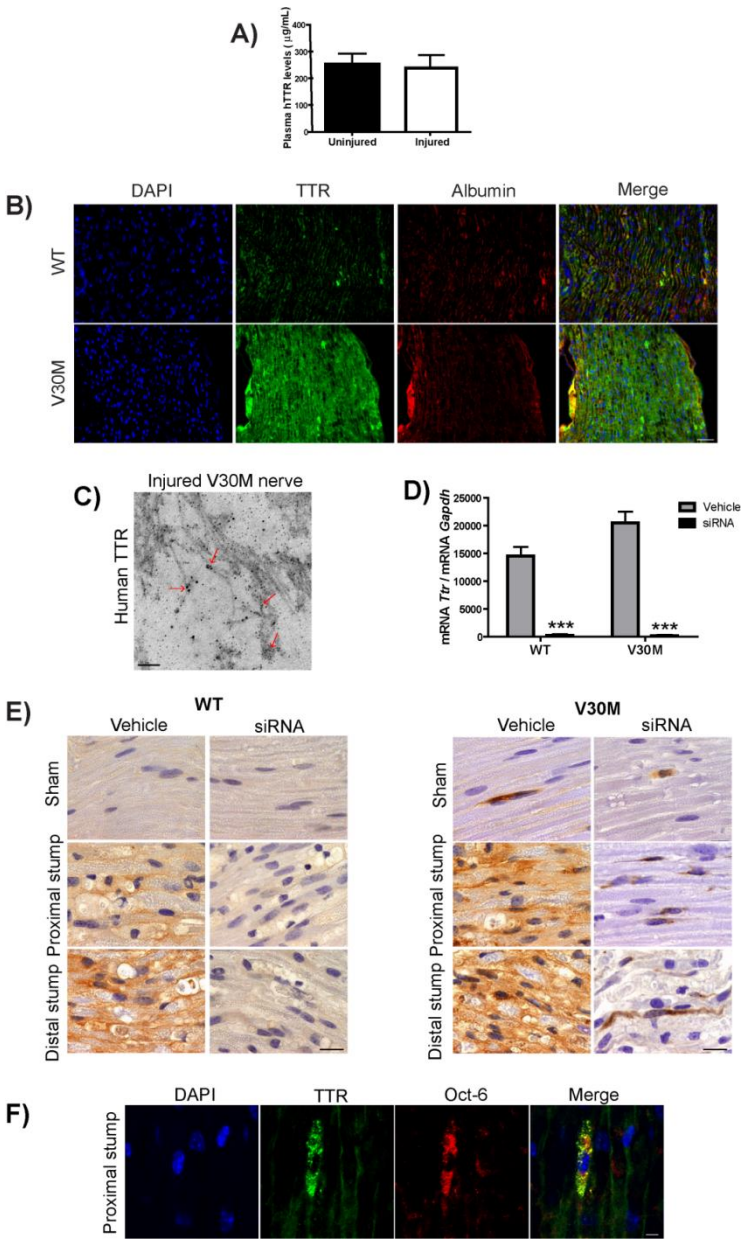

Figure 2 – TTR V30M present in the sciatic nerve after injury, derived for a minor extent from blood and also from local synthesis by Schwann cells. A) TTR V30M plasma levels in uninjured and injured animals (7 days after injury, *n*=6 each). **B)** Double immunofluorescence of TTR (green) and albumin (red). Nuclei stains blue with DAPI. Merged panel shows colocalization in yellow. Scale bar 50 µm, *n*=4. **C)** Representative image obtained by electron microscopy showing TTR V30M aggregates at the nerve extracellular space and in close association with collagen fibrils (pointed by red arrows, *n*=4). Scale bar 100 nm. **D)** Chart represents *Ttr* WT (*n*=5) and *TTR* V30M mRNA (*n*=5) expressed in liver after treatment with siRNA or vehicle (***p<0.001). **E)** Representative pictures obtained with IHC for TTR in sham, proximal and distal stumps of sciatic nerves from WT (left panel, *n*=10) and V30M (right panel, *n*=10) mice receiving siRNA or vehicle (*n*=9 WT and *n*=10 V30M). Scale bar 20 µm. **F)** Double immunofluorescence between TTR (green) and Oct-6 (red) in V30M nerve, denoting colocalization (yellow) and TTR intracellular staining. Superposition of the labels, with DAPI, is shown (merge, *n*=4). Scale bar 5 µm.

Additionally, in the V30M mice, sciatic nerve injury triggered TTR deposition in ipsilateral and contralateral L4, L5 and L6 DRG (Figure 3A), suggesting the importance of a local stimulus in the PNS for mutant TTR deposition. Since TTR deposits in DRG do not colocalize with albumin or TAU (Figure 3B and 3C, top panel), we conclude that they were tissue specific and located in the extracellular space. Also, using TAU as a marker for neurons in the sciatic nerve, TTR presence in axons was ruled out (Figure 3C, bottom panel).

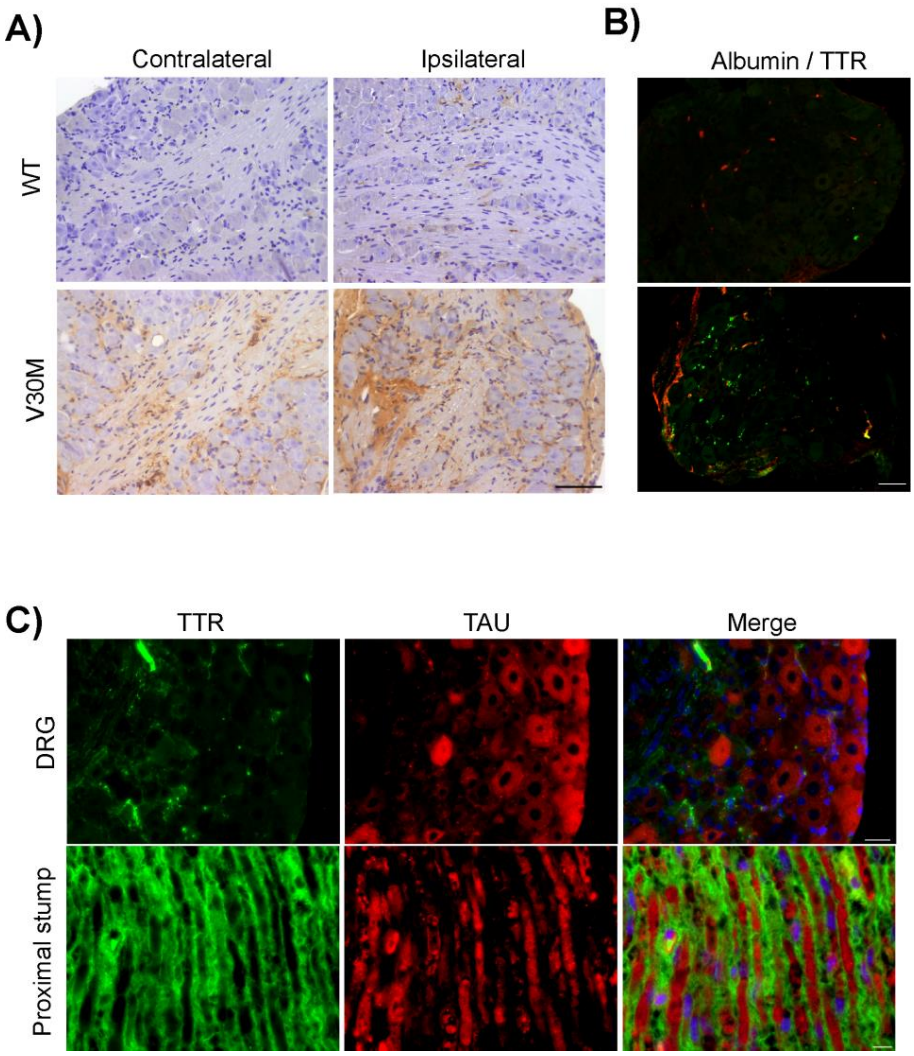

Figure 3 – Nerve injury leads to TTR deposition in lumbar DRGs of V30M mice. A) Representative pictures from IHC for TTR in WT and V30M lumbar DRGs, ipsilateral and contralateral to the injury side, 7 days after damage (*n*=5 WT and *n*=5 V30M). Scale bar 100 µm. **B)** Merged images of double immunofluorescence between TTR (green) and albumin (red), showing that TTR V30M deposition in DRG is not derived from blood contamination (*n*=4 per group). Scale bar 50 µm. **C)** Double immunofluorescence of TTR and TAU, a neuronal marker, in DRG (top panel, scale bar 20 µm) and proximal nerve stump (bottom panel, scale bar 10 µm), ruling out TTR localization in neurons after injury (*n*=4 per group).

In response to nerve injury, V30M mice present downregulation in the innate immune response when compared to WT mice

It has been shown that, after peripheral nerve injury, dedifferentiated Schwann cells produce a pro-inflammatory response which is followed by infiltration of immune cells important for tissue recovery (Ydens et al., 2013). In our study, we started by characterizing the inflammatory infiltrate after injury in both mice strains. Overall, using flow cytometry and SQ-IHC we saw a decrease in the frequency of neutrophils (Figure 4A) and macrophages (Figure 4B) in V30M injured nerves when compared with WT nerves, 7 days after lesion.

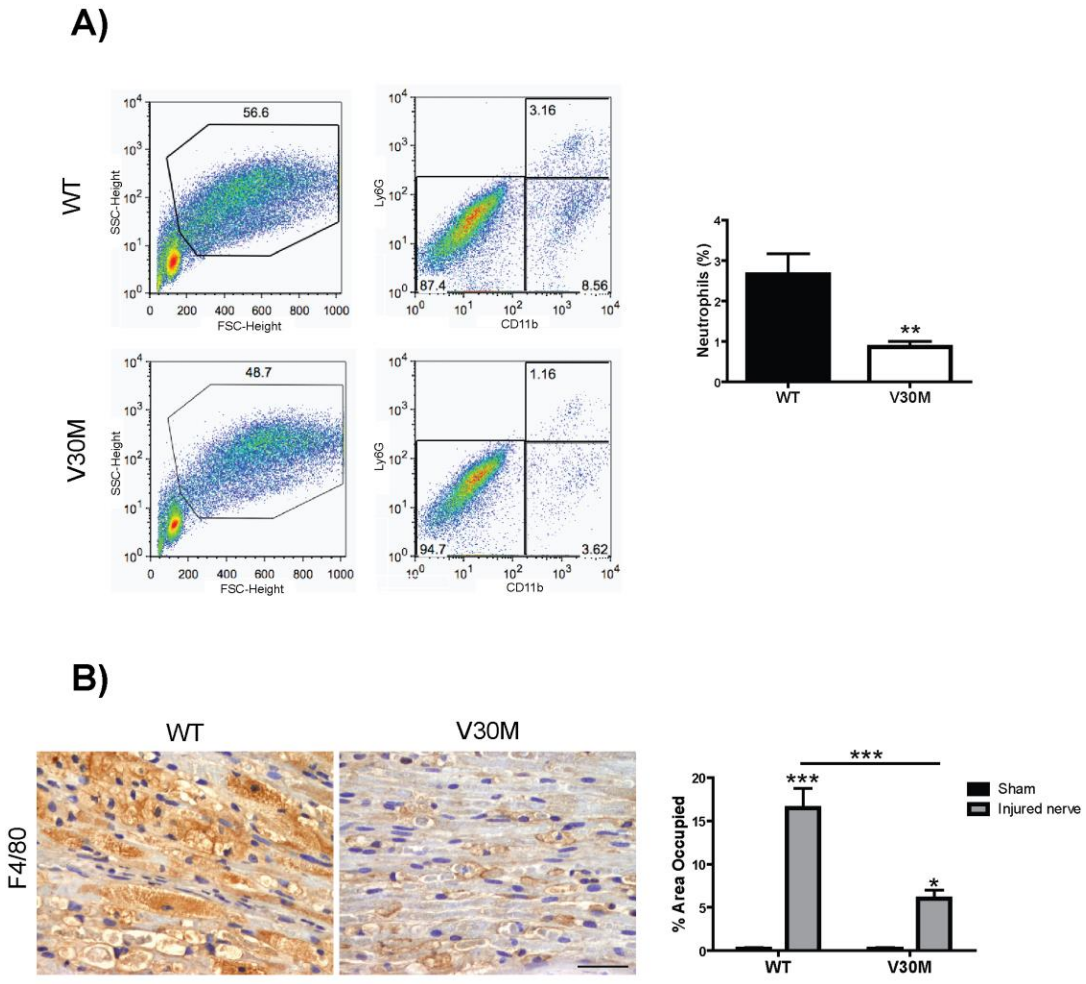

Figure 4 – Decreased innate immune cell infiltration, after injury in the V30M mouse model. **A)** Seven days following nerve injury, cell suspension was analyzed by flow cytometry (*n*=9 mice/group) and the frequency of neutrophils calculated, as shown in the histogram. **B)** Representative SQ-IHC for F4/80, a macrophage marker, in injured sciatic nerves of WT (left panel, *n*=5) and V30M mice (right panel, *n*=5). Scale bar 50 µm. Chart represents the quantification of immunohistochemical images. **p*<0.05, ***p*<0.01 and ****p*<0.001.

Since V30M mice showed a lower frequency of innate cells in the injured sciatic nerve, we next asked if also the production of cytokines was diminished. We found that, after nerve injury, V30M animals had lower expression and production of TNF-α (Figure 5A and 5B) and IL-1β (Figure 5C and 5D), when compared to WT mice. Additionally, when we looked for the expression of another pro-inflammatory cytokine such as *Il-6* no differences were observed when comparing the two mouse strains (Figure 5E). Interestingly, regarding the expression of *Il-10*, an important anti-inflammatory cytokine (Saraiva and O'Garra, 2010), we saw substantial upregulation of this molecule earlier after nerve injury in V30M, in contrast with WT mice (Figure 5F).

Considering the observation that in V30M mice decreased frequency of infiltrating innate cells in the nerve occurs we hypothesized if important cues for their recruitment towards the nerve were also diminished. We started by analyzing the expression of *Cxcl-2*, an essential chemokine for the recruitment of neutrophils (Haraguchi et al., 2012), *Cxcl-3*, a chemokine important for migration and adhesion of monocytes (Smith et al., 2005) and *Cxcl-12* that contributes to neurite growth, axon regeneration and mobilization of hematopoietic cells (Sheu et al., 2012; Heskamp et al., 2013). Indeed, we found that expression of *Cxcl-3*, *Cxcl-2* and *Cxcl-12* was downregulated in ligated V30M nerves compared to those from WT mice (Figure 5G), 7 days after injury. Moreover, the expression of toll-like receptor 1 (*Tlr-1*) that is typically strongly induced after injury (Goethals et al., 2010), was also decreased in V30M mice (Figure 5G). Together, these results indicate an overall decreased inflammatory immune response after nerve injury in the V30M mouse model in contrast with WT mice.

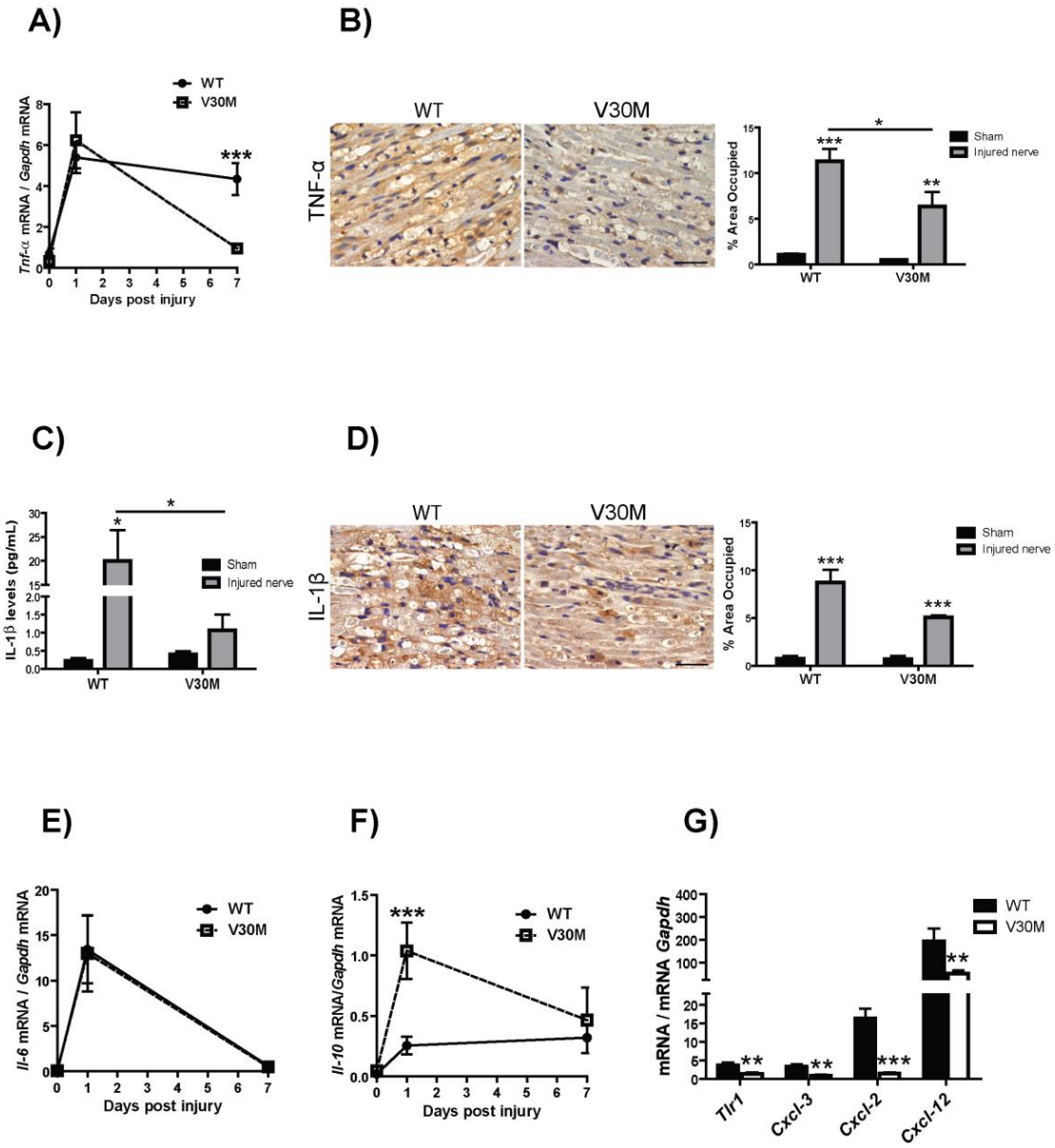

Figure 5 – Decreased innate immune response, after nerve injury, in V30M mice. A) Histogram represents *Tnf-α* mRNA levels, assessed by qPCR, 1 and 7 days after injury in the WT (*n*=6) and V30M mice (*n*=6). **B)** Representative SQ-IHC for TNF-α, 7 days after nerve injury, in both mouse models (*n*=5 each, scale bar 50 μm). Chart represents the quantification of immunohistochemical images. **C)** Levels of IL-1β determined by ELISA, in injured and sham nerves of both mice strains, 7 days after nerve damage (*n*=3 each). **D)** Representative SQ-IHC of IL-1β, 7 days after nerve injury, in both mouse models (*n*=5 each, scale bar 50 μm). Chart represents the quantification of immunohistochemical images. **E)** and **F)** Histograms represent *Il-6* and *Il-10* mRNA levels, assessed by qPCR, 1 and 7 days after injury in the WT (*n*=6) and V30M mice (*n*=6). **G)** Histogram represents *Tlr-1, Cxcl-3, Cxcl-2* and *Cxcl-12* mRNA levels, assessed by qPCR, 7 days after injury in the WT (*n*=6) and V30M mice (*n*=6). **p*<0.05, ***p*<0.01, ****p*<0.001.

After nerve injury, V30M mice present impaired sensory and functional recovery, as compared to WT mice

To compare the sensory response of WT and V30M mice after injury, we performed the hot-plate and Von Frey tests. Hot-plate, a standard procedure to measure nociceptive response to a noxious thermal stimulus was carried out on day 0, 2 and 6 days after injury. In both time points post-injury, WT mice had a quicker response to thermal stimulus compared to V30M mice that took in average 29 s to respond (Figure 6A), indicating severe hypoalgesia to heat.

Five days after injury, mechanical allodynia was assessed with Von Frey hair stimulation and the nominal force necessary for mice to shake or lick its paw was registered. As shown in Figure 6B, even before any nerve injury the values for mechanical pain hypersensitivity were different between the two strains. More specifically, V30M mice were less sensitive to mechanical touch stimulus. When the mechanical stimulus was applied on the plantar surface of the nerve-injured paw, a significant decrease in the paw withdrawal threshold was observed in both strains, as mice developed mechanical allodynia to a normally innocuous stimulation with the Von Frey filaments (Figure 6B). However, V30M mice tended to be less sensitive than WT mice (Figure 6B), suggesting reduced neuropathic pain after nerve lesion.

Finally, recovery of neurological function was also assessed by measuring the sciatic functional index (SFI) at day 0, 2 and 6 days after injury (Figure 6C). No differences were found at day 0 among the two mice groups but after 2 days, a significant difference was revealed as V30M animals presented locomotor deficits compared to WT mice (Figure 6C). Although not statistically significant, a trend for poor functional recovery of V30M mice was also noted 6 days after nerve injury (Figure 6C).

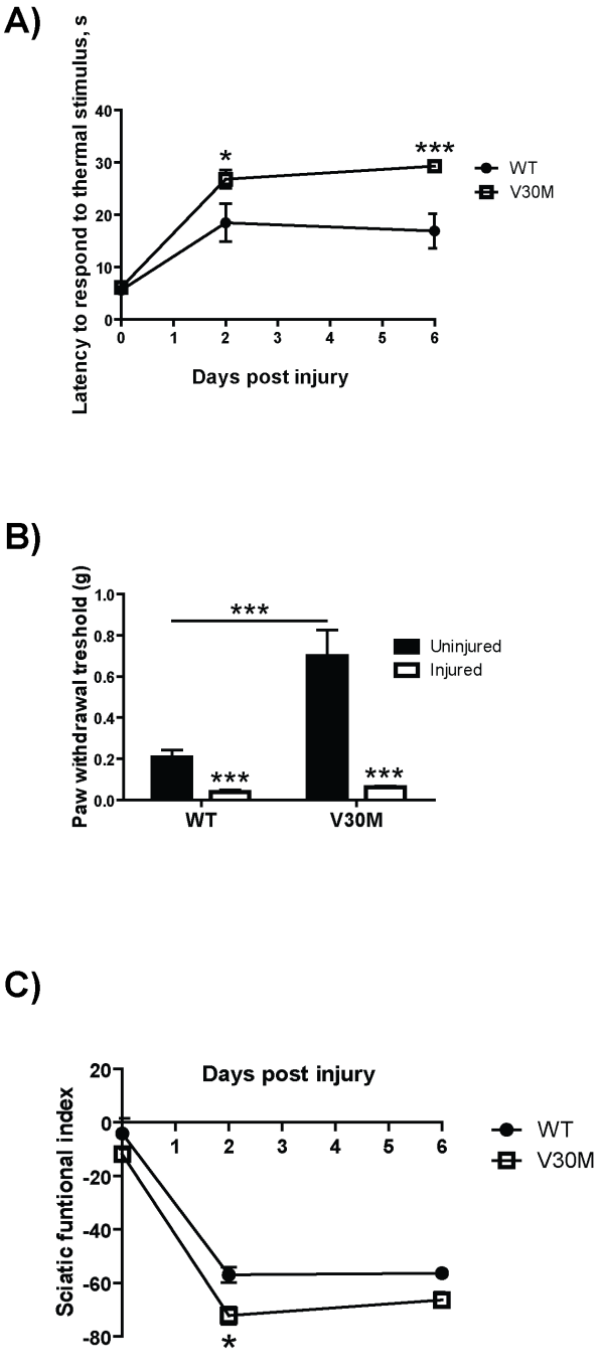

Figure 6 – Delayed sensorimotor recovery after injury in V30M mice. A) Nociception evaluation with the hot-plate test, showing severe hypoalgesia in V30M mice (*n*=10), as compared with WT (*n*=9), 2 and 6 days after injury. **B)** Paw withdrawal threshold evaluated by the Von Frey test, 5 days after sciatic nerve injury (*n*=9 WT and *n*=10 V30M mice), denoting neuropathic pain and a late response in V30M mice before injury. **C)** Walking tract analysis evaluation (*n*=9 WT and *n*=10 V30M mice) with poor sciatic functional index regarding V30M mice. **p*<0.05 and ****p*<0.001.

Nerve injury leads to reduced fiber density and lower levels of regeneration associated molecules

To evaluate the degree of post-injury neurodegeneration, we performed morphometric analysis of the distal stump of ligated nerves *versus* sham nerves, in WT and V30M mice. Thus, we started by analyzing the density of myelinated fibers and found a decrease of 78% and 93% in WT and V30M injured nerves, respectively, as compared with shams (Figure 7A). Using electron microscopy, unmyelinated fiber density was determined indicating a reduction of 90% and 98% in injured nerves of WT and V30M, respectively, in relation to shams (Figure 7B). Moreover, when comparing fiber density between sham nerves, a significant difference was detected, suggesting that mutated non-aggregated TTR or the presence of a heterologous human TTR in the nerve of V30M mice decreases fiber density, even in the absence of an injury stimulus (Figure 7A and 7B).

Since 7 days post-injury is near the mid-point of active axonal regrowth (Arthur-Farraj et al., 2012), we also investigated levels of regenerating factors in injured nerves of V30M mice as compared with WT. Thus, we chose GAP-43, peripherin and ATF-3 as growth association markers since their activation after nerve injury and contribution for nerve regeneration were previously described (Sensenbrenner et al., 1997; Pearson et al., 2003; Girard et al., 2008). As shown in Figure 8, labeling of all biomarkers was significantly higher in WT injured nerves as compared with V30M, suggesting a significant delay in axonal regeneration in the FAP mouse model. Nadeau et al., (2011) showed that the presence of neutrophils is not essential for nerve regeneration; however, macrophages arising from resident endoneurial population (Mueller et al., 2003) and from circulating blood monocytes are necessary for neural repair after injury (Barrette et al., 2008; Niemi et al., 2013). Therefore, it is possible that the phenotype observed for V30M mice regarding regeneration results from lower macrophage infiltration to their injured nerves.

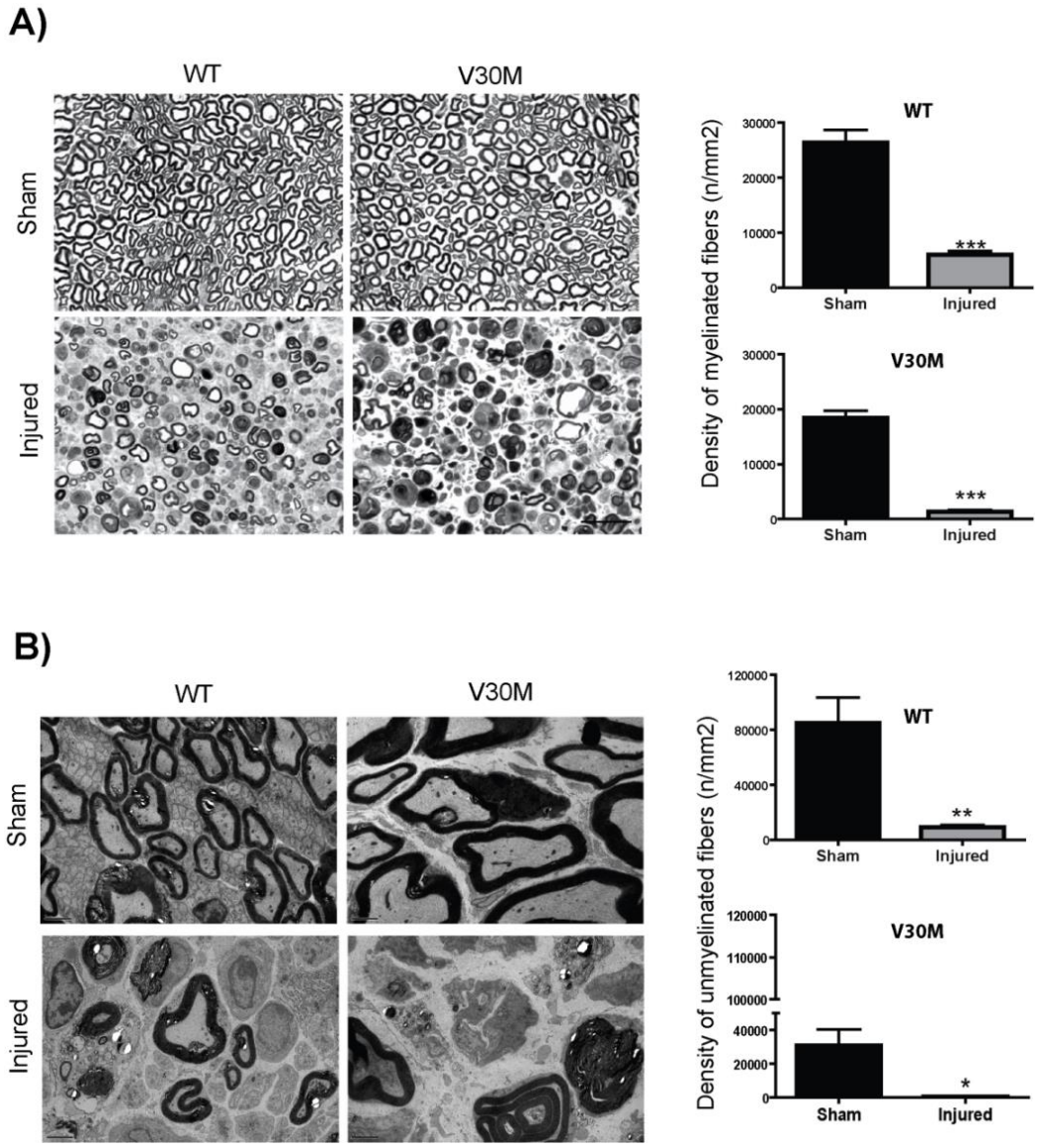

Figure 7 – Prominent nerve degeneration and lower regeneration ability in V30M mice, after injury. A) Morphometric analysis of distal sciatic nerve stumps, 7 days after injury (*n*=4 each strain). Representative images from semithin sections showing decrease in myelinated fibers after injury in both WT and V30M mice. Scale bar 20 µm. **B)** Representative electron microscopy images showing fewer unmyelinated fibers after injury, in both mouse strains. Histograms indicate the corresponding fiber densities (**p*<0.05, ***p*<0.01 and *** *p*<0.001).

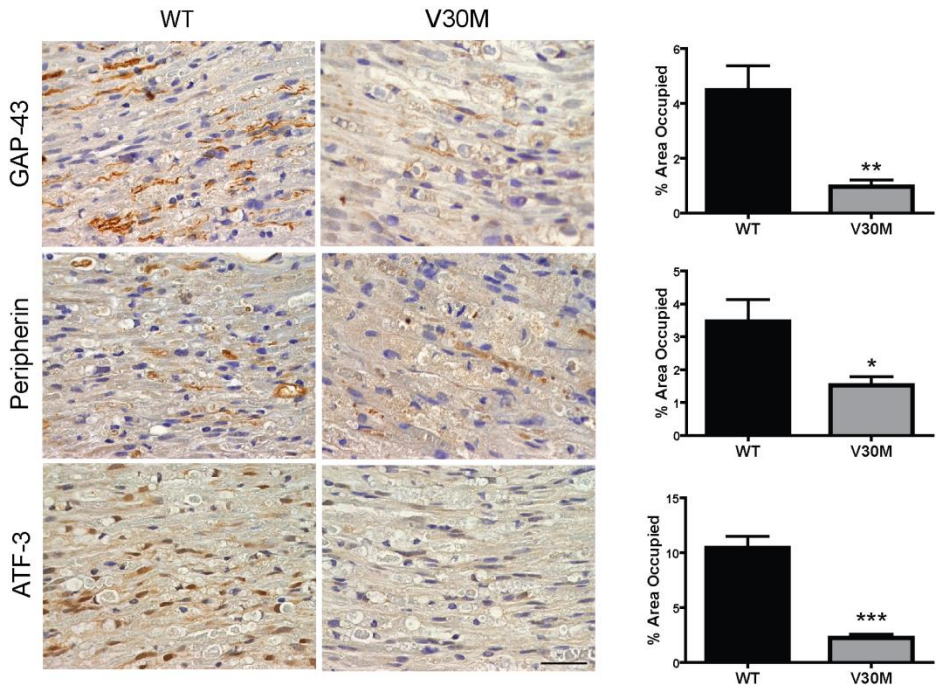

Figure 8 – Impaired activation of regeneration associated molecules in sciatic nerves of V30M mice. Representative SQ-IHC for GAP-43, peripherin and ATF-3, 7 days after injury, in WT (*n*=5) and V30M mice (*n*=5). Scale bar 50 µm. Charts represent the quantification of immunohistological images (**p*<0.05, ***p*<0.01, ****p*<0.001).

Discussion

FAP is a devastating disorder driven by the accumulation of TTR in its amyloidogenic conformation in the PNS (Coimbra and Andrade, 1971b). However, the full spectrum of FAP´s pathophysiology has not been completely characterized. Dissection of the cellular pathways involved in this disease is of utmost importance for the development of new treatment strategies. In FAP patients, with progress of the disease, there is an increase on the inflammatory response associated with higher TTR deposition in the peripheral nerve (Sousa et al., 2001b). Based on this finding, our hypothesis was that inflammation would lead to TTR aggregation and deposition. To answer this question we induced nerve injury in the FAP mouse model carrying the V30M mutation but lacking TTR deposits in the PNS at a basal state.

In a basal situation (no injury), the expression of *TTR* V30M in the sciatic nerve by Schwann cells has been already reported by Murakami et al., (2010). However, our study shows that upon sciatic nerve injury there is an increased in the expression of local *TTR* V30M by Schwann cells, leading to increase deposition as compared with WT mice. Furthermore, we observed that triggering of *TTR* V30M expression was related with the inflammatory threshold since by day 7 following injury, inflammation was considerably lower compared to day 1, but still higher than in sham V30M nerves. Sham nerves of both V30M and WT mice presented a similar inflammatory response; however, only synthesis of *TTR* V30M was upregulated after injury, thus the altered inflammatory profile in V30M mice after nerve lesion can correlate with the TTR mutation itself.

Schwann cells have the ability to regulate local immune responses by secreting cytokines and chemokines thus amplifying the local immune response (Gaudet et al., 2011; Ydens et al., 2013). Typically, in V30M human FAP nerve biopsies, despite the continuous cytokine production, no immune inflammatory cellular infiltrate is observed around TTR aggregates/amyloid deposits thus contributing to slow down TTR clearance and aggravating the pathophysiology of the disease (Misu et al., 1999; Sousa et al., 2001b). In line with this observation, in our V30M model we found that, 7 days post-injury, neutrophil and macrophage infiltration is lower when compared to WT mice. Moreover, it is possible that a non-optimal activation of Schwann cells occurred since, after injury, decreased expression of *Tlr-1*, pro-inflammatory cytokines and chemokines was observed, thus culminating in a diminished immune cellular activation and infiltration in V30M nerves. In accordance with our results, in nerves of FAP patients, Schwann cells are impaired in their ability to express chemokines and neurotrophic factors important to drive tissue regeneration, contributing this way for neuronal dysfunction present in the disease (Sousa et al., 2001b). Additionally, in support of an impaired immune activation, we found a peak

of *Il-10* expression in V30M mice, but not WT mice, early after nerve injury, which could be a hint on the mechanism by which inflammation is hampered in V30M mice in a later time point. In fact, increased levels of IL-10 after TTR fibril deposition in FAP biopsies was noticed (Sousa et al., 2005).

It is known that different pH conditions, namely acidified environments, promote TTR aggregation (Colon and Kelly, 1992; Lai et al., 1996; Noborn et al., 2011). Also, due to its intrinsic unstable quaternary fold, TTR V30M mutant is prone to dissociation into toxic aggregates (Quintas el al., 2001; Sousa et al., 2001a). Additionally, levels of heparan sulfate proteoglycans increase after injury (Murakami and Yoshida, 2012) and have been implicated in the TTR aggregation pathway (Noborn et al., 2011; Gonçalves et al., 2013). Taken together, it is possible that nerve injury results in strong non-fibrillar TTR deposition in the peripheral nerves of V30M mice due to local increase of heparan sulfate promoted by the inflammatory insult and the acidic environment.

Considering that inflammation is an important feature for tissue regeneration (Gaudet et al., 2011; Niemi et al., 2013), we questioned if in our system axonal growth was compromised in V30M mice. We found that V30M mice not only showed less sensorial response but also presented augmented neurodegeneration with decrease densities of both myelinated and unmyelinated fibers, accompanied by decreased levels of regeneration markers. Importantly, it should be noted that fiber loss is likely related to the conformational structure of mutated TTR and/or with non-fibrillar TTR deposition. In fact, Koike et al., (2004) showed that V30M FAP patients with late-onset disease have extensive nerve fiber loss in spite of small amount of amyloid deposition. Altogether, these results indicate that axons degenerate even when only small amyloid deposits are present, supporting cytotoxicity from non-fibrillar TTR (Koike et al., 2004). Differences in neuropathic pain and thermal sensitivity, observed in the present work, could be explained by reduced neutrophil infiltration in V30M injured nerves (Austin and Moalem-Taylor, 2010).

In our model, more than a consequence of absolute increased levels of *TTR* production in nerve, tissue degeneration seen in transgenic mice could also be the direct effect of the V30M mutation. Accordingly, we described for the first time sensory and nerve morphometric differences in naïve V30M mice as compared to WT, which is indicative of a specific phenotype associated with the V30M mutation. In contrast, in WT mice, TTR has been shown to be important in sciatic nerve regeneration as compared with TTR-null mice (Fleming et al., 2007).

Senile systemic amyloidosis (SSA), characterized by TTR WT fibrils deposition in the heart, has been shown to affect 25% of the elderly population (Pitkänen et al., 1984). In a mouse model of SSA, prior to TTR WT local deposition, the heart presents a robust

immune inflammatory transcriptional profile (Buxbaum et al., 2012), which supports previous data that showed local transcription of inflammatory mediators in nerve biopsies from V30M asymptomatic carriers (Sousa et al., 2001b). Based on these observations, and on our study, it is fair to speculate that FAP and SSA patients may lay down TTR in response to multiple subclinical inflammatory traumas and that inflammation might precede TTR deposition in tissues.

In summary, by promoting an inflammatory local insult we were able to show for the first time TTR V30M expression and deposition in the sciatic nerve of a mouse model that usually depicts TTR deposition only in the gastrointestinal tract and skin. Overall, we provide evidence that inflammation plays an important role at the initiation of FAP pathogenesis. This novel finding paves the way to new treatment strategies not only for this disease but also for other neurodegenerative disorders where neuroinflammation play an important role.

Acknowledgements

This work was funded by FEDER funds through the Operational Competitiveness Program – COMPETE and by National Funds through FCT – Fundação para a Ciência e a Tecnologia under the projects FCOMP-01-0124-FEDER-022718 (PEST-c/SAU/LA0002/2011 and PTDC/SAU-ORG/111313/2009), fellowship to NPG (SFRH/BD/74304/2010) and to MTC (ON2-201302-ND-III). The present work was also sponsored by POPH/FSE QREN program.

The authors would like to thank Dr. Mónica Sousa, Dr. Paula Sampaio, Rui Fernandes and Paula Gonçalves from IBMC for helpful discussions and support with confocal, electron microscopy and paraffin tissue processing, respectively. siRNA reagents were kindly provided by Alnylam Pharmaceuticals.

Chapter III

Interleukin-1 signaling pathway as a therapeutic target in transthyretin amyloidosis

Interleukin-1 signaling pathway as a therapeutic target in transthyretin amyloidosis

Nádia Pereira Gonçalves[1,2,3], Paulo Vieira[4], Maria João Saraiva[1,2,3]

1) Instituto de Inovação e Investigação em Saúde (I3S), Universidade do Porto, Portugal
2) Molecular Neurobiology, IBMC – Instituto de Biologia Molecular e Celular, Porto, 4150-180 Portugal
3) Instituto de Ciências Biomédicas de Abel Salazar (ICBAS), Universidade do Porto, Porto, 4050-313 Portugal
4) Unité du Développement des Lymphocytes, Département d'Immunologie, Institut Pasteur, Paris, 75724 CEDEX 15 France

Running title: IL-1 as a novel target in FAP

Abstract

Inflammation is a key pathological hallmark of several neurodegenerative disorders including Alzheimer's disease, Parkinson's disease and Familial Amyloidotic Polyneuropathy (FAP). Among all inflammatory cytokines associated with FAP, IL-1β in particular has been implicated in playing a key pathogenic role. In the present study we sought to investigate whether blocking IL-1β signaling provides disease-modifying benefits in an FAP mouse model.

We assessed the effect of subchronic administration of Anakinra, an IL-1 antagonist, on FAP pathogenesis *in vivo*, using real-time polymerase chain reaction (qPCR), semi-quantitative immunohistochemistry (SQ-IHC), western blot and nerve morphometric analyses. We found that treatment with Anakinra prevents transthyretin (TTR) extracellular deposition in sciatic nerve, protecting unmyelinated nerve fibers from aggregate-induced degeneration. Moreover, Anakinra administration significantly suppressed IL-1 signaling pathway and inhibited apoptosis and endoplasmic reticulum or nitrosative stress. The present work highlights the relevance of the IL-1 signaling pathway in the pathophysiology of FAP. Our results bring to light the importance of non-amyloid targets in the therapeutic strategies for this disorder. Thus, we propose the use of Anakinra as a potential therapeutic agent for TTR-related amyloidosis.

Introduction

Inflammation is an essential protective response being a major cofactor involved in the pathogenesis of numerous conditions that are often considered non-inflammatory such as diabetes (Ehses et al., 2009), atherosclerosis, cancer or amyloid related disorders (Hallegua and Weisman, 2002). Different neurodegenerative diseases share an excessive activation of common pathogenic pathways, including overexpression of tumor necrosis factor α (TNF-α) and interleukin-1β (IL-1β) as in Alzheimer´s, Huntington's, or Parkinson´s disease (Pizza et al., 2011). Inflammation is also observed in Familial Amyloidotic Polyneuropathy (FAP) (Sousa et al., 2001b), an autosomal dominant hereditary disorder characterized by the extracellular deposition of mutant transthyretin (TTR) aggregates and amyloid fibrils, particularly in the peripheral nervous system (PNS). Accumulation of TTR aggregates in the PNS leads to peripheral neuropathy, with reduced nerve fiber density and destruction of endoneurial blood vessels (Coimbra and Andrade, 1971b).

TTR is mainly expressed by the liver and the choroid plexuses of the brain (Soprano et al., 1985) and more than one hundred single point mutations have been described for TTR promoting amyloidogenesis (http://amyloidosismutations.com). The most common TTR mutation in FAP results from an exchange of a methionine for a valine at position 30 – TTR V30M (Saraiva et al., 1984). The mechanism underlying TTR amyloid fibril formation is not fully understood. It has been proposed that fibrillogenesis requires dissociation of TTR homotetrameric structure into misfolded monomers which self-assemble forming non-fibrillar oligomers, protofibrils and finally mature amyloid fibrils (Colon and Kelly, 1992; Quintas et al., 2001).

It has been shown that oligomeric and fibrillar TTR species bind to the receptor for advanced glycation end products (RAGE) leading to activation and nuclear translocation of nuclear factor κB (NF-κB) (Sousa et al., 2000b), which is known to bind as dimers to promoters and enhancers of a variety of inflammation-associated molecules and oxidative stress intermediaries, regulating their transcription (Collins et al., 1995; Rhee et al., 2007). The pro-inflammatory cytokines will in turn promote NF-κB activation (Hayden and Ghosh, 2004) with consequent upregulation of RAGE expression via the NF-κB binding elements in the RAGE promotor (Li and Schmidt, 1997) ending up in a feedback loop that prompts disease, with destructive cell responses. Pro-inflammatory mechanisms are likewise upregulated in FAP, especially in endoneurial axons, with increased expression of TNF-α, macrophage colony-stimulating factor and IL-1β, since earlier stages of disease and increasing with the ongoing neurodegenerative process (Sousa et al., 2001a; Sousa et al., 2001b). IL-1 exists in two forms: IL-1α and IL-1β exerting its pleiotropic effects by binding to the IL-1 type I receptor. IL-1β is a primary regulator of inflammatory and immune

responses being also involved in hypotension, fever, neutrophilia, thrombocytosis and in the production of acute-phase proteins (Gabey et al., 2010). This cytokine can induce apoptosis of different types of cells and stimulate inducible nitric oxide synthase leading to stress responses (Schwarznau et al., 2009). IL-1 receptor antagonist (IL-1Ra) is a member of the IL-1 family and is a natural endogenous inhibitor of both IL-1α and IL-1β, which competitively bind to the IL-1 type I receptor without activating it and thus prevents binding and intracellular IL-1 signal transduction. It is produced by hepatocytes, smooth muscle cells and macrophages as an anti-inflammatory acute-phase protein (Arend et al., 1998).

A non-glycosylated recombinant human IL-1Ra (Anakinra), with similar properties to endogenous IL-1Ra, inhibits IL-1 by binding to the IL-1 type I receptor; it is a Food and Drug Administration approved drug with application in several human diseases (Dinarello, 2011; Dinarello et al., 2012) and successful results in clinical trials of human patients with rheumatoid arthritis (Botsios et al., 2007) or type 2 diabetes (Larsen et al., 2007).

Since neuroinflammation is associated with FAP peripheral nerve, the aim of the present study was to investigate the effect of blockage IL-1 signaling pathway, by Anakinra, on pathological cascades of the disease. To perform this work we used a recent developed mouse model (Santos et al., 2010b), carrying the human *TTR* V30M gene, in a *Ttr* null background and heterozygous for the heat shock factor-1 (*Hsf-1*), here designated as Hsf/V30M mice.

Materials and Methods

Ethics statement

All animal experiments were carried out in accordance with the European Community Council Directive (2010/63/EU) and were approved by the Institutional and National General Veterinarian Board ethical committees.

Experimental groups and treatment

Transgenic mice for human *TTR* V30M, in the 129/Sv and endogenous *Ttr* null background, heterozygous for *Hsf-1* (labeled as Hsf/V30M), with 4.5 months (*n*=10) were treated daily with subcutaneous injections of Anakinra at 25 mg/kg (Kineret®, Biovitrum), over 6 weeks. Age-matched control Hsf/V30M untreated mice were injected with phosphate buffer saline (PBS, *n*=10). Animals were housed in a controlled-temperature room and maintained under a 12 h light/dark period, with water and food *ad libitum*. At the end of treatment, mice were euthanized with a lethal injection of a premixed solution containing ketamine (75 mg/kg) plus medetomidine (1 mg/kg). Unless otherwise mentioned, all reagents were obtained from Sigma-Aldrich and were of analytical grade.

Messenger RNA (mRNA) extraction, cDNA synthesis and quantitative real-time polymerase chain reaction (qPCR)

mRNA from livers was isolated by phenol extraction (Invitrogen) (*n*=10 controls and *n*=10 treated mice). Dorsal root ganglia (DRG) were dissected free from the spinal cord and mRNA extraction (*n*=7 of each group) performed with RNeasy Mini columns (Qiagen). cDNA was synthesized using the SuperScript double-stranded cDNA Kit (Invitrogen). The quality of extracted mRNA was measured using Experion mRNA StdSens Analysis Kit (Bio-Rad); qPCR was performed with duplicates using iQ Syber Green Super Mix (Bio-Rad) and reactions were run on an Bio-Rad iQ5 software.

Primer sequences were designed using Beacon Designer^{TM} 8 (Premier Biosoft, Annex) for the following genes: *TTR*, *Il-1β*, *Tnf-α*, interleukin-1 receptor-associated kinase 1 (*Irak1*), myeloid differentiation primary response gene 88 (*Myd88*), heat shock protein-27 (*Hsp-27*) and glyceraldehyde 3-phosphate dehydrogenase (*Gapdh*). Differential expression was determined by the $2^{-\Delta\Delta CT}$ method using *Gapdh* as housekeeping gene.

Semi-Quantitative Immunohistochemistry (SQ-IHC)

Sciatic nerve, DRG, stomach and colon (*n*=10) were collected to 10% formalin, embedded in paraffin blocks and 3 µm-thick sections were cut, deparaffinated in histoclear (National Diagnostics) and hydrated in a descent alcohol series. Endogenous peroxidase activity was inhibited with 3% hydrogen peroxide solution in methanol and sections blocked in 10% fetal bovine serum and 0.5% Triton X-100 in PBS. Primary antibodies used were: rabbit polyclonal anti-human TTR (1:600, DAKO), goat polyclonal anti-IL-1β (1:25, Santa Cruz Biotechnology), rabbit polyclonal anti-Fas death receptor (1:100, Santa Cruz Biotechnology), rabbit polyclonal anti-cleaved caspase-3 (1:100, R&D Systems), rabbit polyclonal anti-3-nitrotyrosine (1:500, Chemicon, Temecula, CA, USA) and rabbit polyclonal anti-NF-κB p65 (1:25, Santa Cruz Biotechnology). Antigen visualization was performed with biotin-extravidin-peroxidase ABC kit (Vector) using 3.3´-diaminobenzidine (Sigma-Aldrich) as substrate. Semi-quantitative analysis of the immunostaining area was performed with the Image Pro-plus 5.1 software (Media Cybernetics). Results shown represent the area occupied by pixels, corresponding to the immunohistochemical substrate color, normalized relatively to the total area. Immunohistochemistry analysis was blind to treatment and each animal tissue was evaluated in five different areas, with 20 X magnification.

Total protein extracts and Western blot analysis

Protein extracts were obtained by homogenizing, in ice, DRG from control (*n*=7) and Anakinra treated mice (*n*=7), in lysis buffer containing 5 mM ethylenediamine tetraacetic acid, 2 mM ethylene glycol tetraacetic acid, 20 mM 3-(N-morpholino)propanesulfonic acid, 0.5% Triton X-100, 30 mM sodium fluoride, 40 mM sodium pyrophosphate, 1 mM sodium orthovanadate, 1 mM phenylmethylsulphonyl fluoride and a Protease Inhibitor Mix (GE Healthcare). Total protein concentration was determined by the Bradford protein assay (Bio-Rad).

Total protein from each extract (50 µg per lane) was separated in 12% SDS-PAGE gels and transferred onto a nitrocellulose Whatman™ membrane (GE Healthcare) using a Mini Trans-Blot Cell system (Bio-Rad). After blocking in 5% bovine serum albumin in PBS, the membrane was incubated overnight at 4ºC with rabbit polyclonal anti-binding immunoglobulin protein (BiP; 1:1,000, Abcam) and mouse monoclonal anti-α-Tubulin (1:10,0000, Sigma-Aldrich), followed by incubation with anti-rabbit or anti-mouse antibodies conjugated to horsederadish peroxidase (1:5,000, 1:2,500 respectively, The Binding Site). Detection was performed by the Luminata™ Crescendo (enhanced chemiluminescence, Millipore). Quantitative analysis was carried out by densitometry

using Quantity One software (Bio-Rad). Density values were normalized to α-Tubulin levels.

Morphometric analysis

Sciatic nerves from control (*n*=6) and Anakinra treated (*n*=6) animals were removed and fixed overnight in a 0.1 M sodium cacodylate solution containing 1.25% glutaraldehyde and 4% paraformaldehyde. Tissues were washed 3 x 30 min in 0.1 M sodium cacodylate and post-fixed with 2% osmium tetroxide in the cacodylate solution, overnight at 4ºC. After a new wash of 3 x 30 min, the tissue was dehydrated using a series of graded acetone and finally embedded in spurr. Transverse sections were cut (0.5 µm thick) with a SuperNova Reichert Leica ultramicrotome (Wetzlar) and stained with 1% toluidine blue, for 15 s, in an 80°C heating plate, before being examined on a light microscope. For each animal, the total number of myelinated fibers present in one semithin section was determined by counting 40 X magnified photographs covering the whole nerve area. Regarding unmyelinated fibers, ultrathin transverse sections were cut and stained with lead uranyl acetate. Sections were then mounted on 400 mesh copper grids and examined by transmission electron microscopy (Jeol JEM-1400). For unmyelinated fiber density analysis, 40 non-overlapping photographs (12,000 X amplification) per sciatic nerve were selected and fibers counted, normalized to the area of each ultrathin section.

Statistical Analysis

All data are expressed as mean values ± standard error of the mean (SEM). Comparison between Anakinra treated and control group was performed using the Student's t-test. *p*-values of less than 0.05 were considered to be significant (**p*<0.05; ***p*<0.01; ****p*<0.001).

Results

Anakinra prevents non-fibrillar TTR deposition in sciatic nerve and does not alter *TTR* expression by the liver

We decided to test the effect of Anakinra in preventing TTR aggregation using the Hsf/V30M FAP mouse model. In this model, when animals have 6 months of age, non-fibrillar deposits are observed, not only in the gastrointestinal tract but also in the autonomic and PNS (Santos et al., 2010b). We treated 4.5 months-old Hsf/V30M mice, thus before TTR starts to deposit in the PNS. In this way, we were able to evaluate the effect of Anakinra on preventing non-fibrillar TTR aggregates deposition in the PNS and to investigate the contribution of IL-1 signaling in the pathological mechanisms of disease. Some reports show that mice respond to Anakinra in a dose range of 1 mg/kg to 100 mg/kg (Abbate et al., 2008; Salloum et al., 2009) with no signals of toxicity. Based on this and to be as closest as possible to the clinical human dose, in our study we chose the dose of 25 mg/kg. Since Anakinra has a short half-life, daily subcutaneous injections were selected. Accordingly with previous literature (Fleischmann et al., 2006), no major secondary effects besides the topic reaction in the local of the injection were detected.

At the end of the treatment period, animals were 6 months-old and displayed widespread TTR non-fibrillar deposition along the gastrointestinal tract and PNS. Treated mice presented a markedly reduction on TTR deposition in sciatic nerve (43%) as compared to non-treated animals, and a trend, although not statistically significant, was observed in DRG (Figure 1A).

In the gastrointestinal tract, no difference regarding TTR deposition was observed between treated and control mice (data not shown).

We next investigated *TTR* mRNA levels by qPCR and found that Anakinra did not alter liver *TTR* transcription (Figure 1B).

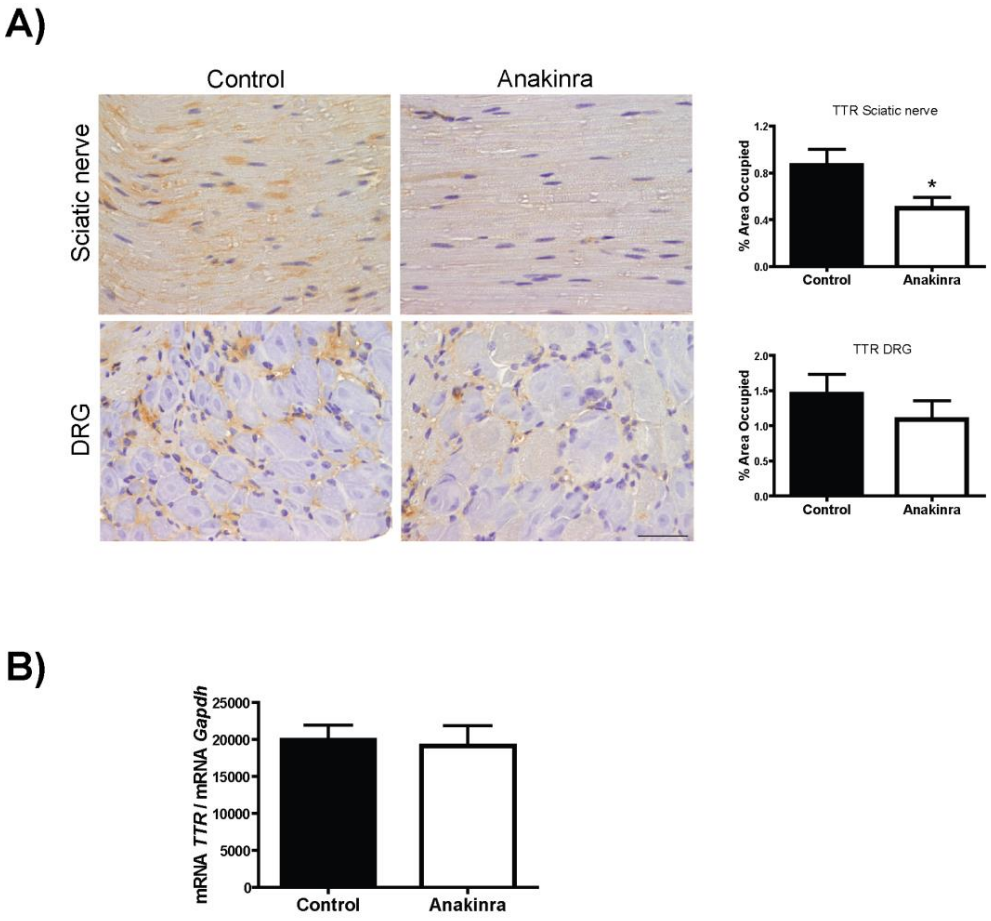

Figure 1 – Anakinra prevents TTR deposition in the sciatic nerve and does not alter *TTR* expression by the liver. A) Representative pictures of TTR load in sciatic nerve and DRG of Hsf/V30M mice treated with Anakinra (right panels, *n*=10) and age-matched controls (left panels, *n*=10). Scale bar 50 µm. Charts represent the quantification of immunohistochemical images. **B)** Histogram represents *TTR* mRNA levels in the liver of Anakinra treated mice (*n*=10), as compared with controls (*n*=10). *Gapdh* was the housekeeping gene for normalization; **p*<0.05.

Anakinra prevents neurodegeneration

Fiber degeneration, first affecting the unmyelinated and low diameter myelinated fibers, is a clinical feature of FAP (Coimbra and Andrade, 1971b). We next analyzed the density of myelinated and unmyelinated fibers in sciatic nerve of Anakinra treated animals and untreated age-matched controls. Treatment prevented loss of 46% of unmyelinated fibers, as compared with controls, with no impact on myelinated fibers (Figure 2).

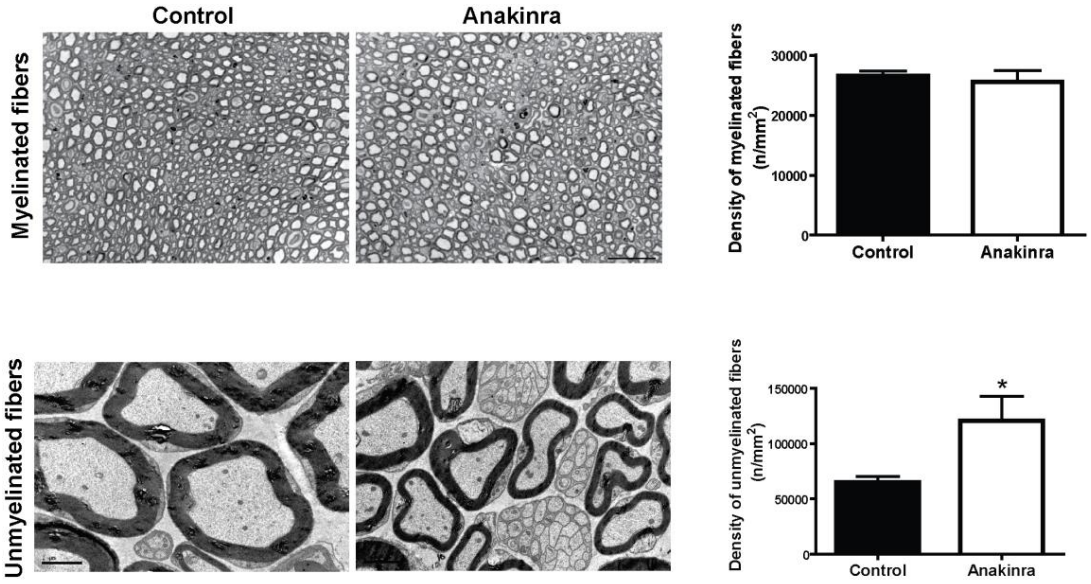

Figure 2 – Anakinra prevents neurodegeneration in the Hsf/V30M transgenic FAP mouse model. Morphometric analyses of sciatic nerve segments in Anakinra treated and control animals. **A)** Fiber density assessed in semithin sections showing no impact of IL-1 blocking on myelinated fibers. Scale bar: 50 µm, *n*=6 animals within each group. **B)** Representative images from electron microscopy and correspondent chart, indicating higher unmyelinated fiber density in Anakinra treated animals, as compared to controls. Scale bar: 2 µm, *n*=6 animals per group; **p*<0.05.

Anakinra decreases expression of IL-1 signaling pathway mediators and NF-κB p65 nucleus translocation

Transcription of pro-inflammatory mediators in DRG was analyzed by qPCR. *Il-1β*, *Myd88* and *Irak1* levels were found reduced in Anakinra treated animals (77%, 36%, 48% reduction, respectively; Figure 3A). Regarding *Tnf-α* expression, we did not observed any significant difference between control and Anakinra treated animals (Figure 3A).

Since *Il-1β* mRNA was downregulated in DRG of Anakinra treated mice, we next assessed IL-1β protein levels in the PNS by SQ-IHC. We found that this pro-inflammatory cytokine was significantly reduced in treated as compared with untreated animals, in both sciatic nerve and DRG (Figure 3B).

A previous report has shown that TTR aggregates bind to RAGE and activate NF-κB (Sousa et al., 2000b). Since Anakinra prevented TTR deposition in nerve tissue, associated with neuroprotection, we next addressed whether these effects influence or might be influenced by NF-κB activation. By SQ-IHC analysis we found minor cytoplasmic and nuclear labeling of NF-κB p65 subunit in sciatic nerve of mice treated with Anakinra, suggesting a reduction of this transcription factor nucleus translocation (Figure 3C,

arrows). Thus, our data indicates Anakinra suppression of the general activity of IL-1 and NF-κB p65 nucleus translocation.

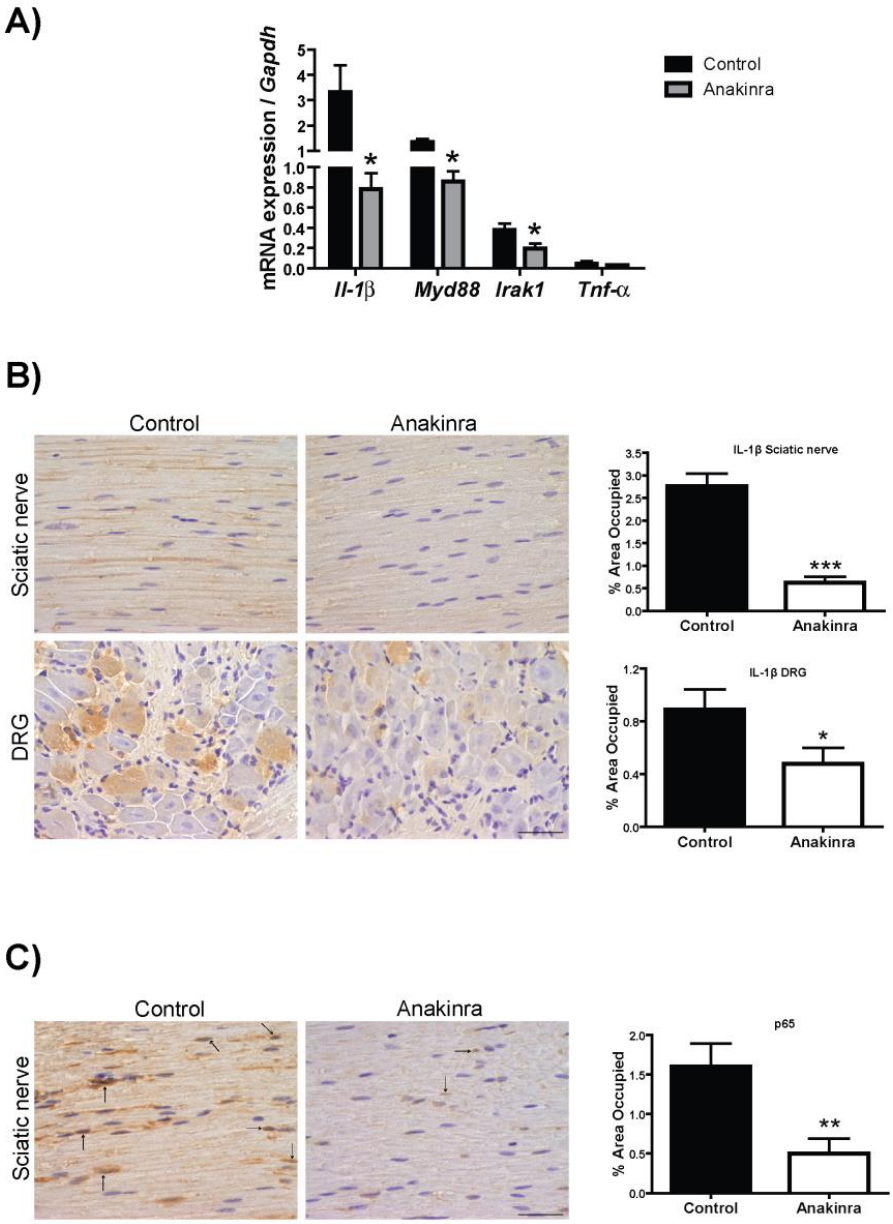

Figure 3 – Expression of IL-1 signaling pathway mediators and evaluation of NF-κB activation throughout p65 subunit translocation to the nucleus. A) Downregulation of pro-inflammatory mediators expression in DRG of Anakinra treated animals (*n*=7), as compared to controls (*n*=7) **B)** IL-1β protein levels in the PNS assessed by SQ-IHC (*n*=10 per group), with respective semi-quantification, demonstrating lower immunostaining in Anakinra treated mice in both nerve and DRG. Scale bar 50 µm. **C)** Representative SQ-IHC pictures of NF-κB p65 subunit in sciatic nerve of mice treated with Anakinra as compared to age-matched controls (*n*=10 in each group). Mice treated with Anakinra presented lower p65 nuclear staining as compared with controls (arrows), suggesting a reduction in p65 nucleus translocation. Scale bar 50 µm. Chart show quantification of immunohistochemical images. *p<0.05, **p<0.01 and ***p<0.001.

Blocking IL-1 activity prevents neuronal apoptosis and *Hsp-27* transcription

Prevention of apoptosis by Anakinra was previously described in a rat islet model and in a model of experimental acute myocardial infarction (Abbate et al., 2008; Schwarznau et al., 2009). Since apoptosis has also been implicated on the pathogenic mechanisms in FAP (Macedo et al., 2008), we next investigated the effect of Anakinra in Fas death receptor and cleaved caspase-3 levels in the PNS. Both apoptotic markers were found significantly reduced in sciatic nerve and DRG of Anakinra treated mice, as compared with untreated age-matched controls (Figure 4A and 4B). These results and the described activation of the heat shock response in FAP (Santos et al., 2008), prompted us to investigate the transcriptional levels of *Hsp-27* in DRG. We observed a significant decrease (70% reduction) in *Hsp-27* mRNA levels in mice treated with Anakinra as compared to the untreated group (Figure 4C).

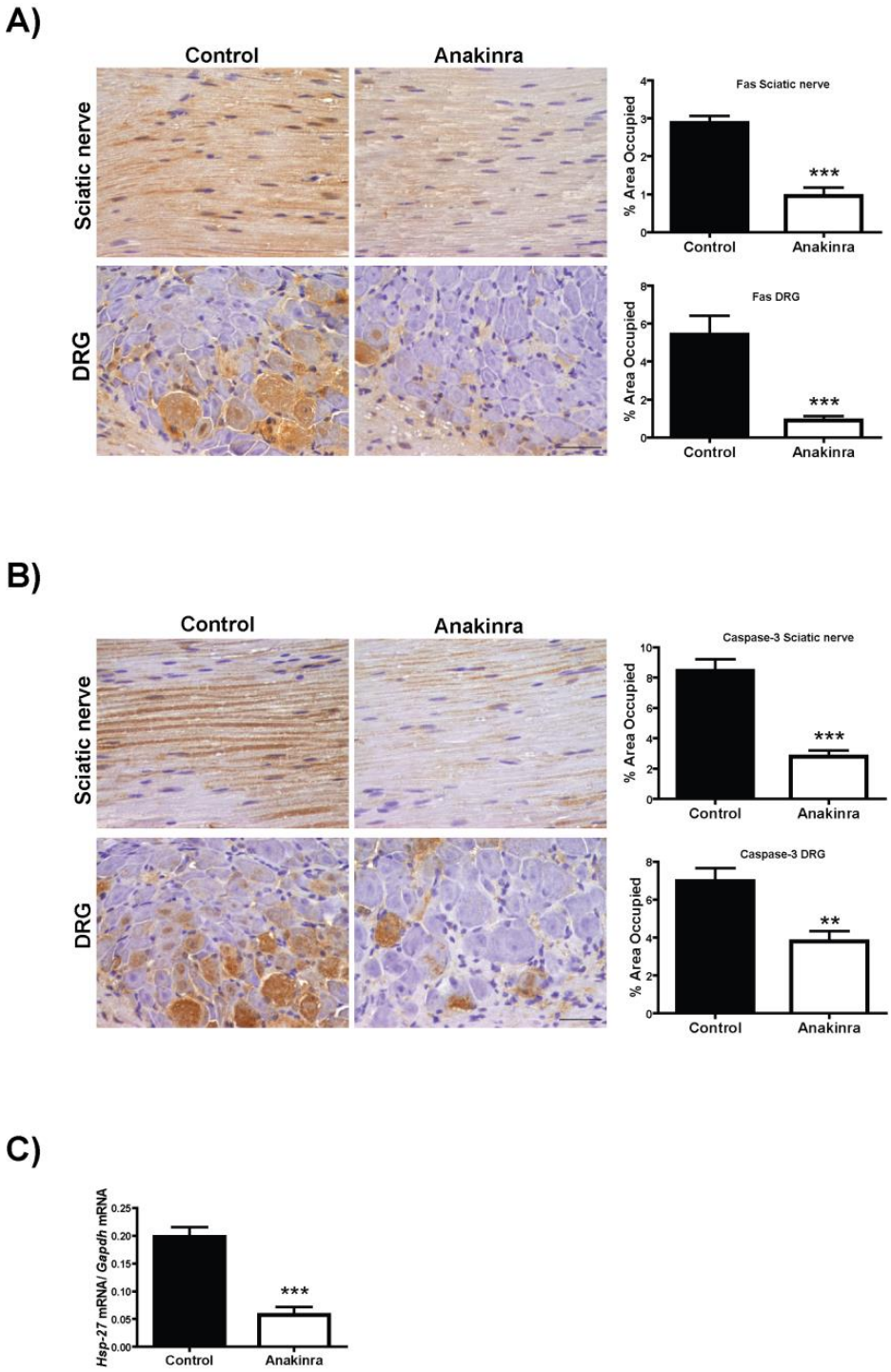

Figure 4 – Anakinra suppresses apoptotic cell death in the PNS and reduce expression of *Hsp-27*. A) Representative SQ-IHC images of Fas death receptor in the PNS and respective quantifications (*n*=10 per group), demonstrating lower levels of Fas in treated animals. **B)** Cleaved caspase-3 immunostaining in sciatic nerve and DRG of Hsf/V30M mice treated with Anakinra (right panels, *n*=10) and age-matched controls (left panels, *n*=10). Scale bar 50 µm. Charts characterize the quantification of immunohistochemical images. **C)** Inhibition of *Hsp-27* mRNA levels in DRG of Anakinra treated mice as compared with controls (*n*=7 of each group). The relative mRNA expression was normalized to *Gapdh.* ***p*<0.01 and ****p*<0.001.

Blocking IL-1 signaling pathway prevents endoplasmic-reticulum (ER) and nitrosative stress

Evidence suggests a link between inflammation driven by IL-1 and ER stress (Amin et al., 2012), pathway also involved in the progress of FAP disease (Teixeira et al., 2006). To test this hypothesis in our model, we decided to evaluate levels of BiP, a central regulator for ER stress, in DRG. By western blotting, we found a significant reduction of BiP in treated mice (Figure 5A), indicating a direct effect of Anakinra in ER stress, since TTR deposition in this organ is not significantly affected.

Nitration of tyrosine residues has been suggested as a marker of peroxynitrite-mediated tissue injury in TTR amyloidosis (Sousa et al., 2004) being the nitrosative stress an integral factor in neurodegeneration. Accordingly, we further investigated whether neuroprotection of unmyelinated axons could also result from decreased levels of peroxynitrite formation. Sciatic nerve was immunohistochemically examined for evidence of 3-nitrotyrosine, a stable biochemical marker for this process. 3-nitrotyrosine reactivity was detected within axons and was remarkably decreased after blocking IL-1 (Figure 5B).

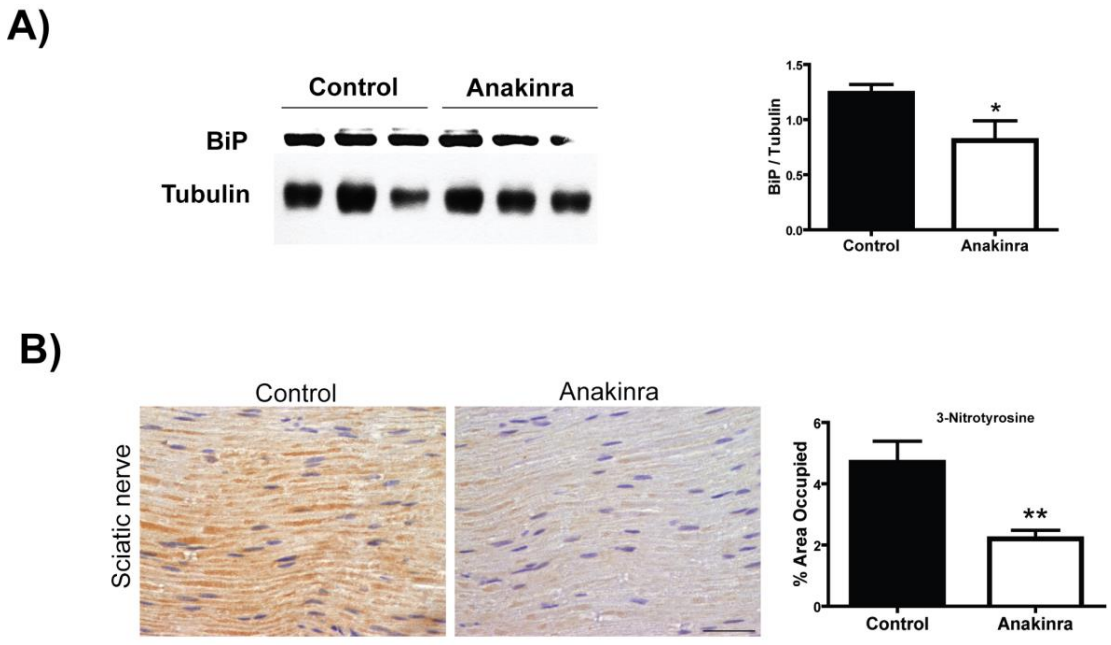

Figure 5 – Anakinra reduced ER and nitrosative stress. A) Western blot quantification of BiP in DRG from mice treated with Anakinra (*n*=7) and non-treated age-matched controls (*n*=7). Histogram denotes normalized BiP/Tubulin density quantification. **B)** Representative SQ-IHC pictures of 3-nitrotyrosine in sciatic nerve of mice treated with Anakinra (right panel, *n*=10) and age-matched controls (left panel, *n*=10). Scale bar 50 µm. Chart represent the quantification of immunohistochemical images. *p<0.05 and **p<0.01.

Discussion

The presence of Congophilic amyloid deposits is a unifying characteristic of the extensive analysis of FAP nerves. Nevertheless, the lack of a cause-effect relationship between amyloid deposition and neurodegeneration in FAP suggests that other TTR molecular intermediaries, namely non-fibrillar oligomeric species, might be the primary neurotoxic culprits (Sousa et al., 2001a; Andersson et al., 2002; Reixach et al., 2004). In fact, it has been shown that nerves from FAP 0 patients (asymptomatic individuals presenting aggregate deposition but lacking amyloid) exhibit early signs of oxidative damage and inflammatory stress (Sousa et al., 2001b). Moreover, TTR non-fibrillar deposition in the sciatic nerves of FAP patients has been shown to induce pro-inflammatory cytokine synthesis by axons and a correlation between increased IL-1β levels and fiber degeneration has been established (Sousa et al., 2001b).

In the present study we investigated the effect of early administration (before aggregate deposition started) of the IL-1 antagonist Anakinra in TTR deposition and neurotoxicity, using a well-established mouse model of FAP.

We found that inhibition of IL-1 lowered non-fibrillar TTR deposition in sciatic nerve, which correlated with increased number of unmyelinated fibers. In contrast, Anakinra treatment did not interfere with TTR deposition in the gastrointestinal tract. This observation might be explained by the presence of endogenous microflora, exposition to oral pathogens and specific immune regulatory networks of the gastrointestinal tract, not operating in the peripheral nerve.

IL-1 has been implicated in several chronic degenerative disease processes, including the development of atherosclerosis and rheumatoid arthritis (Merhi-Soussi et al., 2005; Kay and Calabrese, 2004), being a key player in neuroinflammation and neurodegeneration and regulating the expression of several transcription factors, including NF-κB (Beg et al., 1993). IL-1 activation results in phosphorylation and degradation of IκB proteins, releasing NF-κB and allowing its translocation to the nucleus, where it controls the expression of downstream pro-inflammatory genes (Hayden and Ghosh, 2004). The involvement of NF-κB in FAP has been described (Sousa et al., 2000b; Sousa et al., 2005; Santos et al., 2010b). In this regard, *in vitro* studies have shown that TTR aggregates interact with RAGE triggering nuclear translocation of NF-kB (Sousa et al., 2000b).

In this study, we assessed the effect of IL-1 inhibition on NF-κB activation in sciatic nerve and found a significant reduction of NF-κB p65 nucleus translocation in Anakinra treated animals, which is consistent with decreased TTR extracellular load and increased density of unmyelinated fibers. It is important to emphasize that the influence of NF-κB on cell survival can be protective or deleterious, depending on the cell type, its developmental

stage and the pathological conditions (Kaltschmidt et al., 1997). For instance, in glia, NF-κB is inducible and mediates inflammatory responses that aggravate diseases such as ischemia, autoimmune encephalomyelitis and Alzheimer's disease (Kaltschmidt et al., 1997; Mattson and Camandola, 2001). Thus inhibition of NF-κB in glia might ameliorate disease, whereas activation in neurons might enhance memory (Kaltschmidt et al., 1997). In FAP, NF-κB activation occurs as a response to extracellular aggregate insult. Whether this action is neuroprotective or neurotoxic it is still not fully understood, but there is probably a threshold beyond which NF-κB activation starts to be noxious to cells. Moreover, the fact that other inflammatory mediators such as *Tnf-α* levels were not affected by the treatment supports the specificity of Anakinra action into the IL-1 signaling pathway.

In FAP, like in other neurodegenerative disorders, accumulation of aberrant misfolded proteins activates the unfolded protein response by the ER to restore and maintain homeostasis in the ER (Teixeira et al., 2006; Hoozemans et al., 2009). However, if the ER stress is continued, or the adaptive responses fail, apoptotic cell death ensues. Thus, we further investigate the effect of Anakinra administration on ER chaperone BiP and found that it significantly impairs ER-stress in treated animals.

Compelling evidence has shown that members of the IL-1 family of cytokines are intricately involved in inflammatory and death-inducing signaling platforms. Therefore, IL-1 has been further suggested as rational therapeutic target for several pathological conditions. *In vivo* administration of IL-1Ra in mouse models as diverse as acute myocardial infarction (Abbate et al., 2008), spinal cord injury (Nesic et al., 2001), renal ischemia-reperfusion (Rusai et al., 2008) or cancer chemotherapy (Wu et al., 2011) has been proved efficient in preventing activation of pro-apoptotic molecules or activating pro-survival signaling transduction pathways. In agreement with these observations, in our study early treatment of FAP mice with Anakinra resulted in significantly decreased levels of Fas death-receptor, cleaved caspase-3 and chaperone *Hsp-27* in the PNS.

The reaction of nitric oxide with superoxide produces the peroxynitrite anion (Melo et al., 2011). Peroxynitrite is a powerful oxidant that can nitrate aromatic amino acid residues such as tyrosine to form 3-nitrotyrosine. Hence, 3-nitrotyrosine is a valuable marker of peroxynitrite production. Immunostaining of FAP nerves with antibody to 3-nitrotyrosine demonstrated immunoreactive material in FAP 0 and FAP tissue in an axonal distribution (Sousa et al., 2001b). Our results indicate significant decrease of 3-nitrotyrosine in the sciatic nerve, which is in accordance with Anakinra inhibitory effect on TTR deposition and suggestive of reduction of cytotoxicity and neuroprotection.

Since Anakinra has no effect on TTR stability (data not shown), we hypothesized that decreased TTR aggregation and deposition in tissues might be due to a restored

extracellular environment characterized by decreased levels of inflammatory mediators, nitrosative species and apoptotic cell death. Thus, by interrupting the positive feedback loop between TTR accumulation in tissues and inflammation, Anakinra prevents TTR deposition in the PNS. Future studies will further elucidate the molecular mechanisms behind Anakinra inhibitory effect on TTR deposition.

Therapeutic strategies for FAP, other than orthotropic liver transplantation, have been put forward as it is the case of tetrameric TTR stabilization (Bulawa et al., 2012; Ferreira et al., 2012), inhibition of TTR aggregation (Ferreira et al., 2012; Ferreira et al., 2013) or apoptosis (Macedo et al., 2008), disruption of TTR fibrils (Cardoso and Saraiva, 2006), suppression of liver *TTR* synthesis with small interfering RNA (siRNA) (Kurosawa et al., 2005; Alvarez et al., 2010) and drug combinatorial treatments (Cardoso et al., 2010). In what concerns combinatorial therapeutic strategies in FAP, doxycycline and TUDCA administration were shown to synergize for disruption and clearance of fibrillar deposits and for stabilization of disease progression both in mice and humans, respectively (Cardoso et al., 2010; Obici et al., 2012). Considering the therapeutic potential of Anakinra shown in our study, we hypothesize that it can be a multi-target drug used as an alternative treatment or in a combinatorial approach, improving the efficacy of drugs acting on TTR silencing (Alvarez et al., 2010), TTR stabilization (Bulawa et al., 2012; Ferreira et al., 2012) or amyloid fibril disruption (Cardoso et al., 2006).

Overall, the present study brings to light, for the first time, the therapeutic potential of Anakinra in the context of FAP. Furthermore, data reinforce the importance of inflammation on TTR amyloidosis and further demonstrates an important role of IL-1 in the pathogenesis of FAP.

Acknowledgements

This work was funded by FEDER funds through the Operational Competitiveness Program – COMPETE and by National Funds through FCT – Fundação para a Ciência e a Tecnologia under the project FCOMP-01-0124-FEDER-028406 (PTDC/BIM-MEC/0282/2012) and fellowship to NPG (SFRH/BD/74304/2010). The present work was sponsored by POPH/FSE QREN program and also financed by a grant from Cordex. The authors would like to thank Rui Fernandes and Paula Gonçalves from IBMC for help with electron microscopy, paraffin tissue processing and immunohistochemical analysis, respectively. We also thank Dr. Nelson Ferreira for critical reading.

Chapter IV

Protective role of Anakinra against transthyretin mediated axonal loss and cell death in a mouse model of Familial Amyloidotic Polyneuropathy

Protective role of Anakinra against transthyretin mediated axonal loss and cell death in a mouse model of Familial Amyloidotic Polyneuropathy

Nádia Pereira Gonçalves[1,2,3], Maria Teixeira-Coelho[1,2], Maria João Saraiva[1,2,3]

1) Instituto de Inovação e Investigação em Saúde (I3S), Universidade do Porto, Portugal
2) Molecular Neurobiology, IBMC – Instituto de Biologia Molecular e Celular, Porto, 4150-180 Portugal
3) Instituto de Ciências Biomédicas de Abel Salazar (ICBAS), Universidade do Porto, Porto, 4050-313 Portugal

Running title: Protective role of Anakinra against transthyretin mediated neurodegeneration

Abstract

Familial Amyloidotic Polyneuropathy (FAP) is characterized by a length-dependent axonal loss in the peripheral nervous system (PNS) that results from deposition of extracellular non-fibrillar transthyretin (TTR) and amyloid fibrils. Inflammation is a key factor for the pathophysiology of FAP, aggravating the disease phenotype, suggesting that the immune response in peripheral nerve may have an active role in the progression of the disease. We have previously shown that an inflammatory stimulus in the peripheral nerve of a mouse model of FAP triggers local TTR expression and deposition, leading to poor regeneration. We also demonstrated that blocking interleukin-1 (IL-1) signaling by the IL-1 receptor antagonist Anakinra is beneficial in preventing nerve TTR deposition and associated toxicity. Here, we investigated whether IL-1 signaling influences TTR biology after an injury stimulus in a V30M FAP mouse model. Animals were treated with Anakinra 48 h before sciatic nerve ligation and histopathological changes in sciatic nerve were analyzed 7 days post-lesion. Our data shows that, Anakinra decreased TTR expression by Schwann cells and extracellular deposition after nerve injury, which resulted in improved regeneration. Moreover, treated mice had less apoptotic cell death. In a wild-type (WT) situation, inflammation is important for regeneration to occur. However, in FAP, the threshold of the inflammatory response will differentially regulate *TTR*, becoming detrimental to the system. Taken together, our results show that Anakinra administration before injury can modulate TTR-induced pathology in the PNS corroborating the protective interference of this drug in a FAP pre-clinical model.

Introduction

Familial Amyloidotic Polyneuropathy (FAP), an autosomal dominant hereditary disorder, is primarily characterized by a length-dependent axonal loss consequent to extracellular matrix (ECM) deposition of mutated forms of transthyretin (TTR) (Coimbra and Andrade, 1971b). It is estimated that approximately ten thousand patients are affected worldwide with this disease, with endemic foci in Portugal, Japan and Sweden (Said et al., 2012). TTR is a 55-kDa tetramer made of identical subunits of 127 amino acids, mainly synthesized and secreted by hepatocytes, the choroid plexus and the retinal epithelium (Soprano et al., 1985). However, recently, minute levels of expression were also found in Schwann cells (Murakami et al., 2010; Gonçalves et al., 2014a). More than 100 TTR single point mutations have been reported being the most common mutation associated with FAP a substitution of a methionine for a valine at position 30 (V30M) of the polypeptide chain (Saraiva et al., 1984) (http://amyloidosismutations.com/mut-attr.php). TTR is produced as a monomer and assembles as a tetramer in the endoplasmic reticulum. Amyloidogenic TTR mutants induce the exposure of new structural motifs promoting tetramer destabilization and dissociation into structurally modified unfolded monomers. These unstable and non-native intermediate species lead to the formation of soluble aggregates that further self-assemble into insoluble amyloid fibrils (Colon and Kelly, 1992; Quintas et al., 2001), predominantly accumulating in the PNS and the autonomic nervous system. TTR misfolding, aggregation and deposition culminate in distinct patterns of organ involvement, age of onset, and clinical course of FAP disease. All these stages share a common determinant factor being the cytotoxicity of early TTR non-fibrillar aggregates (Sousa et al., 2001a; Koike et al., 2004). More than mature amyloid fibrils, these intermediate species induce oxidative and inflammatory stress in neuronal cells, ultimately leading to fiber degeneration and death (Sousa et al., 2001a; Sousa et al., 2001b). Additionally, fibrillar TTR binds to the receptor for advanced glycation end products (RAGE) in different cellular structures of the peripheral nerve, such as axons, vascular smooth muscle cells and Schwann cells, resulting in nuclear factor κB (NF-κB) activation and increased IL-1β levels, in a distribution overlapping RAGE expression. Consequently, nerve fiber degeneration occurs creating a feed-forward mechanism that contributes to the maintenance of neuroinflammation and progression of disease (Sousa et al., 2001b; Gonçalves et al., 2014b). In line with this, it has been recently shown that an inflammatory stimulus in the PNS triggers local TTR expression and deposition which supports the notion that neuroinflammation contributes to the pathogenesis and progression of FAP (Gonçalves et al., 2014a).

Anakinra is the recombinant form of the endogenous IL-1 receptor antagonist (IL-1Ra) and is a U.S. FDA approved drug with successful results in rheumatoid arthritis (Botsios et al., 2007) and type 2 diabetes (Larsen et al., 2007). Strong evidence supports a role for inflammation in the progress of FAP, through association of IL-1β production and deterioration of nerve degeneration (Sousa et al., 2001b; Gonçalves et al., 2014b). In an animal model of FAP, Anakinra have proved beneficial when administered prior to TTR deposition, preventing activation of toxic cascades associated with the disease (Gonçalves et al., 2014b). Thus, in the present work we sought to provide additional evidence for the role of IL-1 in the induction and chronicity of FAP. Our goal was to determine the influence of this cytokine in triggering TTR deposition and expression in the PNS. For that, we administered Anakinra to a transgenic human V30M mouse model (Kohno et al., 1997) (V30M), presenting enhanced TTR deposition following nerve injury (Gonçalves et al., 2014a).

Materials and Methods

Animal procedures

Six months-old male and female WT and V30M mice, in the 129/Sv background were used for the experiments. V30M transgenic mice carry the human *TTR* gene bearing the V30M mutation, in a mouse *Ttr* null background (Kohno et al., 1997). Despite the number of *TTR* copies, levels of TTR in plasma are similar in both groups (Oliveira et al., 2011; Ferreira et al., 2013). Animals were maintained in a controlled-temperature room (24 ± 1 °C) under a 12 h light/dark cycle and fed regular chow and tap water *ad libitum*.

Sciatic nerve injury was adapted from the method described by Brumovsky et al., (2004), as previously reported (Gonçalves et al., 2014a) due to the higher inflammatory response that is elicited in response to the ligature. Briefly, sciatic nerve ligation was performed using one ligature placed around the sciatic nerve at the mid-thigh level, with 5.0 silk. A sham operation was similarly performed at the contralateral side, except that the sciatic nerve was not constricted. Mice were kept in a recovery room with infrared heating lamp for 1-2 h and post-surgical pain treatment consisted of butorphanol subcutaneous injections, every 12 h for the first 48 h.

Two days before nerve injury, animals were injected once a day subcutaneously with 50 mg/kg of Anakinra (Kineret®, Biovitrum) and treatment was repeated every day after. Seven days after injury, animals were euthanized with a lethal anesthesia of ketamine/medetomidine.

Mice were handled in accordance with the European Community Council Directive (2010/63/EU) and the number of total animals for this research was approved by ethical committee and by National General Veterinarian Board.

Semi-Quantitative Immunohistochemistry (SQ-IHC)

Immunohistochemical staining of entire or distal stump of sciatic nerves and L4-L6 ipsilateral dorsal root ganglia (DRG) (*n*=5 per group) was carried out using primary antibodies against human TTR (1:600, rabbit polyclonal, DAKO); mouse TTR (1:1,500, rabbit polyclonal, Q-Biogen); growth associated protein 43 (GAP-43, 1,1000, rabbit polyclonal, Abcam); peripherin (1:1,500, rabbit polyclonal, Millipore); cyclic AMP-dependent transcription factor (ATF-3, 1:100, rabbit polyclonal, Santa Cruz Biotechnology); nerve growth factor β (NGF-β, 1:100, rabbit polyclonal, Abcam); cleaved caspase-3 (1:100, rabbit polyclonal, R&D Systems); Fas death receptor (Fas, 1:100, rabbit polyclonal, Santa Cruz Biotechnology), BH3 interacting domain death agonist (Bid, 1:100, rabbit polyclonal, Santa Cruz Biotechnology), myeloid differentiation primary

response gene 88 (Myd88, 1:200, rabbit polyclonal, Abcam) and cAMP response element-binding protein (Creb, 1:500, Cell Signaling). The sections were excised, post-fixed in 10% formalin, embedded in paraffin blocks and cut longitudinally at 3 µm. After tissue deparaffinazation with Histoclear (National Diagnostics) and hydration in descent alcohol series, the sections were quenched for 30 min in 3% hydrogen peroxide in methanol and pre-incubated for 1 h with 10% fetal bovine serum and 0.5% Triton X-100 in PBS. After overnight incubation at 4ºC with primary antibody, a 1:200 dilution of biotinylated anti-rabbit (Vector) for 45 min was performed. Thereafter, sections were washed with PBS, incubated with avidin-biotin-peroxidase complex (ABC Elite, Vector laboratories) and visualized using 3.3´-diaminobenzidine as a chromogen. For semi-quantitative analyses of the immunostained slide, 5 pictures at 20 X magnification were taken from different areas and quantified using the Image pro-plus 5.1 software (Media Cybernetics). The area occupied by chromogen represents the amount of protein present and all types of brown staining were selected by the program. Results shown represent the area occupied by pixels corresponding to the substrate reaction color that is normalized relatively to the total image area, with the corresponding standard error of the mean (SEM).

Double Immunofluorescence

After deparaffinazation and hidration of the entire nerve and L4-L6 ipsilateral DRG sections (*n*=5 per group), primary antibodies used for immunofluorescence were: rabbit anti-human TTR (1:100; DAKO), mouse anti-heparan sulfate proteoglycan (HSPG, 1:100), rabbit anti-cleaved caspase 3 (1:100; R&D Systems), mouse anti-βIII-Tubulin (1:1,000; Promega), mouse anti-S100 (1:50; Abcam) and rat anti-F4/80 (1:50, Serotec). Following 1 h blocking with 10% fetal bovine serum and 0.5% Triton X-100 in PBS, sections were incubated with primary antibodies overnight at 4ºC. Secondary antibodies used were anti-rabbit Alexa Fluor 488, anti-mouse Alexa Fluor 568 and anti-rat Alexa Fluor 594 (1:1,000; Invitrogen Molecular Probes), which were incubated for 2 h at room temperature. After 3 washes with PBS for 10 min each, slides were finally mounted with Vectashield (Vector Laboratories) and visualized in a laser scanning Confocal Microscope Leica TCS SP5 II (Leica Microsystems).

Immunogold Labeling

Ultrathin sections of 2% glutaraldehyde-paraformaldehyde-fixed, LR white-embedded distal injured nerves (*n*=4 in each group) were mounted onto nickel grids, treated with sodium borohydrate for 10 min and subsequently incubated in 2% gelatin for 20 min. After blocking with 2% bovine serum albumin in TBS for 1 h, anti-human TTR (DAKO) was

used as primary antibody diluted 1:100 in blocking buffer. Control sections without secondary antibody were also used. Anti-rabbit immunoglobulins (1:20, British Biocell International) coupled to 10 nm gold particles were used as secondary antibody, 1 h at room temperature. The grids were subsequently washed in pure water 6 times for 10 min each and finally stained with uranyl acetate for 3 min and lead citrate for 30 s. Samples were analyzed in a Jeol JEM-1400 electron microscope.

Messenger RNA (mRNA) isolation, complementary DNA (cDNA) synthesis and real-time polymerase chain reaction (qPCR)

Whole injured nerves (*n*=5 per group) from V30M mice were dissected free from surrounded tissues and immersed in RNA later (Ambion) for 2 h before being frozen at -80ºC. Tissue mRNA was isolated by using the mRNA capture kit (RNA tissue lipid mini-kit, Qiagen) following the manufacturer's instructions. mRNA was reverse transcribed using the SuperScript double-stranded cDNA Kit (Invitrogen) and subjected to qPCR, in duplicate, using iQ Syber Green Super Mix (Bio-Rad). Reactions were analyzed on Bio-Rad iQ5 software. Primer sequences were designed using the Beacon software (Premier Biosoft) for the following genes (Annex): *TTR*, *Myd88*, *Creb*, hepatocyte nuclear factor-4 (*Hnf-4*), hepatocyte nuclear factor 3β (*Hnf-3β*), CCAAT/enhancer binding protein (*C/ebp-β*), *c-Jun*, *Synapsin*, *Persephin*, *Cathepsin B*, *Cathepsin D* and glyceraldehyde 3-phosphate dehydrogenase (*Gapdh*). Calibration curves for target and housekeeping genes were constructed using 10-fold serial cDNA dilutions in duplicates. Differential expression was determined by the $2^{-\Delta\Delta CT}$ method, relative to the housekeeping gene *Gapdh*.

Flow cytometry

Entire injured sciatic nerves from V30M mice (*n*=5 per group) were dissected and subjected to enzymatic digestion using 1.6 mg/mL collagenase type IV, 200 µg/mL DNase I, 10 mM HEPES, 5 mM $CaCl_2$ and 5 mg/mL bovine serum albumin (all from Sigma-Aldrich) in RPMI media for 1 h at 37ºC. Single cell suspensions were filtered through a 70 µm cell strainer (BD Biosciences). Cells were incubated with Fc receptor block (CD16/32, eBioscience) at 4ºC for 15 min and then stained with CD11b, Ly6G, CD45, CD11c and MHCII (Biolegend) in PBS Fluo (2% fetal bovine serum, 0.1% Azide, 5mM EDTA in PBS) at 4ºC for 30 min. Cells were washed, ressuspended in PBS Fluo and run on a FACS CALIBUR flow cytometer and later analyzed using the FlowJo software. The cell population identification for neutrophils, macrophages and dendritic cells was performed as follows: $CD11b^{+}Ly6G^{+}$, $CD11b^{+}$ $Ly6G^{-}$, $CD45^{+}CD11c^{+}MHCII^{+}$, respectively.

Total protein extracts and Western blot analysis

Whole sciatic nerve (*n*=5 per group) was homogenized, at 4ºC, in lysis buffer containing 5 mM ethylenediamine tetraacetic acid, 2 mM ethylene glycol tetraacetic acid, 20 mM 3-(N-morpholino)propanesulfonic acid, 0.5% Triton X-100, 30 mM sodium fluoride, 40 mM sodium pyrophosphate, 1 mM sodium orthovanadate, 1 mM phenylmethylsulphonyl fluoride and a Protease Inhibitor Mix (GE Healthcare, Buckinghamshire). The protein concentration of lysates was determined using the Bradford protein assay (Bio-Rad). Nerve protein lysates were resolved on 12% polyacrylamide gels (50 µg per lane) and transferred to a nitrocellulose Whatman™ membrane (GE Healthcare) using a Mini Trans-Blot Cell system (Bio-Rad). Membranes were blocked with 5 % bovine serum albumin in PBS supplemented with 0.05% Tween 20 and then probed with rabbit polyclonal anti-Arginase-1 (Arg-1, 1:1,000, Cell signaling), rabbit polyclonal anti-iNOS (1:1,000, Cell signaling) or mouse monoclonal anti-GAPDH (1:3,000, Abcam). After washing, membranes were incubated with the appropriate secondary antibodies conjugated to horsederadish peroxidase (The Binding Site) and proteins were visualized with enhanced chemiluminescence using the Luminata™ Crescendo (Millipore). Protein bands were quantified by densitometry using Quantity One software (Bio-Rad). Density values were normalized to GAPDH levels.

Sciatic nerve morphometric analysis

Sciatic nerves were covered with 1.25% glutaraldehyde and 4% paraformaldehyde in a 0.1 M sodium cacodylate solution for 5 min, before dissection. Then, few mm length segments, collected distally from the lesion and proximally to nerve trifurcation (*n*=4 per group) were immersed on fixation solution overnight. After incubation in 2% osmium tetroxide in the cacodylate solution overnight, nerves were dehydrated using a series of graded acetone and finally embedded in spurr. Half µm thick transverse sections covering the complete cross-sectional area of nerves were stained with 1% toluidine blue, for 15 s, in an 80°C heating plate and photographed on an optical microscope. For each animal, the total number of myelinated axons was counted and normalized to the respective nerve area. To determine the density of unmyelinated axons, ultrathin transverse nerve sections were cut, placed on 400-mesh copper grids and stained with uranyl acetate and lead citrate. For each animal, 40 non-overlapping photomicrographs (12,000 X magnification) of each section were taken in a transmission electron microscope (JEOL JEM-1400). The area of the total number of photomicrographs per mice was determined to calculate the density of unmyelinated axons.

Statistical analysis

Statistical comparison of data was performed using the Student t-test with Graph Pad Prism 6 software. Quantitative data are expressed as mean ± SEM. Statistical significance was established for *p<0.05, **p<0.01 and ***p<0.001.

Results

Blocking IL-1 signaling pathway in the V30M FAP mouse model, decreases TTR V30M expression and deposition in sciatic nerve after injury

We have previously reported that TTR expression and deposition in the sciatic nerve is triggered by an injury stimulus, leading to poor nerve regeneration (Gonçalves et al., 2014a). Additionally, we have also found that blocking IL-1 signaling pathway with Anakinra, in a pre-clinical FAP model prevents TTR deposition and associated neurotoxicity (Gonçalves et al., 2014b), reinforcing the role of IL-1 on the pathophysiology of FAP. Since Anakinra was neuroprotective, we hypothesized whether that would also be true in a scenario of sciatic nerve injury in an FAP mouse model. To block IL-1, daily subcutaneous injections of Anakinra were required due to the short half-life of this molecule. The dose used was 50 mg/kg and previously tested (Abbate et al., 2008; Salloum et al., 2009; Sgroi et al., 2011). Blocking IL-1 signals have shown neuroprotective efficacy when performed before ischemia or spinal nerve injury (Banwell et al., 2009; Gabay et al., 2011). Therefore, we started treatment with Anakinra, 48 h before sciatic nerve injury. No secondary effects besides the topic reaction in the local of the injection were detected. Similarly to previous data (Gonçalves et al., 2014a), nerve injury triggered local TTR V30M expression and deposition; however, treatment with Anakinra led to a strong inhibition in both TTR V30M synthesis and nerve deposition (Figure 1A and 1B). TTR V30M deposits in the sciatic nerve after injury were found predominantly in the ECM, as shown with immunogold staining (Figure 1C) and vast colocalization with HSPG, one of the main components of the ECM and basement membranes (Häcker et al., 2005) (Figure 1D, top panel). Moreover, TTR localization in axons was ruled out as no colocalization with βIII-tubulin (an axonal and neuronal marker) was found (Figure 1D, bottom panel).

L4, L5 and L6 DRG, ipsilateral to the injury side, were also analyzed; TTR V30M protein levels were found 85% decreased in DRG from animals treated with Anakinra prior to injury, as compared with untreated mice (Figure 1E, top panel). It was previously described that DRG do not synthesized *TTR* (Sousa and Saraiva, 2008), thus this paradigm probably results from prevention of TTR deposition by Anakinra. Additionally, TTR deposits in DRG do not colocalize with βIII-tubulin (Figure 1E, bottom panel), thus we conclude that they were located in the extracellular space.

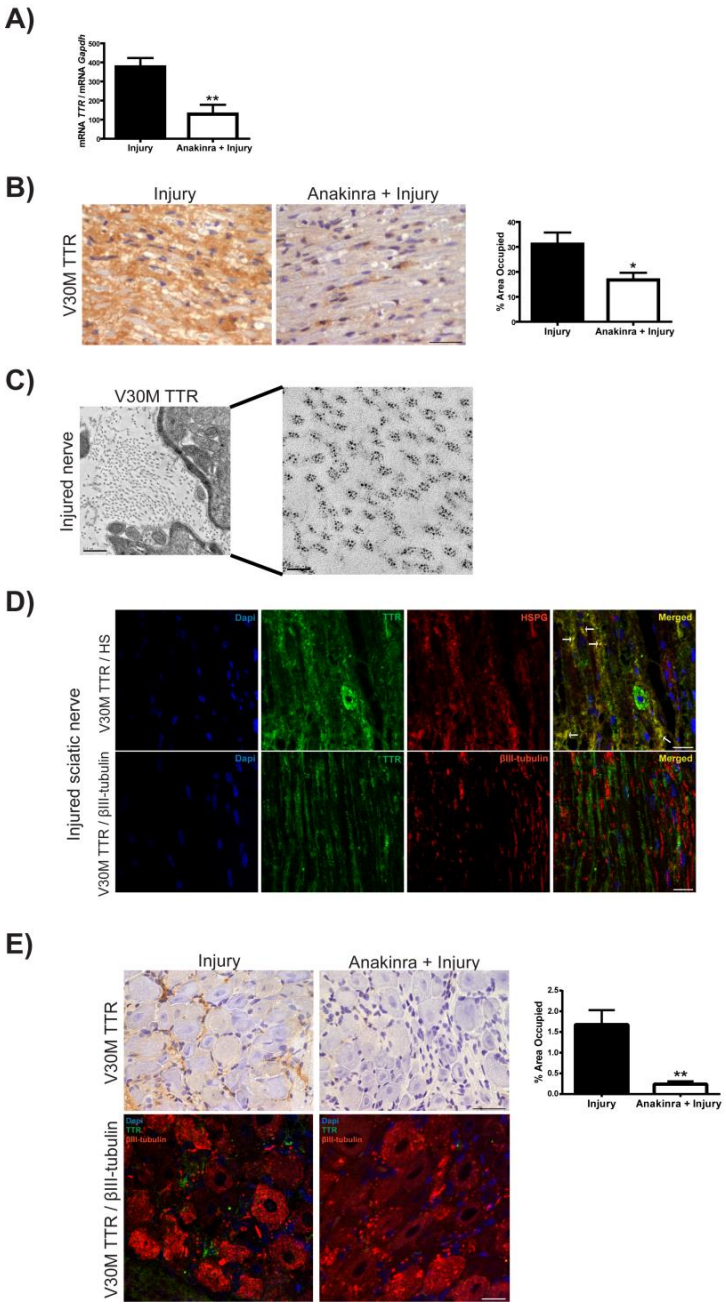

Figure 1 – Blocking IL-1 before nerve injury, decreases local TTR V30M expression and extracellular deposition. A) Histogram represents *TTR* V30M mRNA levels (*n*=5 per group). **B)** Photomicrographs illustrating TTR V30M in injured sciatic nerves; scale bar 50 µm. Chart represent quantification of immunohistochemical images (*n*=5 per group). **C)** Representative electron microscopy pictures of non-treated injured sciatic nerves (scale bars 0.5 µm and 100 nm). **D)** Top panels demonstrate colocalization (arrows) between TTR V30M (green) and HSPG (red) in control injured nerve. Double immunofluorescence between TTR (green) and βIII-tubulin (red, bottom panels). Nuclei stained blue with DAPI. Scale bar 15 µm. **E)** TTR V30M IHC in lumbar DRG ipsilateral to the injury side (top panel). Scale bar 50 µm. Chart demonstrates quantification of histological pictures. Lower panel represents double immunofluorescence between TTR V30M and βIII-tubulin; scale bar 15 µm. **p*<0.05 and ***p*<0.01.

Pre-treatment with Anakinra in V30M mice decreased the levels of Myd88 adaptor and total Creb after injury

Myd88 is an essential effector in the IL-1 signaling pathway (Burns et al., 1998). In injured sciatic nerves from Anakinra treated animals the expression of *Myd88* adaptor and its protein levels were found downregulated (Figure 2A and 2B). Due to lower *TTR* V30M expression by the nerve in mice treated with Anakinra, we next questioned if this drug was affecting the expression of *TTR* transcription factors. Accordingly, we analyzed the expression of *Hnf-3β*, *Hnf-4*, *C/ebp-β* and *c-Jun*, the latter one acting on *TTR* promoter through interaction with AP-1 (Qian et al., 1995). No differences were detected regarding the expression of these molecules in nerve tissue after injury, with or without Anakinra (data not shown). Given the mounting evidence for the interrelation of CREB and IL-1β (Tang et al., 2005, Wen et al., 2010), we next assessed the mRNA and protein levels of this molecule and found lower levels of total CREB in mice treated with Anakinra when compared to non-treated mice (Figure 2C and 2D).

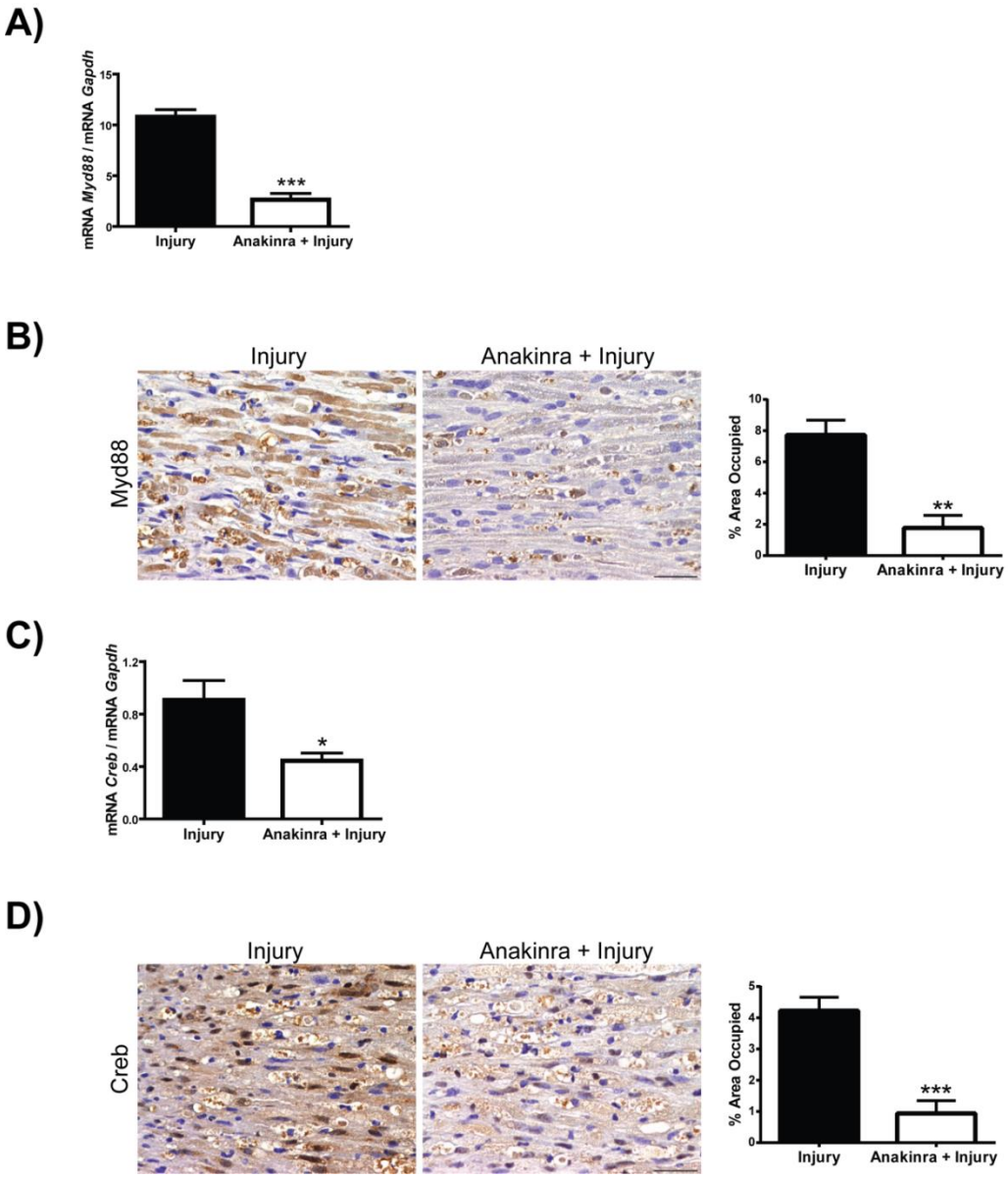

Figure 2 – Treatment with Anakinra reduces the levels of Myd88 and total Creb after injury. **A)** Histogram represents *Myd88* mRNA levels in the sciatic nerve of Anakinra treated animals (*n*=5) as compared with non-treated (*n*=5). **B)** Representative SQ-IHC for Myd88, 7 days after injury, in V30M Anakinra treated mice (*n*=5) and controls (*n*=5). Scale bar 50 µm. Chart represents the quantification of immunohistological images. **C)** Quantification of *Creb* mRNA levels extracted from injured sciatic nerves of mice treated with Anakinra (*n*=5) as compared with untreated ones (*n*=5), analyzed by qPCR. **D)** SQ-IHC against total CREB in injured sciatic nerves of Anakinra treated and untreated V30M mice. Scale bar 50 µm. Plot corresponds to the semi-quantification of CREB staining represented as the ratio of occupied area in the whole tissue; *n*=5 per group. **p*<0.05, ***p*<0.01 and ****p*<0.001.

Treatment with Anakinra before nerve injury decreases levels of pro-apoptotic markers in V30M mice

As soon as 1 week after injury, axonal loss and apoptosis occurs which limits nerve recovery (Scheib and Höke, 2013). Based on previous results showing that Anakinra prevents apoptosis (Abbate et al., 2008; Schwarznau et al., 2009; Gonçalves et al., 2014b), we analyzed the production levels of apoptotic related molecules such as Fas death receptor, Bid (a pro-apoptotic member of the Bcl-2 family) and cleaved caspase-3, in our study model. All apoptotic markers were found significantly reduced in Anakinra treated mice when compared to non-treated animals (Figure 3A). We next searched for cellular localization of cleaved caspase-3 apoptotic marker in untreated animals. With confocal microscopy, staining for cleaved caspase-3 localized mainly in Schwann cells and endoneural macrophages of the sciatic nerve (Figure 3B, arrows, top and middle panels, respectively) while colocalization with axons was barely found (Figure 3B, arrow, bottom panel). Additionally, L4-L6 DRG ipsilateral to the injury side were also analyzed for cleaved caspase-3 and with histological examination this molecule was found downregulated in animals treated with Anakinra (Figure 3C, top panel). Moreover, with immunofluorescence analysis, cleaved caspase-3 was found in neurons of the DRG ganglia, as illustrated with colocalization with βIII-tubulin (Figure 3C, bottom panel, arrows). These results suggest that Anakinra prevents neuronal, glial and immune cell apoptosis after injury. Considering that cathepsins B and D have been implicated in apoptosis in a variety of animal models (Chwieralski et al., 2006), we also asked if these enzymes could be altered in our model. We found that expression of both *Cathepsin B* and *D* was significantly downregulated in response to Anakinra when compared to non-treated animals (Figure 3D). All together, these results indicate an overall decreased apoptotic response after nerve injury in V30M mice receiving Anakinra as compared to untreated mice.

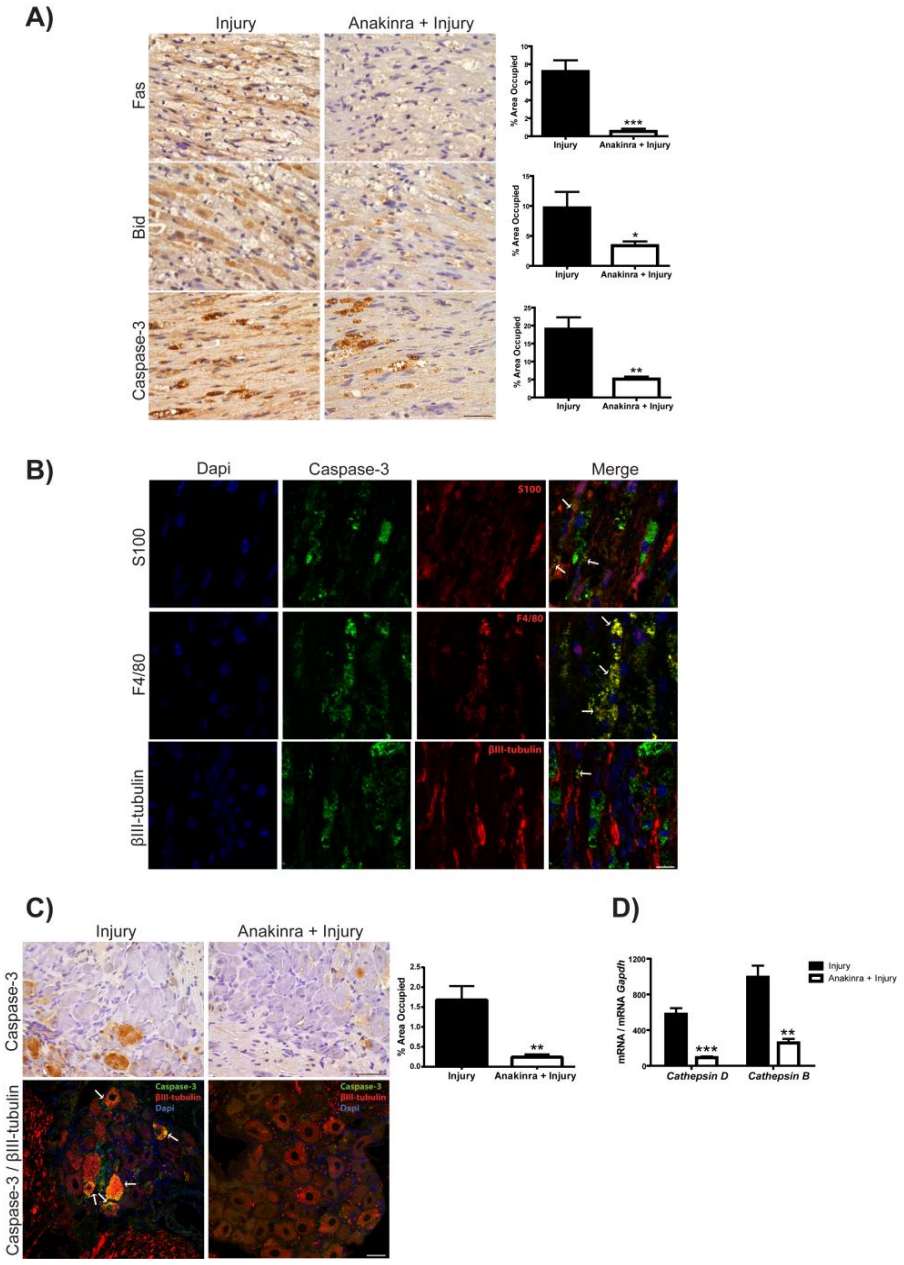

Figure 3 – Mice receiving Anakinra, previously to injury, presented less apoptosis. A) SQ-IHC against Fas death receptor, Bid and cleaved caspase-3 in sciatic nerve of V30M animals treated with Anakinra (*n*=5) or PBS (*n*=5), 7 days post-injury. Scale bar 50 μm. Histograms represent the respective SQ of histological images. **B)** Double immunofluorescence between cleaved caspase-3 and βIII-tubulin (neuronal and axonal marker), S100 (Schwann cell marker) or F4/80 (marker for macrophages) in control injured sciatic nerves. Arrows in merged images denote colocalization. Scale bar 10 μm. **C)** SQ-IHC against cleaved caspase-3 evaluated in L4-L6 ipsilateral DRG (top panels; *n*=5 each group). Scale bar 50 μm. Chart highlights the significant difference obtained with quantification of histological images. In bottom panels, representative picture show cleaved caspase-3 localization in neurons of DRG from non-treated mice. Scale bar 10 μm. **D)** Chart represents *Cathepsin B* and *Cathepsin D* mRNA levels in sciatic nerve, 7 days after injury in Anakinra treated and untreated V30M mice (*n*=5). **p*<0.05, ***p*<0.01 and ****p*<0.001.

Inhibiting IL-1 signaling activity before injury ameliorates the regenerative process in V30M mice

After a PNS lesion, the distal axonal segment undergoes Wallerian degeneration, while the proximal segment regenerates, with Schwann cells playing a crucial role to start remyelination through contact with regenerating axons (Defrancesco-Lisowitz et al., 2014). To evaluate the degree of post-injury neuroregeneration with Anakinra treatment, we performed morphometric analysis distal to the injury site. In treated V30M mice, the myelinated axon density was 1.7 fold increase when compared to untreated mice (Figure 4A). Using electron microscopy, the number of unmyelinated fibers, distally to the injury site, was determined indicating an increase of 86% in Anakinra treated V30M animals as compared with non-treated controls (Figure 4B). No significant changes in the endoneurial space between groups were observed.

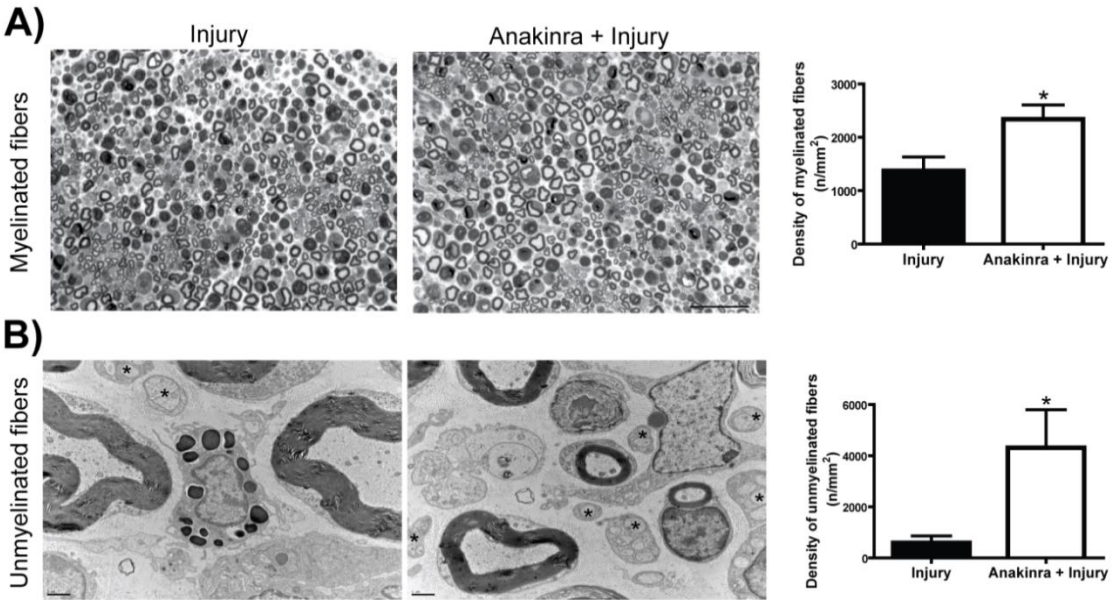

Figure 4 – Increased nerve fiber density in V30M mice receiving Anakinra before injury. Morphometric analyses of distal sciatic nerve stumps, 7 days after injury (*n*=4 animals in each group). **A)** Representative images from semithin sections showing higher number of myelinated fibers in V30M mice treated with Anakinra. Scale bar 50 μm. **B)** Representative electron microscopy pictures demonstrating increased unmyelinated fibers after injury, in Anakinra treated animals (asterisk). Scale bar 1 μm. Charts presented in the right panel indicate the corresponding fiber densities (*p<0.05).

In order to support these findings, we next assessed the levels of NGF-β and regeneration-associated markers GAP-43, peripherin and ATF-3 (Sensenbrenner et al., 1997; Pearson et al., 2003; Girard et al., 2008; Sun et al., 2009) and found that they were

significantly increased in animals treated with Anakinra as compared to non-treated mice (Figure 5A). Additionally, by qPCR, persephin, a member of the glial derived neurotrophic factor family (Milbrandt et al., 1998), important for the support of regenerating axons after injury, and synapsin III, a member of the synapsin gene family implicated in synaptogenesis and in the modulation of neurotransmitter release (Kao et al., 1998), were also upregulated in response to Anakinra when compared to non-treated mice (Figure 5B). All together, these data suggest an improved regenerative response when IL-1 signaling is diminished before injury, in this FAP mouse model.

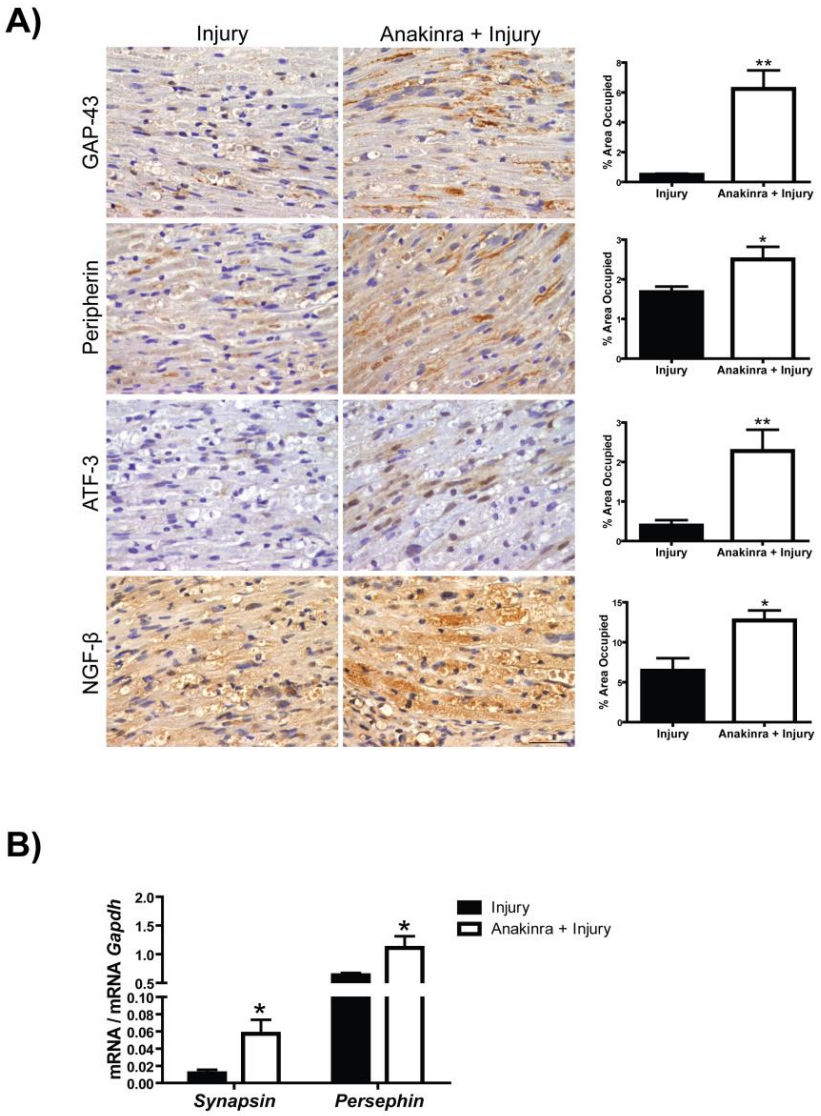

Figure 5 – Increased activation of regenerating markers in sciatic nerve of V30M Anakinra treated mice. A) Representative SQ-IHC for GAP-43, peripherin, ATF-3 and NGF-β, 7 days after injury, in V30M Anakinra treated mice (*n*=5) and controls (*n*=5). Charts represent the quantification of immunohistological images. Scale bar 50 μm. **B)** Bar graph illustrates mRNA levels for *Synapsin* and *Persephin,* normalized to *Gapdh*, in injured V30M sciatic nerves, with and without Anakinra treatment (*n*=5 mice per group). **p*<0.05 and ***p*<0.01.

Improved nerve regeneration after injury, results from the downregulation of TTR V30M expression and deposition and not directly from Anakinra

Next, we wondered if the striking difference in nerve regeneration after injury with Anakinra resulted from the drug itself or from downregulation of TTR V30M expression and deposition in the nerve. To address this question, we treated age-matched WT mice with Anakinra, following the same strategy used for V30M mice. In contrast to the latter condition we found no difference in mouse TTR deposition in nerve tissue after injury in animals receiving the drug as compared with controls (Figure 6A). Similarly, no difference was detected regarding the regenerating markers GAP-43, peripherin or ATF-3 (Figure 6B). However, WT animals treated with Anakinra presented lower nerve fiber density after injury when compared with WT untreated mice (Figure 6C). Therefore, in a WT condition, blocking IL-1 with Anakinra before injury is being deleterious for nerve recovery since IL-1 is an important cytokine for early peripheral regeneration (Nadeau et al., 2011). These results, together with the above mentioned data, strengthen the idea that local TTR V30M expression and deposition impairs nerve regeneration. Also, the presence of a heterologous human TTR in the nerve of V30M mice might contribute to this paradigm.

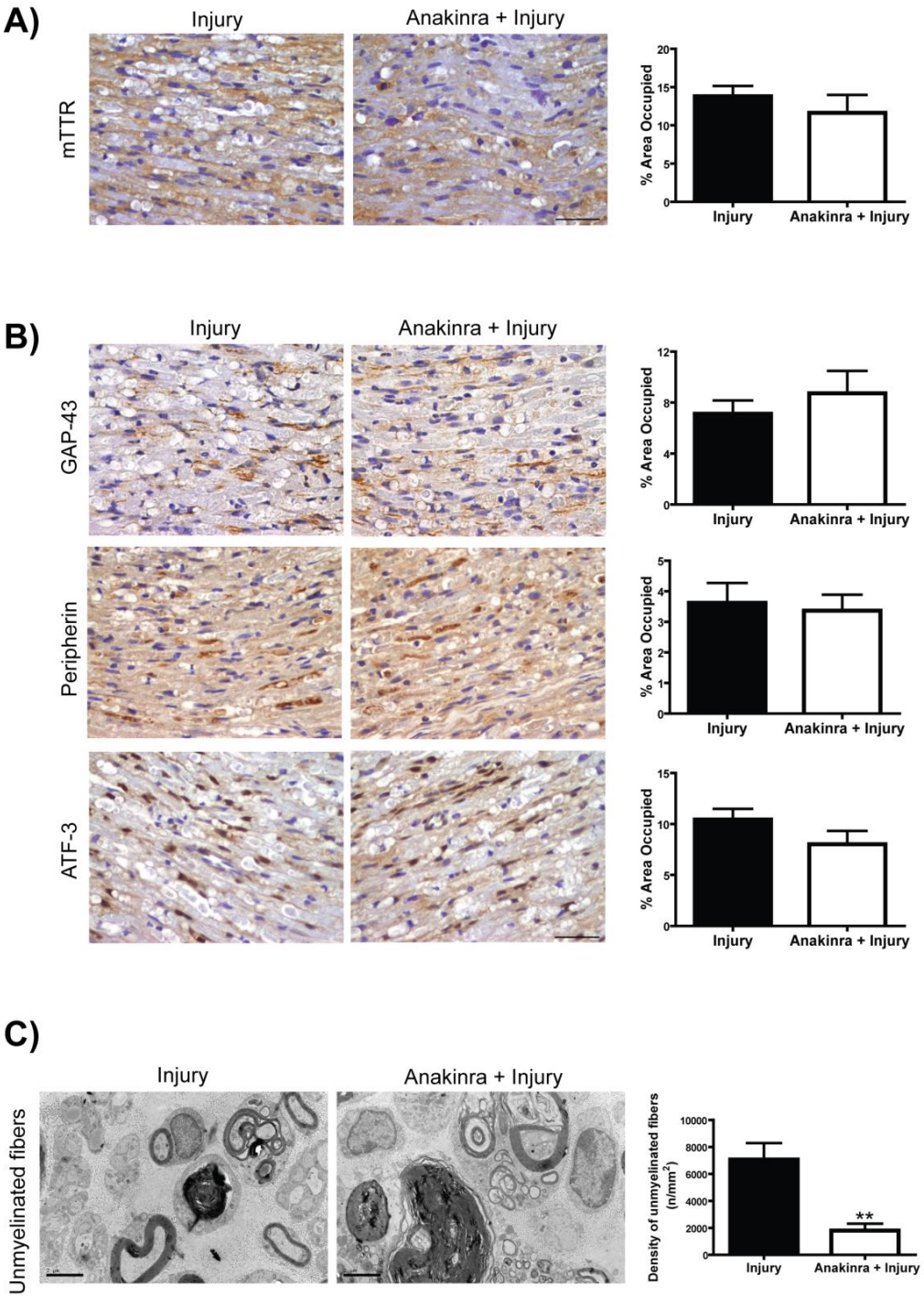

Figure 6 – Increased levels of regenerating markers and fiber density in V30M Anakinra treated mice are consequent to TTR V30M downregulation and not directly from Anakinra. A) Mouse TTR immunohistochemical staining of injured sciatic nerve sections from WT mice, with respective semi-quantification chart (*n*=5 per group). Scale bar 50 µm. **B)** Representative SQ-IHC in WT mice treated with Anakinra (*n*=5) and respective untreated controls (*n*=5), showing no difference regarding GAP-43, peripherin or ATF-3 levels between both groups. Scale bar 50 µm. **C)** Morphometric analyses of injured nerves from WT mice both treated (*n*=4) and untreated with Anakinra (*n*=4). Scale bar 2 µm. ***p*<0.01.

Innate cellular infiltrate to injured nerve and macrophage phenotype are not affected by Anakinra in V30M mice

To compare the inflammatory infiltrate after injury of untreated and Anakinra treated V30M mice, we performed flow cytometry of injured nerves. Overall, we saw no differences regarding the frequency of neutrophils, macrophages or dendritic cells in V30M treated animals when compared with untreated mice (data not shown). Since M2 subsets of monocytes/macrophages are necessary for neural repair after injury (Barrette et al., 2008; Kigerl et al., 2009), we next analyzed the macrophagic phenotype by western blot. A balance between iNOS and Arg-1 production is highly indicative of macrophage phenotypes M1 and M2, respectively (Van Ginderachter et al., 2006; Ydens et al., 2012). In our study, we found a similar induction of these molecules after injury, regardless of Anakinra treatment, indicating a similar M1 and M2 macrophage phenotype pattern in both mice groups (Figure 7).

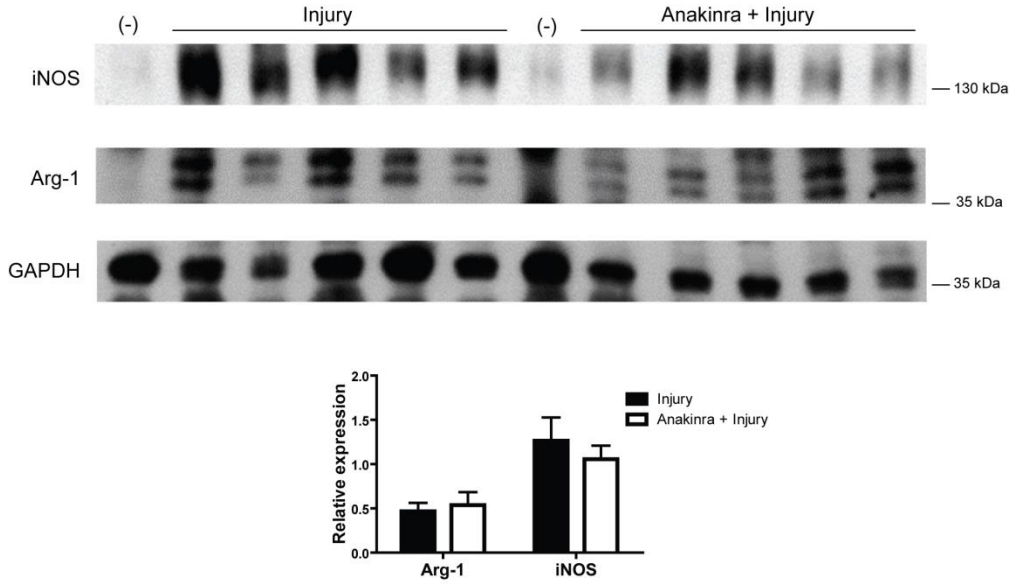

Figure 7 – Treatment with Anakinra did not alter macrophage phenotype. Anti-iNOS and anti-Arg-1 western blots of injured nerves from Anakinra (*n*=5) and PBS treated V30M mice (*n*=5). (-) refers to pooled sham nerves (*n*=5 from each group). Bar graph represents normalized proteins to GAPDH.

Discussion

Overwhelming evidence supports a role for neuroinflammation in the pathophysiology of several neurodegenerative conditions, such as Alzheimer's disease, Parkinson's disease and multiple sclerosis. Activation of microglia, vascular changes with infiltration of peripheral immune cells into the brain, elevated levels of cytokines and neuronal cell death are common deleterious pathways for multiple sclerosis and Parkinson's disease (Van Horssen et al., 2005; Sanchez-Guajardo et al., 2013). In contrast, in Alzheimer's disease, recruitment of monocytes/macrophages from the periphery into the brain would probably be beneficial since brain microglia fails at restricting Aβ plaque formation and degradation (Rezai-Zadeh et al., 2011). Altogether, these data reinforce the importance of new strategies targeting and modulating inflammatory mechanisms in neurodegenerative disorders.

In FAP patients, there is a continuous synthesis of cytokines by peripheral nerve, predominantly of IL-1β (Sousa et al., 2001b), starting as early as the asymptomatic stage of disease. In line with this, it was recently shown that in a mouse model of senile systemic amyloidosis (SSA) the heart presents a robust immune inflammatory transcriptional profile before TTR WT start to accumulate in this tissue (Buxbaum et al., 2012). In accordance with this observation, it has been shown, in a FAP mouse model, that the inflammatory milieu might precede and contribute to non-fibrillar TTR deposition in the PNS (Gonçalves et al., 2014a). Considering these previous studies on the association between inflammation and disease progression, our aim was to evaluate the influence of IL-1 signaling in TTR V30M regulation in peripheral nerve, after an inflammatory stimulus. The IL-1 family consists of 11 molecules which induce a complex network of pro-inflammatory cytokines (Garlanda et al., 2013). The most studied agonists are IL-1α and IL-1β that bind to the IL-1 receptor type I (IL-1RI) and activate signaling via Myd88 adaptor (Burns et al., 1998; Dinarello et al., 2011). When we blocked IL-1RI with Anakinra, the recombinant form of the natural and specific receptor antagonist, Myd88 gene expression and protein levels in nerve were downregulated, proving treatment efficacy, as previously described (Ehses et al., 2009; Gonçalves et al., 2014b). Surprisingly, pre-treatment with Anakinra reduced local nerve *TTR* synthesis induced by sciatic nerve injury in V30M mice. TTR is typically described as a negative acute phase protein whose plasma level decreases during the acute phase inflammatory response (Gruys et al., 2005). This fact was speculated to be secondary to increased protein degradation during inflammation (Rosales et al., 1996) or related to lower *TTR* synthesis by the liver due to decreased levels of hepatocyte nuclear factors (Qian et al., 1995). Regarding sciatic nerve, we previously showed that *TTR* production is dependent of the inflammatory threshold

(Gonçalves et al., 2014a). Therefore, it is plausible that, depending on the insult and threshold of inflammation, the system will regulate *TTR* expression differently from the liver, as it is the case of the present study where inhibition of IL-1 resulted in decreased *TTR* levels in peripheral nerve. *TTR* V30M should be regulated by the same transcription factors known to regulate mouse *TTR*. No difference was found regarding the most important transcription factors known to regulate *TTR* expression, suggesting the direct or indirect modulation by IL-1 of other factors affecting *TTR* regulation. *Creb* was found downregulated with Anakinra treatment and thus, it is a possible candidate for this regulation (Wen et al., 2010). It is also fair to speculate that *TTR* synthesis by sciatic nerve may have a different control mechanism than *TTR* synthesized by the liver or choroid plexus, a topic that will need further investigation.

As a consequence of axonal lesion, breakdown and clearance of distal fibers, in an active self-destruction program, is called Wallerian degeneration (Scheib and Höke, 2013). Early after injury, IL-1β is upregulated promoting apoptotic cell death that will contribute to neurodegeneration (Rothwell et al., 1997). IL-1β appears to be required for apoptosis in several cell types. For example, Mahr et al., (2000) described that IL-1β can trigger cell apoptosis by altering the expression of members of the Bcl-2 family (Mahr et al., 2000). Increased synthesis and release of IL-1β has also been associated with caspase-3 induced apoptosis (Nesic et al., 2001). The inhibitory effect of IL-1Ra on cell apoptosis in different experimental models has been reported (Nesic et al., 2001; Abbate et al., 2008; Rusai et al., 2008; Wu et al., 2011), suggesting that endogenous IL-1 acts at a late stage in the pathway of cell death. Importantly, in nerve biopsies from FAP patients, simultaneously with the increased expression of IL-1β by the nerve, apoptotic cell death becomes evident through activation of caspase-3 (Sousa et al., 2001b). In accordance with these observations, in the present study we found that blocking IL-1 before an injury stimulus prevented axonal activation of pro-apoptotic molecules, such as Fas death receptor, cleaved caspase-3, Bid and cathepsins B/D. Cathepsins are proteases located in lysosomes that can be released into the cytoplasm upon cell damage. In this regard, oxidative stress, growth factor starvation or Fas receptor activation may all cause apoptotic cell death through lysosomal leakage (Brunk and Svensson, 1999). From all cathepsins that might be released under lysosomal destabilization, cathepsins B and D have been found to play an important role in the regulation of apoptosis (Chwieralski et al., 2006). Thus, it is possible that the decreased expression of these enzymes contributed to some extent to the diminished nerve injury response in V30M animals treated with Anakinra. Taken together, our data suggests that *Cathepsins B* and *D* decreased expression may prove beneficial in the regulation of apoptosis and in prevention of death-inducing signaling platforms.

Since it has been previously shown that increased expression of *TTR* V30M impairs nerve regeneration after injury (Gonçalves et al., 2014a), we questioned if in animals treated with Anakinra nerve regeneration was ameliorated. We found that V30M mice treated with Anakinra not only showed higher nerve fiber densities but also presented increased levels of regenerating markers, not related with macrophage infiltration or differentiation stage. Treatment with IL-1Ra has been shown to be neuroprotective in hippocampal slice cultures after excitotoxic damage (Hailer et al., 2005), in models of focal cerebral ischemia (Relton et al., 1996; Loddick et al., 1997; Banwell et al., 2009), in a fluid percussion brain injury model (Toulmond and Rothwell, 1995; Lawrence et al., 1998) and on a rat model of spinal cord injury (Zong et al., 2012). Thus, to understand if in our model neuroprotection was due to direct effects of Anakinra or indirectly, consequent to the downregulation of TTR V30M in nerve tissue, we treated WT mice with Anakinra before injury. Our data clearly indicate that the increased regeneration after neuronal injury in V30M mice receiving Anakinra was due to decreased levels of TTR V30M transcription and deposition since treated WT mice showed no difference regarding regenerating markers and, importantly, presented lower density of unmyelinated nerve fibers. In naïve mice, IL-1 has been associated with early peripheral nerve regeneration; however, the mechanisms by which this cytokine mediate regenerating effects remains to be fully elucidated (Nadeau et al., 2011). Additionally, the role of IL-1 in axonal growth of WT mice was confirmed by the inhibitory action of IL-1Ra on regeneration after axotomy (Guénard et al., 1971). Moreover, in contrast with TTR V30M, mouse TTR has an important role regarding peripheral nerve regeneration (Fleming et al., 2007). Since Anakinra did not alter mouse TTR levels in nerve after injury, the lower fiber density might be explained by decrease levels of IL-1 in WT mice. Previous data show that increased TTR V30M deposition in nerve after injury, compromise the immune response with lower innate cell infiltration (Gonçalves et al., 2014a). In the present work, despite IL-1 signaling inhibition by Anakinra, treated V30M mice were able to produce NGF-β and to recruit different immune cell subsets, such as neutrophils, pro-inflammatory M1 macrophages and dendritic cells.

In summary, our results further substantiate the importance of inflammation mediated by IL-1 in the regulation of human mutated TTR and, consequently in the pathomechanisms activated after nerve injury. Treatment with Anakinra before sciatic nerve injury partially rescues the phenotype of FAP mice caused by abnormal TTR V30M synthesis and protein deposition in the PNS after an inflammatory stimulus. Despite many recent advances, prevention/treatment for FAP or TTR-related amyloidosis is highly complex and will most likely require a combination of approaches. We believe that targeting neuroinflammation might be one of those approaches and more detailed studies on the subject will open new windows of action to improve the neuropathology of these disorders.

Acknowledgements

This work was funded by FEDER funds through the Operational Competitiveness Program – COMPETE and by National Funds through FCT – Fundação para a Ciência e a Tecnologia under the projects FCOMP-01-0124-FEDER-022718 (PEST-c/SAU/LA0002/2011, PTDC/SAU-ORG/111313/2009 and PTDC/BIM-MEC/0282/2012) and fellowships to NPG (SFRH/BD/74304/2010) and to MTC (ON2-201302-ND-III). The present work was also sponsored by POPH/FSE QREN program.

We thank Dr. Paulo Vieira from Pasteur Institute for useful discussions. At IBMC we thank Rui Fernandes and Paula Gonçalves for support with electron microscopy and paraffin tissue processing, respectively.

Chapter V

Glial cells in Familial Amyloidotic Polyneuropathy

Glial cells in Familial Amyloidotic Polyneuropathy

Nádia Pereira Gonçalves[1,2,3], Susete Costelha[1,2], Maria João Saraiva[1,2,3]

1) Instituto de Inovação e Investigação em Saúde (I3S), Universidade do Porto, Portugal
2) Molecular Neurobiology, IBMC – Instituto de Biologia Molecular e Celular, Porto, 4150-180 Portugal
3) Instituto de Ciências Biomédicas de Abel Salazar (ICBAS), Universidade do Porto, Porto, 4050-313 Portugal

Running title: Glial cells in FAP

Abstract

Transthyretin (TTR) V30M mutation is the most common variant leading to Familial Amyloidotic Polyneuropathy (FAP). In this genetic disorder, TTR accumulates preferentially in the extracellular matrix (ECM) of peripheral and autonomic nervous systems leading to cell death and dysfunction. Thus, knowledge regarding important biological systems for TTR clearance might unravel novel insights into FAP pathophysiology. Herein, our aim was to evaluate the ability of glial cells from peripheral and autonomic nervous systems in TTR uptake and degradation. We assessed the role of glial cells in FAP pathogenesis with real-time polymerase chain reaction, immunohistochemistry, interference RNA and confocal microscopy.

Histological examination revealed that Schwann cells and satellite cells, from an FAP mouse model, internalize and degrade non-fibrillar TTR. Immunohistochemical studies of human nerve biopsies from V30M patients and disease controls showed intracellular TTR immunoreactivity in Schwann cells, corroborating animal data. Additionally, we found *TTR* expression in colon of this FAP mouse model, probably being synthesized by satellite cells of the myenteric plexus.

Overall, these findings bring to light the closest relationship between TTR burden and clearance from the nervous system extracellular milieu.

Introduction

Familial Amyloidotic Polyneuropathy (FAP) is a rare but fulminant and life-threatening neurodegenerative disorder. Approximately ten thousand patients are affected worldwide with endemic foci in Portugal, Japan and Sweden (Said et al., 2012). Major neuropathological and neurochemical hallmarks of this autosomal dominant hereditary disease included extracellular accumulation of mutated transthyretin (TTR) aggregates and amyloid fibrils, particularly in autonomic and peripheral nervous systems (ANS and PNS, respectively), leading to sensorimotor, motor and autonomic neuropathy (Coimbra and Andrade, 1971b).

Transthyretin is a tetramer of identical subunits of 127 amino acid residues each (Blake et al., 1974). It is primarily synthesized by the liver and the choroid plexuses of the brain (Soprano et al., 1985; Dikson et al., 1986) and functions as a protein carrier for thyroxine and retinol (Kanai et al., 1968; Raz and Goodman, 1969). More than 100 single point TTR mutations have been discovered, being the exchange of a methionine for a valine at position 30 (V30M) the most common in FAP (Saraiva et al., 1984). TTR is mainly produced by the liver as a monomer that assembles into a tetramer and is efficiently secreted. This process occurs in most FAP associated mutations, including carriers of the V30M mutation (Sekijima et al., 2005). Particular high amyloidogenic mutations, such as the L12P associated with leptomeningeal amyloidosis, form intracellular aggregates that are transported into liver lysosomes (Batista et al., 2013) and thus these mutants are poorly secreted. Contrarily to other TTR amyloidoses, L12P cases present liver TTR deposition (Brett et al., 1999).

The original amyloid cascade hypothesis proposed that circulating TTR dissociation into non-native monomers is a determinating step for misfolding. Thus, monomers with low conformational stability self-assemble forming non-fibrillar aggregates, protofibrils and mature amyloid fibrils (Colon and Kelly, 1992; Quintas et al., 2001) that accumulate in the ECM of the gastrointestinal tract, skin, heart, kidney and PNS (Sousa and Saraiva, 2003).

A particular feature of FAP is organ and tissue tropism for TTR deposition. The mechanistic and functional principles that underlie this fact are not fully understood. Hence, converging evidence revealed the importance of a dynamic balance between formation and clearance of extracellular deposited TTR (Tsuchiya et al., 2008). Cellular uptake of soluble TTR by hepatocytes, mouse embryonic fibroblasts, yolk sac cells and sensory neurons, was previously demonstrated *in vitro* (Sousa et al., 2000a; Sousa and Saraiva, 2001; Fleming et al., 2009). More recently, intracellular material has been observed in fibroblasts and macrophages, through analysis of skin biopsies from FAP patients and TTR transgenic mice (Misumi et al., 2013).

Since important target tissues of TTR load belong to the ANS and PNS, the aim of the present study was to investigate TTR localization in tissues and cells of these systems. To perform this work we take advantage of human nerve biopsies and tissues from a well-established FAP mouse model, carrying the human *TTR* V30M gene.

We analyzed *TTR* expression in the peripheral nerve of the FAP mouse model using qPCR analysis and determined the subcellular localization of TTR in satellite cells from mice dorsal root ganglia (DRG) and Schwann cells. Schwann cells from patients and control subjects were also evaluated, through confocal double immunofluorescence. An interference RNA (RNAi) approach was used to study TTR expression/internalization by satellite cells from the myenteric plexus.

Materials and Methods

Ethics statement

All mouse protocols followed the European Union Directive (2010/63/EU) and were previously approved by the Institutional and National General Veterinarian Board ethical committees. Human tissue biopsy was performed after informed consent and approval from the Ethics Committee of the Hospital Geral de Santo António (Porto, Portugal), following the declaration of Helsinki.

Human Samples

Archival sural nerve biopsy samples obtained from FAP V30M patients (*n*=4) and normal disease control subjects (*n*=4) were previously characterized, after informed consent, for TTR and amyloid deposition, with immunohistochemistry and Congo red staining, respectively. Samples were kindly provided by the Hospital Geral de Santo António (Porto, Portugal). FAP samples analyzed in this study presented TTR amyloid deposition. Disease control patients were near-relatives of FAP patients who ultimately turned out not to have mutations in TTR. This material was obtained as part of the clinical diagnosis and evaluation of polyneuropathy, before the current use of less invasive methods, as previously described (Sousa et al., 2001b).

Animals

Six months transgenic mice for human *TTR* V30M, in the 129/Sv and endogenous *Ttr* null background, heterozygous for the heat shock factor-1 (*Hsf-1*), here designated as Hsf/V30M (Santos et al., 2010b), were used for the experiments. Although not presenting amyloid fibrils in PNS or ANS, non-fibrillar TTR material is widespread in the extracellular milieu of these systems at 6 months of age. Additionally, 6 months-old wild-type (WT) and TTR knockout (KO) mice (Episkopou et al., 1993), in a 129/Sv background were used as controls. Animals were housed in a controlled-temperature room, maintained under a 12 h light/dark cycle, with water and food *ad libitum* and euthanized with a lethal injection of a premixed solution containing ketamine (75 mg/kg) and medetomidine (1 mg/kg).

Liver TTR silencing *in vivo* with RNAi

For *TTR*-silencing studies, TTR or control siRNA (vehicle) were formulated into a lipid nanoparticle delivery system (Semple et al., 2010). Five months-old Hsf/V30M mice were injected in the tail vein with human TTR siRNA (*n*=6), at a concentration of 1 mg/kg.

Untreated age-matched controls received vehicle intravenously (*n*=6). One injection per week was performed during 4 weeks and animals were sacrificed 48 h after the last injection. Liver and colon were divided and collected to 10% formalin and frozen at -80ºC.

Messenger RNA (mRNA) isolation, complementary DNA (cDNA) synthesis and real-time quantitative polymerase chain reaction (qPCR)

Liver and colon mRNA (*n*=6 per group Hsf/V30M; *n*=5 WT) was isolated using phenol extraction (Invitrogen). Sciatic nerve from Hsf/V30M mice was dissected free from surrounding tissue (*n*=5) and mRNA extraction performed using RNeasy Mini columns (Qiagen). cDNA was synthesized with the SuperScript double-stranded cDNA Kit (Invitrogen). The quality of extracted RNA was assessed with Experion RNA StdSens Analysis Kit (Bio-Rad); qPCR was performed in duplicates using iQ Syber Green Super Mix (Bio-Rad) and reactions were run on an Bio-Rad iQ5 software.
Primer sequences were designed using Beacon Designer 8^{TM} (Premier Biosoft) for human *TTR,* mouse *Ttr,* glyceraldehyde 3-phosphate dehydrogenase *(Gapdh)* and *18S.* Differential expression was determined by the 2^-$^{\Delta\Delta CT}$ method.

Immunohistochemistry

Liver and colon from animals subjected to TTR siRNA treatment and respective controls were excised, post-fixed in 10% formalin, embedded in paraffin and cut longitudinally at 3 µm. Colon from WT and KO mice was used as controls (*n*=4). Histoclear (National Diagnostics) was used to deparaffinate sections that were thereafter hydrated in a descent alcohol series. Endogenous peroxidase activity was inhibited with 3% hydrogen peroxide in methanol and sections were blocked with 10% fetal bovine serum and 0.5% Triton X-100, in PBS. Primary antibodies against human TTR (1:600, rabbit polyclonal, DAKO) and mouse TTR (1:1,500, rabbit polyclonal, Q-Biogen) were used. After incubation with secondary antibody (anti-rabbit IgG, 1:200, Vector), sections were incubated with avidin-biotin-peroxidase complex (ABC Elite, Vector) and visualized using 3.3´-diaminobenzidine as a chromogen.

Immunofluorescent double labeling

For double immunofluorescence analyses, sciatic nerve, DRG and colon from Hsf/V30M animals were excised and processed as described above. Human sural nerve biopsies were also used. Rabbit polyclonal anti-human TTR (1:100, DAKO), sheep polyclonal anti-human TTR (1:100, Abcam), goat polyclonal anti-Octamer transcription factor 6 (Oct-6,

1:25, Santa Cruz Biotechnology), rabbit polyclonal anti-S100 (1:100, DAKO), rabbit polyclonal anti-early endosome antigen 1 (EEA1, 1:100, Sigma-Aldrich) and mouse monoclonal anti-lysosomal-associated membrane protein 1 (Lamp1, 1:75, Abcam) were used as primary antibodies. Secondary antibodies included donkey anti-rabbit Alexa Fluor 488, donkey anti-goat Alexa Fluor 568, donkey anti-sheep Alexa Fluor 488, goat anti-rabbit Alexa Fluor 568, goat anti-mouse Alexa Fluor 568 and 488 (1:1,000, Molecular Probes). Slides were mounted with Vectashield containing 4'.6-diamino-2-phenylindole (DAPI) (Vector) and visualized in a laser scanning Confocal Microscope Leica TCS SP5 II (Leica Microsystems).

TTR-immunopositive Schwann cells in human sural nerve biopsies were detected by merged images with anti-TTR antibody and a Schwann cell marker (Oct-6). The number of TTR-immunopositive Schwann cells in each group was calculated as an average of 5 visual fields (447.63 µm x 335.40 µm) per sample (n=4 per group) at an original magnification of 20 X, in a Axio Imager Microscope.

Statistical analysis

Two or three groups' comparison was performed with Student T-test or One-way ANOVA, respectively. For One-way ANOVA, Bonferroni was used as the post-test. Data are expressed as mean values ± standard error of the mean (SEM) and p-values of less than 0.05 were considered to be significant (*p<0.05, **p<0.01 and ***p< 0.001).

Results

Non-fibrillar TTR is degraded by Schwann cells of the FAP mouse model Hsf/V30M

Expression of *TTR* by Schwann cells of sciatic nerve in a mouse model carrying the TTR V30M mutation but missing TTR deposition in the PNS and ANS was previously described (Murakami et al., 2010). Thus, we questioned whether this feature is recapitulated in an FAP mouse model deficient for the *Hsf-1* (Hsf/V30M). In this model, non-fibrillar TTR deposition is widespread along the gastrointestinal tract since the first month of age. Furthermore regarding the nervous system, TTR deposits are found in the ECM of sciatic nerve, DRG and parasympathetic ganglia approximately at 6 months of age (Santos et al., 2010b). For this reason, animals with 6 months-old were chosen for subsequent analyses.
Using qPCR, TTR expression by the sciatic nerve of Hsf/V30M mice was found (61.7 units ratio of TTR mRNA and Gapdh mRNA ± 16.2 SEM). With double immunofluorescence between TTR and Oct-6, a Schwann cell marker, TTR intracellular staining in these cells was noticed (Figure 1A, arrows), suggesting them as the primary source of *TTR* in nerve, in accordance with previous results from other FAP mouse models (Murakami et al., 2010; Gonçalves et al., 2014a).
To localize TTR within Schwann cells, additional studies were performed using double immunofluorescence between TTR and a marker for the early endosome antigen 1 (EEA1). Looking for cells previously stained with Oct-6, consecutive cross-sectional images revealed that indeed Schwann cells presented intracellular punctuate material, visible in higher magnification, that colocalize with EEA1 (Figure 1B, arrows). Further labeling with TTR and Lamp1 demonstrated colocalization of TTR V30M with lysosomes (Figure 1C), indicating that Schwann cells, might also be important for TTR clearance.

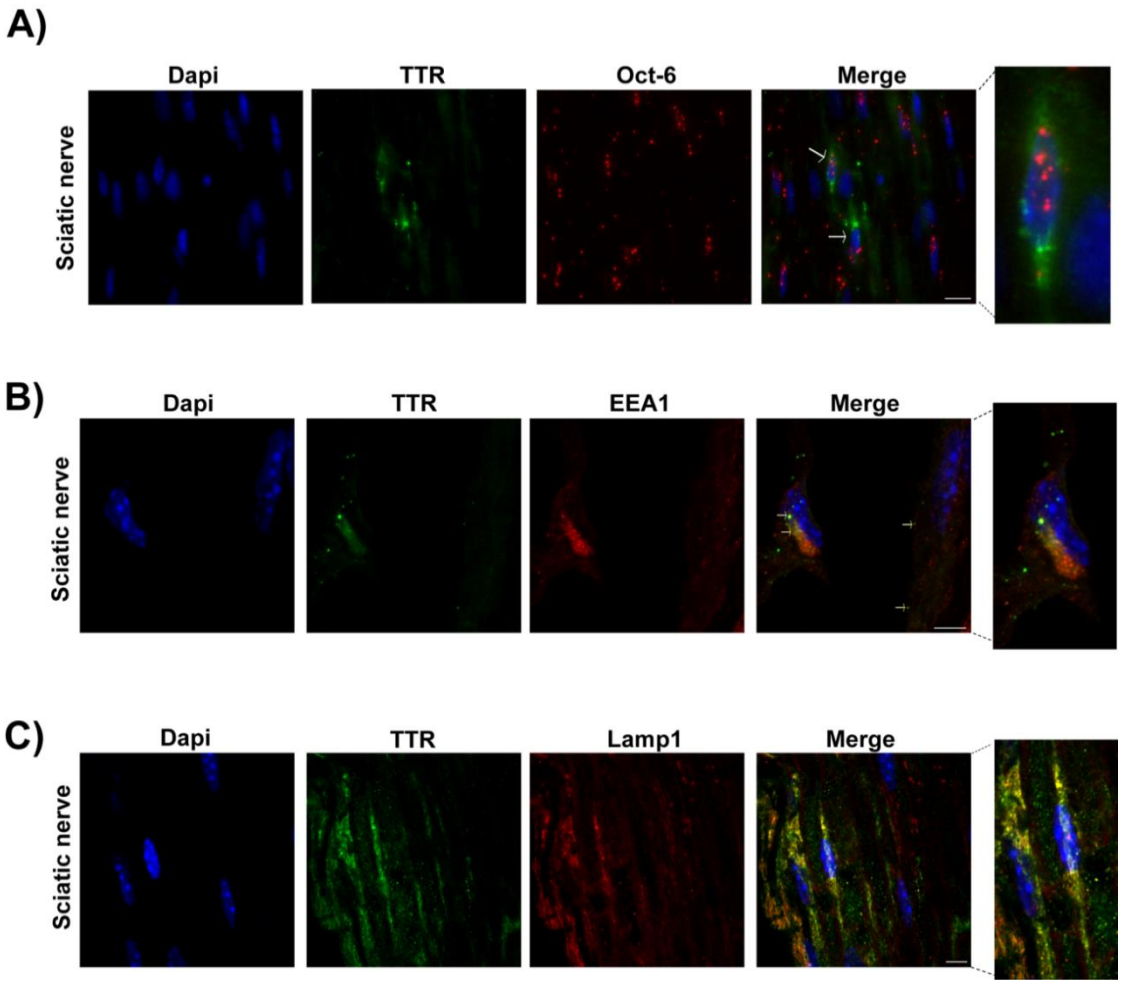

Figure 1 – Schwann cells express and internalize TTR in the Hsf/V30M FAP mouse model. A) Representative picture of double immunofluorescence between TTR (green) and Oct-6 (red) in Hsf/V30M nerves, demonstrating TTR intracellular staining in Schwann cells (arrows). Superposition of the labels, with DAPI (blue), is shown (merge, *n*=4). Scale bar 10 μm. **B)** Double immunofluorescence of TTR (green) and EEA1 (red) demonstrating colocalization between the 2 proteins in Schwann cells of Hsf/V30M mice (arrows). Scale bar 5 μm. **C)** Confocal representative image of a sciatic nerve section stained with anti-TTR antibody (green) and a lysosome marker (Lamp1; red). Colocalization between both markers was noticed in yellow; scale bar 5 μm.

Non-fibrillar TTR is internalized by glial cells of sensory ganglia

Data reported so far indicate that Schwann cells, besides being a source of *TTR* might also be important for TTR clearance in the sciatic nerve. We next investigated TTR immunoreactive glial cells from DRG of Hsf/V30M mice. In fact, with double immunofluorescence between TTR and S100, TTR intracellular staining was found in glial cells of DRG (possibly satellite cells; Figure 2A). Since it was previously shown that *TTR* is not synthesized by cells of DRG (Sousa and Saraiva, 2008) and in this work we found

colocalization of TTR with EEA1 (Figure 2B), we hypothesized that satellite cells have an active role in TTR internalization. Moreover, we found TTR signal partially colocalized with lysosomes (Figure 2C); therefore we can conclude that these cells participate in TTR clearance in this animal model.

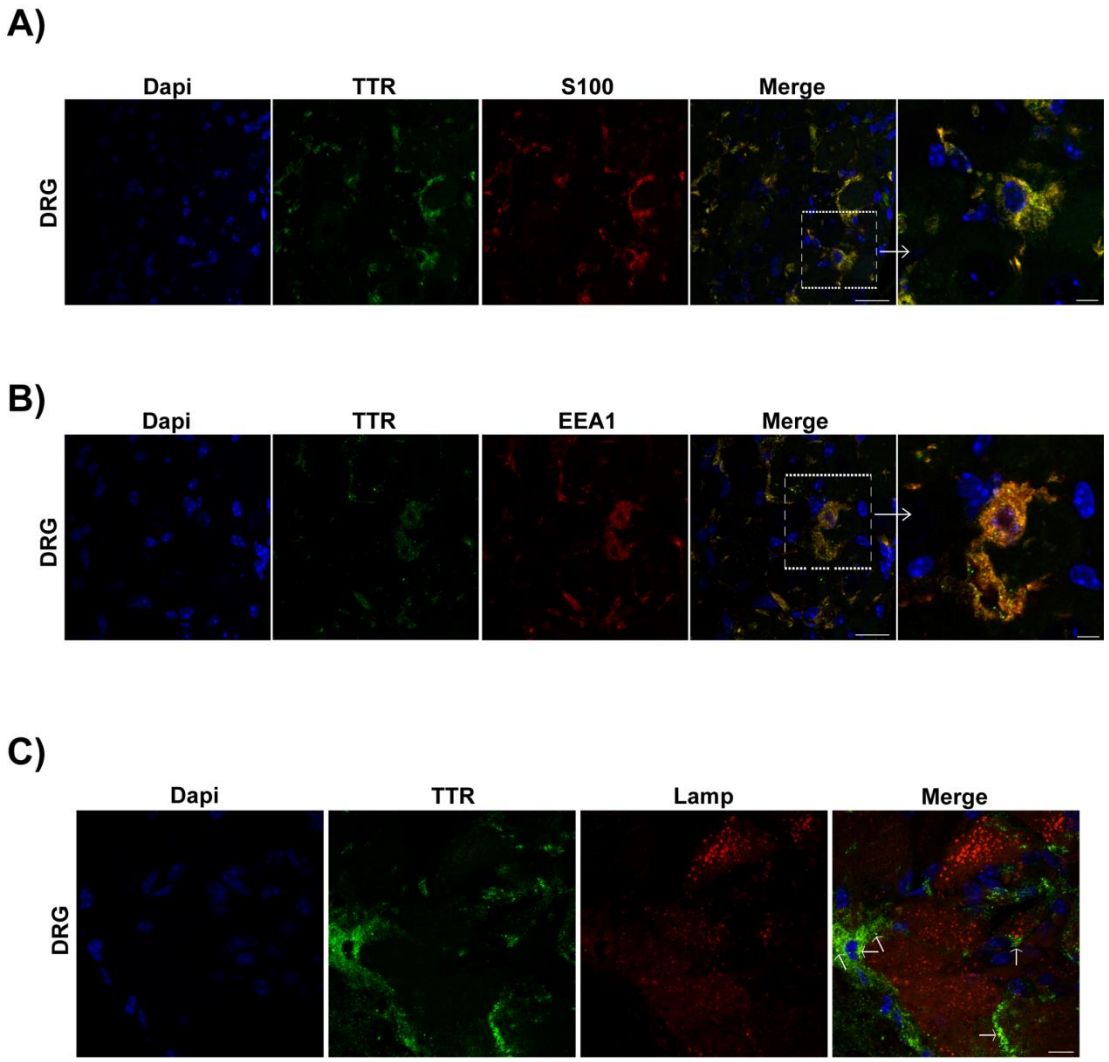

Figure 2 – Glial cells from DRG internalize TTR, in a mouse model of FAP. A) Double immunofluorescence of TTR (green) and S100 (red), a marker for glial cells, in DRG of Hsf/V30M mice, showing TTR localized inside satellite cells. Scale bar 20 µm; higher magnification 5 µm. **B)** TTR colocalizing with EEA1 in satellite cells from DRG of Hsf/V30M animals. Scale bar 20 µm; higher magnification 5 µm. **C)** Representative confocal image demonstrating colocalization between TTR (green) and lysosomes (Lamp1; red) in satellite cells from DRG (arrows). Scale bar 8 µm.

Intracellular TTR in human Schwann cells

Following the previous results with the FAP mouse model, we wondered if intracellular TTR could also be observed in nerves from FAP patients. To address this issue, we also used sural nerve biopsies from normal individuals (disease free) as controls. In disease control individuals, the majority of Schwann cells were negative for TTR WT intracellular staining; surprisingly, few positive cells presented TTR WT immunoreactive punctuate material (Figure 3A, top panel, and 3B), suggesting that Schwann cells might have an important role for uptake and degradation of TTR WT reaching the nerve though the blood stream. In FAP carriers, some Schwann cells had generalized TTR V30M intracellular staining (Figure 3A, bottom panel, and 3B) and the percentage of TTR positive cells was significantly higher than for disease control patients (Figure 3C).

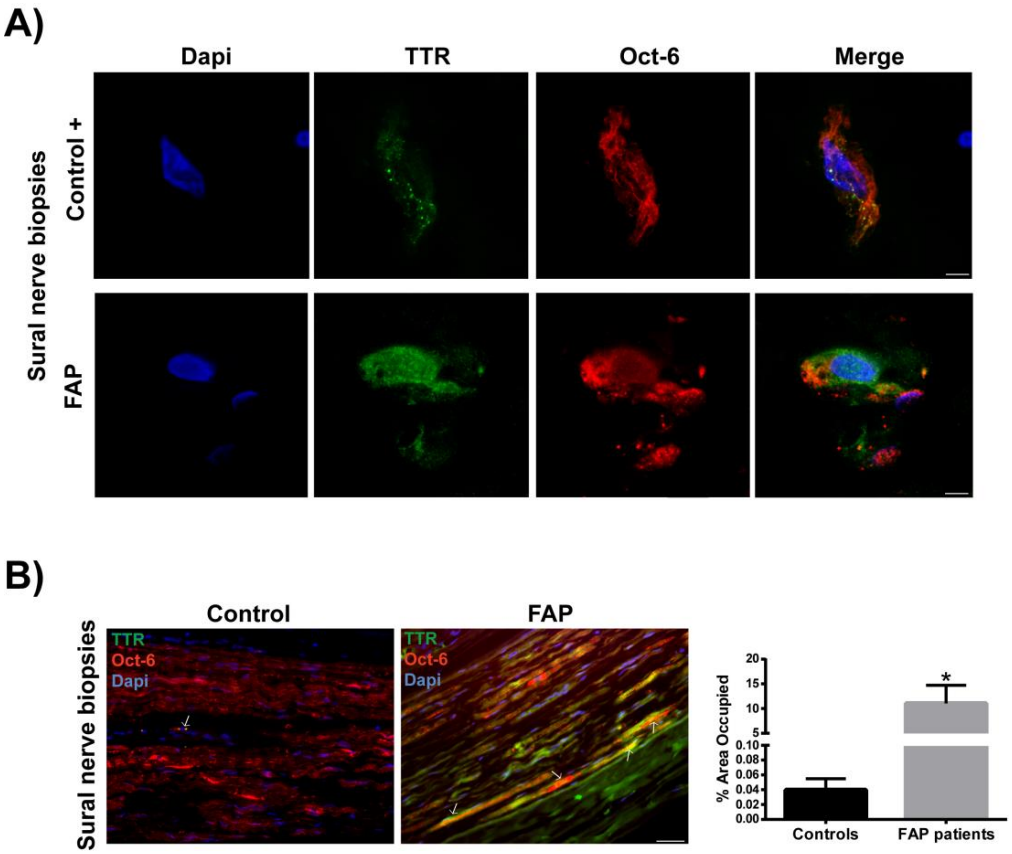

Figure 3 – Intracellular TTR in Schwann cells of human nerve biopsies. A) Representative images from double immunofluorescence between TTR (green) and Oct-6 (red) in sural nerve biopsies from disease control individuals and FAP patients, demonstrating TTR intracellular staining in Schwann cells. Superposition of the labels, with DAPI (blue), is shown (merge, *n*=4). Scale bar 4 µm. **B)** Low magnification images from longitudinal sections of human sural nerves showing colocalization between TTR and Oct-6 (arrows); scale bar 40 µm. Chart represents quantification of TTR positive Schwann cells, related to total Oct-6 positive Schwann cells in nerve sections. **p*<0.05.

TTR colocalization with EEA1 was observed in both cases (Figure 4A, arrows), corroborating the notion that punctuate intracellular material arise from TTR internalization and probably not from cell synthesis. Colocalization between TTR and lysosomes was scarce (Figure 4B, arrow), most likely related to sample storage and processing.

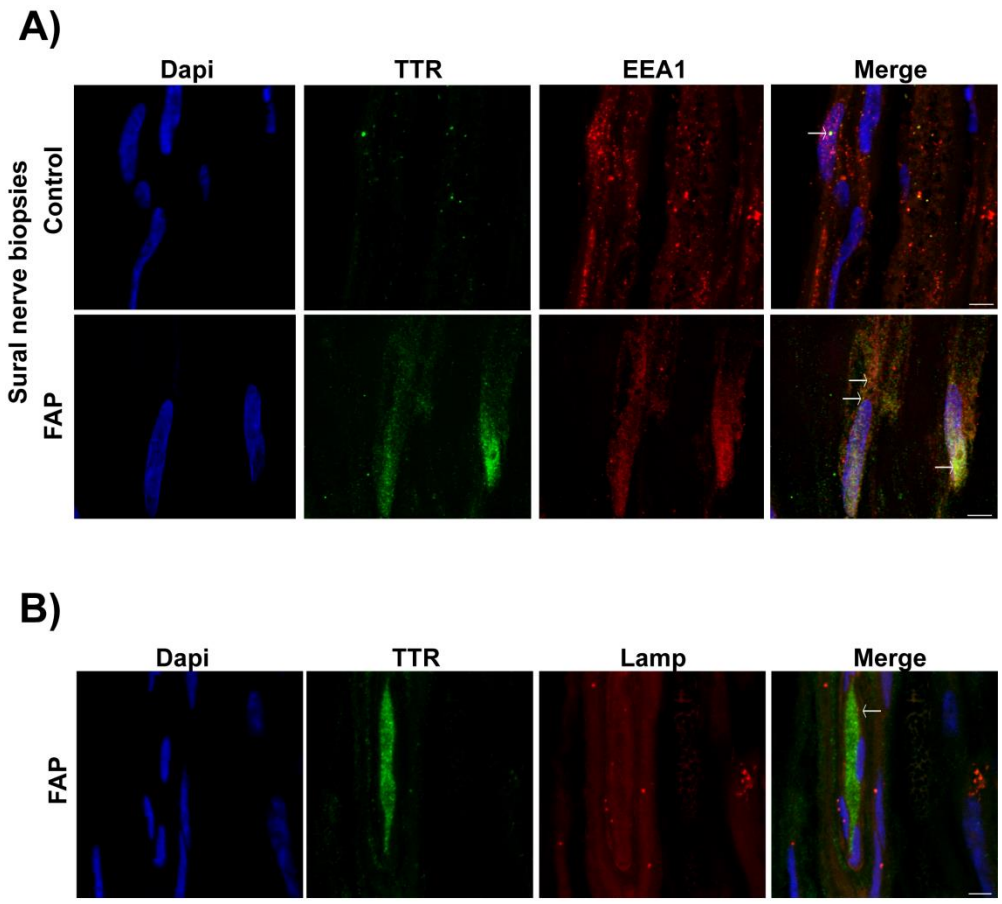

Figure 4 – TTR is internalized by human Schwann cells. A) Double immunofluorescence of TTR (green) and EEA1 (red) showing colocalization spots between the 2 proteins in Schwann cells of FAP patients and normal control individuals (arrows). Scale bar 4 µm. **B)** Confocal representative image showing scarce colocalization between TTR (green) and lysosomes (red). Scale bar 3 µm.

Intracellular TTR in satellite cells from the myenteric plexus

In FAP disease, ANS is severely affected by TTR deposition ultimately leading to bladder dysfunction, diarrhea, malabsorption and motility disturbances (Sousa and Saraiva, 2003). Thus, we questioned whether satellite cells from the myenteric plexus may also be able to internalize TTR in FAP. By histological analysis of Hsf/V30M mice colon, non-fibrillar TTR immunostaining was found in Auerbach plexus (myenteric plexus) especially inside

smaller cells surrounding the nerve cell bodies (compatible with satellite cells), in contrast with WT and TTR KO animals that were negative for TTR (Figure 5A). Following these results, we performed double immunofluorescence between TTR and S100 in colon sections of Hsf/V30M animals. Colocalization between the two proteins was observed (Figure 5B). Since the TTR staining present in these cells partially colocalized with EEA1 (Figure 5C, arrows) and Lamp1 (Figure 5D, arrows), it is reasonable to suggest that satellite cells have an important role in non-fibrillar TTR uptake and internalization. However, we could not discard the possibility of *TTR* synthesis by these cells of the myenteric plexus, especially when *TTR* production in colon was already previously suggested (Loughna et al., 1995).

To address this question we treated 5 months-old Hsf/V30M mice with TTR siRNA, to inhibit TTR deposition in the gastrointestinal tract. With this treatment we were able to silence 92% *TTR* expression by the liver (Figure 6A and B), avoiding TTR circulation in plasma and burden in tissues, as previously described (Alvarez et al., 2010). Nevertheless, TTR immunostaining in satellite cells from myenteric plexus was equally observed in animals treated with TTR siRNA or controls (vehicle treated mice) (Figure 6C). By qPCR we found *TTR* expression in colon of Hsf/V30M mice, with similar levels of relative expression between siRNA and vehicle treated mice (Figure 6D). Additionally, mouse *Ttr* expression in colon from WT mice was considerably lower than in Hsf/V30M mice (Figure 6D). This, together with the fact that no TTR reactivity was found in satellite cells from myenteric plexus in WT mice, suggests that FAP colonic myenteric plexus might be able to synthesize and clear TTR.

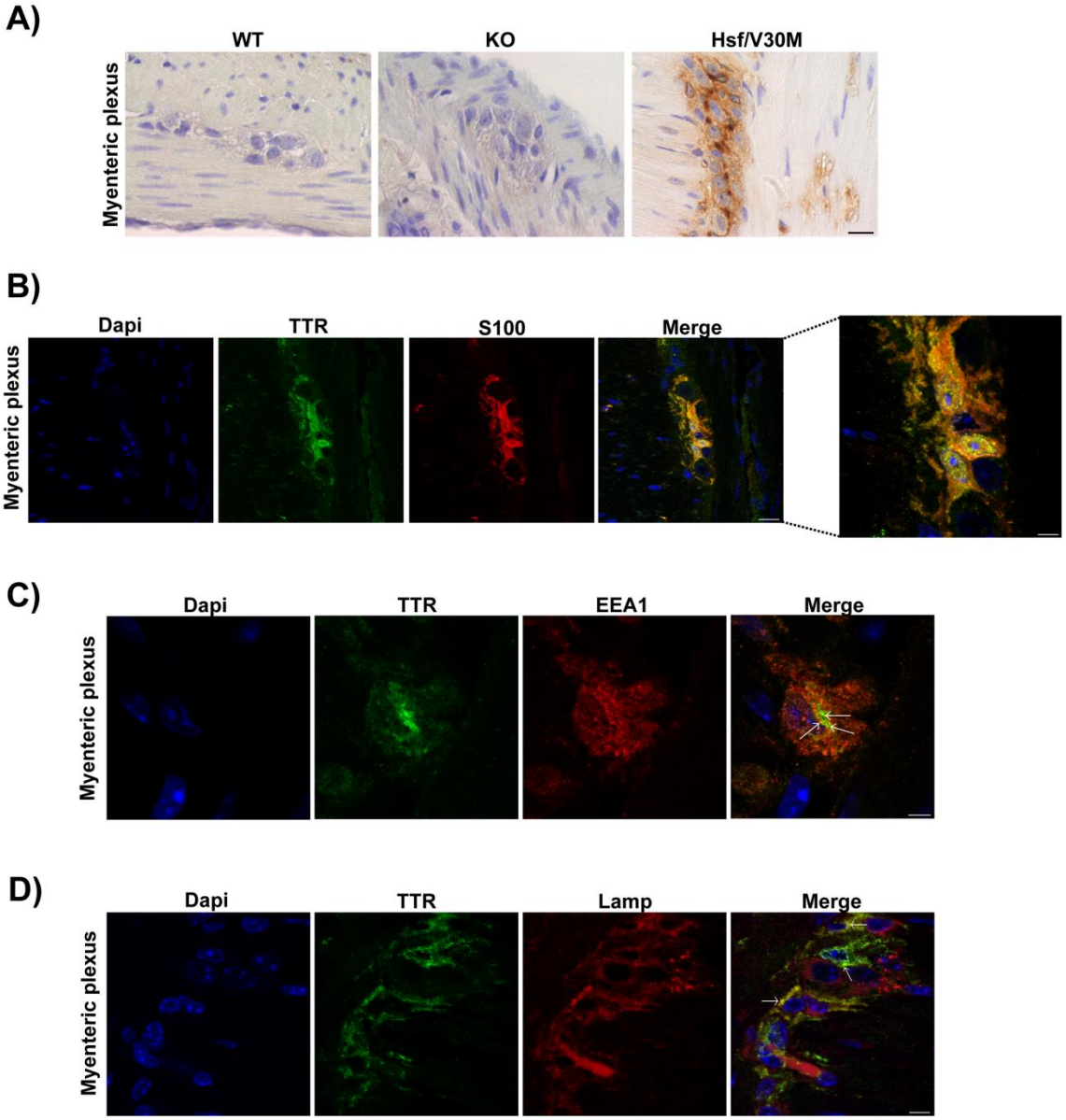

Figure 5 – TTR is internalized by satellite cells from the myenteric plexus. A) TTR immunohistochemical staining on colon myenteric plexus from WT, TTR KO and Hsf/V30M animals. Scale bar 20 µm. **B)** Double immunofluorescence between TTR (green) and S100 (red), a satellite cell marker, showing TTR inside these cells. Scale bar 14 µm; higher magnification 5 µm. **C)** Representative confocal image of myenteric plexus section showing a satellite cell with intracellular TTR staining (green) colocalizing with EEA1 (red) (arrows). Scale bar 4 µm. **D)** Confocal microscopy image with anti-TTR antibody (green) and lysosome marker (Lamp1; red). Nuclei stained blue with DAPI. Arrows indicate colocalization of TTR with lysosomes. Scale bar 5 µm.

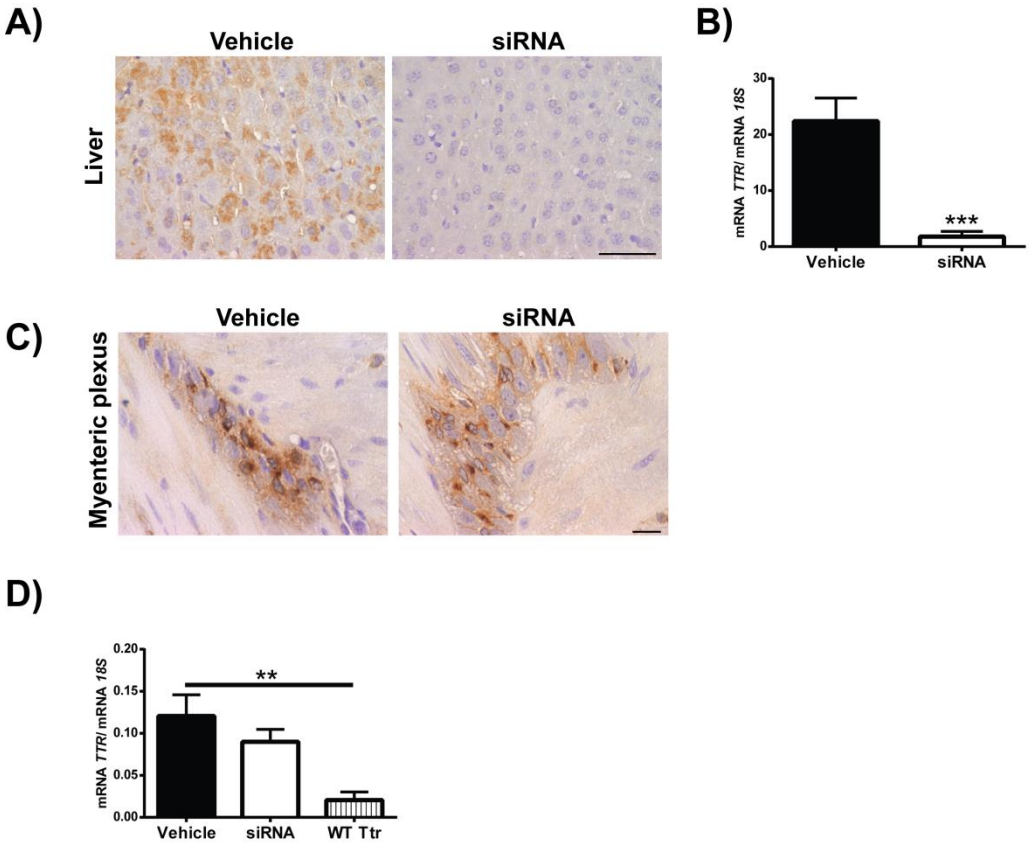

Figure 6 – *TTR* is expressed by colon of the Hsf/V30M FAP mouse model. A) Photomicrographs illustrating TTR staining in liver of Hsf/V30M mice, treated with TTR siRNA or vehicle; scale bar 50 µm. **B)** Histogram represents *TTR* mRNA levels in liver of Hsf/V30M mice treated with TTR siRNA as compared with control animals receiving only vehicle. Data was normalized using *18S* as the housekeeping gene (***p<0.001). **C)** Histological images of colonic myenteric plexus from Hsf/V30M mice treated with TTR siRNA as compared with vehicle treated animals. Scale bar 20 µm. **D)** Histogram denoting *TTR* mRNA expression in colon from Hsf/V30M mice treated with vehicle or siRNA and *Ttr* mRNA from WT animals. Data was normalized using *18S* as the housekeeping gene (**p<0.01).

Discussion

FAP is a peculiar form of neuropathy with clinical symptoms generally occurring in the second or third decade of life. However, a late-onset form of disease has also been described, affecting individuals over 50 years of age and characterized by low penetrance rate and different pathological presentations (Koike et al., 2004). Sensory impairment, wasting and weakness results from neuronal and axonal loss consequent to obliteration/dysfunction of small vessels supplying the nerve tissue, nerve fiber compression by TTR deposits or toxic effects of amyloid precursors (Koike et al., 2004; Sousa et al., 2001a). Additionally, motor sensory type is often found in FAP, characterized by muscle atrophy with distal predominance and decreased motor conduction velocity (Yoshioka et al., 2001).

In peripheral nerve, TTR deposits are predominantly found in the endoneurium, in close contact with Schwann cells and collagen fibrils (Coimbra and Andrade, 1971b). Thus, an impairment of axon-Schwann cell interaction due to cell dysfunction might contribute to axonopathy. Similarly, in nervous ganglia, TTR deposition occurs in the stroma in close association to satellite cells (Hofer and Anderson, 1975; Sobue et al., 1990). Satellite cells covering sensory neurons are similar to Schwann cells of the peripheral nerve as they are both derived from the neural crest of the embryo during development (Hall and Landis, 1992). They are known as glial supporting cells of the nervous system and have important roles on mechanical support to neurons, nutrients/oxygen supply and removal of cell debris (Hanani, 2005). *TTR* expression by glial cells of sensory neurons was previously suggested (Murakami et al., 2008). However, this hypothesis was later disputed and the results were attributed to TTR contamination by the meninges (Sousa and Saraiva, 2008).

Glial cells regulate neuron microenvironment and appear to be actively engaged in the control of ECM composition (Hanani, 2005). Thus, several studies indicate the ability of these cells in the uptake of different substances (Schlaepfer, 1969; Kumamoto et al., 1986; Paresce et al., 1996; Pannese and Procacci, 2002). Since TTR non-fibrillar deposits are found in the ECM in close association with glial cells, we decided to investigate whether these cells in sensory neurons and peripheral nerve might be important for TTR uptake *in vivo*. In fact we found immunoreactive TTR in satellite and Schwann cells, both in the Hsf/V30M transgenic model and in tissues from FAP patients. Occasionally, the observed intracellular TTR presented a punctate-like pattern, compatible with its presence within vesicles. Once in the cell, endocytic vesicles are rapidly targeted to the early endosomes. Thus, despite the existence of numerous internalization routes, early endosomes are a focal point of the endocytic pathway (Jovic et al., 2010). EEA1 is a widely used marker for early endosomes due to its colocalization with the transferrin

receptor (Mu et al., 1995). In this work, TTR colocalization with EEA1 and a lysosome marker (Lamp1) in glial cells of peripheral nerve and sensory ganglia indicate internalization and consequent vesicular transport of TTR through early endosomes for degradation.

In Alzheimer disease, A*β* internalization by glia has been observed *in vitro* and *in vivo* (Paresce et al., 1996; Wyss-Coray et al., 2003) suggesting an important role for these cells in Alzheimer pathology. Nevertheless, exposure of glial cells to A*β* aggregates could have detrimental consequences with upregulation of inflammatory mediators and nitric oxide, resulting in glia and neuron cell death (Mohamed and Posse de Chaves, 2011).

Another striking feature of FAP is severe autonomic nervous dysfunction, affecting particularly the gastrointestinal tract (Sousa and Saraiva, 2003; Koike et al., 2004). Initial gastrointestinal symptoms are severe constipation alternating with periods of diarrhea, nausea and vomiting (Suhr et al., 1992). Evidence suggests that environmental and genetic factors have impact on the clinical pattern of FAP (Ando et al., 2000). For instance, in Japanese FAP patients no significant destruction of the enteric nervous system is observed (Anan et al., 2001) while Portuguese FAP patients present infiltration of amyloid material in the space between two adjacent ganglia, accompanied by different degrees of neuronal loss (Guimarães et al., 1980). However, the mechanisms leading to neuron cell death remain poorly understood. Some factors that have been associated with the pathogenesis of gastrointestinal dysfunction are a depletion of neuroendocrine cells, such as serotonin, somatostatin or PYY immunoreactive cells (Anan et al., 1999), accumulation of advanced glycation end products (Matsunaga et al., 2002), loss of interstitial cells of Cajal (Wixner et al., 2013) and amyloid deposition in sympathetic ganglia (Koike et al., 2011). Although amyloid deposits have not been found in the myenteric plexus of Hsf/V30M FAP mouse model, this was the first animal model presenting non-fibrillar TTR deposition in the ANS of the gastrointestinal tract (Santos et al., 2010b). Therefore, we next investigated whether satellite cells were able to internalize TTR, also in this system. TTR colocalization with EEA1 and lysosomes indicated that endocytic trafficking pathways are activated in satellite cells from the myenteric plexus of Hsf/V30M mice. Importantly, this is the first study showing *TTR* synthesis by the enteric tissue, in this FAP mouse model. Therefore, it is reasonable to suggest that satellite cells may also be synthesizing mutated *TTR* which in turn might contribute for the non-fibrillar TTR deposition. It would be interesting to confirm these results in biopsy colon specimens from FAP patients; however, such specimens are very difficult to obtain since the conditions of these patients not often calls for colonoscopy.

Overall, the present study brings to light new insights into the FAP pathophysiology. Besides TTR endocytosis by fibroblasts demonstrated both *in vitro* and *in vivo* (Misumi et

al., 2013), TTR internalization *in vivo* by glial cells of peripheral nerve, sensory ganglia and myenteric plexus was here demonstrated. However, whether TTR uptake by these cells is neuroprotective or neurotoxic leading to glial and neuronal cell death with autonomic dysfunction needs further investigation. Furthermore, additional studies are needed to clarify the molecular mechanisms and signaling platforms involved in these particular systems.

Acknowledgments

This work was funded by FEDER funds through the Operational Competitiveness Program – COMPETE and by National Funds through FCT – Fundação para a Ciência e a Tecnologia under the project FCOMP-01-0124-FEDER-028406 (PTDC/BIM-MEC/0282/2012) and fellowship to NPG (SFRH/BD/74304/2010). The present work was sponsored by POPH/FSE QREN program and also financed by a grant from Cordex. We would like to thank Paula Gonçalves from IBMC for paraffin tissue processing and Alnylam Pharmaceuticals (Boston) for the kind supply of siRNA reagents.

Conclusions and Future Perspectives

Conclusions and future perspectives

FAP is a severe condition characterized by a loss of sensitive, motor and autonomic functions, culminating with lifetime medical care, since the only available therapy halting the disease progression is liver transplantation. Thus, development of novel effective therapies ameliorating the patient quality of life are still needed. For that purpose, basic knowledge regarding disease pathophysiological mechanisms is awaited.

TTR fibril formation and amyloid deposition is a dynamic process influenced by other factors, such as proteoglycans or glycosaminoglycans (GAGs) (Noborn et al., 2011). In this regard, we found colocalization of heparan sulfate proteoglycans with TTR in amyloid laden nerves from FAP patients. Additionally, to confirm the role of heparan sulfate in FAP nerve-specific deposition, in chapter I we proposed a novel nanoparticle delivery system targeting the sciatic nerve tissue. This innovative combinatorial approach using heparin/CH nanotherapeutics allowed for a sustained release of heparin throughout the ECM, without a markedly inflammatory reaction. By immunohistochemistry, levels of TTR deposition were markedly increased in sciatic nerves receiving the heparin/CH nanoparticles thereby suggesting a positive role for this GAG in TTR pathogenesis. In the future, these observations should be taken into consideration for the establishment of new animal models or for the development of novel therapeutical strategies.

Neurodegeneration in FAP has so far been suggested to partially relate to binding of TTR aggregates to RAGE with activation of inflammatory cascades, apoptosis and oxidative stress. However, one should not exclude the possibility that an inflammatory stimulus might also trigger TTR deposition in the PNS, leading to a positive feedback loop. In chapter II, we evaluated the effect of neuroinflammation and stress on TTR deposition after sciatic nerve ligation. Seven days following injury, non-fibrillar TTR was widespread in the PNS of an FAP mouse model initially depicting TTR deposition only in the gastrointestinal tract and skin. This observation could be attributed to the lower pH and increased levels of heparan sulfate after injury (Figure 1); however, in depth studies are needed in the future to clarify this issue. Importantly, we also found that *TTR* expression in Schwann cells is regulated by an inflammatory threshold. A striking feature of FAP is the lack of an immune infiltrate despite the production of pro-inflammatory cytokines by axons. Accordingly, in our injury model, FAP mice presented lower frequency of neutrophils and macrophages as well as less production of *Tnf-α*, *Il-1β*, *Tlr-1* and chemokines, as compared with WT animals (Figure 1). A previous study shows that Schwann cells from FAP patients are impaired on their ability to produce neurotrophins in a context of neuronal stress (Sousa et al., 2001b). The lack of trophic factors, immune cells and regenerating molecules might be relevant for neuronal dysfunction, poor functional

recovery and lower regenerative abilities observed in the injured FAP transgenic mice. Moreover, nerve deposition of toxic TTR aggregates in uninjured conditions most probably impairs Schwann cells and their role in regeneration after toxic events, leading to disruption in the crosstalk between Schwann cells and axons. Therefore, it would be interesting to address at transcriptional and translational levels whether a naïve situation recapitulates in some features the injury condition. In this regard, Schwann cells from naïve sciatic nerves of FAP transgenic mice, and corresponding controls, might be sorted for future microarray analysis, particularly for the search of regenerating and survival-related genes. Thereafter, studies with primary Schwann cells, stimulated with different intermediate TTR species, might give novel insights into new molecular pathways underlying FAP pathology or provide information about drugs able to rescue cell impairment.

Based on results from chapter II demonstrating the importance of inflammation in the progress of FAP, in chapter III we explored an anti-inflammatory approach to this disorder in a mouse model of disease. IL-1 is a major pro-inflammatory cytokine involved in the pathogenesis of different neurodegenerative conditions, such as Alzheimer's disease, multiple sclerosis or FAP. Several studies have shown that blocking the IL-1 signaling pathway with Anakinra prevents activation of pro-apoptotic molecules or increase pro-survival signaling transduction pathways, culminating in neuroprotection. Thus, we performed daily treatment in early-stage pathology with Anakinra, in the FAP mouse model heterozygous for the *Hsf-1*. Nerve TTR deposition was found significantly decreased in treated animals as well as secondary associated neurotoxic cascades, such as NF-κB activation, apoptosis, heat-shock response, ER and nitrosative stress, highlighting the importance of IL-1 signaling in the pathogenesis of FAP.

If IL-1 influenced TTR deposition in the PNS of naïve FAP transgenic mice, in chapter IV we questioned whether blocking this cytokine could also inhibit *TTR* expression after nerve injury, rescuing the observed phenotype. By treating FAP animals with Anakinra, 48 h before sciatic nerve ligation, we were able to prevent TTR deposition and decrease *TTR* nerve expression after damage (Figure 1). In addition, apoptotic cascades were diminished accompanied by an improved regenerative response. Furthermore, our data suggest that CREB is probably associated with TTR expression/deposition and highlight new possible disease biomarker molecules, such as cathepsins B/D, synapsin and persephin. After treatment with Anakinra, no differences were found regarding immune cell infiltration, so future studies should address how to improve chemotaxis pharmacologically. These will probably encompass the development of more suitable animals models, with amyloid deposits in peripheral nerves, closely resembling human pathology. Application of heparan sulfate proteoglycans into the sciatic nerve of an FAP

mouse model failed in triggering fibrillar deposition, possibly due to different ECM environments between mouse and human patients. Therefore, future studies in transgenic mice should address the modulation of ECM remodeling in FAP nerves through stimulation with different types of proteoglycans. In this regard, comparative analyses of human and rodent nerve proteoglycan composition should be addressed.

Schwann cells are the immunocompetent cells of the PNS. After peripheral nerve injury, Schwann cells dedifferentiate and are able to phagocyte myelin debris for regeneration to occur. TTR aggregates deposition lead to activation of pro-inflammatory cytokines in nerves from FAP patients thus possibly functioning as an injury stimulus. *TTR* expression by Schwann cells was previously suggested (Murakami et al., 2010) and corroborated in our FAP mouse models; we questioned whether these cells might also be able to internalize TTR. In chapter V of the present work, we show *in vivo* colocalization between TTR/EEA1 and TTR/Lamp-1 in nerve Schwann cells and glial cells from DRG, indicating protein internalization and degradation. These results prompt us to proceed and analyse Schwann cells from human patients. Surprisingly, TTR punctuate material was found, also in Schwann cells from disease control individuals, suggesting that these cells might be important for the clearance of TTR reaching the nerve through the blood-stream. ANS is also a target for TTR deposition, particularly at the myenteric plexus. Using confocal microscopy we show that satellite cells from the myenteric plexus internalize and deliver TTR to lysosomes for degradation. Additionally, using RNAi, *TTR* expression by colon was observed and attributed to satellite cells since these were the only TTR positive cells after treatment with TTR siRNA. The study of TTR internalization is of outmost importance since an imbalance of this system might trigger or accelerate TTR aggregates deposition in target tissues. These novel data regarding the physiopathology of FAP might open new windows of action in the design of new therapeutics to modulate TTR clearance from ECM. However, there are some questions that are certainly worth studying, namely: 1) TTR uptake by these cells is neuroprotective or neurotoxic ending in glial and neuronal cell death? 2) What are the molecular mechanisms and signaling platforms involved in these particular systems? 3) Is internalized TTR recycled to cell surface? Answering these questions could help to further understand the intracellular TTR processing steps and the mechanisms that participate in TTR internalization, or in the identification of putative receptors for TTR binding, in addition to megalin and RAGE.

In summary, this project reinforces the importance of inflammation on TTR amyloidosis and further demonstrates the key role of IL-1 in the pathogenesis of FAP. Overall, we propose to counteract toxicity in this neurodegenerative disorder by modulating inflammation, ECM remodeling and cellular uptake of TTR, possible through combinatorial approaches, paving the way for future clinical trials.

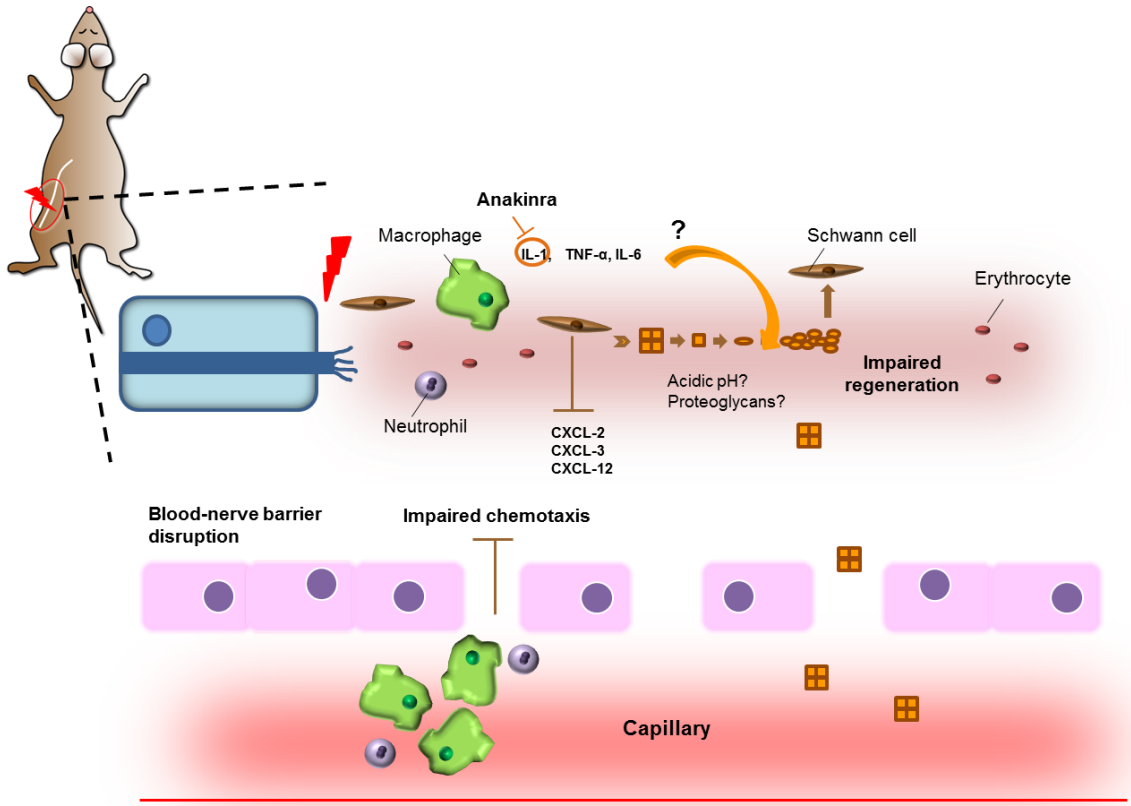

Figure 1 – Schematic representation of crosstalk events studied in this thesis. Nerve injury triggered local TTR expression and non-fibrillar deposition, possibly due to low pH or ECM remodeling, characterized by increased levels of heparan sulfate GAGs. Schwann cells are able to express and internalize TTR species and are impaired in their normal functions, with compromised production of growth factors, pro-inflammatory cytokines and chemokines, ultimately affecting nerve regeneration. In fact, despite disruption of the blood-nerve barrier with entrance of systemic TTR into nerve tissue, lower frequency of macrophages and neutrophils was found in injured nerves from FAP transgenic mice, contributing for the lower production of pro-inflammatory cytokines and factors driven regeneration. Blocking IL-1 with Anakinra partially rescue this phenotype and prevents TTR non-fibrillar deposition as well as neurotoxic cascades.
With ageing, a similar scenario in naïve FAP mice might occur with toxic TTR aggregates leading to impairment of Schwann cells and threshold of pro or anti-inflammatory intermediaries.

References

References

Abbate A, Salloum FN, Vecile E, Das A, Hoke NN, et al., (2008) Anakinra, a recombinant human interleukin-1 receptor antagonist, inhibits apoptosis in experimental acute myocardial infarction. Circulation 117:2670-2683.

Ackermann EJ, Guo S, Booten S, Alvarado L, Benson M, et al., (2012) Clinical development of an antisense therapy for the treatment of transthyretin-associated polyneuropathy. Amyloid 19 Suppl 1:43-44.

Adams D, Cauquil C, Theaudin M, Rousseau A, Algalarrondo V, et al., (2014) Current and future treatment of amyloid neuropathies. Expert Rev Neurother 14(12):1437-1451.

Alapatt P, Guo F, Komanetsky SM, Wang S, Cai J, et al., (2013) Liver retinol transporter and receptor for serum retinol-binding protein (RBP4). J Biol Chem 288(2):1250-1265.

Almeida MR, Macedo B, Cardoso I, Alves I, Valencia G, et al., (2004) Selective binding to transthyretin and tetramer stabilization in serum from patients with familial amyloidotic polyneuropathy by an iodinated diflunisal derivative. Biochem J 381(Pt 2):351-356.

Alvarez R, Borland T, Chen Q, Milstein S, Nguyen T, et al., (2010) ALN-TTR, an RNAi therapeutic for the treatment of transthyretin-mediated amyloidosis. Amyloid-J Protein Fold Disord 17:51-52.

Amin A, Choi SK, Galan M, Kassan M, Partyka M, et al., (2012) Chronic inhibition of endoplasmic reticulum stress and inflammation prevents ischaemia-induced vascularpathology in type II diabetic mice. J Pathol 227:165-174.

Anan I, El-Salhy M, Ando Y, Forsgren S, Nyhlin N, et al., (1999) Colonic enteric nervous system in patients with familial amyloidotic neuropathy. Acta Neuropathol 98:48-54.

Anan I, El-salhy M, Ando Y, Terazaki H, Suhr OB (2001) Comparison of amyloid deposits and infiltration of enteric nervous system in the upper with those in the lower gastrointestinal tract in patients with familial amyloidotic polyneuropathy. Acta Neuropathol 102:227-232.

Ancsin JB (2003) Amyloidogenesis: historical and modern observations point to heparan sulfate proteoglycans as a major culprit. Amyloid 10(2):67-79.

Andersson K, Olofsson A, Nielsen EH, Svehag SE, Lundgren E (2002) Only amyloidogenic intermediates of transthyretin induce apoptosis. Biochem Biophys Res Commun 294:309-314.

Andersson K, Pokrzywa M, Dacklin I, Lundgren E (2013) Inhibition of TTR aggregation-induced cell death--a new role for serum amyloid P component. PLoS ONE 8:e55766.

Andersson R (1976) Familial amyloidosis with polyneuropathy. A clinical study based on patients living in northern Sweden. Acta Med Scand Suppl 590:1-64.

Ando Y, Nyhlin N, Suhr O, Holmgren G, Uchida K, et al., (1997) Oxidative stress is found in amyloid deposits in systemic amyloidosis. Biochem Biophys Res Commun 232:497-502.

Ando Y, Ohtsu Y, Terazaki H, Kibayashi K, Nakamura M, et al., (2000) Japanese monozygotic twins with familial amyloidotic polyneuropathy (FAP) (ATTR Val30Met). Amyloid 7:133-136.

Ando Y, Terazaki H, Nakamura M, Ando E, Haraoka K, et al., (2004) A different amyloid formation mechanism: de novo oculoleptomeningeal amyloid deposits after liver transplantation. Transplantation 77(3):345-349.

Ando Y (2005) Liver transplantation and new therapeutic approaches for familial amyloidotic polyneuropathy (FAP). Med Mol Morphol 38:142-154.

Ando Y, Nakamura M, Araki S (2005) Transthyretin-related familial amyloidotic polyneuropathy. Arch Neurol. 62(7):1057-1062.

Ando Y, Coelho T, Berk JL, Cruz MW, Ericzon BG, et al., (2013) Guideline of transthyretin-related hereditary amyloidosis for clinicians. Orphanet J Rare Dis 8:31.

Andrade C (1952) A peculiar form of peripheral neuropathy; familiar atypical generalized amyloidosis with special involvement of the peripheral nerves. Brain 75:408-427.

Apfel SC (1999) Neurotrophic factors in peripheral neuropathies: therapeutic implications. Brain Pathol 9(2):393-413.

Araki S, Mawatari S, Ohta M, Nakajima A, Kuroiwa Y (1968) Polyneuritic amyloidosis in a Japanese family. Arch Neurol 18(6):593-602.

Arend WP, Malyak M, Guthridge CJ, Gabay C (1998) Interleukin-1 receptor antagonist: role in biology. Annu Rev Immunol 16:27-55.

Arthur-Farraj PJ, Latouche M, Wilton DK, Quintes S, Chabrol E, et al., (2012) c-Jun reprograms Schwann cells of injured nerves to generate a repair cell essential for regeneration. Neuron 75(4):633-647.

Austin PJ, Moalem-Taylor G (2010) The neuro-immune balance in neuropathic pain: involvement of inflammatory immune cells, immune-like glial cells and cytokines. J Neuroimmunol 229:26-50.

Azevedo E, Silva PF, Palhano F, Braga CA, Foguel D (2013) Transthyretin-Related Amyloidoses: A Structural and Thermodynamic Approach, Amyloidosis, Dr. Dali Feng (Ed), ISBN: 978-953-51-1100-9, InTech.

Bain JR, Mackinnon SE, Hunter DA (1989) Functional evaluation of complete sciatic, peroneal, and posterior tibial nerve lesions in the rat. Plast Reconstr Surg 83:129-136.

Baldrick P (2010) The safety of chitosan as a pharmaceutical excipient. Regul Toxicol Pharmacol 56(3):290-299.

Banwell V, Sena ES, Macleod MR (2009) Systematic review and stratified meta-analysis of the efficacy of interleukin-1 receptor antagonist in animal models of stroke. J Stroke Cerebrovasc Dis 18:269-276.

Barnat M, Enslen H, Propst F, Davis RJ, Soares S, et al., (2010) Distinct roles of c-Jun N-terminal kinase isoforms in neurite initiation and elongation during axonal regeneration. J Neurosci 30(23):7804-7816.

Barrette B, Hébert MA, Filali M, Lafortune K, Vallières N, et al., (2008) Requirement of myeloid cells for axon regeneration. J Neurosci 28(38):9363-9376.

Bartalena L (1990) Recent achievements in studies on thyroid hormone-binding proteins. Endocr Rev 11(1):47-64.

Bartalena L, Robbins J (1993) Thyroid hormone transport proteins. Clin Lab Med 13:583-598.

Bastien D, Lacroix S (2014) Cytokine pathways regulating glial and leukocyte function after spinal cord and peripheral nerve injury. Exp Neurol 258:62-77.

Batista AR, Sena-Esteves M, Saraiva MJ (2013) Hepatic production of transthyretin L12P leads to intracellular lysosomal aggregates in a new somatic transgenic mouse model. Biochim Biophys Acta 1832(8):1183-1193.

Batista AR, Gianni D, Ventosa M, Coelho AV, Almeida MR, et al., (2014) Gene therapy approach to FAP: in vivo influence of T119M in TTR deposition in a transgenic V30M mouse model. Gene Ther 21(12):1041-1050.

Be'eri H, Reichert F, Saada A, Rotshenker S (1998) The cytokine network of wallerian degeneration: IL-10 and GM-CSF. Eur J Neurosci 10(8):2707-2713.

Beg AA, Finco TS, Nantermet PV, Baldwin AS Jr (1993) Tumor necrosis factor and interleukin-1 lead to phosphorylation and loss of I kappa B alpha: a mechanism for NF-kappa B activation. Mol Cell Biol 13:3301-3310.

Benarroch EE (2011) Heat shock proteins: multiple neuroprotective functions and implications for neurologic disease. Neurology 76(7):660-667.

Ben-Neriah Y, Karin M (2011) Inflammation meets cancer, with NF-κB as the matchmaker. Nat Immunol 12(8):715-723.

Benson MD, Kluve-Beckerman B, Zeldenrust SR, Siesky AM, Bodenmiller DM, et al., (2006) Targeted suppression of an amyloidogenic transthyretin with antisense oligonucleotides. Muscle Nerve 33:609-618.

Benson MD, Kincaid JC (2007) The molecular biology and clinical features of amyloid neuropathy. Muscle Nerve 36:411-423.

Ben-Yaakov K, Dagan SY, Segal-Ruder Y, Shalem O, Vuppalanchi D, et al., (2012) Axonal transcription factors signal retrogradely in lesioned peripheral nerve. EMBO J 31(6):1350-1363.

Berg I, Thor S, Hammarstrom P (2009) Modeling familial amyloidotic polyneuropathy (Transthyretin V30M) in Drosophila melanogaster. Neurodegener Dis 6:27-138.

Bergström J, Gustavsson A, Hellman U, Sletten K, Murphy CL, et al., (2005) Amyloid deposits in transthyretin-derived amyloidosis: cleaved transthyretin is associated with distinct amyloid morphology. J Pathol 206(2):224-232.

Blake CC, Geisow MJ, Swan ID, Rerat C, Rerat B (1974) Structure of human plasma prealbumin at 2-5 A resolution. A preliminary report on the polypeptide chain conformation, quaternary structure and thyroxine binding. J Mol Biol 88:1-12.

Blake C, Serpell L (1996) Synchrotron X-ray studies suggest that the core of the transthyretin amyloid fibril is a continuous beta-sheet helix. Structure 4(8):989-998.

Boddohi S, Moore N, Johnson PA, Kipper MJ (2009) Polysaccharide-based polyelectrolyte complex nanoparticles from chitosan, heparin and hyaluronan. Biomacromolecules 10:1402-1409.

Bodin K, Ellmerich S, Kahan MC, Tennent GA, Loesch A, et al., (2010) Antibodies to human serum amyloid P component eliminate visceral amyloid deposits. Nature 468(7320):93-97.

Boivin A, Pineau I, Barrette B, Filali M, Vallières N, et al., (2007) Toll-like receptor signaling is critical for Wallerian degeneration and functional recovery after peripheral nerve injury. J Neurosci 27(46):12565-12576.

Bourgault S, Solomon JP, Reixach N, Kelly JW (2011) Sulfated glycosaminoglycans accelerate transthyretin amyloidogenesis by quaternary structural conversion. Biochemistry 50(6):1001-1015.

Botsios C, Sfriso P, Furlan A, Ostuni P, Biscaro M, et al., (2007) Anakinra, a recombinant human IL-1 receptor antagonist, in clinical practice. Outcome in 60 patients with severe rheumatoid arthritis. Reumatismo 59:32-37.

Bradke F, Fawcett JW, Spira ME (2012) Assembly of a new growth cone after axotomy: the precursor to axon regeneration. Nat Rev Neurosci 13(3):183-193.

Brambilla F, Lavatelli F, Di Silvestre D, Valentini V, Palladini G, et al., (2013) Shotgun protein profile of human adipose tissue and its changes in relation to systemic amyloidoses. J Proteome Res 12(12):5642-5655.

Brett M, Persey MR, Reilly MM, Revesz T, Booth DR, et al., (1999) Transthyretin Leu12Pro is associated with systemic, neuropathic and leptomeningeal amyloidosis. Brain 122:183-190.

Brosius Lutz A, Barres BA (2014) Contrasting the glial response to axon injury in the central and peripheral nervous systems. Dev Cell 28(1):7-17.

Brück W, Friede RL (1990) Anti-macrophage CR3 antibody blocks myelin phagocytosis by macrophages in vitro. Acta Neuropathol 80(4):415-418.

Brumovsky PR, Bergman E, Liu HX, Hökfelt T, Villar MJ (2004) Effect of a graded single constriction of the rat sciatic nerve on pain behavior and expression of

immunoreactive NPY and NPY Y1 receptor in DRG neurons and spinal cord. Brain Res 1006:87-99.

Brunk UT, Svensson I (1999) Oxidative stress, growth factor starvation and Fas activation may all cause apoptosis through lysosomal leak. Redox Rep 4:3-11.

Bulawa CE, Connelly S, Devit M, Wang L, Weigel C, et al., (2012). Tafamidis, a potent and selective transthyretin kinetic stabilizer that inhibits the amyloid cascade. Proc Natl Acad Sci USA 109:9629-9634.

Burns K, Martinon F, Esslinger C, Pahl H, Schneider P, et al., (1998) MyD88, an adapter protein involved in interleukin-1 signaling. J Biol Chem 273:12203-12209.

Buxbaum JN, Ye Z, Reixach N, Friske L, Levy C, et al., (2008) Transthyretin protects Alzheimer's mice from the behavioral and biochemical effects of Abeta toxicity. Proc Natl Acad Sci USA 105:2681-2686.

Buxbaum JN, Tagoe C, Gallo G, Walker JR, Kurian S, et al., (2012) Why are some amyloidoses systemic? Does hepatic "chaperoning at a distance" prevent cardiac deposition in a transgenic model of human senile systemic (transthyretin) amyloidosis? FASEB J 26(6):2283-2293.

Buxbaum JN, Roberts AJ, Adame A, Masliah E (2014) Silencing of murine transthyretin and retinol binding protein genes has distinct and shared behavioral and neuropathologic effects. Neuroscience 275:352-364.

Cai D, Deng K, Mellado W, Lee J, Ratan RR, et al., (2002) Arginase I and polyamines act downstream from cyclic AMP in overcoming inhibition of axonal growth MAG and myelin in vitro. Neuron 35(4):711-719.

Cardoso I, Merlini G, Saraiva MJ (2003) 4'-iodo-4'-deoxydoxorubicin and tetracyclines disrupt transthyretin amyloid fibrils in vitro producing noncytotoxic species: screening for TTR fibril disrupters. FASEB J 17:803-809.

Cardoso I, Saraiva MJ (2006) Doxycycline disrupts transthyretin amyloid: evidence from studies in a FAP transgenic mice model. FASEB J 20:234-239.

Cardoso I, Brito M, Saraiva MJ (2008) Extracellular matrix markers for disease progression and follow-up of therapies in familial amyloid polyneuropathy V30M TTR-related. Dis Markers 25(1):37-47.

Cardoso I, Martins D, Ribeiro T, Merlini G, Saraiva MJ (2010) Synergy of combined doxycycline/TUDCA treatment in lowering Transthyretin deposition and associated biomarkers: studies in FAP mouse models. J Transl Med 8:74.

Cascella R, Conti S, Mannini B, Li X, Buxbaum JN, et al., (2013) Transthyretin suppresses the toxicity of oligomers formed by misfolded proteins in vitro. Biochim Biophys Acta;1832(12):2302-2314.

Cecchi C, Baglioni S, Fiorillo C, Pensalfini A, Liguri G, et al., (2005) Insights into the molecular basis of the differing susceptibility of varying cell types to the toxicity of amyloid aggregates. J Cell Sci 118:3459-3470.

Chen MC, Wong HS, Lin KJ, Chen HL, Wey SP, et al., (2009) The characteristics, biodistribution and bioavailability of a chitosan-based nanoparticulate system for the oral delivery of heparin. Biomaterials 30:6629-6637.

Chen ZL, Yu WM, Strickland S (2007) Peripheral regeneration. Annu Rev Neurosci 30:209-233.

Cho Y, Sloutsky R, Naegle KM, Cavalli V (2013) Injury-induced HDAC5 nuclear export is essential for axon regeneration. Cell 155(4):894-908.

Chu H, Johnson NR, Mason NS, Wang YA (2010) A [polycation:heparin] complex releases growth factors with enhanced bioactivity. J Control Release 150(2):157-163.

Chwieralski CE, Welte T, Buhling F (2006) Cathepsin-regulated apoptosis. Apoptosis 11:143-149.

Coelho T, Maia LF, Martins da Silva A, Waddington Cruz M, Plante-Bordeneuve V, et al., (2012) Tafamidis for transthyretin familial amyloid polyneuropathy: a randomized, controlled trial. Neurology 79:785-792.

Coelho T, Adams D, Silva A, Lozeron P, Hawkins PN, et al., (2013) Safety and efficacy of RNAi therapy for transthyretin amyloidosis. N Engl J Med 369(9):819-829.

Coimbra A, Andrade C (1971a) Familial amyloid polyneuropathy: an electron microscope study of the peripheral nerve in five cases. I. Interstitial changes. Brain 94(2):199-206.

Coimbra A, Andrade C (1971b) Familial amyloid polyneuropathy: an electron microscope study of the peripheral nerve in five cases. II. Nerve fibril changes. Brain 94(2):207-212.

Colgan SM, Hashimi AA, Austin RC (2011) Endoplasmic reticulum stress and lipid dysregulation. Expert Rev Mol Med 13:e4.

Collins T, Read MA, Neish AS, Whitley MZ, Thanos D, et al., (1995) Transcriptional regulation of endothelial cell adhesion molecules: NF-kappa B and cytokine-inducible enhancers. FASEB J 9:899-909.

Colon W, Kelly JW (1992) Partial denaturation of transthyretin is sufficient for amyloid fibril formation in vitro. Biochemistry 31(36):8654-8660.

Conceição I, Costa J, Castro J, de Carvalho M (2014) Neurophysiological techniques to detect early small-fiber dysfunction in transthyretin amyloid polyneuropathy. Muscle Nerve 49(2):181-186.

Conejos-Sánchez I, Cardoso I, Oteo-Vives M, Romero-Sanz E, Paul A, et al., (2015) Polymer-doxycycline conjugates as fibril disrupters: An approach towards the treatment of a rare amyloidotic disease. J Control Release 198:80-90.

Costa PP, Figueira AS, Bravo FR (1978) Amyloid fibril protein related to prealbumin in familial amyloidotic polyneuropathy. Proc Natl Acad Sci USA 75(9):4499-4503.

Costa R, Ferreira-da-Silva F, Saraiva MJ, Cardoso I (2008a) Transthyretin protects against A-beta peptide toxicity by proteolytic cleavage of the peptide: a mechanism sensitive to the Kunitz protease inhibitor. PLoS ONE 3:e2899.

Costa R, Goncalves A, Saraiva MJ, Cardoso I (2008b) Transthyretin binding to A-Beta peptide-impact on A-Beta fibrillogenesis and toxicity. FEBS Lett 582:936-942.

Costa RH, Lai E, Darnell JE Jr (1986) Transcriptional control of the mouse prealbumin (transthyretin) gene: both promoter sequences and a distinct enhancer are cell specific. Mol Cell Biol 6(12):4697-4708.

Costa RH, Van Dyke TA, Yan C, Kuo F, Darnell JE Jr (1990) Similarities in transthyretin gene expression and differences in transcription factors: liver and yolk sac compared to choroid plexus. Proc Natl Acad Sci USA 87(17):6589-6593.

de Carvalho M, Conceição I, Bentes C, Luís ML (2002) Long-term quantitative evaluation of liver transplantation in familial amyloid polyneuropathy (Portuguese V30M). Amyloid 9(2):126-133.

DeFrancesco-Lisowitz A, Lindborg JA, Niemi JP, Zigmond RE (2014) The neuroimmunology of degeneration and regeneration in the peripheral nervous system. Neuroscience. pii: S0306-4522(14)00769-6 [Epub ahead of print].

Dekki N, Refai E, Holmberg R, Köhler M, Jörnvall H, et al., (2011) Transthyretin binds to glucose-regulated proteins and is subjected to endocytosis by the pancreatic β-cell. Cell Mol Life Sci 69(10):1733-1743.

de Medinaceli L, Freed WJ, Wyatt RJ (1982) An index of the functional condition of rat sciatic nerve based on measurements made from walking tracks. Exp Neurol 77(3):634-643.

Dickson PW, Aldred AR, Marley PD, Bannister D, Schreiber G (1986) Rat choroid plexus specializes in the synthesis and the secretion of transthyretin (prealbumin). Regulation of transthyretin synthesis in choroid plexus is independent from that in liver. J Biol Chem 261(8):3475-3478.

Dickson PW, Howlett GJ, Schreiber G (1982) Metabolism of prealbumin in rats and changes induced by acute inflammation. Eur J Biochem 129(2):289-293.

Di Domizio J, Zhang R, Stagg LJ, Gagea M, Zhuo M, et al., (2012) Binding with nucleic acids or glycosaminoglycans converts soluble protein oligomers to amyloid. J Biol Chem 287(1):736-747.

Dinarello CA (2011) A clinical perspective of IL-1β as the gatekeeper of inflammation. Eur J Immunol 41:1203-1217.

Dinarello CA, Simon A, Van der Meer JW (2012) Treating inflammation by blocking interleukin-1 in a broad spectrum of diseases. Nat Rev Drug Discov 11:633-652.

Ehses JA, Lacraz G, Giroix MH, Schmidlin F, Coulaud J, et al., (2009) IL-1 antagonism reduces hyperglycemia and tissue inflammation in the type 2 diabetic GK rat. Proc Natl Acad Sci USA 33:13998-14003.

Episkopou V, Maeda S, Nishiguchi S, Shimada K, Gaitanaris GA, et al., (1993) Disruption of the transthyretin gene results in mice with depressed levels of plasma retinol and thyroid hormone. Proc Natl Acad Sci USA 90(6):2375-2379.

Ferreira N, Cardoso I, Domingues MR, Vitorino R, Bastos M, et al., (2009) Binding of epigallocatechin-3-gallate to transthyretin modulates its amyloidogenicity. FEBS Lett 583(22):3569-3576.

Ferreira N, Saraiva MJ, Almeida MR (2011) Natural polyphenols inhibit different steps of the process of transthyretin (TTR) amyloid fibril formation. FEBS Lett 585(15):2424-2430.

Ferreira N, Saraiva MJ, Almeida MR (2012) Epigallocatechin-3-gallate as a potential therapeutic drug for TTR-related amyloidosis: "in vivo" evidence from FAP mice models. PLoS One 7(1):e29933.

Ferreira N, Santos SA, Domingues MR, Saraiva MJ, Almeida MR (2013) Dietary curcumin counteracts extracellular transthyretin deposition: insights on the mechanism of amyloid inhibition. Biochim Biophys Acta 1832(1):39-45.

Ferreira N, Pereira-Henriques A, Attar A, Klärner FG, Schrader T, et al., (2014) Molecular tweezers targeting transthyretin amyloidosis. Neurotherapeutics 11(2):450-461.

Fleischmann R (2006) Anakinra in the treatment of rheumatic disease. Expert Rev Clin Immunol 2:331-340.

Fleming CE, Saraiva MJ, Sousa MM (2007) Transthyretin enhances nerve regeneration. Journal of Neurochem 103:831-839.

Fleming CE, Mar FM, Franquinho F, Saraiva MJ, Sousa MM (2009) Transthyretin internalization by sensory neurons is megalin mediated and necessary for its neuritogenic activity. J Neurosci 29(10):3220-3232.

Foss TR, Kelker MS, Wiseman RL, Wilson IA, Kelly JW (2005). Kinetic stabilization of the native state by protein engineering: implications for inhibition of transthyretin amyloidogenesis. J Mol Biol 347(4):841-854.

Frank-Cannon TC, Alto LT, McAlpine FE, Tansey MG (2009) Does neuroinflammation fan the flame in neurodegenerative diseases? Mol Neurodegener 4:47.

Fricker FR, Lago N, Balarajah S, Tsantoulas C, Tanna S, et al., (2011) Axonally derived neuregulin-1 is required for remyelination and regeneration after nerve injury in adulthood. J Neurosci 31(9):3225-3233.

Gabey C, Lamacchia C, Palmer G (2010) IL-1 pathways in inflammation and human diseases. Nat Rev Rheumatol 6:232-241.

Gabay E, Wolf G, Shavit Y, Yirmiya R, Tal M (2011) Chronic blockade of interleukin-1 (IL-1) prevents and attenuates neuropathic pain behavior and spontaneous ectopic neuronal activity following nerve injury. Eur J Pain 15:242-248.

Galluzzi L, Kepp O, Trojel-Hansen C, Kroemer G (2012) Mitochondrial control of cellular life, stress, and death. Circ Res 111(9):1198-1207.

Garlanda C, Dinarello CA, Mantovani A (2013) The interleukin-1 family: Back to the future. Immunity 39:1003-1018.

Gaudet AD, Popovich PG, Ramer MS (2011) Wallerian degeneration: gaining perspective on inflammatory events after peripheral nerve injury. J Neuroinflammation 8:110.

George EB, Glass JD, Griffin JW (1995) Axotomy-induced axonal degeneration is mediated by calcium influx through ion-specific channels. J Neurosci 15(10):6445-6452.

Gharagozloo M, Majewski S, Foldvari M (2015) Therapeutic applications of nanomedicine in autoimmune diseases: From immunosuppression to tolerance induction. Nanomedicine pii: S1549-9634(15)00008-8 [Epub ahead of print].

Ghavami S, Shojaei S, Yeganeh B, Ande SR, Jangamreddy JR, et al., (2014) Autophagy and apoptosis dysfunction in neurodegenerative disorders. Prog Neurobiol 112:24-49.

Girard C, Liu S, Cadepond F, Adams D, Lacroix C, et al., (2008) Etifoxine improves peripheral nerve regeneration and functional recovery. Proc Natl Acad Sci USA 105:20505-20510.

Glenn TD, Talbot WS (2013) Signals regulating myelination in peripheral nerves and the Schwann cell response to injury. Curr Opin Neurobiol 23(6):1041-1048.

Goethals S, Ydens E, Timmerman V, Janssens S (2010) Toll-like receptor expression in the peripheral nerve. Glia 58(14):1701-1709.

Goldsmith BM, Munson S (1987) Rate nephelometry and radial immunodiffusion compared for measuring serum prealbumin. Clin Chem 33:161-163.

Gonçalves NP, Pêgo AP, Saraiva MJ (2013) Heparin/Chitosan nanoparticle delivery system for in vivo evaluation of glycosaminoglycans influence on transthyretin deposition. In: Hazenberg, Bouke PC, Bijzet Johan (Eds), XIIIth International Symposium on Amyloidosis. GUARD, Groningen, Netherlands, 118-121.

Gonçalves NP, Teixeira-Coelho M, Saraiva MJ (2014a) The inflammatory response to sciatic nerve injury in a familial amyloidotic polyneuropathy mouse model. Exp Neurol 257:76-87.

Gonçalves NP, Vieira P, Saraiva MJ (2014b) Interleukin-1 signaling pathway as a therapeutic target in transthyretin amyloidosis. Amyloid 21:175-184.

Gruys E, Toussaint MJ, Niewold TA, Koopmans SJ (2005) Acute phase reaction and acute phase proteins. J Zhejiang Univ Sci B 61:1045-1056.

Gudas LJ (2012) Emerging roles for retinoids in regeneration and differentiation in normal and disease states. Biochim Biophys Acta 1821(1):213-221.

Guénard V, Dinarello CA, Weston PJ, Aebischer P (1991) Peripheral nerve regeneration is impeded by interleukin-1 receptor antagonist released from a polymeric guidance channel. J Neurosci Res 29:396-400.

Guimarães A, Monteiro L, Coutinho P (1980) Pathology of the autonomic nervous system in andrade type of familial amyloidotic polyneuropathy. In: Glenner GG, Costa PP, de Freitas AF (Eds) Amyloid and Amyloidosis. Excerpta Medica, Amsterdam, 88-98.

Häcker U, Nybakken K, Perrimon N (2005) Heparan sulphate proteoglycans: the sweet side of development. Nat Rev Mol Cell Biol 6(7):530-541.

Hailer NP, Vogt C, Korf HW, Dehghani F (2005) Interleukin-1beta exacerbates and interleukin-1 receptor antagonist attenuates neuronal injury and microglial activation after excitotoxic damage in organotypic hippocampal slice cultures. Eur J Neurosci 21:2347-2360.

Hall AK, Landis SC (1992) Division and migration of satellite glia in the embryonic rat superior cervical ganglion. J Neurocytol 21:635-647.

Hallegua DS, Weisman MH (2002) Potential therapeutic uses of interleukin 1 receptor antagonists in human diseases. Ann Rheum Dis 61:960-967.

Hamilton JA, Steinrauf LK, Braden BC, Liepnieks J, Benson MD, et al., (1993) The x-ray crystal structure refinements of normalhuman transthyretin and the amyloidogenic Val-30-Met variant to 1.7-A resolution. J Biol Chem 268:2416-2424.

Hamilton SK, Hinkle ML, Nicolini J, Rambo LN, Rexwinkle AM, et al., (2011) Misdirection of regenerating axons and functional recovery following sciatic nerve injury in rats. J Comp Neurol 519:21-33.

Hammarström P, Schneider F, Kelly JW (2001) Trans-suppression of misfolding in an amyloid disease. Science 293:2459-2462.

Han SH, Jung ES, Sohn JH, Hong HJ, Hong HS, et al., (2011) Human serum transthyretin levels correlate inversely with Alzheimer's disease. J Alzheimers Dis 25(1):77-84.

Hanani M (2005) Satellite glial cells in sensory ganglia: from form to function. Brain Res Brain Res Rev 48:457-476.

Hanna M (2014) Novel drugs targeting transthyretin amyloidosis. Curr Heart Fail Rep 11(1):50-57.

Haraguchi K, Kawamoto A, Isami K, Maeda S, Kusano A, et al., (2012) TRPM2 contributes to inflammatory and neuropathic pain through the aggravation of pronociceptive inflammatory responses in mice. J Neurosci 32:3931-3941.

Hare GMT, Evans PJ, Mackinnon SE, Best TJ, Bain JR, et al., (1992) Walking track analysis: a long-term assessment of peripheral nerve recovery. Plast Reconstr Surg 89:251-258.

Hawkins PN, Pepys MB (1995) Imaging amyloidosis with radiolabelled SAP. Eur J Nucl Med 22(7):595-599.

Hayden MS, Ghosh S (2004) Signaling to NF-κB. Genes Dev 18:2195-2224.

Hennebry SC, Wright HM, Likic VA, Richardson SJ (2006) Structural and functional evolution of transthyretin and transthyretin-like proteins. Proteins 64:1024-1045.

Heskamp A, Leibinger M, Andreadaki A, Gobrecht P, Diekmann H, et al., (2013) CXCL12/SDF-1 facilitates optic nerve regeneration. Neurobiol Dis 55:76-86.

Hirai S, Cui de F, Miyata T, Ogawa M, Kiyonari H, et al., (2006) The c-Jun N-terminal kinase activator dual leucine zipper kinase regulates axon growth and neuronal migration in the developing cerebral cortex. J Neurosci 26(46):11992-12002.

Hofer PA, Anderson R (1975) Postmortem findings in primary familial amyloidosis with polyneuropathy. Acta Pathol Microbiol Scand 83:309-322.

Hoozemans JJ, van Haastert ES, Nijholt DA, Rozemuller AJ, Eikelenboom P, et al., (2009) The unfolded protein response is activated in pretangle neurons in Alzheimer's disease hippocampus. Am J Pathol 174:1241-1251.

Hou X, Parkington HC, Coleman HA, Mechler A, Martin LL, et al., (2007) Transthyretin oligomers induce calcium influx via voltage-gated calcium channels. J Neurochem 100(2):446-457.

Huang M, Ma Z, Khor E, Lim LY (2002) Uptake of FITC-chitosan nanoparticles by A549 cells. Pharm Res 19:1488-1494.

Ihse E, Ybo A, Suhr O, Lindqvist P, Backman C, et al., (2008) Amyloid fibril composition is related to the phenotype of hereditary transthyretin V30M amyloidosis. J Pathol 216(2):253-261.

Inoue S, Kuroiwa M, Saraiva MJ, Guimarães A, Kisilevsky R (1998) Ultrastructure of familial amyloid polyneuropathy amyloid fibrils: examination with high-resolution electron microscopy. J Struct Biol 124(1):1-12.

Irace G, Edelhoch H (1978) Thyroxine-induced conformational changes in prealbumin. Biochemistry 17(26):5729-5733.

Jacobson DR, McFarlin DE, Kane I, Buxbaum JN (1992) Transthyretin Pro55, a variant associated with early-onset, aggressive, diffuse amyloidosis with cardiac and neurologic involvement. Hum Genet 89(3):353-6.

Jacobson DR, Pastore R, Pool S, Malendowicz S, Kane I, et al., (1996) Revised transthyretin Ile 122 allele frequency in African-Americans. Hum Genet 98(2):236-238.

Jendresen CB, Cui H, Zhang X, Vlodavsky I, Nilsson LN, et al., (2014) Overexpression of heparanase lowers amyloid burden in AβPP transgenic mice. J Biol Chem. pii: jbc.M114.600569 [Epub ahead of print].

Jessen KR, Mirsky R (2005) The origin and development of glial cells in peripheral nerves. Nat Rev Neurosci 6(9):671-682.

Jessen KR, Mirsky R (2008) Negative regulation of myelination: relevance for development, injury, and demyelinating disease. Glia. 56(14):1552-1565.

Jono H, Anno T, Motoyama K, Misumi Y, Tasaki M, et al., (2011) Cyclodextrin, a novel therapeutic tool for suppressing amyloidogenic transthyretin misfolding in transthyretin-related amyloidosis. Biochem J 437(1):35-42.

Jovic M, Sharma M, Rahajeng J, Caplan S (2010) The early endosome: a busy sorting station for proteins at the crossroads. Histol Histopathol 25:99-112.

Kabat EA, Moore DH, Landow H (1942) An Electrophoretic Study of the Protein Components in Cerebrospinal Fluid and Their Relationship to the Serum Proteins. J Clin Invest 21:571-577.

Kaltschmidt B, Uherek M, Volk B, Baeuerle PA, Kaltschmidt C (1997) Transcription factor NF-kappaB is activated in primary neurons by amyloid beta peptides and in neurons surrounding early plaques from patients with Alzheimer disease. Proc Natl Acad Sci USA 94:2642-2647.

Kanai M, Raz A, Goodman DS (1968) Retinol-binding protein: the transport protein for vitamin A in human plasma. J Clin Invest 47(9):2025-2044.

Kao HT, Porton B, Czernik AJ, Feng J, Yiu G, et al., (1998) A third member of the synapsin gene family. Proc Natl Acad Sci USA 95:4667-4672.

Kassem NA, Deane R, Segal MB, Preston JE (2006) Role of transthyretin in thyroxine transfer from cerebrospinal fluid to brain and choroid plexus. Am J Physiol Regul Integr Comp Physiol 291(5):R1310-1315.

Kawaguchi R, Yu J, Honda J, Hu J, Whitelegge J, et al., (2007) A membrane receptor for retinol binding protein mediates cellular uptake of vitamin A. Science 315(5813):820-825.

Kay J, Calabrese L (2004) The role of interleukin-1 in the pathogenesis of rheumatoid arthritis. Rheumatology(Oxford) 43:iii2-iii9.

Kigerl KA, Gensel JC, Ankeny DP, Alexander JK, Donnelly DJ, et al., (2009) Identification of two distinct macrophage subsets with divergent effects causing either neurotoxicity or regeneration in the injured mouse spinal cord. J Neurosci 29:13435-13444.

Kofuji K, Ito T, Murata Y, Kawashima S (2002) Effect of chondroitin sulphate on the biodegradation and drug release of chitosan gel beads in subcutaneous air pouches of mice. Biol Pharm Bull 25(2):268-271.

Kohno K, Palha JA, Miyakawa K, Saraiva MJ, Ito S, et al., (1997) Analysis of amyloid deposition in a transgenic mouse model of homozygous familial amyloidotic polyneuropathy. Am J Pathol 150:1497-1508.

Koike H, Misu K, Sugiura M, Iijima M, Mori K, et al., (2004) Pathology of early vs late-onset TTR Met30 familial amyloid polyneuropathy. Neurology 63(1):129-138.

Koike H, Kiuchi T, Iijima M, Ueda M, Ando Y, et al., (2011) Systemic but asymptomatic transthyretin amyloidosis 8 years after domino liver transplantation. J Neurol Neurosurg Psychiatry 82:1287-1290.

Kollmer J, Hund E, Hornung B, Hegenbart U, Schönland SO, et al., (2014) In vivo detection of nerve injury in familial amyloid polyneuropathy by magnetic resonance neurography. Brain [Epub ahead of print].

Kuhlmann T, Bitsch A, Stadelmann C, Siebert H, Brück W (2001) Macrophages are eliminated from the injured peripheral nerve via local apoptosis and circulation to regional lymph nodes and the spleen. J Neurosci 21(10):3401-3408.

Kumamoto T, Fukuhara N, Miyatake T, Araki K, Takahashi Y, et al., (1986) Experimental neuropathy induced by methyl mercury compounds: autoradiographic study of GABA uptake by dorsal root ganglia. Eur Neurol 25:269-277.

Kurosawa T, Igarashi S, Nishizawa M, Onodera O (2005) Selective silencing of a mutant transthyretin allele by small interfering RNAs. Biochem Biophys Res Commun 337:1012-1018.

Lai Z, Colón W, Kelly JW (1996) The acid-mediated denaturation pathway of transthyretin yields a conformational intermediate that can self-assemble into amyloid. Biochemistry 35(20):6470-6482.

Landers KA, McKinnon BD, Li H, Subramaniam VN, Mortimer RH, et al., (2009) Carrier-mediated thyroid hormone transport into placenta by placental transthyretin. J Clin Endocrinol Metab 94(7):2610-2616.

Larsen CM, Faulenbach M, Vaag A, Volund A, Ehses JA, et al., (2007) Interleukin-1-receptor antagonist in type 2 diabetes mellitus. N Engl J Med 356:1517-1526.

Lawrence CB, Allan SM, Rothwell NJ (1998) Interleukin-1beta and the interleukin-1 receptor antagonist act in the striatum to modify excitotoxic brain damage in the rat. Eur J Neurosci 10:1188-1195.

Lemos C, Coelho T, Alves-Ferreira M, Martins-da-Silva A, Sequeiros J, et al., (2014) Overcoming artefact: anticipation in 284 Portuguese kindreds with familial amyloid polyneuropathy (FAP) ATTRV30M. J Neurol Neurosurg Psychiatry 85(3):326-330.

Li J, Schmidt AM (1997) Characterization and functional analysis of the promoter of RAGE, the receptor for advanced glycation end products. J Biol Chem 272:16498-16506.

Li X, Wang W, Wei G, Wang G, Zhang W, et al (2010) Immunophilin FK506 loaded in chitosan guides promotes peripheral nerve regeneration. Biotechnol Lett 32(9):1333-1337.

Li X, Masliah E, Reixach N, Buxbaum JN (2011) Neuronal production of transthyretin in human and murine Alzheimer's disease: is it protective? J Neurosci 31(35):12483-12490.

Li X, Zhang X, Ladiwala AR, Du D, Yadav JK, et al., (2013) Mechanisms of transthyretin inhibition of β-amyloid aggregation in vitro. J Neurosci 33(50):19423-19433.

Lilje O (2002) The processing and presentation of endogenous and exogenous antigen by Schwann cells in vitro. Cell Mol Life Sci 59:2191-2198.

Lin YH, Chang CH, Wu YS, Hsu YM, Chiou SF, et al., (2009) Development of pH-responsive chitosan/heparin nanoparticles for stomach-specific anti-Helicobacter pylori therapy. Biomaterials 30:3332-3342.

Liu J, Lan J, Zhao P, Zheng F, Song J, et al., (2014) Evidence of the presence of amyloid substance in the blood of familial amyloidotic polyneuropathy patients with ATTR Val30Met mutation. Int J Clin Exp Pathol 7(11):7795-7800.

Liu Z, Jiao Y, Liu F, Zhang Z (2007) Heparin/chitosan nanoparticle carriers prepared by polyelectrolyte complexation. J Biomed Mater Res A 83(3):806-812.

Liz MA, Faro CJ, Saraiva MJ, Sousa MM (2004) Transthyretin, a new cryptic protease. J Biol Chem 279:21431-21438.

Liz MA, Gomes CM, Saraiva MJ, Sousa MM (2007) ApoA-I cleaved by transthyretin has reduced ability to promote cholesterol efflux and increased amyloidogenicity. J Lipid Res 48:2385-2395.

Liz MA, Fleming CE, Nunes AF, Almeida MR, Mar FM, et al., (2009) Substrate specificity of transthyretin: identification of natural substrates in the nervous system. Biochem J 419:467-474.

Liz MA, Mar FM, Franquinho F, Sousa MM (2010) Aboard transthyretin: From transport to cleavage. IUBMB Life 62(6):429-435.

Liz MA, Leite SC, Juliano L, Saraiva MJ, Damas AM, et al., (2012) Transthyretin is a metallopeptidase with an inducible active site. Biochem J 443(3):769-778.

Liz MA, Mar FM, Santos TE, Pimentel HI, Marques AM, et al., (2014) Neuronal deletion of GSK3β increases microtubule speed in the growth cone and enhances axon regeneration via CRMP-2 and independently of MAP1B and CLASP2. BMC Biol 12:47.

Loddick SA, Wong ML, Bongiorno PB, Gold PW, Licinio J, et al., (1997) Endogenous interleukin-1 receptor antagonist is neuroprotective. Biochem Biophys Res Commun 234:211-215.

Longo Alves I, Hays MT, Saraiva MJ (1997) Comparative stability and clearance of [Met30]transthyretin and [Met119]transthyretin. Eur J Biochem 249(3):662-668.

Loughna S, Bennett P, Moore G (1995) Molecular analysis of the expression of transthyretin in intestine and liver from trisomy 18 fetuses. Hum Genet 95:89-95.

Lu P, Takai K, Weaver VM, Werb Z (2011) Extracellular matrix degradation and remodeling in development and disease. Cold Spring Harb Perspect Biol 3(12) pii: a005058.

Luo Y, Wang Q (2014) Recent development of chitosan-based polyelectrolyte complexes with natural polysaccharides for drug delivery. Int J Biol Macromol 64:353-367.

Macedo B, Batista AR, do Amaral JB, Saraiva MJ (2007) Biomarkers in the assessment of therapies for familial amyloidotic polyneuropathy. Mol Med 13:584-591.

Macedo B, Batista AR, Ferreira N, Almeida MR, Saraiva MJ (2008) Anti-apoptotic treatment reduces transthyretin deposition in a transgenic mouse model of Familial Amyloidotic Polyneuropathy. Biochim Biophys Acta 1782(9):517-522.

Macedo B, Magalhães J, Batista AR, Saraiva MJ (2010) Carvedilol treatment reduces transthyretin deposition in a familial amyloidotic polyneuropathy mouse model. Pharmacol Res 62(6):514-522.

Magalhães J, Santos SD, Saraiva MJ (2010) αB-crystallin (HspB5) in familial amyloidotic polyneuropathy. Int J Exp Pathol 91(6):515-521.

Magalhães J, Saraiva MJ (2011) Clusterin overexpression and its possible protective role in transthyretin deposition in familial amyloidotic polyneuropathy. J Neuropathol Exp Neurol 70(12):1097-1106.

Mahr S, Neumayer N, Gerhard M, Classen M, Prinz C (2000) IL-1betaYinduced apoptosis in rat gastric enterochromaffin-like cells is mediated by iNOS, NF-kappaB, and Bax protein. Gastroenterology 118:515-524.

Maia LF, Magalhães R, Freitas J, Taipa R, Pires MM, et al., (2015) CNS involvement in V30M transthyretin amyloidosis: clinical, neuropathological and biochemical findings. J Neurol Neurosurg Psychiatry 86(2):159-167.

Makover A, Moriwaki H, Ramakrishnan R, Saraiva MJ, Blaner WS, et al., (1988) Plasma transthyretin. Tissue sites of degradation and turnover in the rat. J Biol Chem 263(18):8598-8603.

Malik R, Roy I (2011) Making sense of therapeutics using antisense technology. Expert Opin Drug Discov 6(5):507-526.

Mangione PP, Porcari R, Gillmore JD, Pucci P, Monti M, et al., (2014) Proteolytic cleavage of Ser52Pro variant transthyretin triggers its amyloid fibrillogenesis. Proc Natl Acad Sci USA 111(4):1539-1544.

Mao HQ, Roy K, Troung-Le VL, Janes KA, Lin KY, et al., (2001) Chitosan-DNA nanoparticles as gene carriers: synthesis, characterization and transfection efficiency. J Control Release 70:399-421.

Mar FM, Bonni A, Sousa MM (2014) Cell intrinsic control of axon regeneration. EMBO Rep 15(3):254-263.

Matsunaga N, Anan I, Forsgren S, Nagai R, Rosenberg P, et al., (2002) Advanced glycation end products (AGE) and the receptor for AGE are present in gastrointestinal tract of familial amyloidotic polyneuropathy patients but do not induce NF-kappaB activation. Acta Neuropathol 104:441-447.

Mattson MP, Camandola S (2001) NF-κB in neuronal plasticity and neurodegenerative disorders. J Clin Invest 107:247-254.

Mattson MP (2012) Parkinson's disease: don't mess with calcium. J Clin Invest 122: 1195-1198.

McKinnon B, Li H, Richard K, Mortimer R (2005) Synthesis of thyroid hormone binding proteins transthyretin and albumin by human trophoblast. J Clin Endocrinol Metab 90(12):6714-6720.

Melo A, Monteiro L, Lima RM, Oliveira DM, Cerqueira MD, et al., (2011) Oxidative stress in neurodegenerative diseases: mechanisms and therapeutic perspectives. Oxid Med Cell Longev 2011:467180.

Merhi-Soussi F, Kwak BR, Magne D, Chadjichristos C, Berti M, et al., (2005) Interleukin-1 plays a major role in vascular inflammation and atherosclerosis in male apolipoprotein E-knockout mice. Cardiovasc Res 66:583-593.

Merlini G, Ascari E, Amboldi N, Bellotti V, Arbustini E, et al., (1995) Interaction of the anthracycline 4'- iodo-4'-deoxydoxorubicin with amyloid fibrils: inhibition of amyloidogenesis. Proc Natl Acad Sci USA 92:2959-2963.

Milbrandt J, de Sauvage FJ, Fahrner TJ, Baloh RH, Leitner ML, et al., (1998) Persephin, a novel neurotrophic factor related to GDNF and neurturin. Neuron 20:245-253.

Miroy GJ, Lai Z, Lashuel HA, Peterson SA, Strang C, et al., (1996) Inhibiting transthyretin amyloid fibril formation via protein stabilization. Proc Natl Acad Sci USA 93:15051-15056.

Misu Ki, Hattori N, Nagamatsu M, Ikeda Si, Ando Y, et al., (1999) Late-onset familial amyloid polyneuropathy type I (transthyretin Met30-associated familial amyloid polyneuropathy) unrelated to endemic focus in Japan. Clinicopathological and genetic features. Brain 122:1951-1962.

Misumi Y, Ando Y, Ueda M, Obayashi K, Jono H, et al., (2009) Chain reaction of amyloid fibril formation with induction of basement membrane in familial amyloidotic polyneuropathy. J Pathol 219(4):481-490.

Misumi Y, Ando Y, Gonçalves NP, Saraiva MJ (2013) Fibroblasts endocytose and degrade transthyretin aggregates in transthyretin related amyloidosis. Lab Invest 93:911-920.

Miyata M, Sato T, Kugimiya M, Sho M, Nakamura T, et al., (2010) The crystal structure of the green tea polyphenol (-)-epigallocatechin gallate-transthyretin complex reveals a novel binding site distinct from the thyroxine binding site. Biochemistry 49(29):6104-6114.

Mizisin AP, Weerasuriya A (2011) Homeostatic regulation of the endoneurial microenvironment during development, aging and in response to trauma, disease and toxic insult. Acta Neuropathol 121(3):291-312.

Mizoguchi H, Yamada K, Nabeshima T (2011) Matrix metalloproteinases contribute to neuronal dysfunction in animal models of drug dependence, Alzheimer's disease, and epilepsy. Biochem Res Int 2011:681385.

Moalem G, Xu K, Yu L (2004) T lymphocytes play a role in neuropathic pain following peripheral nerve injury in rats. Neuroscience 129(3):767-777.

Mohamed A, Posse de Chaves E (2011) Aβ Internalization by neurons and glia. Int J Alzheimers Dis 2011:127984.

Monaco HL, Rizzi M, Coda A (1995) Structure of a complex of two plasma proteins: transthyretin and retinol-binding protein. Science 268:1039-1041.

Monteiro FA, Cardoso I, Sousa MM, Saraiva MJ (2006a) In vitro inhibition of transthyretin aggregate-induced cytotoxicity by full and peptide derived forms of the soluble receptor for advanced glycation end products (RAGE). FEBS Lett 580:3451-3456.

Monteiro FA, Sousa MM, Cardoso I, do Amaral JB, Guimarães A, et al., (2006b) Activation of ERK1/2 MAP kinases in familial amyloidotic polyneuropathy. J Neurochem 97(1):151-161.

Moore KW, de Waal Malefyt R, Coffman RL, O'Garra A (2001) Interleukin-10 and the interleukin-10 receptor. Annu Rev Immunol 19:683-765.

Moreira C, Oliveira H, Pires LR, Simões S, Barbosa MA, et al., (2009) Improving chitosan-mediated gene transfer by the introduction of intracellular buffering moieties into the chitosan backbone. Acta Biomaterialia 5:2995-3006.

Mu FT, Callaghan JM, Steele-Mortimer O, Stenmark H, Parton RG, et al., (1995) EEA1, an early endosome associated protein. EEA1 is a conserved alpha-helical peripheral membrane protein flanked by cysteine? fingers? and contains a calmodulin-binding IQ motif. J Biol Chem 270:13503-13511.

Mueller M, Leonhard C, Wacker K, Ringelstein EB, Okabe M, et al., (2003) Macrophage response to peripheral nerve injury: the quantitative contribution of resident and hematogenous macrophages. Lab Invest 83(2):175-185.

Murakami K, Yoshida S (2012) Nerve injury induces the expression of syndecan-1 heparan sulfate proteoglycan in peripheral motor neurons. Neurosci Lett 527(1):28-33.

Murakami T, Ohsawa Y, Sunada Y (2008) The transthyretin gene is expressed in human and rodend dorsal root ganglia. Neurosci Lett 436:335-339.

Murakami T, Ohsawa Y, Zhenghua L, Yamamura K, Sunada Y (2010) The transthyretin gene is expressed in Schwann cells of peripheral nerves. Brain Res 1348:222-225.

Nadeau S, Filali M, Zhang J, Kerr BJ, Rivest S, et al., (2011) Functional recovery after peripheral nerve injury is dependent on the pro-inflammatory cytokines IL-1β and TNF: implications for neuropathic pain. J Neurosci 31:12533-12542.

Nagata Y, Tashiro F, Yi S, Murakami T, Maeda S, et al., (1995) A 6-kb upstream region of the human transthyretin gene can direct developmental, tissue-specific, and quantitatively normal expression in transgenic mouse. J Biochem 117:169-175.

Nakagawa T, Yuan J (2000) Cross-talk between two cysteine protease families. Activation of caspase-12 by calpain in apoptosis. J Cell Biol 150(4):887-894.

Nakagawa T, Zhu H, Morishima N, Li E, Xu J, et al., (2000) Caspase-12 mediates endoplasmic-reticulum-specific apoptosis and cytotoxicity by amyloid-beta. Nature 403(6765):98-103.

Nesic O, Xu GY, McAdoo D, High KW, Hulsebosch C, et al., (2001) IL-1 receptor antagonist prevents apoptosis and caspase-3 activation after spinal cord injury. J Neurotrauma 18:947-956.

Neumann B, Coakley S, Giordano-Santini R, Linton C, Lee ES, et al., (2015) EFF-1-mediated regenerative axonal fusion requires components of the apoptotic pathway. Nature 517(7533):219-222.

Niemi JP, Defrancesco-Lisowitz A, Roldán-Hernández L, Lindborg JA, Mandell D, et al., (2013) A critical role for macrophages near axotomized neuronal cell bodies in stimulating nerve regeneration. J Neurosci 33:16236-16248.

Noborn F, O'Callaghan P, Hermansson E, Zhang X, Ancsin JB, et al., (2011) Heparan sulfate/heparin promotes transthyretin fibrillization through selective binding to a basic motif in the protein. Proc Natl Acad Sci USA 108(14):5584-5589.

Nunes AF, Saraiva MJ, Sousa MM (2006) Transthyretin knockouts are a new mouse model for increased neuropeptide Y. FASEB J 20:166-168.

Obici L, Cortese A, Lozza A, Lucchetti J, Gobbi M, et al., (2012) Doxycycline plus tauroursodeoxycholic acid for transthyretin amyloidosis: a phase II study. Amyloid 19 Suppl 1:34-36.

Oeckinghaus A, Hayden MS, Ghosh S (2011) Crosstalk in NF-κB signaling pathways. Nat Immunol 12(8):695-708.

Oliveira H, Pires LR, Fernandez R, Martins MC, Simões S, et al., (2010) Chitosan-based gene delivery vectors targeted to the peripheral nervous system. J Biomed Mater Res A 95(3):801-810.

Oliveira SM, Ribeiro CA, Cardoso I, Saraiva MJ (2011) Gender-dependent transthyretin modulation of brain amyloid-β levels: evidence from a mouse model of Alzheimer's disease. J Alzheimers Dis 27:429-439.

Ong DE, Davis JT, O'Day WT, Bok D (1994) Synthesis and secretion of retinol-binding protein and transthyretin by cultured retinal pigment epithelium. Biochemistry 33(7):1835-1842.

Palha JA, Episkopou V, Maeda S, Shimada K, Gottesman ME, et al., (1994) Thyroid hormone metabolism in a transthyretin-null mouse strain. J Biol Chem 269:33135-33139.

Palha JA, Hays MT, Morreale de Escobar G, Episkopou V, Gottesman ME, et al., (1997) Transthyretin is not essential for thyroxine to reach the brain and other tissues in transthyretin-null mice. Am J Physiol 272:E485-493.

Palha JA (2002) Transthyretin as a thyroid hormone carrier: function revisited. Clin Chem Lab Med 40:1292-1300.

Pannese E, Procacci P (2002) Ultrastructural localization of NGF receptors in satellite cells of the rat spinal ganglia. J Neurocytol 31:755-763.

Paresce DM, Ghosh RN, Maxfield FR (1996) Microglial cells internalize aggregates of the Alzheimer's disease amyloid beta-protein via a scavenger receptor. Neuron 17:553-565.

Pavinatto FJ, Pavinatto A, Caseli L, Santos DS Jr, Nobre TM, et al., (2007) Interaction of chitosan with cell membrane models at the air-water interface. Biomacromolecules 8:1633-1640.

Pearson AG, Gray CW, Pearson JF, Greenwood JM, During MJ, et al., (2003) ATF3 enhances c-Jun-mediated neurite sprouting. Brain Res Mol Brain Res 120:38-45.

Pepys MB (2001) Pathogenesis, diagnosis and treatment of systemic amyloidosis. Philos Trans R Soc Lond B Biol Sci 356:203-210.

Pepys MB, Herbert J, Hutchinson WL, Tennent GA, Lachmann HJ, et al., (2002) Targeted pharmacological depletion of serum amyloid P component for treatment of human amyloidosis. Nature 417(6886):254-259.

Pepys MB (2006) Amyloidosis. Annu Rev Med 57:223-241.

Pitkänen P, Westermark P, Cornwell GG 3rd (1984) Senile systemic amyloidosis. Am J Pathol 117(3):391-399.

Pizza V, Agresta A, D'Acunto CW, Festa M, Capasso A (2011) Neuroinflamm-aging and neurodegenerative diseases: an overview. CNS Neurol Disord Drug Targets 10:621-634.

Planté-Bordeneuve V, Said G (2011) Familial amyloid polyneuropathy. Lancet Neurol 10(12):1086-1097.

Pokrzywa M, Dacklin I, Hultmark D, Lundgren E (2007) Misfolded transthyretin causes behavioral changes in a Drosophila model for transthyretin-associated amyloidosis. Eur J Neurosci 26:913-924.

Pokrzywa M, Dacklin I, Vestling M, Hultmark D, Lundgren E, et al., (2010) Uptake of aggregating transthyretin by fat body in a Drosophila model for TTR-associated amyloidosis. PLoS One 5(12):e14343.

Potter MA, Luxton G (1999) Prealbumin measurement as a screening tool for protein calorie malnutrition in emergency hospital admissions: a pilot study. Clin Invest Med 22(2):44-52.

Puchtler H, Sweat F (1965) Congo red as a stain for fluorescence microscopy of amyloid. J Histochem Cytochem 13(8):693-694.

Qian X, Samadani U, Porcella A, Costa RH (1995) Decreased expression of hepatocyte nuclear factor 3 alpha during the acute-phase response influences transthyretin gene transcription. Mol Cell Biol 15:1364-1376.

Quintas A, Vaz DC, Cardoso I, Saraiva MJ, Brito RM (2001) Tetramer dissociation and monomer partial unfolding precedes protofibril formation in amyloidogenic transthyretin variants. J Biol Chem 276(29):27207-27213.

Ramon y Cajal S, May RM (1928) Degeneration and regeneration of the nervous system. Oxford London: Oxford University Press; Humphrey Milford.

Raoul C, Pettmann B, Henderson CE (2000) Active killing of neurons during development and following stress: a role for p75(NTR) and Fas? Curr Opin Neurobiol 10(1):111-117.

Raz A, Goodman DS (1969) The interaction of thyroxine with human plasma prealbumin and with the prealbumin-retinol-binding protein complex. J Biol Chem 244:3230-3237.

Refai E, Dekki N, Yang SN, Imreh G, Cabrera O, et al., (2005) Transthyretin constitutes a functional component in pancreatic beta-cell stimulus-secretion coupling. Proc Natl Acad Sci USA 102(47):17020-17025.

Reixach N, Deechongkit S, Jiang X, Kelly JW, Buxbaum JN (2004) Tissue damage in the amyloidoses: Transthyretin monomers and nonnative oligomers are the major cytotoxic species in tissue culture. Proc Natl Acad Sci USA 101:2817-2822.

Relton JK, Martin D, Thompson RC, Russell DA (1996) Peripheral administration of interleukin-1 receptor antagonist inhibits brain damage after focal cerebral ischemia in the rat. Exp Neurol 138:206-213.

Rezai-Zadeh K, Gate D, Gowing G, Town T (2011) How to get from here to there: Macrophage recruitment in Alzheimer's disease. Curr Alzheimer Res 8:156-163.

Rhee JW, Lee KW, Kim D, Lee Y, Jeon OH, et al., (2007) NF-kappaB-dependent regulation of matrix metalloproteinase-9 gene expression by lipopolysaccharide in a macrophage cell line RAW 264.7. J Biochem Mol Biol 40:88-94.

Ribeiro CA, Santana I, Oliveira C, Baldeiras I, Moreira J, et al., (2012) Transthyretin decrease in plasma of MCI and AD patients: investigation of mechanisms for disease modulation. Curr Alzheimer Res 9:881-889.

Ribeiro CA, Saraiva MJ, Cardoso I (2012) Stability of the transthyretin molecule as a key factor in the interaction with a-beta peptide--relevance in Alzheimer's disease. PLoS One 7(9):e45368.

Richter K, Haslbeck M, Buchner J (2010) The heat shock response: life on the verge of death. Mol Cell 40(2):253-266.

Rodriguez FJ, Valero-Cabre A, Navarro X (2004) Regeneration and functional recovery following peripheral nerve injury. Drug Discov Today 1(2):177-185.

Rogers J (1995) Inflammation as a pathogenic mechanism in Alzheimer's disease. Arzneimittelforschung 45:439-442.

Rosales FJ, Ritter SJ, Zolfaghari R, Smith JE, Ross AC (1996) Effects of acute inflammation on plasma retinol, retinol-binding protein, and its mRNA in the liver and kidneys of vitamin AY sufficient rats. J Lipid Res 37:962-971.

Rothwell N, Allan S, Toulmond S (1997) The role of interleukin 1 in acute neurodegeneration and stroke: Pathophysiological and therapeutic implications. J Clin Invest 100:2648-2652.

Roy S, Zhang B, Lee VM, Trojanowski JQ (2005) Axonal transport defects: a common theme in neurodegenerative diseases. Acta Neuropathol 109:5-13.

Rusai K, Huang H, Sayed N, Strobl M, Roos M, et al., (2008) Administration of interleukin-1 receptor antagonist ameliorates renal ischemia-reperfusion injury. Transpl Int 21:572-580.

Saada A, Reichert F, Rotshenker S (1996) Granulocyte macrophage colony stimulating factor produced in lesioned peripheral nerves induces the up-regulation of cell surface expression of MAC-2 by macrophages and Schwann cells. J Cell Biol 133(1):159-167.

Said G, Planté-Bordeneuve V (2009) Familial amyloid polyneuropathy: a clinico-pathologic study. J Neurol Sci 284(1-2):149-154.

Said G, Grippon S, Kirkpatrick P (2012) Tafamidis. Nat Rev Drug Discov 11:185-186.

Salloum FN, Chau V, Varma A, Hoke NN, Toldo S, et al., (2009) Anakinra in experimental acute myocardial infarction-does dosage or duration of treatment matter? Cardiovasc Drugs Ther 23:129-135.

Sanchez-Guajardo V, Barnum CJ, Tansey MG, Romero-Ramos M (2013) Neuroimmunological processes in Parkinson’s disease and their relation to α-synuclein: Microglia as the referee between neuronal processes and peripheral immunity. ASN Neuro 5:113-139.

Santos SD, Cardoso I, Magalhães J, Saraiva MJ (2007) Impairment of the ubiquitin-proteasome system associated with extracellular transthyretin aggregates in familial amyloidotic polyneuropathy. J Pathol 213(2):200-209.

Santos SD, Magalhães J, Saraiva MJ (2008) Activation of the heat shock response in familial amyloidotic polyneuropathy. J Neuropathol Exp Neurol 67(5):449-455.

Santos SD, Lambertsen KL, Clausen BH, Akinc A, Alvarez R, et al., (2010a) CSF transthyretin neuroprotection in a mouse model of brain ischemia. Journal of Neurochem 115:1434-1444.

Santos SD, Fernandes R, Saraiva MJ (2010b) The heat shock response modulates transthyretin deposition in the peripheral and autonomic nervous systems. Neurobiol Aging 31:280-289.

Saraiva M, O'Garra A (2010) The regulation of IL-10 production by immune cells. Nat Rev Immunol 10:170-181.

Saraiva MJ, Birken S, Costa PP, Goodman DS (1984) Amyloid fibril protein in familial amyloidotic polyneuropathy, Portuguese type. Definition of molecular abnormality in transthyretin (prealbumin). J Clin Invest 74:104-119.

Saraiva MJ, Costa PP, Goodman DS (1985) Biochemical marker in familial amyloidotic polyneuropathy, Portuguese type. Family studies on the transthyretin (prealbumin)-methionine-30 variant. J Clin Invest 76(6):2171-2177.

Saraiva MJ, Magalhaes J, Ferreira N, Almeida MR (2012) Transthyretin deposition in familial amyloidotic polyneuropathy. Curr Med Chem 19(15):2304-2311.

Sasaki H, Yoshioka N, Takagi Y, Sakaki Y (1985) Structure of the chromosomal gene for human serum prealbumin. Gene 37(1-3):191-197.

Sasaki H, Tone S, Nakazato M, Yoshioka K, Matsuo H, et al., (1986) Generation of transgenic mice producing a human transthyretin variant: a possible mouse model for familial amyloidotic polyneuropathy. Biochem Biophys Res Commun 139:794-799.

Sasaki H, Nakazato M, Saraiva MJ, Matsuo H, Sakaki Y (1989) Activity of a metallothionein-transthyretin fusion gene in transgenic mice. Possible effect of plasmid sequences on tissue-specific expression. Mol Biol Med 6:345-353.

Scheib J, Höke A (2013) Advances in peripheral nerve regeneration. Nat Rev Neurol 9(12):668-676.

Schlaepfer WW (1969) Experimental lead neuropathy: a disease of the supporting cells in the peripheral nervous system. J Neuropathol Exp Neurol 28:401-418.

Schwarznau A, Hanson MS, Sperger JM, Schram BR, Danobeitia JS, et al., (2009) IL-1beta receptor blockade protects islets against pro-inflammatory cytokine induced necrosis and apoptosis. J Cell Physiol 220:341-347.

Schwarzman AL, Gregori L, Vitek MP, Lyubski S, Strittmatter WJ, et al., (1994) Transthyretin sequesters amyloid beta protein and prevents amyloid formation. Proc Natl Acad Sci USA 91:8368-8372.

Seibert FB, Nelson JW (1942) Electrophoretic study of the blood protein response in tuberculosis. J Biol Chem 143:29-38.

Seijffers R, Mills CD, Woolf CJ (2007) ATF3 increases the intrinsic growth state of DRG neurons to enhance peripheral nerve regeneration. J Neurosci 27(30):7911-7920.

Sekijima Y, Wiseman RL, Matteson J, Hammarström P, Miller SR, et al., (2005) The biological and chemical basis for tissue-selective amyloid disease. Cell 121(1):73-85.

Sekijima Y, Kelly JW, Ikeda S (2008) Pathogenesis of and therapeutic strategies to ameliorate the transthyretin amyloidoses. Curr Pharm Des 14:3219-3230.

Semple SC, Akinc A, Chen J, Sandhu AP, Mui BL, et al., (2010) Rational design of cationic lipids for siRNA delivery. Nat Biotechnol 28:172-176.

Sensenbrenner M, Lucas M, Deloulme JC (1997) Expression of two neuronal markers, growth-associated protein 43 and neuron-specific enolase, in rat glial cells. J Mol Med (Berl) 75:653-663.

Serot JM, Christmann D, Dubost T, Couturier M (1997) Cerebrospinal fluid transthyretin: aging and late onset Alzheimer's disease. J Neurol Neurosurg Psychiatr 63:506-508.

Sgroi A, Gonelle-Gispert C, Morel P, Baertschiger RM, Niclauss N, et al., (2011) Interleukin-1 receptor antagonist modulates the early phase of liver regeneration after partial hepatectomy in mice. PLoS One 6(9):e25442

Shin JE, Cho Y, Beirowski B, Milbrandt J, Cavalli V, et al., (2012) Dual leucine zipper kinase is required for retrograde injury signaling and axonal regeneration. Neuron 74(6):1015-1022.

Sheu ML, Cheng FC, Su HL, Chen YJ, Chen CJ, et al., (2012) Recruitment by SDF-1α of CD34-positive cells involved in sciatic nerve regeneration. J Neurosurg 116:432-444.

Sierra-Filardi E, Nieto C, Domínguez-Soto A, Barroso R, Sánchez-Mateos P, et al., (2014) CCL2 shapes macrophage polarization by GM-CSF and M-CSF: identification of CCL2/CCR2-dependent gene expression profile. J Immunol 192(8):3858-3867.

Simon DJ, Weimer RM, McLaughlin T, Kallop D, Stanger K, et al., (2012) A caspase cascade regulating developmental axon degeneration. J Neurosci 32(49):17540-17553.

Sinha S, Lopes DH, Du Z, Pang ES, Shanmugam A, et al., (2011) Lysine-specific molecular tweezers are broad-spectrum inhibitors of assembly and toxicity of amyloid proteins. J Am Chem Soc 133:16958-16969.

Skene JH, Willard M (1981) Characteristics of growth-associated polypeptides in regenerating toad retinal ganglion cell axons. J Neurosci 1(4):419-426.

Smith DF, Galkina E, Ley K, Huo Y (2005) GRO family chemokines are specialized for monocyte arrest from flow. Am J Physiol Heart Circ Physiol 289:1976-1984.

Soares ML, Centola M, Chae J, Saraiva MJ, Kastner DL (2003) Human transthyretin intronic open reading frames are not independently expressed in vivo or part of functional transcripts. Biochim Biophys Acta 1626(1-3):65-74.

Sobue G, Nakao N, Murakami K, Yasuda T, Sahashi K, et al., (1990) Type I familial amyloid polyneuropathy. A pathological study of the peripheral nervous system. Brain 113:903-919.

Socolow EL, Woeber KA, Purdy RH, Holloway MT, Ingbar SH (1965) Preparation of I-131-labeled human serum prealbumin and its metabolism in normal and sick patients. J Clin Invest 44(10):1600-1609.

Soprano DR, Herbert J, Soprano KJ, Schon EA, Goodman DS (1985) Demonstration of transthyretin mRNA in the brain and other extrahepatic tissues in the rat. J Biol Chem 260:11793-11798.

Sorokin L (2010) The impact of the extracellular matrix on inflammation. Nat Rev Immunol 10(10):712-723.

Sousa JC, Grandela C, Fernández-Ruiz J, De Miguel R, De Sousa L, et al., (2004) Transthyretin is involved in depression-like behaviour and exploratory activity. Journal of Neurochem 88:1052-1058.

Sousa MM, Norden AG, Jacobsen C, Willnow TE, Christensen EI, et al., (2000a) Evidence for the role of megalin in renal uptake of transthyretin. J Biol Chem 275(49):38176-38181.

Sousa MM, Yan SD, Stern D, Saraiva MJ (2000b) Interaction of the receptor for advanced glycation end products (RAGE) with transthyretin triggers nuclear transcription factor kB (NF-kB) activation. Lab Invest 80:1101-1110.

Sousa MM, Berglund L, Saraiva MJ (2000c) Transthyretin in high density lipoproteins: association with apolipoprotein A-I. J Lipid Res 41:58-65.

Sousa MM, Saraiva MJ (2001) Internalization of transthyretin. Evidence of a novel yet unidentified receptor-associated protein (RAP)-sensitive receptor. J Biol Chem 276(17): 14420-14425.

Sousa MM, Cardoso I, Fernandes R, Guimarães A, Saraiva MJ (2001a) Deposition of transthyretin in early stages of familial amyloidotic polyneuropathy: evidence for toxicity of nonfibrillar aggregates. Am J Pathol 159:1993-2000.

Sousa MM, Du Yan S, Fernandes R, Guimaraes A, Stern D, et al., (2001b) Familial amyloid polyneuropathy: receptor for advanced glycation end products-dependent triggering of neuronal inflammatory and apoptotic pathways. J Neurosci 21(19):7576-7586.

Sousa MM, Fernandes R, Palha JA, Taboada A, Vieira P, et al., (2002) Evidence for early cytotoxic aggregates in transgenic mice for human transthyretin Leu55Pro. Am J Pathol 161:1935-1948.

Sousa MM, Saraiva MJ (2003) Neurodegeneration in familial amyloid polyneuropathy: from pathology to molecular signaling. Prog Neurobiol 71(5):385-400.

Sousa MM, Ferrão J, Fernandes R, Guimarães A, Geraldes JB, et al., (2004) Deposition and passage of transthyretin through the blood-nerve barrier in recipients of familial amyloid polyneuropathy livers. Lab Invest 84:865-873.

Sousa MM, do Amaral JB, Guimarães A, Saraiva MJ (2005) Up-regulation of the extracellular matrix remodeling genes, biglycan, neutrophil gelatinase-associated

lipocalin, and matrix metalloproteinase-9 in familial amyloid polyneuropathy. FASEB J 19(1):124-126.

Sousa MM, Saraiva MJ (2008) Transthyretin is not expressed by dorsal root ganglia cells. Exp Neurol 214:362-365.

Stangou AJ, Heaton ND, Hawkins PN (2005) Transmission of systemic transthyretin amyloidosis by means of domino liver transplantation. N Engl J Med 352:2356.

Su Y, Jono H, Misumi Y, Senokuchi T, Guo J, et al., (2012) Novel function of transthyretin in pancreatic alpha cells. FEBS Lett 586(23):4215-4222.

Suhr O, Danielsson A, Steen L (1992) Bile acid malabsorption caused by gastrointestinal motility dysfunction? an investigation of gastrointestinal disturbances in familial amyloidosis with polyneuropathy. Scand J Gastroenterol 27:201-207.

Sun W, Sun C, Lin H, Zhao H, Wang J, et al., (2009) The effect of collagen-binding NGF-beta on the promotion of sciatic nerve regeneration in a rat sciatic nerve crush injury model. Biomaterials 30:4649-4656.

Surmeier DJ, Schumacker PT (2013) Calcium, bioenergetics, and neuronal vulnerability in Parkinson's disease. J Biol Chem 288:10736-10741.

Szegezdi E, Logue SE, Gorman AM, Samali A. (2006) Mediators of endoplasmic reticulum stress-induced apoptosis. EMBO Rep 7(9):880-885.

Takahashi R, Ono K, Shibata S, Nakamura K, Komatsu J, et al., (2014) Efficacy of diflunisal on autonomic dysfunction of late-onset familial amyloid polyneuropathy (TTR Val30Met) in a Japanese endemic area. J Neurol Sci 345(1-2):231-235.

Takaoka Y, Tashiro F, Yi S, Maeda S, Shimada K, et al., (1997) Comparison of amyloid deposition in two lines of transgenic mouse that model familial amyloidotic polyneuropathy, type I. Transgenic Res 6:261-269.

Tang C, Sula MJ, Bohnet S, Rehman A, Taishi P, et al., (2005) Interleukin-1beta induces CREB-binding protein (CBP) mRNA in brain and the sequencing of rat CBP. Brain Res Mol Brain Res 137:213-222.

Tawara S, Nakazato M, Kangawa K, Matsuo H, Araki S (1983) Identification of amyloid prealbumin variant in familial amyloidotic polyneuropathy (Japanese type). Biochem Biophys Res Commun 116(3):880-888.

Tedeschi A, Bradke F (2013) The DLK signalling pathway--a double-edged sword in neural development and regeneration. EMBO Rep 14(7):605-614.

Teixeira AC, Saraiva MJ (2013) Presence of N-glycosylated transthyretin in plasma of V30M carriers in familial amyloidotic polyneuropathy: an escape from ERAD. J Cell Mol Med 17(3):429-435.

Teixeira PF, Cerca F, Santos SD, Saraiva MJ (2006) Endoplasmic reticulum stress associated with extracellular aggregates. Evidence from transthyretin deposition in familial amyloid polyneuropathy. J Biol Chem 281(31):21998-22003.

Tendi EA, Cunsolo R, Bellia D, Messina RL, Paratore S, et al., (2010) Drug target identification for neuronal apoptosis through a genome scale screening. Curr Med Chem 17:2906-2920.

Teng M, Gallo G, Buxbaum J (1995) Is an amyloidogenic substrate enough? Transgenic mice producing human TTR Pro55 do not develop amyloid. Neuromuscul Disord 6, Supplement 1, S30.

Teng MH, Yin JY, Vidal R, Ghiso J, Kumar A, et al., (2001) Amyloid and nonfibrillar deposits in mice transgenic for wild-type human transthyretin: a possible model for senile systemic amyloidosis. Lab Invest 81:385-396.

Terazaki H, Ando Y, Fernandes R, Yamamura K, Maeda S, et al., (2006) Immunization in familial amyloidotic polyneuropathy: counteracting deposition by immunization with a Y78F TTR mutant. Lab Invest 86:23-31.

Thomas PK, King RH (1974) Peripheral nerve changes in amyloid neuropathy. Brain 97(2):395-406.

Tofaris GK, Patterson PH, Jessen KR, Mirsky R (2002) Denervated Schwann cells attract macrophages by secretion of leukemia inhibitory factor (LIF) and monocyte chemoattractant protein-1 in a process regulated by interleukin-6 and LIF. J Neurosci 22(15):6696-6703.

Tojo K, Sekijima Y, Kelly JW, Ikeda S (2006) Diflunisal stabilizes familial amyloid polyneuropathy-associated transthyretin variant tetramers in serum against dissociation required for amyloidogenesis. Neurosci Res 56:441-449.

Toulmond S, Rothwell NJ (1995) Interleukin-1 receptor antagonist inhibits neuronal damage caused by fluid percussion injury in the rat. Brain Res 671:261-266.

Trapani A, Di Gioia S, Ditaranto N, Cioffi N, Goycoolea FM, et al., (2013) Systemic heparin delivery by the pulmonary route using chitosan and glycol chitosan nanoparticles. Int J Pharm 447(1-2):115-123.

Tsuchiya A, Yazaki M, Kametani F, Takei Y, Ikeda S (2008) Marked regression of abdominal fat amyloid in patients with familial amyloid polyneuropathy during long-term follow-up after liver transplantation. Liver Transpl 14:563-570.

Tsuzuki T, Mita S, Maeda S, Araki S, Shimada K (1985) Structure of the human prealbumin gene. J Biol Chem 260(22):12224-12227.

Ueda M, Ando Y, Hakamata Y, Nakamura M, Yamashita T, et al., (2007) A transgenic rat with the human ATTR V30M: a novel tool for analyses of ATTR metabolisms. Biochem Biophys Res Commun 352:299-304.

Ueda M, Ando Y (2014) Recent advances in transthyretin amyloidosis therapy. Transl Neurodegener. 3:19.

Uttara B, Singh AV, Zamboni P, Mahajan RT (2009) Oxidative stress and neurodegenerative diseases: a review of upstream and downstream antioxidant therapeutic options. Curr Neuropharmacol 7(1):65-74.

van Bennekum AM, Wei S, Gamble MV, Vogel S, Piantedosi R, et al., (2001) Biochemical basis for depressed serum retinol levels in transthyretin-deficient mice. J Biol Chem 276(2):1107-1113.

Van Ginderachter JA, Movahedi K, Hassanzadeh Ghassabeh G, Meerschaut S, Beschin A, et al., (2006) Classical and alternative activation of mononuclear phagocytes: Picking the best of both worlds for tumor promotion. Immunobiology 211:487-501.

van Horssen J, Bö L, Vos CM, Virtanen I, de Vries HE (2005) Basement membrane proteins in multiple sclerosis-associated inflammatory cuffs: Potential role in influx and transport of leukocytes. J Neuropathol Exp Neurol 64:722-729.

Vargas ME, Watanabe J, Singh SJ, Robinson WH, Barres BA (2010) Endogenous antibodies promote rapid myelin clearance and effective axon regeneration after nerve injury. Proc Natl Acad Sci USA 107(26):11993-11998.

Vatassery GT, Quach HT, Smith WE, Benson BA, Eckfeldt JH (1991) A sensitive assay of transthyretin (prealbumin) in human cerebrospinal fluid in nanogram amounts by ELISA. Clin Chim Acta 197:19-25.

Vieira M, Saraiva MJ (2013) Transthyretin regulates hippocampal 14-3-3ζ protein levels. FEBS Lett 587(10):1482-1488.

Vieira M, Gomes JR, Saraiva MJ (2014) Transthyretin Induces Insulin-like Growth Factor I Nuclear Translocation Regulating Its Levels in the Hippocampus. Mol Neurobiol [Epub ahead of print].

Vieira M, Saraiva MJ (2014) Transthyretin: a multifaceted protein. Biomol Concepts 5(1):45-54.

Walker AK, Gong Z, Park WM, Zigman JM, Sakata I (2013) Expression of Serum Retinol Binding Protein and Transthyretin within Mouse Gastric Ghrelin Cells. PLoS One 8(6):e64882.

Waller A (1850) Experiments on the section of the glossopharyngeal and hypoglossal nerves of the frog, and observations of the alterations produced thereby in the structure of their primitive fibres. Philosophical Transactions of the Royal Society of London 140:423-429.

Wang J, Maldonado MA (2006) The ubiquitin-proteasome system and its role in inflammatory and autoimmune diseases. Cell Mol Immunol 3(4):255-261.

Wen AY, Sakamoto KM, Miller LS (2010) The role of the transcription factor CREB in immune function. J Immunol 185:6413-6419.

Westermark P (1998) The pathogenesis of amyloidosis: understanding general principles. Am J Pathol 152(5):1125-1127.

Westermark P (2005) Aspects on human amyloid forms and their fibril polypeptides. FEBS J 272:5942-5949.

Westermark GT, Westermark P (2008) Transthyretin and amyloid in the islets of Langerhans in type-2 diabetes. Exp Diabetes Res 2008:429274.

Whitehead AS, Skinner M, Bruns GA, Costello W, Edge MD, et al., (1984) Cloning of human prealbumin complementary DNA. Localization of the gene to chromosome 18 and detection of a variant prealbumin allele in a family with familial amyloid polyneuropathy. Mol Biol Med 2(6):411-423.

Wixner J, Obayashi K, Ando Y, Karling P, Anan I (2013) Loss of gastric interstitial cells of Cajal in patients with hereditary transthyretin amyloidosis. Amyloid 20:99-106.

Wu ZQ, Han XD, Wang Y, Yuan KL, Jin ZM, et al., (2011) Interleukin-1 receptor antagonist reduced apoptosis and attenuated intestinal mucositis in a 5-fluorouracil chemotherapy model in mice. Cancer Chemother Pharmacol 68:87-96.

Wyss-Coray T, Loike JD, Brionne TC, Lu E, Anankov R, et al., (2003) Adult mouse astrocytes degrade amyloid-beta in vitro and in situ. Nat Med 9:453-457.

Xu C, Bailly-Maitre B, Reed JC (2005) Endoplasmic reticulum stress: cell life and death decisions. J Clin Invest 115(10):2656-2664.

Ydens E, Cauwels A, Asselbergh B, Goethals S, Peeraer L, et al., (2012) Acute injury in the peripheral nervous system triggers an alternative macrophage response. J Neuroinflammation 9:176.

Ydens E, Lornet G, Smits V, Goethals S, Timmerman V, et al., (2013) The neuroinflammatory role of Schwann cells in disease. Neurobiol Dis 55:95-103.

Yoshioka A, Yamaya Y, Saiki S, Hirose G, Shimazaki K, et al., (2001) A case of familial amyloid polyneuropathy homozygous for the transthyretin Val30Met gene with motor-dominant sensorimotor polyneuropathy and unusual sural nerve pathological findings. Arch Neurol 58:1914-1918.

Zong S, Zeng G, Wei B, Xiong C, Zhao Y (2012) Beneficial effect of interleukin-1 receptor antagonist protein on spinal cord injury recovery in the rat. Inflammation 35:520-526.

Annex

Gene	Forward	Reverse
Human *TTR*	5'-ATTCTTGGCAGGATGGCTTC-3'	5'-CAGAGGACACTTGGATTCACC-3'
Mouse *Ttr*	5'-AGCCCTTTGCCTCTGGGAAGAC-3'	5'-TGCGATGGTGTAGTGGCGATGG-3'
Il-1β	5'-ACCTTCCAGGATGAGGACATGA-3'	5'-AACGTCACACACCAGCAGGTTA-3'
Il-6	5'-CTGTCTATACCACTTCAC-3'	5'-GCTTATCTGTTAGGAGAG-3'
Tnf-α	5'-ACAAGGCTGCCCCGACTAC-3'	5'-TGGAAGACTCCTCCCAGGTATATG-3'
Il-10	5'-CTAACCGACTCCTTAATG-3'	5'-ATCATCATGTATGCTTCTA-3'
Cxcl-2	5'-CCAACCACCAGGCTACAG-3'	5'-CTTCAGGGTCAAGGCAAAC-3'
Cxcl-3	5'-CCAACCACCAGGCTACAG-3'	5'-AACTTCTTGACCATCCTTGA-3'
Cxcl-12	5'-AGAGCCACATCGCCAGAG-3'	5'-AGCTTTCTCCAGGTACTCTT-3'
Myd88	5'-CCTGTGTCTGGTCCATTGC-3'	5'-AGTCCTTCTTCATCGCCTTG-3'
Irak1	5'-GCCACCACTACCATCTTC-3'	5'-TCTCCAATCCTGAGTTCTTC-3'
Hsp-27	5'-GAGTACGAATTTGCCAAC-3'	5'-AACATAGTAGCCGTGATA-3'
Creb	5'-CCACAGATTGCCACATTAG-3'	5'-TGGAGACTGGATAACTGATG-3'
Hnf-4	5'-GAGGTTCTGTCCCAGCAG-3'	5'-TGTGATGTTGGCAATCTTCTT-3'
Hnf-3β	5'-GACTGGAGCAGCTACTAC-3'	5'-TATGTGTTCATGCCATTCAT-3'
C/ebp-β	5'-CTGAGCGACGAGTACAAG-3'	5'-CTGCTCCACCTTCTTCTG-3'
c-jun	5'-CCTTCTACGACGATGCCCTC-3'	5'-GGTTCAAGGTCATGCTCTGTTT-3'
Synapsin III	5´-ATCCGCATACAGAAGATTGG-3'	5´-GCCTTGACAGCACAGATG-3'
Persephin	5´-AAGATGGCAGAGACTAGAG-3'	5'-CACAGTATCGGAAGATGAC-3'
Cathepsin B	5'-CTGCTTACCATACACCATC-3'	5'-CTCCTTCACACTGTTAGAC-3'
Cathepsin D	5'-CTGGCTTCGTCCTCCTTC-3'	5´-CTGGCTCCGTGGTCTTAG-3'
Gapdh	5'-GCCTTCCGTGTTCCTACC-3'	5'-AGAGTGGGAGTTGCTGTTG-3'
18S	5´-AAATCAGTTATGGTTCCTTTGGTC-3'	5´-GCTCTAGAATTACCACAGTTATCCAA-3'

Table 1 – Primer sequences used for qPCR.